SAPIENZA
UNIVERSITÀ DI ROMA

LPTMS
Laboratoire de Physique Théorique
et Modèles Statistiques

UNIVERSITÉ PARIS SUD
FACULTÉ DES SCIENCES D'ORSAY
université PARIS-SACLAY

Scuola di Dottorato Vito Volterra - XXXII ciclo
École Doctorale 564, Physique en Île-de-France

PhD Thesis

The mixed p-spin model:
selecting, following and losing states

Giampaolo Folena

Supervisors

Federico Ricci-Tersenghi & Silvio Franz

November 2019

Anecdote: this thesis has been discussed in Rome on the 10 of March 2020, one day after the national lockdown and one day before the declaration of the pandemic from the world health organization because of coronavirus.

Luca Leuzzi Ricercatore, CNR-Nanotec, Roma (IT)	President of the Jury
Chiara Cammarota Senior Lecturer, King's College, London (GB)	External Reviewer
Patrick Charbonneau Associate Professor, Duke University, Durham (USA)	External Reviewer
Florent Krzakala Professeur, Sorbonne Université, Paris (FR)	Jury Member
Luca Dall'Asta Professore Associato, Politecnico di Torino (IT)	Jury Member
Pierfrancesco Urbani Chargé de Recherche, IPhT, CEA/Saclay (FR)	Jury Member

Federico Ricci-Tersenghi Professore ordinario, "La Sapienza", Università di Roma (IT)	Thesis Director
Silvio Franz Professeur des Universités, LPTMS, Orsay (FR)	Thesis Director

Thesis Summary - English

The main driving notion behind my thesis research is to explore the connection between the dynamics and the static in a prototypical model of glass transition, i.e. the mean-field p-spin spherical model. This model was introduced more than 30 years ago with the purpose of offering a simplified model that had the same equilibrium dynamical slowing down, theoretically described a few years earlier by mode-coupling theory. Over the years, the p-spin spherical model has shown to be a very meaningful and promising model, capable of describing many equilibrium and out-of-equilibrium aspects of glasses. Eventually it came to be considered as a prototypical model of glassiness. Having such a simple but rich reference model allows a coherent examination of a subject, in our case the glass behavior, which presents a very intricate phenomenology. Thus, the main purpose is not to have a quantitative prediction of the phenomena, but rather a broader view with a strong analytical basis. In this sense the p-spin model has assumed a role for disordered systems which is comparable to that of the Ising model for understanding ferromagnetism. My research is a natural path to reinforce our knowledge and comprehension of this model.

In the first chapter, we provide a general introduction to supercooled liquids and their phenomenology. The introduction is brief, and the main goal is to give a general overview, mainly from the point of view of the Random First Order Transition, while considering other perspectives on the subject and attempting to provide a 'fair' starting bibliography to whomever wants to study supercooled liquids. The last section focuses on the Potential Energy Landscape paradigm (PEL), which in my view, gives a very solid modelization of glassy phenomenology, and shares many aspects with mean-field analysis.

In the second chapter, the p-spin spherical model is presented in details. The equilibrium analysis is performed with the replica formalism, with a focus on the ultrametric structure. Then, different tools to study its free energy landscape are introduced: the TAP approach, the Franz-Parisi potential and the Monasson method. These three different ways of selecting states are carefully contrasted and their analogies and differences are underlined, in particular highlighting the different behavior played by pure and mixed p-spin models. Then the equilibrium dynamics is discussed, and a selection of classical results on the dynamical slowing down are analyzed by numerical integration. To conclude, the out-of-equilibrium dynamics in the two temperature protocol is analyzed. This shows two different regimes, the state following and the aging. For both, an asymptotic analysis and a numerical integration are performed and compared. A strong emphasis is given to the possibility of describing the asymptotic dynamics with a static potential.

The third chapter presents all the new results that emerged during my research. The study focuses on the two temperature protocol, starting in equilibrium and setting the second temperature to zero, which corresponds to a gradient descent dynamics. This protocol is especially interesting because it corresponds to the search of inherent structure of the energy landscape. The integrated dynamics, depending on the starting temperature, shows three different regimes, one that corresponds to a new phase, which shows aging together with memory of the initial condition. This new phase is not present in pure p-spin models, only in mixed ones. In order to theoretically describe this new phase, a constrained analysis of the stationary points of the energy landscape is performed. A numerical simulation of the system is also presented to confirm this new scenario.

Résumé de la Thèse - Français

L'objectif principal de cette thèse est d'explorer le lien entre la dynamique et la statique dans un modèle prototypique de transition vitreuse, i.e. le modèle à champ moyen du p-spin sphérique. Ce modèle a été introduit il y a plus de 30 ans dans le but d'offrir un modèle simplifié ayant, à l'équilibre, le même ralentissement dynamique décrit théoriquement quelques années plus tôt par la théorie des modes couplés. Au fil des ans, le modèle du p-spin sphérique s'est révélé être un modèle très significatif et prometteur, capable de décrire de nombreux aspects d'équilibre et hors équilibre des verres. Avoir un tel modèle de référence simple mais riche permet un examen cohérent d'un sujet, dans notre cas le comportement du verre qui présente une phénoménologie très complexe. Ainsi, le but principal n'est pas d'avoir une prédiction quantitative des phénomènes, mais plutôt une vue plus large avec une forte base analytique. En ce sens, le modèle du p-spin a assumé un rôle pour les systèmes désordonnés qui est comparable à celui du modèle Ising pour comprendre le ferromagnétisme. Ma recherche est une voie naturelle pour renforcer notre connaissance et notre compréhension de ce modèle.

Dans le premier chapitre, nous donnons une introduction générale aux liquides surfondus et leur phénoménologie. L'introduction est brève, et l'objectif principal est de donner un aperçu général, principalement du point de vue de la transition aléatoire du premier ordre, tout en tenant compte d'autres points de vue sur le sujet et en essayant de fournir une 'bonne' bibliographie de départ à quiconque veut étudier les liquides surfondus. La dernière section se concentre sur le paradigme du surface d'énergie potentielle (PEL), qui, à mon avis, donne une modélisation très solide de la phénoménologie vitreuse, et partage de nombreux aspects avec l'analyse du champ moyen.

Dans le deuxième chapitre, le modèle du p-spin sphérique est présenté en détail. L'analyse d'équilibre est réalisée avec le formalisme des répliques, avec un accent sur la structure ultramétrique. Ensuite, différents outils pour étudier son paysage d'énergie libre sont présentés: l'approche TAP, le potentiel de Franz-Parisi et la méthode de Monasson. Ces trois manières différentes de sélectionner les états sont soigneusement contrastées et leurs analogies et différences sont soulignées, en particulier le comportement différent joué par les modèles du p-spin purs et mixtes. Ensuite, la dynamique d'équilibre est discutée, et une sélection de résultats classiques sur le ralentissement dynamique sont analysés par intégration numérique. Pour conclure, la dynamique hors équilibre dans le protocole à deux températures est analysée. Cela montre deux régimes différents, des états suivables et du vieillissement. Pour les deux, une analyse asymptotique et une intégration numérique sont effectuées et comparées. L'accent est mis sur la possibilité de décrire la dynamique asymptotique avec un potentiel statique.

Le troisième chapitre présente tous les nouveaux résultats qui ont émergé au cours de mes recherches. L'étude se concentre sur le protocole à deux températures, commençant à l'équilibre et fixant la deuxième température à zéro, ce qui correspond à une dynamique de descente du gradient. Ce protocole est particulièrement intéressant car il correspond à la recherche de la structure inhérente du paysage énergétique. La dynamique intégrée, en fonction de la température de départ, montre trois régimes différents. Une de ceux-ci corresponde à une nouvelle phase, qui présente le vieillissement avec la mémoire de la condition initiale. Cette nouvelle phase n'est pas présente dans les modèles du p-spin pure, seulement dans les modèles mixtes. Afin de décrire théoriquement cette nouvelle phase, une analyse des points stationnaires du paysage énergétique est effectuée. Une simulation numérique du système est également présentée pour confirmer ce nouveau scénario.

Riassunto della Tesi - Italiano

L'obiettivo principale di questa tesi è di esplorare il legame tra la dinamica e la statica in un modello prototipico di transizione vetrosa, i.e. il modello di campo medio del p-spin sferico. Questo modello è stato introdotto più di 30 anni, come modello prototipico per il rallentamento critico all'equilibrio, quale era stato descritto alcuni anni prima dalla teoria dei modi accoppiati. Nel corso degli anni, il modello del p-spin sferico si è rivelato molto pregnante, capace di descrivere diversi aspetti dei vetri, sia all'equilibrio che fuori dall'equilibrio. Avere un simile modello di riferimento, semplice ma ricco, permette un esame coerente di un soggetto, quale è il comportamento dei vetri, con una fenomenologia molto complessa. Lo scopo principale non è quello di avere una previsione quantitativa dei fenomeni, ma piuttosto una visione più ampia con una forte base analitica. In questo senso, il modello del p-spin ha assunto un ruolo per i sistemi disordinati che è paragonabile a quello del modello di Ising per il ferromagnetismo. La mia ricerca è volta a rafforzare la nostra conoscenza e comprensione di questo modello.

Nel primo capitolo è fornita un'introduzione generale ai liquidi sopraffusi e alla loro fenomenologia. L'introduzione è breve, e l'obiettivo principale è quello di fornire una panoramica generale, soprattutto dal punto di vista della transizione disordinata del primo ordine (RFOT), pur tenendo conto di altri punti di vista sul soggetto e cercando di fornire una 'buona' bibliografia di partenza a chiunque voglia studiare i liquidi sopraffusi. L'ultima sezione si concentra sul paradigma della superficie di energia potenziale (PEL), che, a mio parere, fornisce una modellazione molto solida della fenomenologia vetrosa, e condivide molti aspetti con l'analisi di campo medio.

Nel secondo capitolo è presentato in dettaglio il modello del p-spin sferico. L'analisi dell'equilibrio è realizzata con il formalismo delle repliche, con un accenno alla struttura ultrametrica. Vengono poi presentati vari strumenti per studiare il paesaggio di energia libera: l'approccio TAP, il potenziale di Franz-Parisi e il metodo di Monasson. Questi tre diversi modi di selezionare gli stati sono accuratamente confrontati e le loro analogie e differenze sono messe in evidenza, in particolare il diverso comportamento dei modelli di p-spin puri e misti. Poi viene discussa la dinamica di equilibrio, e alcuni risultati classici sul rallentamento dinamico sono analizzati attraverso l'integrazione numerica della dinamica. In conclusione, si analizza la dinamica fuori dall'equilibrio nel protocollo a due temperature. Questo mostra due diversi regimi dinamici, di inseguimento degli stati e di invecchiamento. In entrambi i casi, sono effettuate e confrontate l'analisi asintotica e l'integrazione numerica. L'accento è posto sulla possibilità di descrivere la dinamica asintotica attraverso un potenziale statico.

Il terzo capitolo presenta i nuovi risultati emersi nel corso della mia ricerca. Lo studio si concentra sul protocollo a due temperature, iniziando dall'equilibrio e fissando la seconda temperatura a zero, il che corrisponde ad una dinamica di discesa del gradiente. Questo protocollo è particolarmente interessante perché corrisponde alla ricerca delle strutture inerenti nel paesaggio energetico. Questa dinamica, in funzione della temperatura di partenza, mostra tre differenti regimi. Uno di questi corrisponde ad una nuova fase, che presenta invecchiamento insieme alla memoria della condizione iniziale. Questa nuova fase non è presente nei modelli di p-spin puro, ma solo nei modelli misti. Per descrivere teoricamente questa nuova fase, si effettua un'analisi dei punti stazionari del paesaggio energetico. Inoltre, per confermare questo nuovo scenario, viene presentata una simulazione numerica del sistema.

alla mamma

Contents

Details that could throw doubt on your interpretation must be given, if you know them. You must do the best you can – if you know anything at all wrong, or possibly wrong – to explain it. If you make a theory, for example, and advertise it, or put it out, then you must also put down all the facts that disagree with it, as well as those that agree with it.

Richard P. Feynman

Introduction

The main driving notion behind my thesis research is to explore the connection between the dynamics and the static in a prototypical model of glass transition, i.e. the mean-field p-spin spherical model. This model was introduced more than 30 years ago with the purpose of offering a simplified model that had the same equilibrium dynamical slowing down, theoretically described a few years earlier by mode-coupling theory. Since its birth, statistical mechanics has always searched in the static analysis of some 'carefully' defined landscape; a path to avoid impossible dynamical calculations. One first fundamental concept is the idea of mapping temporal averages of observables into measures over phase space. This approach has allowed us to attain many fundamental relations between equilibrium observables. The same emphasis, in identifying the ensemble of dynamical paths in a static measure, continues to nourish the spirit of many researchers, and has been the drive all along my PhD research.

Over the years, the p-spin spherical model has shown to be a very meaningful and promising model, capable of describing many equilibrium and out-of-equilibrium aspects of glasses. Eventually it came to be considered as a prototypical model of *glassiness*. Having such a simple but rich reference model allows a coherent examination of a subject, in our case the glass behavior, which presents a very intricate phenomenology. Thus, the main purpose is not to have a quantitative prediction of the phenomena, but rather a broader view with a strong analytical basis. In this sense the p-spin model has assumed a role for disordered systems which is comparable to that of the Ising model for understanding ferromagnetism. My research is a natural path to reinforce our knowledge and comprehension of this model.

Over my three years of PhD research, I have concentrated on the out-of-equilibrium phenomenology of p-spin models, and in particular on a specific, two temperature protocol: a system prepared at one temperature and relaxed at another one. In the study of this out-of-equilibrium dynamics some unexpected phenomena were discov-

ered, which revealed a new interesting path of research and added a new brick to this prototypical structure of glassiness. In particular, we can assert now with certainty that there is no absolute threshold in the energy landscape of mean-field models. The region of phase space asymptotically explored by the dynamics depends on the chosen cooling path from high temperature. This was already known for finite-dimensional models, but not for mean-field ones. This new observation questions some paradigms that were built because of a pathological symmetry, present only in a subclass of these models, i.e., pure models.

In our attempt to understand this new unexpected behavior, my supervisors and me, have tackled the problem from many different angles; from the numerical integration of the long-time dynamics to the analytical study of the asymptotic dynamics, from the numerical simulation of finite-size systems to the theoretical study of the energy landscape. All these studies have clarified the origin of this anomalous behavior, and in particular, the parallelism aforementioned between static and dynamics. The major result of this work has been to introduce a new out-of-equilibrium mean-field phase and to characterize it in great detail.

In the first chapter, we provide a general introduction to supercooled liquids and their phenomenology. The introduction is brief, and the main goal is to give a general overview, mainly from the point of view of the Random First Order Transition, while considering other perspectives on the subject and attempting to provide a 'fair' starting bibliography to whomever wants to study supercooled liquids. The last section focuses on the Potential Energy Landscape paradigm, which in my view, gives a very solid modelization of glassy phenomenology, and shares many aspects with mean-field analysis.

In the second chapter, the p-spin spherical model is presented in details. The equilibrium analysis is performed with the replica formalism, with a focus on the ultrametric structure. Then, different tools to study its free energy landscape are introduced: the TAP approach, the Franz-Parisi potential and the Monasson method. These three different ways of selecting states are carefully contrasted and their analogies and differences are underlined, in particular highlighting the different behavior played by pure and mixed p-spin models. Then the equilibrium dynamics is discussed, and a selection of classical results on the dynamical slowing down are analyzed by numerical integration. To conclude, the out-of-equilibrium dynamics in the two temperature protocol is analyzed. This shows two different regimes, the state following and the aging. For both, an asymptotic analysis and a numerical integration are performed and compared. A strong emphasis is given to the possibility of describing the asymptotic dynamics with a static potential.

The third chapter presents all the new results that emerged during my research.

The study focuses on the two temperature protocol, starting in equilibrium and setting the second temperature to zero, which corresponds to a gradient descent dynamics. This protocol is especially interesting because it corresponds to the search of inherent structure of the energy landscape (PEL perspective). The integrated dynamics, depending on the starting temperature, shows three different regimes, one that corresponds to a new phase, which shows aging together with memory of the initial condition. This new phase is not present in pure p-spin models, only in mixed ones. In order to theoretically describe this new phase, a constrained analysis of the stationary points of the energy landscape is performed. A numerical simulation of the system is also presented to confirm this new scenario.

I wish to remark that all the thesis has been written with the continuous attention of providing my personal view over each subject. Therefore, sometimes things are not presented in a customary way, but I hope that this can stimulate a further understanding of the subject matter.

1

Glass Transition

1.1 Super-Cooled Liquids

A *supercooled liquid* is a liquid followed down to temperatures at which the crystal would be the stable phase. It is possible to follow this metastable branch if the cooling is fast enough so that the characteristic time to nucleate the *crystal* is much larger than the equilibrium relaxation time of the supercooled liquid (SCL). If this is the case, the SCL can be followed down in temperature until it starts to develop a fast increase of the relaxation time, such that it is no longer possible to equilibrate it on an experimental time scale τ_{exp}, thus the observed system is out of equilibrium. This marks the temperature T_g at which the "non-equilibrated" SCL is considered a *glass*. Conventionally T_g has been fixed to the temperature at which the viscosity overcomes the threshold $\nu_g = 10^{13}$ Poise*. This convention however is 'dangerous' because the temperature at which the system gets out of equilibrium strictly depends on the protocol used to prepare it. The glass is a *memorius* phase of matter†. In a *normal* phase of matter physical properties are uniquely defined by a small set of intensive variables $(T, P, ...)$, while each glass has its own properties, depending on how it has been prepared. This is very clear when thinking of commercial silica-based glasses. The dependence on the preparation protocol is closely related to the way in which the system has gone out of equilibrium, which in turn is connected to the experimental time scale considered. Therefore the properties of the glass depend on the time scale at which we observe it. Waiting for an incredibly long time τ_{SCL} the system is expect to relax to the equilibrium underlying SCL. And by waiting for an even longer period

*which corresponds to relaxation times of the order of 10-100s for molecular and atomic glass formers

†if it can be defined so

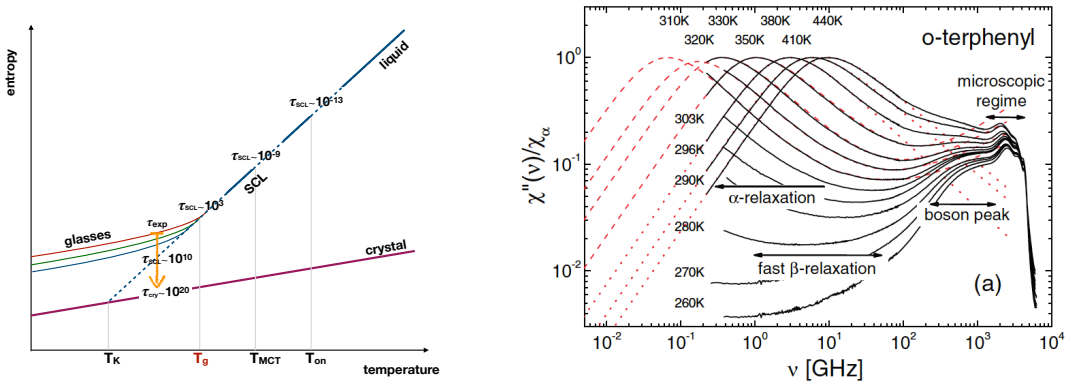

Figure 1.1: (**left**): idealized plot of entropy vs temperature in a SCL and in the relative crystal. The arrow highlights the enormous difference in time scales$\tau_{exp} \ll \tau_{SCL} \ll \tau_{cry}$ when the system gets out of equilibrium (**right**): dynamic susceptibility of o-terphenyl as a function of frequency, with different relaxations regimes highlighted. [Pet+13],

of time τ_{cry} the system should find the really stable crystalline phase. Each relaxation time is expected to depend on some activated dynamics (nucleation-type). As long as $\tau_{exp} \ll \tau_{SCL} \ll \tau_{cry}$ the glass is "well defined" and its properties depend on its history and in particular on the path it has been driven through, in the space of intensive variables, from the point it has fallen out-of-equilibrium ($\tau_{exp} \approx \tau_{SCL}$).

From this discussion the difficulties in building a theory that embodies all this history dependence should appear clear. As it is custom in statistical mechanics, such a theory should transform the average over dynamical path into a measure upon the phase space, which at equilibrium is the well known Boltzmann-Gibbs distribution ($e^{-\beta H}$). One of the main foci of this thesis is to build such a measure for a two-temperatures protocol: a quench from an initial temperature T' to a final temperature T.

In the following sections, in order to elucidate the major peculiarities of SCL we will follow the perspective of random first order transition RFOT, which drives all the modelization from a mean-field viewpoint (see [BB09] for a comprehensive review). We will simplify as much as possible the discussion and not introduce spatial description if not indispensable - even hough in recent years spatial and temporal heterogeneities have acquired an essential role in the description of 'glassiness' [Edi00; Ber11]. For the interested reader a plethora of very interesting reviews about SCL are available, each one with its theoretical background dependent on the community of reference. For a very brief and in-depth panorama of the glass transition

[DS01; Cha+14a]. From the MCT perspective [GS92]. For a short and dense review of RFOT [LW07]. For a pedestrian introduction to SCL with a RFOT-replica perspective [Cav09]. For a perspective RFOT closer to the numerical results [BB11]. To focus only on the dynamical (and not thermodynamical) description of the glass transition[CG10]. For a question-answer experimental point of view [Ang+00c]. For other experimental perspectives [Dyr06; EH12]. For an introduction to the Potential Energy Landscape paradigm [Sci05]. For a very detailed analysis of PEL [Heu08]. For a theoretical focus towards out-of-equilibrium dynamics [Cug02].

1.1.1 Equilibrium Regimes

We wish here to sketch the equilibrium regimes of a SCL, upon changing temperature T. In the following we use s to denote a configuration in phase space. This configuration evolves following a Hamiltonian dynamics. One very effective observable to characterize this dynamics - in and out-of-equilibrium - is the overlap of the configuration at a time t' with the configuration at a subsequent time t:

$$C(t, t') = s(t) \cdot s(t') \tag{1.1}$$

where $\cdot$ is a scalar product in phase space. This correlation function gives a direct characterization of different regimes and phases of matter. The system is *at equilibrium* if:

$$C(t, t') = C(t - t') \tag{1.2}$$

together with the fact there is no energy flux in and out of the system, i.e. fluctuation dissipation theorem (FDT) holds. The system is *ergodic* if:

$$\lim_{t \to 0} C(t) = 0 \tag{1.3}$$

At equilibrium, an ergodic SCL is in the liquid phase, while a non-ergodic SCL is considered in the glassy phase.

Given this observable, let's sketch what happens to a SCL starting from high temperatures (a cartoon of the transition is shown in figure 1.2.1). Above a so-called onset temperature T_{on} the equilibrium SCL is ergodic and a fast exponential relaxation occurs:

$$C(t) \propto \exp(-t/\tau_\alpha)) \qquad \tau_\alpha \propto \exp(T^{-1}) \tag{1.4}$$

where τ_β is the relaxation time of the system and follows an Arrhenius law. In this regime the kinetic energy dominates.

Around T_{on} the system starts feeling the presence of the energy landscape, kinetic and potential energies compete and the dynamics becomes sluggish. The relaxation

dynamics decouples into two different regimes, α-relaxation (slow) and β-relaxation (fast), which in terms of the correlation $C(t)$ signifies the development of a plateau. This is often described as a "cage forming" behavior. On short time scale τ_β each constituent of the system is trapped in a cage and experiences a fixed landscape. On another time scale τ_α the cages deform and the system diffuses. At this point the role of the observation τ_{exp} time in the modelization of the system starts to become appreciable. In fact if $\tau_\beta \ll \tau_{exp} \ll \tau_\alpha$ the system can be considered a fully-fledged glass.

Going down in temperature the largest time scale τ_α diverges with a power-law and the correlation $C(t)$ shows a critical behavior in the development of a plateau:

$$C(t) \simeq (t/\tau_\beta)^{-a} + q_{MCT} \sim q_{MCT} - (t/\tau_\alpha)^b \qquad \tau_\alpha \propto (T - T_{MCT})^{-\gamma} \tag{1.5}$$

where a, b are the exponents that govern the approach to and the depart from the plateau, respectively. All this behavior is predicted by the mode coupling theory (MCT)* (see [RC05] for a review). This is a critical theory and for this reason it has some sort of universality, however it ignores activated events which occur before reaching T_{MCT}. Thus in finite dimensional systems T_{MCT} flags a crossover region, which, in the extreme case of mean-field models (fully connected, infinite dimensional,...), becomes a sharp thermodynamic transition that separates the SCL from glass states. In finite dimensional systems, however, no metastable state is well defined because activated events are always possible with finite probability and the system can diffuse from one pseudo-glass to another†. While there is one ergodic SCL, there exist many (pseudo-)glasses, which in mean-field correspond to metastable states. The logarithm of their number S_c is extensive, it is called 'configurational entropy' and it goes linearly to zero at a finite temperature T_K, the Kauzmann temperature.

Further decreasing the temperature below T_{MCT}, the system keeps ergodic but the divergence of the time scale τ_α then scales as:

$$\tau_\alpha \propto \exp(\Delta F) \approx \exp(\sigma^d / S_c^\theta)^{1/(d-\theta)} \approx (T - T_K)^{\theta/(d-\theta)} \tag{1.6}$$

where σ is the surface tensions between pseudo-glasses. Thus the relaxation dynamics is directly connected to the structure of free energy landscape through the configurational entropy. Behind this prediction lies a nucleation 'argument', which in the literature is dubbed "mosaic picture" (see section 1.1.2). Glasses nucleate inside

*each exponent is given by the theory

†'pseudo-glass' is obtained whenever one considers the short time dynamics below T_{MCT} in a real system

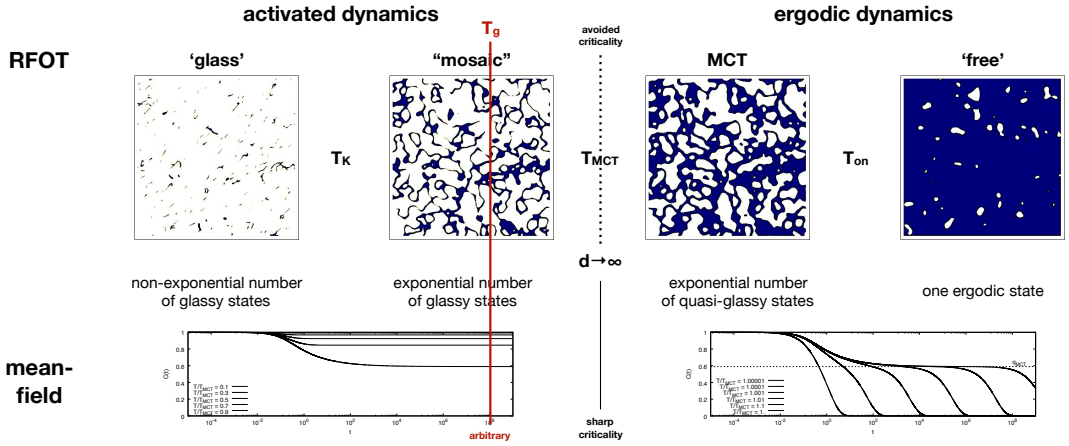

Figure 1.2: Random First Order Transition stems from the perspective that the real 'glass' can be described around an underlying mean-field core

glasses and the plateau continue to elongate. The mosaic picture is the most debated and weakest part of the RFOT perspective, but it continues to be stringently supported since it is powered by a strong mean-field core. One of the strongest mathematical prediction of mean-field in this temperature region is the partitioning of the phase space in many 'well separated' basins * which gives a total free energy partitioned in a 'large' number of states $\mathscr{S}$:

$$-\beta F = \log\Big(\sum_{\mathscr{I}}\sum_{s\in\mathscr{S}} e^{-\beta H[s]}\Big) = \log\Big(\sum_{\mathscr{I}} e^{-\beta f_{\mathscr{S}}}\Big) = \log\Big(\int df\, e^{-\beta f + S_c(f)}\Big) \qquad (1.7)$$

which, in mean-field models, is dominated by the saddle point $\partial_f S_c(f^*) = \beta$, which is analogous to the equilibrium relation $\partial_E S(E^*) = \beta$, but at the level of states $\mathscr{S}$. We see that the temperature T plays the role of an equilibrium parameter (Legendre transform) at two different scales. Inside basins the temperature is what defines the thermal bath perceived at a configuration level and between basins it regulates the exchange of free energy. This suggests an abstract interpretation of the decoupling of time scales described at the level of the correlations.

Below T_K, the dynamics is non-ergodic also for a real system, at least with the RFOT perspective. At T_K there is a true thermodynamic transition, below which phase space is ergodically broken and the system is confined into one of many glassy state. However, given the nature of the transition there is no direct way to verify

*basin and state are used interchangeably

this prediction. Whether the glass formation is a purely dynamical effect or the result of an underlying static transition is far from understood, but following the Occam's razor principle, RFOT* has for now all the ingredients to be considered a 'good candidate' to describe the SCL phenomenology.

1.1.2 Statical vs Dynamical Signatures

In this section we briefly overview the main theoretical interpretation and experimental observations concerning the aforementioned temperatures T_K, T_{MCT}, T_{on} which constitute the backbone of RFOT interpretation. For each temperature a brief historical account will be presented together with some different theoretical perspective on the transition, with a particular emphasis on the contrast between statical and dynamical perspectives.

The Onset Temperature

The onset temperature T_{on}† marks the passage from uncorrelated dynamics above to the "landscape dominated dynamics" below. It is a 'quite sharp' crossover that appears in a variety of materials, such as molecular liquids, colloids, metallic liquids... [Wee+00; Sas02; Jai+16]. And it has been studied in many numerical simulations [KA95a; SDS98; Sas00; Sin+12; Ban+17]. Above T_{on} the characteristic relaxation time of the system follows an Arrhenius law and two times observables presents an exponential decay:

$$\tau_\alpha \propto \exp(T^{-1}) \qquad C(t) \propto \exp(-t/\tau_\alpha) \tag{1.8}$$

Below T_{on} cooperative behavior between constituents of the system begins which find the way to continue their motion while in a very crowded environment. This deep change can be seen in many different aspects. First the deviation from the Arrhenius law and the stretching of the exponential relaxations‡:

$$\tau_\alpha \not\propto \exp(T^{-1}) \qquad C(t) \propto \exp\Big(-(t/\tau_\alpha)^\beta \Big) \tag{1.9}$$

where $\beta \in [0,1]$ is a stretching exponent that decreases with temperature. Another very crucial aspects is the decoupling of time scales τ_α and τ_β, respectively the scale of fast vibration in "cages" and the scale of slow rearrangement of "cages". This is

*by design MCT is compatible with RFOT, since the birth of the second [KT87b]

†in literature it is also called T_A, for Arrhenius or ,T_o

‡Kohlrausch–Williams–Watts law

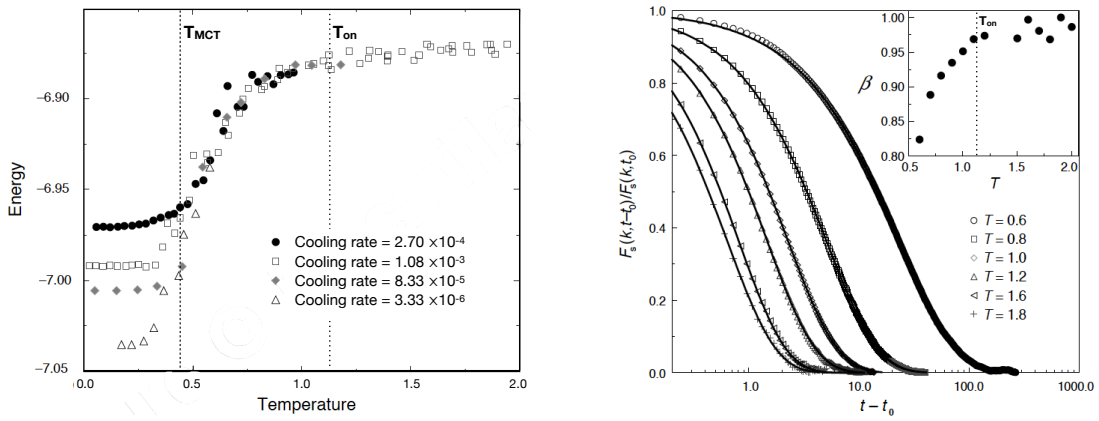

Figure 1.3: Landscape vs Equilibrium Dynamics around the T_{on}. Simulation of a Lennard Jones binary mixture [SDS98] (**left**): average energy of sampled Inherent Structures changing the temperature. For $T < T_{on}$ the dynamics becomes "landscape dominated". $T_{MCT} \approx 0.44$ (**right**): stretched exponential relaxation dynamics below T_{on}. For $T > T_{on}$ almost exponential relaxation $\beta \approx 1$.

to say that the spectrum of vibration in the frequency domain develops two peaks. Moreover the violation of Stokes-Einstein relation is observed:

$$D\tau_\alpha \not\sim T \tag{1.10}$$

The diffusion coefficient D and the relaxation time τ_α are not inversely proportional as is the case with a simple Brownian motion. This is a direct consequence of the presence of more than one relaxation times [CE96] and it is a signature together with the stretched exponential relaxation of an underneath emerging phenomenon, the spatially heterogeneous dynamics [Kob+97].

What about the "landscape dominated dynamics" definition? In 1998 S.Sastry, P.G.Debenedetti and F.H.Stillinger found a correspondence between equilibrium dynamics and potential energy landscape in a simulation of Lennard Jones binary mixture [SDS98]. The idea was to run a gradient descent dynamics to find the closest energy minimum (Inherent Structure) to the starting equilibrated configuration and study the statistical properties of these minima. They found that below T_{on} the average IS energy was dependent on the starting temperature.

Another static concept recently introduced, which again marks the onset temperature is the "residual multiparticle entropy", which is the contribution to the entropy that comes from correlations of more than two particles. This entropy is found to vanish at T_{on}, and becomes positive below, in the range of temperature of cooperative behavior [Ban+17].

Let's briefly mention that T_{on} has a very special role from another theoretical perspective, that of dynamical facilitations. It has the same role of T_{MCT} for MCT, it defines a reference temperature around which to develop an 'expansion'. It follows a prediction for the divergence of relaxation time $\tau_\alpha = \exp\left((T - T_{on})^2\right)$ for $T < T_{on}$. This law was shown to be very good in fitting the behavior of very different liquids down to T_g [ECG09]. It has been later recovered in another work with completely different theoretical assumption and in place of T_{on} a melting temperature [Wei+16].

Finally, all the aforementioned phenomenology can be found exactly in the p-spin mixed spherical model, which will be our mean-field reference model throughout this thesis. Mixed, because in the pure version, as we will see in great detail in chapter 2, the potential energy landscape is trivial and does not show any connection with the equilibrium dynamics. In particular in the mixed model we found evidence of IS energy dependence on temperature around T_{on} [FFR19], which will be carefully illustrated in chapter 3. It is striking that despite the lack of spatial dimension, and thus the lack of heterogeneity, the same picture arises. There are two possible resolutions of to this apparent paradox, either space is not really necessary in the picture, or 'distances' arise in a non trivial way, even in models without spatial dimensions.

The Mode Coupling Temperature

The mode-coupling temperature T_{MCT}* takes its name from the homonymous theory developed by W. Götze and collaborators [Göt09], starting from the two seminal papers in 1984 [BGS84; Leu84]†. This theory is fully dynamical, but takes as input the static structure factor $S(k)$, which is Fourier transform of the spatial density correlation. It has great predictive power and it has been tested very intensively both numerically and experimentally, over the years [KA95a; Göt99; DP01; Nan+15]. The MCT formulation departs from the equation that describes the equilibrium dynamics at temperature T of a tagged-particle of mass m in the SCL:

$$\partial_t^2 F(k,t) + \frac{k^2 T}{m S(k)} F(k,t) = -\int_0^t ds M(k, t-s) \partial_s F(k,s) \tag{1.11}$$

where $F(k,t)$ is the Fourier transform of time-dependent spatial density correlation ‡ with $F(k,0) = S(k)$. The lhs is just the (pseudo-)diffusive motion of the particle, while $M(k, t-s)$ is a memory kernel. In the MCT approximation, this can be

*in literature it is also called $T_\times$ whenever the focus is more on Goldstein

†written concomitantly by different groups

‡also known as van Hove's correlation function

written as a function of the correlation $F(k,t)$, which closes the equation. The past trajectory of the particle influences the actual dynamics in a feedback loop. For a short review with all calculations see [RC05], while for a reference book [Göt09].

In absence of spatial dependence, $F(k,t) \to C(t)$, the equation becomes purely temporal and it coincides with the dynamics of the correlation function in p-spin models:

$$\partial_t C(t) + TC(t) = -\int_0^\tau ds M[C(\tau - s)]\partial_s C(s) \tag{1.12}$$

where we considered the limit of overdamped dynamics. We will study this equation in detail in section 2.6. The temperature T_{MCT} fixes a critical point, in the asymptotic evaluation of this equation, at which the dynamics develops an infinite plateau with two power-laws approaching and departing from it (see fig. 1.4). The elongation of the plateau represents the further decoupling of fast and slow time scales.

In real systems at T_{MCT} there is no singularity, because activated processes intervene. This idea of a crossover temperature that sets "activated dynamics" was already present before MCT; Martin Goldstein introduced it in 1969 [Gol69; Ang88]. It is interesting that T_{MCT} defines a sharp thermodynamic transition in the mean-field limit, usually referred to as "dynamical transition". It marks the temperature below which the dynamics is non-ergodic and glasses dominate Gibbs measure. In real systems, below this crossover, the most accepted view - remaining in RFOT paradigm - is the "mosaic picture", which we will discuss in the following section.

To conclude the section we go back to the PEL perspective. It has been shown in computer simulations that the Goldstein crossover can be quantified and it was found that the temperature so obtained $T_\times \approx T_{MCT}$, which confirms a correspondence between dynamical MCT and statical PEL [Sch+00]. The idea behind this analysis was to mirror at the level of IS the molecular dynamics and to find the temperature at which dynamics become dominated by IS jumps. In another couple of almost equivalent works it has been shown that at T_{MCT} the typical closest saddle to an equilibrium configuration has a spectrum that is marginal, which means with a zero lowest eigenvalue [Ang+00b; Bro+00]. In a very recent work this correspondence between the geometry of the landscape and the equilibrium dynamics has been reformulated by distinguish between localized and delocalized modes and noticing that only the seconds take part to the geometric transition [CNB19].

The Kauzmann Temperature

The Kauzmann transition temperature T_K is perhaps the most debated and at the same time the least characteristic temperature. In fact it is deep in the experimentally

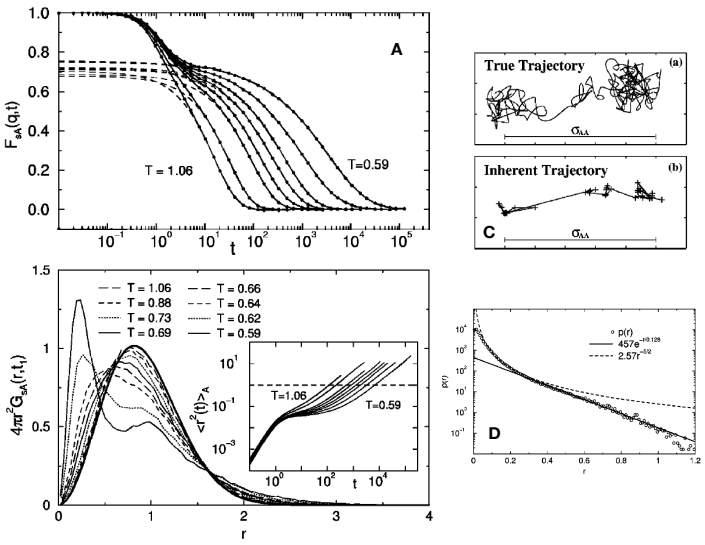

Figure 1.4: Towards "activated dynamics" around T_{MCT}. Simulation of a Lennard Jones binary mixture for which $T_{MCT} \approx 0.59$ [Sch+00] (**A**): elongation of the plateau of the correlation function. (**B**): double-well development in the diffusion of particles (**C**): correspondence between real motion and motion between underlying Inherent Structures. (**D**): Distribution of typical jumps between ISs.

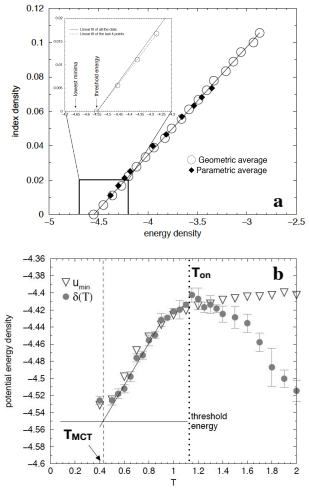

Figure 1.5: Landscape signature of T_{MCT} through the Hessian of ISs. Same simulation of fig. 1.3, from [Bro+00]. (**a**): marginal Hessian of ISs at T_{MCT} (**b**): the harmonic approx for the energy around ISs $\delta(T)$ works between T_{MCT} and T_{on}.

unreachable zone. It becomes strictly fundamental when some theory is based on it. In 1948 Walter Kauzmann wrote "the nature of the glassy state and the behavior of liquids at low temperatures" [Kau48], where he describes that:

> [...] trends seem to indicate that the entropies and enthalpies, but not the free energies, of many non-vitreous liquids would become less than those of the corresponding crystalline phases at temperatures well above the absolute zero. This paradoxical result [...] the existence of such a "pseudocritical temperature".

The Pandora's box was opened. Here we won't discuss the philosophical questions, we just reread Kauzmann's result in the perspective of RFOT, and thus in regard to a mean-field core. The first and largest step in this direction was took by Gerold Adam and Julian H. Gibbs in 1965 [AG65]. They connected the configurational entropy S_c and the dynamical most accepted fit - at the time and still now - for the diverseness of relaxation times in SCL, the Vogel-Fulcher-Tamman-(Hesse) empirical

law (VFT):

$$\tau_\alpha \propto \exp\Big(\frac{1}{TS_c}\Big) \Longleftrightarrow \tau_\alpha \propto \exp\Big(\frac{1}{K_{VFT}(T/T_{VFT}-1)}\Big) \tag{1.13}$$

where T_0 is a fitted temperature and K_{VFT} is a material-specific parameter quantifying the kinetic fragility. Assuming the Kauzmann's thermodynamic result for entropy, $S_{SCL}(T_K) - S_{cry}(T_K) = (\partial_T S_{SCL}(T_K) - \partial_T S_{cry}(T_K))(T - T_K) + o(T - T_K)$ and this is considered a good approximation for the configurational entropy:

$$S_c \approx \Delta C_p (T/T_K - 1) \tag{1.14}$$

where $\Delta C_p = (\partial_T S_{SCL}(T_K) - \partial_T S_{cry}(T_K))$ is the liquid-crystal difference in specific heat around T_K*. Plugging this expression into (1.13) we find the double correspondence:

$$T_{VFT} \approx T_K \qquad K_{VFT} \approx T\Delta C_p \tag{1.15}$$

This fixes two parameters of the VFT fit from calorimetric calculations, which are very well verified in experiments [RA98]. If we accept the picture this tells us two important things: the T_{VFT} is a thermodynamic transition and the fragility K_{VFT} is proportional to the jump of the specific heat at the glass transition.

To obtain lhs of (1.13) Adam and Gibbs adopted the concept of cooperative rearranging region (CRR), the smallest region that can rearrange into another configuration independently of its environment. This perspective has been developed during the years and was reformulated in 1989 by Kirkpatrick, Thirumalai and Wolynes, into the so-called "mosaic picture", to connect it to mean-field models [KTW89]. This association is considered to be the birth of RFOT. Here we briefly describe their argument in a revisited formulation [BB04]. In a SCL equilibrated at T, let's take a spherical cavity of radius ξ and fix all particles† outside. The smaller the cavity, the stabler the particles inside. Let's admit that they form a state α that is stable. The partition function for the cavity in d-dimensions is:

$$Z = Z_{in} + Z_{out} = e^{-\beta f_\alpha \xi^d + \beta\sigma\xi^\theta} + \int df e^{-\beta f \xi^d + S_c(f)\xi^d} \tag{1.16}$$

here f_α is the free energy density which gives the bulk contribution, σ is the surface cost given by the borders of the cavity and $S_c(f)$ is the configurational entropy density. Z_{out} can be on first approximation given by the saddle point (see 1.7),

*considered almost constant in the range around T_g

†molecules, granules, ...

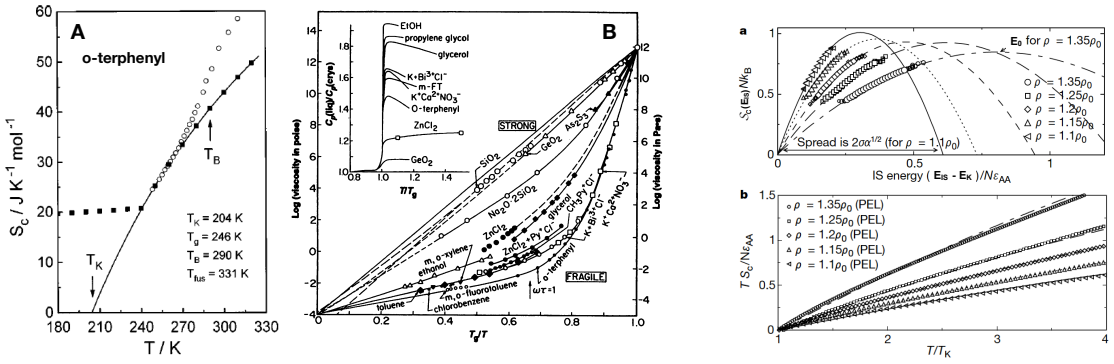

Figure 1.6: Configurational Entropy and Activated Dynamics near T_K. (**A**): Configurational entropy from calorimetric analysis (CA) extrapolate to zero at finite T_K. Open circles are from VFT fit of relaxation dynamics. From [RA98] (**B**): Glasses of different fragilities and liquid-solid specific heat ratio [Ang95]

Figure 1.7: Inherent Structures near T_K LJ simulation [Sas01]. (**a**): configurational entropy $S_c(E_{IS})$ vs IS energy E_{IS} from PEL analysis. (**b**): S_c obtained from CA (lines), and from analysis of the PEL (points) plotted against temperature T.

which gives the typical free energy density f^*. Moreover the free energy $f_\alpha = f^*$ because at equilibrium we expect the reference state α to be a typical one. This gives a standard nucleation argument. The free energy of such a nucleus (cavity) is:

$$\Delta F = S_c(f^*)\xi^d - \beta\sigma\xi^\theta \qquad \text{with} \quad \partial_f S_c(f^*) = \beta \tag{1.17}$$

and following an Arrhenius approximation, the relaxation time behaves as:

$$\tau_\alpha \propto \exp\big(\arg\max \beta\Delta F\big) = \exp\left[\Big(\frac{\sigma^d}{S_c^\theta}\Big)^{1/(d-\theta)}\right] \tag{1.18}$$

in the case of $\theta = d/2$ we re-obtain the famous VFT law (1.13). The reason for this equality is not clear and the question is still debated. This concludes our fast excursion on the "mosaic picture".

All this supports the idea that the dynamical divergence of relaxation time is the reflection of a true thermodynamic transition, at which the configurational entropy becomes zero. Many experiments tested this correspondence [AS82; Ric84; RA98].

There are also opposite views on the problem. Certain papers disagree with a VFT law [Hec+08] and propose other possible perspectives which do not consider thermodynamic T_K to have any influence on the SCL dynamics (see [BG13] for a critical review).

What is sure is that in p-spin spherical models, a true thermodynamic transition takes place at T_K, which corresponds to the temperature at which the Gibbs measure condenses on the deepest available states. However there is not any dynamical divergence because above T_K, glassy states were already well defined, ergodicity was broken at T_{MCT}.

To conclude the section we again consider the PEL perspective. Srikanth Sastry in a work of 2001 shows how the fragility of a system is connected to the multiplicity of states, their spread and the changes in each basin entropy [Sas01]. It is a direct application of the Gaussian harmonic approximation, which we will briefly explore in the next section.

There are still many unresolved question about this transition, for a broader view see [BB09; Cav09].

1.2 Potential Energy Landscape

Martin Goldstein in 1969 in the abstract of its famous paper "Viscous Liquids and the Glass Transition: A Potential Energy Barrier Picture" wrote:

> The model is based on the idea that in "viscous" liquids (shear relaxation time $\geq 10^{-9}$ sec) flow is dominated by potential barriers high compared to thermal energies, while at higher temperature, this will no longer be true.

This is the picture that every scholar of supercooled liquid has in mind. Nowadays T_{MCT} is considered by many to be the crossover temperature to activated dynamics, and we will see that the Goldstein picture is often a good approximation until the onset of temperature T_{on}.

Following the path of Goldstein, F.H.Stillinger and T.A.Weber wrote in 1982 "Hidden structure in liquids" [SW82], which was the first of a series of papers in which they developed one of the major paradigms in the investigation of SCL, the Potential Energy Landscape approach [SW83; SW84; SW85]. The central idea is to build both the thermodynamic and the dynamics starting from the structure of the underneath PEL.

Over the years, this perspective has grown fast, made possible by the increase of computer's power. In fact since the beginning this theory has build a strong connection with computer simulations which are necessary to validate the theory. In some sense this paradigm follows the epistemology:

$$\text{PEL} \Longleftrightarrow \text{numcerical simulations} \Longleftrightarrow \text{real experiments} \tag{1.19}$$

numerical simulations are a necessary 'medium' between nature and theory. This is a path that an ever-increasing area of science has been pursuing in the last 30 years, which is very fascinating, and new to history [Win99].

1.2.1 Inherent Structures Partitioning

In this introduction to PEL we will more or less follow the review of F. Sciortino [Sci05], who is one of the greatest contributors to the development of PEL. The first thing is to define a model of SLC. A N-particles system, whose evolution is described by a Hamiltonian H, which has a kinetic K and potential contribution U. Usually the potential is given by the sum of pair potentials:

$$U = \sum_{ij} U^{ij}(r_i, r_j) \qquad U_{LJ}(r) = 4\varepsilon \cdot \left[\left(\frac{\sigma}{r}\right)^{12} - \left(\frac{\sigma}{r}\right)^{6} \right] \tag{1.20}$$

in the simplest case it depends only on the distance $|r_i - r_j|$ between particles. The suffix ^{ij} refers to the possibility of having different kinds of particles. One of the most studied systems is the Lennard-Jones binary mixture (LJBM), where two kinds of particles interact through U_{LJ}. The most famous of all is the so-called Kob-Andersen model [KA94], a LJBM which has a fine-tuned composition to avoid crystallization*. This is all we will say about the numerical part, which requires a huge effort, for now we are interested to the theoretical part.

The PEL of the system is a very rough landscape defined by the coordinates r_i of the N particles. In order to study it thermodynamically, the fundamental concept is that of the Inherent Structure (IS), which denotes the configuration that lies at a local minimum of the PEL.

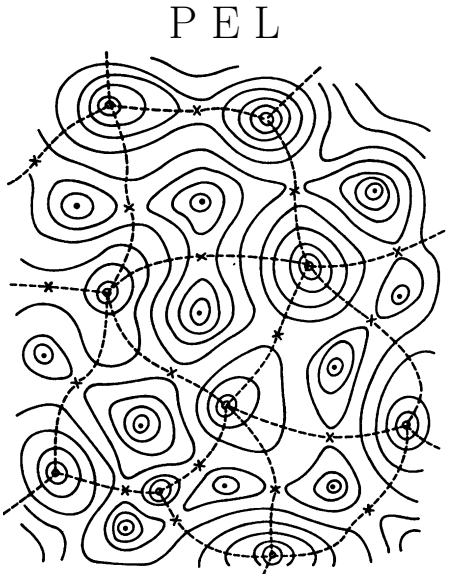

Each IS ι labels a basin of attraction $\mathscr{B}(\iota)$, which is defined by the locus of configurations which are connected to IS by a gradient descent path. In this way all the PEL is unambiguously partitioned in basins of attraction, each labeled by its IS (filled circles). The interesting thing about this partitioning is that it can be further explored, considering that each border between basins is an $(N-1)$-dimensional space for which one can define the IS, which would be in the original landscape a saddle of order 1 (crosses). Thus defining an ulterior partitioning in basins of dimension $(N-1)$ on the border of the original basins.

This procedure can be repeated an arbitrary number of times, giving a hierarchical partitioning of borders, which has been give an interesting perspective in the study of the aging dynamic [KL95]. In this brief overview we concentrate on ISs (minima) and we will just allude to the role of saddles.

Having partitioned the phase space in basins, we rewrite the partition function as a sum of the free energy of each basin:

$$Z(\beta) = \sum_{\iota} \sum_{\sigma \in \mathscr{B}(\iota)} e^{-\beta H[\sigma]} = \sum_{\iota} e^{-\beta E(\iota) + F(\mathscr{B}(\iota))} \tag{1.21}$$

where $\sigma \in \mathscr{B}(\iota)$ stands for the configurations that belongs to the basin $\mathscr{B}(\iota)$, $E(\iota)$

*crystallization still occurs for long enough simulations [PSD18]

is the energy of the inherent structure ι and $F(\mathscr{B}(\iota))$ the free energy of the relative basin. Each basin has its own volume $V(\mathscr{B}(\iota))$ and its free energy is given by:

$$F(\mathscr{B}(\iota)) = \Delta E(\mathscr{B}(\iota)) - T \log V(\mathscr{B}(\iota)) \tag{1.22}$$

where $\Delta E(\mathscr{B}(\iota))$ is the internal energy of the basin having subtracted the energy of bottom $E(\iota)$. If each basin is considered an independent system all its thermodynamic properties can be characterized. But one should keep in mind that basins are not 'truly' independent. The borders that separate them are typically not extensive. Thus in each canonical computation, which is typically the simplest one, all basins are connected through thermal paths. It is better to rethink this partitioning in microcanonical terms. In this perspective, low energy orbits are non ergodic whenever restricted inside a basin. Anyhow, canonical or micronanonical, the point is that this decomposition in basins gives a valid method of approximation. Selecting basins on the base of the energy of their inherent structure $E(\iota)$, in the thermodynamic limit we expect them to have a 'well defined' * free energy $F(\mathscr{B}(\iota))$. Thus the partition function can be rewritten as:

$$Z(\beta) = \int dE_{IS} \sum_{\iota} \delta(E_{IS} - E_{\iota}) e^{-\beta\left(E(\iota)+F(\mathscr{B}(\iota))\right)} = \int dE_{IS} \mathscr{N}(E_{IS}) e^{-\beta\left(E_{IS}+F(E_{IS})\right)} \tag{1.23}$$

where $F(E_{IS})$ is the typical free energy for a basin with energy $E(\iota) = E_{IS}$. The last $\mathscr{N}(E_{IS})$ is the number of inherent structures of energy E_{IS}, from which the concept of configurational entropy is derived:

$$S_c(E_{IS}) = \log(\mathscr{N}(E_{IS})) \tag{1.24}$$

Thus we have that the total partition function can be decomposed in a two-layer hierarchy, configuration in basins, and basins in system. This is a typical feature of mean-field models with Random First Order Transition, and in particular our reference model, the p-spin spherical model. The key difference is that in mean-field models this partitioning has no ambiguity, since barriers between basins are extensive and each basin corresponds to a well defined thermodynamic state. This is not the case in finite dimensional systems, but in many cases it is a very good approximation, because over the temperature range studied by PEL, activated dynamics dominate ($T \leq T_{MCT}$), therefore the relaxation time scale inside the basin $\tau_{\mathscr{B}}$ is well separated from the time scale for jumping between basins τ_{α}.

*delta distributed

1.2.2 The Gaussian PEL Approximation

In the previous section we have seen how to partition the configuration space on the base of the potential energy landscape and consequently rewrite the partition function. Here we concentrate on one effective approximation, the so-called "Gaussian harmonic" approximation. *Gaussian* refers to the distribution of inherent structure energies, while *harmonic* refers to the approximation of free energy for each basin. Let's start with the first:

$$\mathscr{N}_{Gauss}(E_{IS}) = \mathscr{N}_{tot} N(E_0, \Delta E_0) \tag{1.25}$$

$N(E_0, \Delta E_0)$ is a normal distribution with average E_0 and standard deviation ΔE_0, and $\mathscr{N}_{tot} = \exp(\alpha N)$ is the total number of inherent structures and its logarithm is extensive in the dimension of the system. This is the Gaussian part of the approximation and it corresponds exactly to what is known as Random Energy Model [Der80]. On top of this REM modelization of IS energies, another layer is added, the structure of each basin. The simplest possible approximation is to consider each basin as a harmonic well. It follows that the free energy of each basin is given by normal modes around the IS:

$$F_{harm}(E_{IS}) = \sum_i^N \log(\frac{1}{\beta\omega_i}) = -3N\log(\beta\omega_0) - \int d\omega D(\omega)\log(\omega/\omega_0) \tag{1.26}$$

which says that the total free energy is the sum of free energy of independent harmonic oscillators with spectral density $D(\omega)$. And we rescaled all the frequencies by the lowest one ω_0. Both ω_0 and $D(\omega)$ are strictly dependent on E_{IS}. This is the general form for the harmonic approximation. We remark that the frequencies are simply given by the diagonalization of the Hessian matrix at the IS. We do a further simplification considering that the harmonic free energy F_{harm} has a linear dependence on E_{IS} around the most probable inherent structure energy E_0:

$$F_{harm}(E_{IS}) = F_{harm}(E_0) + b(E_{IS} - E_0) \tag{1.27}$$

Here we introduce another parameter b which must be added to $E_0, \Delta E_0$ and α. All these parameters have an implicit dependence on volume and should be inferred from computer simulations. Putting all these approximations together we obtain the free energy (1.23):

$$\begin{aligned} -\beta F(\beta) =& S_{Gauss}(E_{IS}) - \beta\big(E_{IS} + F_{harm}(E_{IS})\big) \\ =& N\alpha - \frac{(E_{IS} - E_0)^2}{2\Delta E_0^2} - \beta E_{IS} - \beta F_{harm}(E_0) - \beta b(E_{IS} - E_0) \end{aligned} \tag{1.28}$$

In order to find the IS that dominate the measure, this free energy must be extremized with respect to E_{IS}, which gives the equation:

$$E_{IS} = E_0 - (\beta + b)\Delta E_0^2 \tag{1.29}$$

which defines the temperature dependence of the IS energy, which is linear in inverse temperature β. The two parameters E_0, b can be directly fitted from simulations. Reinserting it in the configurational entropy one obtains:

$$S_{Gauss}(E_{IS}) = \alpha N - \frac{(\beta + b)^2}{2\Delta E_0^2} \tag{1.30}$$

from which one can fit the parameters α and ΔE_0. Thus the model is completely defined. Remember, however, that for each volume the four parameters must be refitted. Then one can deduce many thermodynamic properties, such as the existence of a Kauzmann transition ($S_{Gauss}(E_{IS}) = 0$) at:

$$T_K = 1/(\sqrt{2\alpha N}/\Delta E_0 - b) \qquad E_K = E_0 - \sqrt{2\alpha N}\Delta E_0 \tag{1.31}$$

Here we have considered the simplest possible model of PEL which has all the essential ingredients to describe a supercooled liquid. The Gaussian distribution of ISs (REM like) is the most robust feature, since it comes directly from the central limit theorem*, for what concern the free energy of each basin, many possible approximations have been considered, considering anharmonicities as well as different dependences on the E_{IS}. The literature is vast. Here we wanted only to draw the picture given by PEL's perspective of analyzing the thermodynamics properties of disordered systems. Moreover, the general ideas given in this brief introduction to PEL will be very useful in understanding our reference mean-field model.

*consider the extraction of independent basins

Chapter 1 References

[AG65] Gerold Adam and Julian H. Gibbs. "On the Temperature Dependence of Cooperative Relaxation Properties in Glass-Forming Liquids". In: *The Journal of Chemical Physics* 43.1 (1965).

[Ang+00b] L. Angelani et al. "Saddles in the Energy Landscape Probed by Supercooled Liquids". In: *Physical Review Letters* 85.25 (2000).

[Ang+00c] C. A. Angell et al. "Relaxation in glassforming liquids and amorphous solids". In: *Journal of Applied Physics* 88.6 (2000).

[Ang88] C. A. Angell. "Perspective on the glass transition". en. In: *Journal of Physics and Chemistry of Solids* 49.8 (1988).

[Ang95] C. A. Angell. "The old problems of glass and the glass transition, and the many new twists". en. In: *Proceedings of the National Academy of Sciences* 92.15 (1995).

[AS82] C. A. Angell and D. L. Smith. "Test of the entropy basis of the Vogel-Tammann-Fulcher equation. Dielectric relaxation of polyalcohols near Tg". In: *The Journal of Physical Chemistry* 86.19 (1982).

[Ban+17] Atreyee Banerjee et al. "Determination of onset temperature from the entropy for fragile to strong liquids". In: *The Journal of Chemical Physics* 147.2 (2017).

[BB04] Jean-Philippe Bouchaud and Giulio Biroli. "On the Adam-Gibbs-Kirkpatrick-Thirumalai-Wolynes scenario for the viscosity increase in glasses". In: *The Journal of Chemical Physics* 121.15 (2004).

[BB09] G. Biroli and J. P. Bouchaud. "The Random First-Order Transition Theory of Glasses: a critical assessment". In: *arXiv:0912.2542 [cond-mat]* (2009).

[BB11] Ludovic Berthier and Giulio Biroli. "Theoretical perspective on the glass transition and amorphous materials". In: *Reviews of Modern Physics* 83.2 (2011).

[Ber11] Ludovic Berthier. "Dynamic heterogeneity in amorphous materials". In: *Physics* 4 (2011).

[BG13] Giulio Biroli and Juan P. Garrahan. "Perspective: The glass transition". In: *The Journal of Chemical Physics* 138.12 (2013).

[BGS84] U. Bengtzelius, W. Gotze, and A. Sjolander. "Dynamics of supercooled liquids and the glass transition". en. In: *Journal of Physics C: Solid State Physics* 17.33 (1984).

[Bro+00] Kurt Broderix et al. "Energy Landscape of a Lennard-Jones Liquid: Statistics of Stationary Points". In: *Physical Review Letters* 85.25 (2000).

[Cav09] Andrea Cavagna. "Supercooled Liquids for Pedestrians". In: *Physics Reports* 476.4-6 (2009).

[CE96] Marcus T. Cicerone and M. D. Ediger. "Enhanced translation of probe molecules in supercooled o-terphenyl: Signature of spatially heterogeneous dynamics?" In: *The Journal of Chemical Physics* 104.18 (1996).

[CG10] David Chandler and Juan P. Garrahan. "Dynamics on the Way to Forming Glass: Bubbles in Space-Time". In: *Annual Review of Physical Chemistry* 61.1 (2010).

[Cha+14a] Patrick Charbonneau et al. "Fractal free energy landscapes in structural glasses". en. In: *Nature Communications* 5 (2014).

[CNB19] Daniele Coslovich, Andrea Ninarello, and Ludovic Berthier. "A localization transition underlies the mode-coupling crossover of glasses". en. In: *SciPost Physics* 7.6 (2019).

[Cug02] Leticia F. Cugliandolo. "Dynamics of glassy systems". In: *arXiv:cond-mat/0210312* (2002).

[Der80] B. Derrida. "Random-Energy Model: Limit of a Family of Disordered Models". In: *Physical Review Letters* 45.2 (1980).

[DP01] Catherine. Dreyfus and Robert M. Pick. "Relaxations and vibrations in supercooled liquids". en. In: *Comptes Rendus de l'Académie des Sciences - Series IV - Physics-Astrophysics* 2.2 (2001).

[DS01] Pablo G. Debenedetti and Frank H. Stillinger. "Supercooled liquids and the glass transition". en. In: *Nature* 410.6825 (2001).

[Dyr06] Jeppe C. Dyre. "Colloquium: The glass transition and elastic models of glass-forming liquids". In: *Reviews of Modern Physics* 78.3 (2006).

[ECG09] Yael S. Elmatad, David Chandler, and Juan P. Garrahan. "Corresponding States of Structural Glass Formers". In: *The Journal of Physical Chemistry B* 113.16 (2009).

[Edi00] M. D. Ediger. "Spatially Heterogeneous Dynamics in Supercooled Liquids". In: *Annual Review of Physical Chemistry* 51.1 (2000).

[EH12] M. D. Ediger and Peter Harrowell. “Perspective: Supercooled liquids and glasses”. In: *The Journal of Chemical Physics* 137.8 (2012).

[FFR19] Giampaolo Folena, Silvio Franz, and Federico Ricci-Tersenghi. “Memories from the ergodic phase: the awkward dynamics of spherical mixed p-spin models”. In: *arXiv:1903.01421 [cond-mat]* (2019).

[Gol69] Martin Goldstein. “Viscous Liquids and the Glass Transition: A Potential Energy Barrier Picture”. In: *The Journal of Chemical Physics* 51.9 (1969).

[Göt09] W. Götze. *Complex Dynamics of Glass-Forming Liquids: A Mode-Coupling Theory*. OUP Oxford, 2009.

[Göt99] Wolfgang Götze. “Recent tests of the mode-coupling theory for glassy dynamics”. en. In: *Journal of Physics: Condensed Matter* 11.10A (1999).

[GS92] W. Gotze and L. Sjogren. “Relaxation processes in supercooled liquids”. en. In: *Reports on Progress in Physics* 55.3 (1992).

[Hec+08] Tina Hecksher et al. “Little evidence for dynamic divergences in ultraviscous molecular liquids”. en. In: *Nature Physics* 4.9 (2008).

[Heu08] Andreas Heuer. “Exploring the potential energy landscape of glass-forming systems: from inherent structures via metabasins to macroscopic transport”. en. In: *Journal of Physics: Condensed Matter* 20.37 (2008).

[Jai+16] Abhishek Jaiswal et al. “Onset of Cooperative Dynamics in an Equilibrium Glass-Forming Metallic Liquid”. In: *The Journal of Physical Chemistry B* 120.6 (2016).

[KA94] Walter Kob and Hans C. Andersen. “Scaling Behavior in the $\ensuremath{\beta}$-Relaxation Regime of a Supercooled Lennard-Jones Mixture”. In: *Physical Review Letters* 73.10 (1994).

[KA95a] Walter Kob and Hans C. Andersen. “Testing mode-coupling theory for a supercooled binary Lennard-Jones mixture I: The van Hove correlation function”. In: *Physical Review E* 51.5 (1995).

[Kau48] Walter. Kauzmann. “The Nature of the Glassy State and the Behavior of Liquids at Low Temperatures.” In: *Chemical Reviews* 43.2 (1948).

[KL95] Jorge Kurchan and Laurent Laloux. “Phase space geometry and slow dynamics”. en. In: (1995).

[Kob+97] Walter Kob et al. "Dynamical Heterogeneities in a Supercooled Lennard-Jones Liquid". In: *Physical Review Letters* 79.15 (1997).

[KT87b] T. R. Kirkpatrick and D. Thirumalai. "p-spin-interaction spin-glass models: Connections with the structural glass problem". In: *Physical Review B* 36.10 (1987).

[KTW89] T. R. Kirkpatrick, D. Thirumalai, and P. G. Wolynes. "Scaling concepts for the dynamics of viscous liquids near an ideal glassy state". In: *Physical Review A* 40.2 (1989).

[Leu84] E. Leutheusser. "Dynamical model of the liquid-glass transition". In: *Physical Review A* 29.5 (1984).

[LW07] Vassiliy Lubchenko and Peter G. Wolynes. "Theory of Structural Glasses and Supercooled Liquids". In: *Annual Review of Physical Chemistry* 58.1 (2007).

[Nan+15] Manoj Kumar Nandi et al. "Unraveling the success and failure of mode coupling theory from consideration of entropy". In: *The Journal of Chemical Physics* 143.17 (2015).

[Pet+13] N. Petzold et al. "Evolution of the dynamic susceptibility in molecular glass formers: Results from light scattering, dielectric spectroscopy, and NMR". In: *The Journal of Chemical Physics* 138.12 (2013).

[PSD18] Ulf R. Pedersen, Thomas B. Schrøder, and Jeppe C. Dyre. "Phase diagram of Kob-Andersen type binary Lennard-Jones mixtures". In: *Physical Review Letters* 120.16 (2018).

[RA98] R. Richert and C. A. Angell. "Dynamics of glass-forming liquids. V. On the link between molecular dynamics and configurational entropy". In: *The Journal of Chemical Physics* 108.21 (1998).

[RC05] David R. Reichman and Patrick Charbonneau. "Mode-coupling theory". en. In: *Journal of Statistical Mechanics: Theory and Experiment* 2005.05 (2005).

[Ric84] Pascal Richet. "Viscosity and configurational entropy of silicate melts". en. In: *Geochimica et Cosmochimica Acta* 48.3 (1984).

[Sas00] Srikanth Sastry. "Onset temperature of slow dynamics in glass forming liquids". en. In: *PhysChemComm* 3.14 (2000).

[Sas01] Srikanth Sastry. "The relationship between fragility, configurational entropy and the potential energy landscape of glass-forming liquids". en. In: *Nature* 409.6817 (2001).

[Sas02] Srikanth Sastry. "Onset of slow dynamics in supercooled liquid silicon". en. In: *Physica A: Statistical Mechanics and its Applications* 315.1 (2002).

[Sch+00] Thomas B. Schrøder et al. "Crossover to potential energy landscape dominated dynamics in a model glass-forming liquid". In: *The Journal of Chemical Physics* 112.22 (2000).

[Sci05] Francesco Sciortino. "Potential energy landscape description of supercooled liquids and glasses". en. In: *Journal of Statistical Mechanics: Theory and Experiment* 2005.05 (2005).

[SDS98] Srikanth Sastry, Pablo G. Debenedetti, and Frank H. Stillinger. "Signatures of distinct dynamical regimes in the energy landscape of a glass-forming liquid". en. In: *Nature* 393.6685 (1998).

[Sin+12] Murari Singh et al. "Structural correlations and cooperative dynamics in supercooled liquids". In: *The Journal of Chemical Physics* 137.2 (2012).

[SW82] Frank H. Stillinger and Thomas A. Weber. "Hidden structure in liquids". In: *Physical Review A* 25.2 (1982).

[SW83] Frank H. Stillinger and Thomas A. Weber. "Dynamics of structural transitions in liquids". In: *Physical Review A* 28.4 (1983).

[SW84] Frank H. Stillinger and Thomas A. Weber. "Packing Structures and Transitions in Liquids and Solids". en. In: *Science* 225.4666 (1984).

[SW85] Frank H. Stillinger and Thomas A. Weber. "Computer simulation of local order in condensed phases of silicon". In: *Physical Review B* 31.8 (1985).

[Wee+00] Eric R. Weeks et al. "Three-Dimensional Direct Imaging of Structural Relaxation Near the Colloidal Glass Transition". en. In: *Science* 287.5453 (2000).

[Wei+16] Nicholas B. Weingartner et al. "A Phase Space Approach to Supercooled Liquids and a Universal Collapse of Their Viscosity". English. In: *Frontiers in Materials* 3 (2016).

[Win99] Eric Winsberg. "Sanctioning Models: The Epistemology of Simulation". en. In: *Science in Context* 12.2 (1999).

2

Prototypical model of Supercooled Liquid

2.1 The p-spin spherical model

2.1.1 A short History

The p-spin model with ising spin was firstly introduced in 1980 *en passant* by B.Derrida as a model for which the limit ($p \to \infty$) gives the famous "Random Energy Model" [Der80]. In 1987 T.R.Kirkpatrick and D.Thirumalai introduced the spherical (soft) version of the p-spin model and put forward the analogy between this model and the structural glasses [KT87b; KT87a]. In particular, they focused on the equilibrium dynamics, extending the work of H.Sompolinsky and A.Zippelius on the 2-spin (soft) dynamics [SZ82]. In 1992-1993 in two coupled works, A.Crisanti, H.-J. Sommers and (in the second) H. Horner firstly solved, by means of a 1RSB scheme, the statics of the model in presence of an external field and analyzed the equilibrium and out-of-equilibrium dynamics of the model [CS92; CHS93]. At the same time L.F.Cugliandolo and J.Kurchan were solving the out of equilibrium dynamics from random conditions and confronted it with results gained about the free energy landscape from TAP analysis [KPV93; CS95].

In 1995 S.Franz and G.Parisi introduced a potential to select equilibrium states and follow them in temperature, strengthening the correspondence between dynamics and statics of p-spin models [FPV92]. This analysis was later extended to mixed models [Bar97]. In the subsequent years in a series of papers A.Cavagna, I. Giardina and G.Parisi explored in more details the energy landscape and TAP free energy in the pure p-spin model [CGP97a; CGP98; CGP01]. Starting in 2003, L.Leuzzi

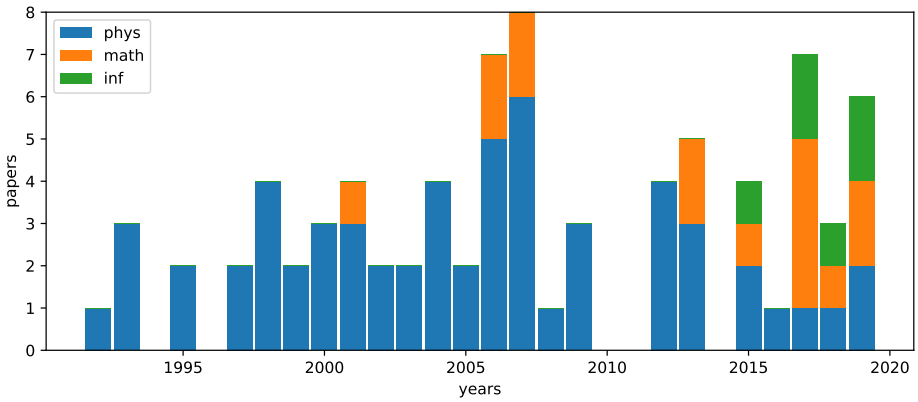

Figure 2.1: Number of publications about the "spherical p-spin"

and A.Cristanti have revealed the zoology of phases achievable with mixed models [CL04; CL06; CL07], and coincidently was understood that the mixed model can reach different asymptotic states depending on the cooling schedule [Cap+06].

Nearly a decade later, Y. Sun and collaborators asserted that the asymptotic dynamics cannot be described with standard replica calculations in mixed models [Sun+12]. In the same years the p-spin model was gaining interest in a small mathematical community led by G.Ben Arous, and the many of the aforementioned results were recasted in a mathematical framework [ADG01; ASZ18]. In recent years, in the attempt of making the model attractive to computer scientists, it has been sometimes referred to as "spiked tensor model" [Ros+19; Man+19]. Finally in 2019 we have understood that in mixed model the out-of-equilibrium dynamics preserves *memory of the ergodic phase* [FFR19].

2.1.2 The Model

The p-spin spherical model is a fully connected model with continuous spins $\sigma_i \in \Re$ constrained over a sphere ($\sum_i \sigma_i^2 = N$) whose Hamiltonian reads*:

$$H[\sigma] = \sum_p \alpha_p J_p \bullet \sigma^{\otimes p} \tag{2.1}$$

where $J_p \equiv J_{i_1 i_2 \dots i_p}$ are rank-p N-dimensional symmetric Gaussian tensors (natural extension of Wigner matrices) [Com+08; LNV18], i.e. their elements are indepen-

*for example: $J_3 \bullet \sigma^{\otimes 3} \equiv \sum_{i_1<i_2<i_3} J_{i_1 i_2 i_3} \sigma_{i_1} \sigma_{i_2} \sigma_{i_3}$

dently extracted from a Gaussian distribution of zero mean and variance:

$$\overline{J^2_{i_1 i_2 \dots i_p}} = \frac{1}{2} N / \binom{N}{p} \tag{2.2}$$

where $\binom{N}{p}$ is the total number number of p-couplings*. The coefficients α_p define the mixture of the model. In the case of only one non zero p-body interaction α_p, the model is called *pure*. In all other cases the model is *mixed*. Throughout this thesis, we will focus in particular on the pure 3-spin model ($\alpha_3 = 1$) and the mixed (3+4)-spin model ($\alpha_3 = 1$ and $\alpha_4 = 1$). The disorder of the couplings Js is quenched, in the sense that all the statistical equilibrium and out-of-equilibrium averages are performed with a given realization of them (model). There are two different levels of statistics: the disorder averaging which will be marked by an overline $\overline{\ }$ and the thermal averaging which will be marked by angle brackets $\langle \ \ \rangle$.

One first observation that will be crucial in all future calculations is that, the quenched disorder of the couplings can be read as a fluctuation of Hamiltonian in different models, when changing the distance of two reference configurations (σ and τ)†:

$$\overline{H[\sigma]H[\tau]} = N \sum_p \frac{\alpha_p^2}{2} q^p \equiv N f(q) \tag{2.3}$$

where $q \equiv \sum_i \sigma_i \tau_i / N$ is the overlap between configuration σ and τ. Moreover, if one evaluates higher order of correlations, these are subdominant in N. Therefore, in the thermodynamic limit ($N \to \infty$) the Hamiltonian of different samples are Gaussian correlated:

$$\overline{\exp(H[\sigma] + H[\tau])} = \exp(\overline{(H[\sigma] + H[\tau])^2}/2) \tag{2.4}$$

more details can be found in appendix section A.1. This way of threating disorder has been introduced in the context of Random Media [KZ87; Hal89; MP90]. The function $f(q)$ fully defines the structure of the Gaussian quenched disorder. In the pure model this function is homogeneous ($f(q) = \alpha_p^2 q^p / 2$) and this will have very strong effects on both static and dynamics properties of the system.

2.1.3 Replica Trick

In models with quenched disorder, one is interested in evaluating the free energy:

$$F_J(\beta) = -\frac{1}{\beta} \log(\sum_{\sigma \in \Sigma} e^{-\beta H_J[\sigma]})$$

*$\binom{N}{p} \equiv \frac{N!}{(N-p)!p!} = \sum_{i_1 < i_2 < \dots < i_p}$

†for the p-spin pure model: $\overline{H[\sigma]H[\tau]} = \overline{J_p \bullet \sigma^{\otimes p} J_p \bullet \tau^{\otimes p}} \approx \frac{1}{2} N / \binom{N}{p} \sigma_{\otimes p} \bullet \tau^{\otimes p} = \frac{N}{2} q^p$

where the subscript $_J$ means that one particular coupling sample* was extracted. Now, to simplify the calculus, the important consideration is that $F_J(\beta)$, since it is an extensive quantity (in N), must be self-averaging with regard to the disorder. Thus, we can substitute its value on a typical sample with its average over different samples:

$$-\beta F(\beta) = \overline{\log(\sum_{\sigma\in\Sigma} e^{-\beta H_J[\sigma]})} = \overline{\log Z}$$

The problem is that we do not know how to calculate the $\overline{\log Z}$ (quenched average). Because we know how to calculate $\log \overline{Z}$ (annealed average), the *replica trick* [EA75], which is a formal substitution that will bring us a lot of physical interpretations, can be considered instead. We just use one of the following equivalences:

$$\overline{\log Z} = \lim_{n\to 0} \frac{\overline{Z^n} - 1}{n} = \lim_{n\to 0} \frac{\log(\overline{Z^n})}{n} = \lim_{n\to 0} \partial_n \overline{Z^n} \tag{2.5}$$

where Z is the partition function. The idea is very common in physics, we bring the calculus to some discretization that we know how to deal with, and then we do an analytic continuation. It is a sort of moment transformation, in the sense that from the moments of the distribution $P(Z)$ we rebuilt the moments of the distribution $P(\log Z)$. The annealed calculation gives us a lower bound to the free energy, by Jensen's inequality: $\overline{\log Z} \geq \log \overline{Z}$. Using the replica trick (2.5) the free energy becomes:

$$F(\beta) = -\frac{1}{\beta} \lim_{n\to 0} \frac{\overline{(\sum_{\sigma\in\Sigma} e^{-\beta H_J[\sigma]})^n} - 1}{n} \tag{2.6}$$

This expression is our point of departure to evaluate the free energy of the p-spin spherical model.

2.1.4 The Replicated Free Energy

Let's specialize (2.6) to our prototypical p-spin spherical model. In the thermodynamic limit ($N\to\infty$) the average n-replicated partition function gets †:

$$\overline{Z^n} = \int_{S_N} \mathscr{D}\sigma\, \overline{e^{\sum_{a=1}^n \beta H[\sigma^a]}} = \int_{S_N} \mathscr{D}\sigma\, e^{\sum_{a,b=1}^n \frac{N}{2}\beta^2 f(\frac{\sigma_a\cdot\sigma_b}{N})} \tag{2.7}$$

where S_N recalls the N-dimensional spherical constraint and the Gaussianity of Hamilitonian fluctuations is used (2.3). The next step is to make a change of integration variables from configurations σ_i to overlaps $q_{ab} = \sigma_a\cdot\sigma_b/N$. This transformation

*using sample for J couplings and configurations for σ spins

†$\mathscr{D}\sigma \equiv \prod_i^N \prod_{\alpha=1}^n d\sigma_i^\alpha$

will induce a volume contraction (determinant of the Jacobian) which needs to be evaluated. The standard approach is to use Lagrange multipliers [CC05], however, to get more intuition we here follow a direct geometrical approach.

The goal is to measure the total volume of configurations $\sigma_1, \sigma_2, ...\sigma_n$ that lie on the S_N sphere and are constrained by fixing their reciprocal overlaps $\{q_{ab}\}_{a=1,b=1}^{n}$. Since all the replicas are equivalent, we take the first one σ_1 as the reference replica. This will give the total volume of the N-dimensional sphere S_N of radius $r_1 = \sqrt{N}$. The second replica is constrained at a fixed overlap q_{12} from the first one. Thus, we can decompose its vector as:

$$\sigma_2 = \sqrt{N q_{12}}\hat{\sigma}_1 + \sqrt{N(1-q_{12})}\hat{\sigma}_{2\perp 1} \tag{2.8}$$

where $\hat{\sigma}_1$ is a unit vector parallel to σ_1 and $\hat{\sigma}_{2\perp 1}$ a generic unit vector orthogonal to σ_1. The volume spanned by $\hat{\sigma}_{2\perp 1}$ is the volume (S_{N-1}) of a sphere of $N-1$ dimensions and radius $r_2 = \sqrt{N(1-q_{12})}$. In the thermodynamic limit $N \to \infty$ the total entropic contribution of the first two replicas gets:

$$\log\left(S_N r_1^{N/2} S_{N-1} r_2^{(N-1)/2}\right) \quad \overset{N\to\infty}{=} \quad 2\frac{N}{2}(1+\log 2\pi) + \frac{N}{2}\log(1-q_{12})) \tag{2.9}$$

The third replica is at fixed overlap q_{12} from the first replica and q_{23} from the second. At this point we notice that we can decompose σ_3 in an orthonormal basis $\hat{\sigma}_1$,$\hat{\sigma}_{2\perp 1}$,$\hat{\sigma}_{3\perp 1\&2}$. This is the second step of the Gram–Schmidt decomposition. We continue this procedure till the vector σ_n. Therefore, the total volume available to n replicas, having fixed all the reciprocal overlaps, q_{ab} is given by the product of the volume spanned by the $\hat{\sigma}_{k\perp 1\to(k-1)}$, each one with its own radius r_k:

$$V_n = \prod_{k=1}^{n-1}(S_{N-k}) r_{k+1}^{(N-k)/2} \quad \overset{N\to\infty}{=} \quad S_N^n \prod_{k=1}^{n-1} r_{k+1}^{N/2} \tag{2.10}$$

But $\prod_{k=1}^{n-1} r_{k+1}$ is by definition the volume of the parallelotope of vertices $\sigma_1, ..., \sigma_n$ that lies on a sphere, which is equal to the determinant of the scalar product matrix $\{\sqrt{N}q_{ab}\}_{a=1,b=1}^{n} = \sqrt{N}Q$:

$$V_n = \quad S_N^n \; vol(\sigma_1, ..., \sigma_n) = (S_N\sqrt{N})^n \sqrt{\det Q} \tag{2.11}$$

This is the volume factor connected to the change of variables from configurations σ_i to overlaps q_{ab}. Let's finally rewrite (2.7) as a function of the overlaps:

$$\overline{Z^n} = \int \mathscr{D}Q \; e^{\frac{N}{2}\left(n\log S_\infty + \log\det Q + \sum_{a,b=1}^{n}\beta^2 f(q_{ab})\right)} \tag{2.12}$$

where $\log S_\infty = \lim_{N\to\infty} \log(S_N N^{N/2})/N = 1 + \log 2\pi$. Now we come back to the replica trick, and here, an inversion of limits must be considered. First, we evaluate the thermodynamic limit $N \to \infty$ which concentrates the measure on saddle points of the overlap action and only after the replica $n \to 0$ limit. This inversion is canonical in replica calculations and has been demonstrated to be "safe" for some particular models [Gue03]. Finally the free energy gets:

$$-\beta F(\beta) = \lim_{n\to 0} \partial_n \lim_{N\to\infty} \frac{1}{N} \overline{Z^n} = \lim_{n\to 0} \partial_n e^{\frac{1}{2}\left(n \log S_\infty + G[Q^*]\right)} \tag{2.13}$$

where

$$G[Q] = \beta^2 \sum_{a,b}^{n} f(q_{ab}) + \log\det[Q] \tag{2.14}$$

Q^* stands for the dominant(s) saddle point of the action. As it is always the case in mean-field calculations, the problem stands in extremizing an action. In this case, the action is defined over the space of overlap matrices Q of dimension shrinking to zero ($n \to 0$).

2.1.5 Replica Symmetric Ansatz

The simplest route is the annealed average, which in the p-spin model is given by:

$$-\beta N F_\beta^{an} = \log \overline{Z} = \log\Big(\int_{S_N} \mathscr{D}\sigma \; e^{\frac{N}{2}\beta^2 f(1)}\Big) = N\Big(\log S_\infty + \frac{1}{2}\beta^2 f(1)\Big) \tag{2.15}$$

where we used (2.7) applied to the case $n = 1$. This is the annealed free energy which is also referred to as the paramagnetic free energy, since it is the correct solution at high temperature. As we have seen, this fixes the lower bound for any quenched average.

Now let's proceed to estimate $\overline{\log Z}$. We need to find the dominant saddle point Q^* of the action $G[Q]$ (given in 2.14).
Since the space of all overlap matrices Q is tremendously huge, we have to restrict it, fixing a structure for the saddle point Q^* and *a posteriori* verifying that the chosen Q^* is stable if the structure is relaxed. The simplest choice is the Replica Symmetric matrix Q^{RS}:

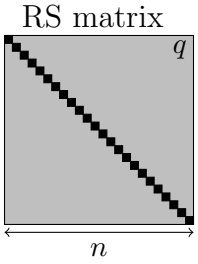

$$q_{ab} = \delta_{ab} + (1 - \delta_{ab})q \tag{2.16}$$

in which each configuration has the same overlap with all the others and the self-overlap $q_{aa} = 1$ for the spherical constraint.

This matrix has two eigenvalues:

$$\begin{aligned} 1+(n-1)q \qquad & \text{with degeneracy} \qquad 1 \\ 1-q \qquad & \text{with degeneracy} \qquad n-1 \end{aligned}$$

Plugging Q^{RS} into (2.14) and taking the $n \to 0$ limit:

$$\begin{aligned} &\lim_{n\to 0} \partial_n G[Q^{RS}] = \\ &= \lim_{n\to 0} \partial_n \Big(n\beta^2 \big(f(1) + (n-1)f(q)\big) + \log\big(1+(n-1)q\big) + (n-1)\log\big(1-q\big)\Big) \\ &= \beta^2\big(f(1)-f(q)\big) + \frac{q}{1-q} + \log(1-q) \end{aligned}$$

And substituting this in (2.13) the RS free energy reads:

$$F_\beta^{RS}(q) = -\frac{1}{2\beta}\Big(\beta^2\big(f(1)-f(q)\big) + \frac{q}{1-q} + \log(1-q) + \log S_\infty\Big) \tag{2.17}$$

Now we need to extremize it over q, which is the only free parameter having chosen the RS ansatz. This gives the equation for the saddle point q^*:

$$\partial_q F_\beta^{RS}(q) = 0 \qquad \Longrightarrow \qquad \beta^2 f'(q^*) = \frac{q^*}{(1-q^*)^2} \tag{2.18}$$

which in order to be stable has to satisfy:

$$\partial_q^2 F_\beta^{RS}(q) > 0 \qquad \Longrightarrow \qquad \beta^2 f''(q^*) < \frac{1+q^*}{(1-q^*)^3} \tag{2.19}$$

This is the so-called *longitudinal* stability. For a generic matrix Q it is the stability with regard to homogeneous scaling $Q \to \alpha Q$. But what if the Q^{*RS} that satisfies 2.18 is not stable to a change of the shape of the matrix i.e. there is a generic small perturbation δQ such that:

$$F_\beta[Q^{*RS} + \delta Q] < F_\beta[Q^{*RS}] \tag{2.20}$$

To verify this possibility, we go back to (2.14) and evaluate first and second order Taylor expansion in the overlap matrix space (see appendix section A.3):

$$\begin{aligned} \partial_{q_{ab}} G[Q] &= \beta^2 f'(q_{ab}) + [q^{-1}]_{ab} \\ \partial_{q_{cd}}\partial_{q_{ab}} G[Q] &= \delta_{ac}\delta_{bd}\beta^2 f''(q_{ab}) - [q^{-1}]_{ac}[q^{-1}]_{bd} \end{aligned} \tag{2.21}$$

where we implicitly considered only ordered indexes: $a < b$ and $c < d$. Inserting the Q^{RS} matrix into the stability condition:

$$\partial_{q_{cd}}\partial_{q_{ab}} G[Q^{RS}] = \delta_{ac}\delta_{bd}\big(\beta^2 f''(q) - \frac{1}{(1-q)^2}\big) + (\delta_{ac}+\delta_{bd})\frac{q}{(1-q)^3} + \frac{q^2}{(1-q)^4}$$

to study the eigenspaces, we project this expression in ad-hoc directions. In particular, homogeneous perturbations $\delta q^L_{ab} = \epsilon$ are eigenmatrices and correspond to the longitudinal eigenvalue:

$$\lambda_{L}(q) = -(\beta^2 f''(q) - \frac{1}{(1-q)^2}) + 2\frac{q}{(1-q)^3} \tag{2.22}$$

thus, to second order $G[Q^{*RS}+\epsilon] = G[Q^{*RS}] - \lambda_L(q^*)\epsilon^2 + O(\epsilon^3)$. For $\lambda_L(q^*) > 0$ the RS solution is stable against longitudinal perturbations and, as it should, it gives back the stability condition (2.19). Another eigenspace of perturbations is represented by δq^R_{ab} s.t. $\sum_b \delta q^R_{ab} = 0$ for each a. We are perturbing the system in such a way, not to change the average overlap of every replica with all the others:

$$\overline{q_a} = \sum_b q_{ab} = \sum_b (q_{ab} + \delta q^R_{ab}) = \overline{q_a + \delta q^R_a}$$

The relative eigenvalue of this pertubation is the so-called *replicon* mode:

$$\lambda_{R} = -(\beta^2 f''(q) - \frac{1}{(1-q)^2}) \tag{2.23}$$

There is a third eigenspace called *anomalous* that is represented by perturbations δq^A_{ab} that satisfy the condition $\sum_{ab} \delta q_{ab} = 0$ but $\sum_b \delta q_{ab} \neq 0$. It is called anomalous, because it is projecting in the direction in which replicas are not equivalent; the average $\overline{q_a} \neq \overline{q_a + \delta q_a}$ but at the same time $\sum_a \overline{\delta q_a} = 0$. The relative eigenvalue turns out to be equal to the replicon one: $\lambda_A = \lambda_R$.

From this fast excursion on the stability of the solutions, we have obtained two independent stability conditions $\lambda_L > 0$ and $\lambda_R = \lambda_A > 0$. The first one is directly obtained by evaluating stability in the restricted space of matrices considered, in our case Q^{RS}. The second condition is related to the stability with regard to the change in shape of the matrix and it directly breaks the symmetry between replicas (RSB) in the sense that the perturbed matrix no longer has a constant overlap $q_{ab} = q^* + \delta q^R_{ab}$. This stability against the change in shape will be further explored in the section subsection 2.1.7. The complete analysis of the stability of the RS solution can be found in [CS92].

We are ready to explore the RS solution (2.18). We first notice that, as long as q is positive $\lambda_{L} > \lambda_{R}$, therefore, we only need to consider λ_{R}. The solution $q^{*} = 0$ is always stable and gives back the annealed (paramagnetic) free energy (2.15), and, any solution with $q \neq 0$ is always unstable. Therefore, the search for another structure of the overlap matrix Q is needed and the Replica Symmetry Breaking must be introduced.

2.1.6 One Step of Replica Symmetric Breaking

Because we were unable to find a stable solution other than the paramagnetic one within an RS ansatz Q^{RS}, we propose a new structure of overlap matrix Q^{1RSB}, a one step of replica symmetry breaking. This was one of the greatest intuitions of Giorgio Parisi [Par79b; Par02]. Instead of considering the typical configuration σ_a to have the same overlap with all other configurations σ_b, we consider that there are two possible overlaps $q_0 < q_1$ with different weights.
Transferred in the language of overlap matrices, this prescribes a block matrix (see figure), where each row and each column is a permutation of the structure:

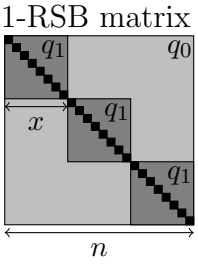

$$(1, \underbrace{q_1, ..., q_1}_{x-1}, \underbrace{q_0, ..., q_0}_{n-x}) \tag{2.24}$$

Any matrix with this shape belongs to Q^{1RSB}. Ordering in blocks and sub-blocks is essential to understand the physical hierarchical organization of configurations.

Configurations that are far from each other have the smallest overlap q_0 (*inter-state*) and in the matrix are far from the diagonal. Configurations that are close to each other have the largest overlap q_1 (*intra-state*) and in the matrix are close to the diagonal. On the diagonal, the self-overlap of each configuration is identically 1 for a spherical model. It is clear from the structure of matrices Q^{1RSB} that each replica σ_a has the same role, since each row (column) has the same entries. The weight x is directly connected to the probability of finding a configuration that has overlap q_0 or q_1 between each other. This is seen after the computation of the $n \to 0$ limit. Let's define the probability of one typical configuration σ_a of having overlap q:

$$P_a(q) = \lim_{n\to 0} \frac{1}{n-1} \sum_{b\neq a} \delta(q - q_{ab}) = \lim_{n\to 0} \frac{x-1}{n-1}\delta(q-q_1) + \frac{n-x}{n-1}\delta(q-q_0) \tag{2.25}$$

Therefore, picking randomly a second configuration σ_b, with probability x their overlap is q_0 and with probability $1-x$ their overlap is q. Having introduced the new

class of matrices Q^{1RSB} that depends on three parameters q_0, q_1, x, we need to plug this matrix shape into (2.14) and extremize it. To do so, the first difficulty is computing the entropic term $\log\det[Q^{1RSB}]$, which requires a diagonalization. We leave this task to the following section in which we will diagonalize a general k-steps RSB matrix Q^{kRSB}. For now, let's write directly the result free energy:

$$\begin{aligned} F_\beta^{1RSB}(q_0,q_1,x) =& \frac{\beta}{2}\Big(x(f(q_1)-f(q_0)) + (f(1)-f(q_1))\Big) \\ &+ \frac{\beta^{-1}}{2}\Big(\frac{q_0}{\lambda(q_0)} + x^{-1}\log\frac{\lambda(q_0)}{\lambda(q_1)} + \log\lambda(q_1)\Big) + const \end{aligned} \tag{2.26}$$

where

$$\lambda(q_0) = 1-(1-x)q_1 - xq_0 \qquad \lambda(q_1) = 1-q_1 \tag{2.27}$$

are the two eigenvalues of the overlap matrix Q^{1RSB}. This must be extremized to find the optimal q_0, q_1, x:

$$\begin{cases} \partial_{q_0} F_\beta^{1RSB} \\ \partial_{q_1} F_\beta^{1RSB} \\ \partial_x F_\beta^{1RSB} \end{cases} \Rightarrow \begin{cases} \beta^2 f'(q_0) = q_0\lambda(q_0)^{-2} \\ \beta^2\Big(f'(q_1)-f'(q_0)\Big) = x(\lambda(q_1)^{-1}-\lambda(q_0)^{-1}) \\ \beta^2\Big(f(q_1)-f(q_0)\Big) = -x^{-2}\log\frac{\lambda(q_0)}{\lambda(q_1)} - (q_1-q_0)\big(x^{-1}\lambda(q_0)^{-1} - q_0\lambda(q_0)^{-2}\big) \end{cases} \tag{2.28}$$

For a general $f(q)$ these three equations are not analytically solvable. One must then rely on a numerical approach. Once all possible solutions are found, their stability should be checked, which, as we will see in the next section, gives the conditions:

$$\begin{cases} \lambda(q_0)^{-2} \geq \beta^2 f''(q_0) \\ \lambda(q_1)^{-2} \geq \beta^2 f''(q_1) \end{cases} \tag{2.29}$$

The second condition is the *marginal condition* that corresponds to the stability of thermodynamics states. Thus corresponds to what we have defined in the previous section as the stability of the overlap matrix in the replicon direction ($\lambda_R > 0$). As we will see in chapter 3, this condition is strongly connected to the out-of-equilibrium dynamics. Taking the first inequality (2.29) together with the first extremization condition (2.28) gives the inequality:

$$f'(q_0) \geq q_0 f''(q_0) \tag{2.30}$$

which is satisfied only by the value $q_0 = 0$. Physically this result is quite intuitive. Two arbitrary configurations taken on the sphere, will typically be orthogonal to

each other. The only way to break this condition is to put an external field (or a reference configuration), which breaks the spherical symmetry.

Thus, eq. (2.28) simplifies to:

$$\begin{cases} \beta^2 f'(q_1) = \frac{q_1}{(1-q_1)(1-(1-x)q_1)} \\ \beta^2 f(q_1) = -x^{-2}\log\frac{\lambda(q_0)}{\lambda(q_1)} - q_1\big(x^{-1}\lambda(q_0)^{-1} - q_0\lambda(q_0)^{-2}\big) \end{cases} \tag{2.31}$$

together with the marginal condition $(1-q_1)^{-2} \geq \beta^2 f''(q_1)$. The first equation fixes x, which can be plugged into the second one, that is solved numerically to find q_1. It is found that for any $T < T_{TAP}$ there is a stable solution, which has a free energy lower than the paramagnetic for $T < T_K < T_{TAP}$. Thus, following this solution branch in the space of overlap matrices, there is a first order transition at T_K and a spinodal transition at T_{TAP}. As we will see using other methods to probe the free energy landscape, this solution corresponds to deepest states, which below T_K dominate the Gibbs measure; here a sort of 'condensation' occurs. We further discuss the general picture in the next sections.

2.1.7 k-RSB Solution

Our point of departure is the p-spin free energy functional (see 2.13):

$$G[Q] = \beta^2 \sum_{a,b}^{n} f(Q_{ab}) + \log(\det[Q]) \tag{2.32}$$

where $Nf(Q_{ab}) = \overline{H[\sigma_a]H[\sigma_b]}$ and $Q = (Q_{ab}) = (\langle \sigma_a \cdot \sigma_a \rangle / N)$ is the overlap matrix and a, b are the replica indices. The free energy of the model reads:

$$-2\beta F_\beta = \log S_\infty - \lim_{n\to 0} \frac{G[Q]}{n}$$

The Ultrametric Structure

In order to minimize the functional (2.32) we restrict the space of overlap matrices to ultrametric matrices $\tilde{Q}$ [Par79a]. These matrices depend on $(2k+1)$ parameters (see figure on the right): x_i with $i = 1..k$ are the length of sub-boxes, q_i with $i = 0..k$ the overlap inside the relative sub-boxes, and k is the number of replica symmetry breaking (RSB) steps. The structure of the matrix does not privilege any of the replicas and, as a consequence, any two columns (or rows) can be mapped on each other by permutation. Our goal is to recover a general formula for (2.32) that can handle a k-RSB replica broken $\tilde{Q}$.

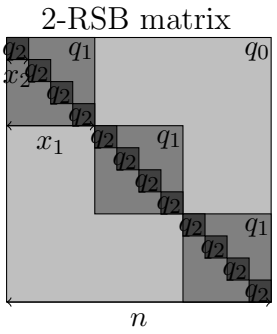

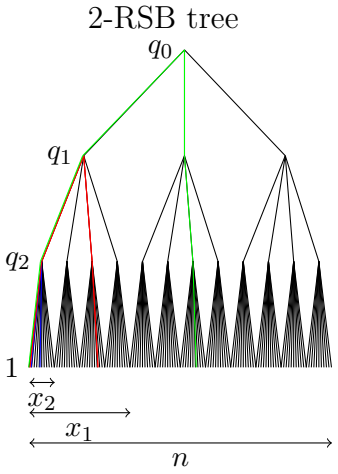

Any ultrametric matrix $\tilde{Q}$ can be mapped into an ultrametric tree [RTV86]. In order to have a physical ultrametric tree, we require that $q_a < q_b$ and $x_a < x_b$ for every $a < b$. The tree can be thought as a probability flux, starting from the major branch of overlap q_0 (the smallest possible overlap) end ending with the smallest branch of overlap $q_k = q_{EA}$ (self-overlap within a state). The probability that two configurations have overlap $q \geq q_r$ is given by the ratio between the number of paths that connect one given configuration to another configuration in the same cluster $x_r - 1$ and the number of paths to another whatever configuration $n - 1$. Thus:

$$P(q \geq q_r) = (x_r - 1)/(n - 1)$$

In the limit $n \to 0$ the probability that two extracted configurations belong to a same cluster is:

$$\begin{aligned} P(q = q_r) &= P(q \geq q_r) - P(q \geq q_{r+1}) \\ &= x_{r+1} - x_r \end{aligned} \tag{2.33}$$

By convention $x_0 \equiv n \to 0$. For convenience, we also define $q_{k+1} = 1$ which is the norm of a single configuration (from the spherical constraint) and $x_{k+1} = 1$.

Recursive Diagonalization

Let's define the average overlap inside a r-cluster:

$$\overline{q_r} \equiv \int_{q_r^-}^{1} dq P(q) q = \lim_{n\to 0} \frac{1}{n-1} \sum_{b=2}^{x_r} Q_{1b} \tag{2.34}$$

where $P(q) \equiv \sum_{r=0}^{k} \delta(q-q_r)(x_{r+1}-x_r)$. We also introduce the cumulant distribution:

$$x(q) \equiv \int_0^{q^-} dq' P(q') \tag{2.35}$$

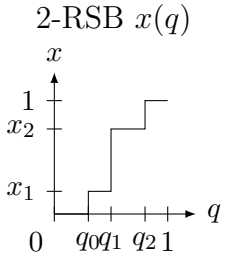

In the following, we will see that $\overline{q_r}$ are directly connected to the eigenvalues of $\tilde{Q}$.

Let's recall that since the matrices considered are symmetric, their eigenspaces are mutually orthogonal. Now we build a recursive procedure to diagonalize $\tilde{Q}$. Since all replicas are equivalent, we concentrate on the first row of $\tilde{Q}$ (overlaps with replica 1). We introduce the 00-eigenspace (related to the overlap q_0) as the homogeneous eigenvector:

$$\vec{v}_{00} = \underbrace{(1,1,...,1)}_{n}$$

$$\lambda_{00} = \tilde{Q}\vec{v}_0 = Q_{11} + \sum_{b=2}^{n} Q_{1b} = 1 - \overline{q_0} + nq_0$$

$$\mu_{00} = 1$$

where λ_0 is the eigenvalue and μ_0 is the dimension of the space. The 0-eigenspace is spanned by eigenvectors homogeneous in sub-blocks of dimension x_1 and orthogonal to the 00-eigenspace:

$$\vec{v}_0 = \underbrace{(1,...,1}_{x_1}, \underbrace{-x_1/(n-x_1),...,-x_1/(n-x_1))}_{n-x_1} \qquad \text{s.t.} \qquad \vec{v}_0 \cdot \vec{v}_{00} = 0$$

$$\lambda_0 = \tilde{Q}\vec{v}_0 = Q_{11} + \sum_{b=2}^{x_1} Q_{1b} - x_1 q_0 = 1 - (\overline{q_1} + x_1 q_0) = 1 - \overline{q_0}$$

$$\mu_0 = \frac{n}{x_1} - 1 = n(x_1^{-1} - n^{-1})$$

The recursive structure then appears. The 1-eigenspace is spanned by homogeneous eigenvectors in n/x_2 blocks of dimension x_2, but orthogonal to the $(00\oplus 0)$-eigenspace.

Considering that the blocks of dimension x_2 are inside x_1-blocks, we can consider this recursion equal to the previous one from the 00-eigenspace to the 0-eigenspace. Remembering that there are n/x_1 of such recursions, we have:

$$\begin{aligned}
&\vec{v}_1 = \underbrace{(1,...,1}_{x_2},\underbrace{-x_2/(x_1-x_2),...,-x_2/(x_1-x_2))}_{x_2-x_1} \qquad \text{s.t.} \qquad \vec{v}_1\cdot\vec{v}_0 = 0\\
&\lambda_1 = \tilde{Q}_0\vec{v}_1 = Q_{11} + \sum_{b=2}^{x_2} Q_{1b} - x_2 q_1 = 1 - (\overline{q_2} + x_2 q_1)\\
&\mu_1 = (\frac{x_1}{x_2} - 1)\frac{n}{x_1} = n(x_2^{-1} - x_1^{-1})
\end{aligned}$$

where $\tilde{Q}_0$ is the matrix restricted inside one x_1-block. Iterating this procedure we obtain:

$$\begin{aligned}
&\vec{v}_r = \underbrace{(1,...,1}_{x_{r+1}},\underbrace{-x_{r+1}/(x_r-x_{r+1}),...,-x_{r+1}/(x_r-x_{r+1})}_{x_{r+1}-x_r} \qquad \text{s.t.} \qquad \vec{v}_r\cdot\vec{v}_{r-1} = 0\\
&\lambda_r = \tilde{Q}_{r-1}\vec{v}_r = Q_{11} + \sum_{b=2}^{x_{r+1}} Q_{1b} - x_{r+1} q_r \underset{\mathrm{n}\to 0}{=} 1 - (\overline{q_{r+1}} + x_{r+1} q_r)\\
&\mu_r = (\frac{x_r}{x_{r+1}} - 1)\frac{n}{x_r} = n(x_{r+1}^{-1} - x_r^{-1})
\end{aligned} \tag{2.36}$$

With k-RSB steps the last eigenvalue is $\lambda_k = 1 - q_k$. The first two eigenvalues λ_{00} and λ_0 have a non-trivial n-dependence and must be treated carefully to get a finite $n \to 0$ limit. To this aim, we define two mixed eigenvalues:

$$\begin{aligned}
&\lambda_{01} = \lambda_0/\lambda_1 = 1 + \frac{n q_0}{1-\overline{q_0}} \quad \text{with} \quad \mu_{01} = 1\\
&\lambda_{02} = \lambda_1 = 1 - \overline{q_0} \quad \text{with} \quad \mu_{02} = n x_1^{-1}
\end{aligned} \tag{2.37}$$

All the other eigenvalues are ordered $\lambda_{r+1} < \lambda_r$ till the smallest λ_{k+1} one which is connected to perturbations inside a state $q = q_k$. Equations (2.36) can be recasted in the continuous form $\lambda_r \to \lambda(q)$:

$$\begin{aligned}
&\lambda(q) = 1 - \Big(q\int_0^{q^-} dq' P(q') + \int_{q^-}^1 dq' P(q') q'\Big) = \int_q^1 dq' x(q')\\
&\mu(q) = \frac{\partial x^{-1}(q)}{\partial q} \qquad\qquad \text{for} \qquad q_0 < q < q_k
\end{aligned} \tag{2.38}$$

the first line results from an integration by parts. Taking $\lambda_r = \frac{1}{q_{r+1}-q_r}\int_{q_r}^{q_{r+1}} \lambda(q)dq$ and $\mu_r = \frac{1}{q_{r+1}-q_r}\int_{q_r}^{q_{r+1}} \mu(q)dq$ gives back (2.36). The function $\lambda(q)$ is directly connected to the probability measure $P(q) > 0$:

$$P(q) = \partial_q x(q) \qquad x(q) = -\partial_q \lambda(q) \tag{2.39}$$

this forces $\lambda(q)$ to be a concave and monotonously decreasing function, which satisfies the Cauchy boundary conditions:

$$\lambda(1) = 1 \qquad \text{and} \qquad \partial_q \lambda(1) = -1 \tag{2.40}$$

In case of a k-RSB ansatz we have:

$$\begin{aligned}
\hat{P}(q) &= \sum_{i=0}^{k} \delta(q - q_i)(x_{i+1} - x_i) \\
\hat{x}(q) &= \sum_{i=0}^{k} \theta(q - q_i) x_{i+1} \\
\hat{\lambda}(q) &= \sum_{i=0}^{k+1} \theta(q_i - q)(q_i - q)(x_i - x_{i+1}) \qquad\qquad x_{k+2} \equiv 0
\end{aligned} \tag{2.41}$$

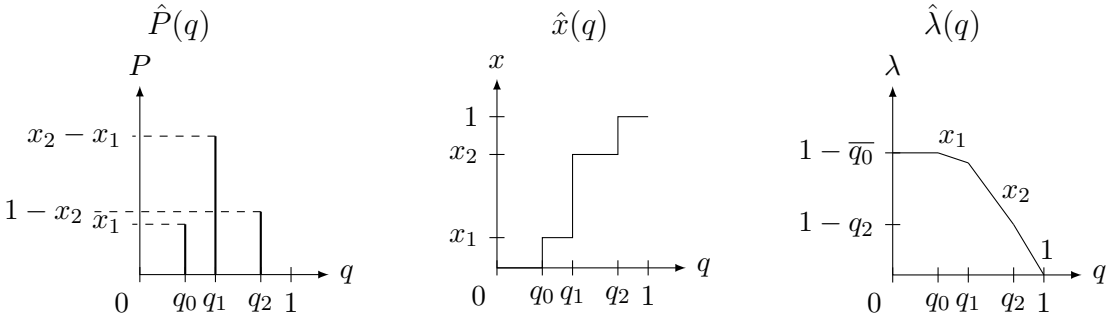

The k-RSB free energy and stability

Let's rewrite the free energy (2.32) using the diagonal form (eqs. (2.36) to (2.38)):

$$\frac{1}{n} G[\tilde{Q}] = \beta^2 \sum_{b=1}^{n} f(Q_{1b}) + \frac{1}{n} \log(\prod_{i=0}^{k+1} \lambda_i^{\mu_i})$$

In the functional formalism the energy term becomes:

$$\begin{aligned}\beta^2 \sum_{b=1}^{n} f(Q_{1b}) &= \beta^2 \Big(f(1) - \int_{q_0^-}^{1} dq P(q) f(q) \Big) \\ &= \beta^2 \int_{q_0}^{1} dq\; x(q) f'(q) \\ &= \beta^2 \int_{0}^{1} dq\; \lambda(q) f''(q)\end{aligned} \tag{2.42}$$

where we used two consecutive integrations by parts together with (2.39), and the entropic contribution:

$$\begin{aligned}\lim_{n\to 0} \frac{1}{n} \log(\prod_{i=0}^{k+1} \lambda_i^{\mu_i}) &= \lim_{n\to 0} \Big(\frac{1}{n} \log(\lambda_{01}^{\mu_{01}}) + \frac{1}{n} \log(\lambda_{02}^{\mu_{02}}) + \frac{1}{n} \log(\prod_{i=2}^{k+1} \lambda_i^{\mu_i}) \Big) \\ &= \frac{q_0}{1-\overline{q_0}} + x_1^{-1} \log(1-\overline{q_0}) + \int_{q_0^+}^{q_k} dq\; \mu(q) \log \lambda(q) \\ &= \int_{0}^{q_k} dq \lambda^{-1}(q) + \log \lambda(q_k)\end{aligned} \tag{2.43}$$

where to get the last line we used an integration by parts *. Finally, the free energy of the system in terms of the eigenvalues $\lambda(q)$ of the overlap matrix $\tilde{Q}$ reads:

$$F_\beta[\lambda(q)] = \frac{1}{2} \int_0^1 dq \left(\beta \lambda(q) f''(q) + \beta^{-1} \lambda(q)^{-1} \right) + \log(0) - (1 + \log 2\pi) \tag{2.44}$$

where we have a little abuse of notation $\log(0)$, which compensates the divergence in $\int_{1-\epsilon}^{1} dq\; \beta^{-1}\lambda^{-1}(q)$. To find the thermodynamic free energy we need to minimize $F_\beta[\lambda(q)]$ with regards to $\lambda(q)$. This minimization is not made easy by the auxiliary condition that $\lambda(q)$ must be a concave and monotonic function (see eq. 2.39). Let's first consider the minimization of $F[\lambda(q)]$ without any restriction to the space of functions $\lambda(q)$:

$$0 = \frac{\delta F_\beta[\lambda(q)]}{\delta \lambda(q)} = \frac{\beta}{2} f''(q) - \frac{\beta^{-1}}{2} \lambda^{-2}(q) \tag{2.45}$$

$\lambda^\circ(q) = \beta^{-1} f''(q)^{-1/2}$ is the solution.

Now let's specialize to the pure 3-spin model (fig.2.2): $\lambda^\circ(q) = \beta\sqrt{3q}$. This solution is convex, but we know that the optimal $\lambda^*(q)$ should be concave. The

* $\mu \log \lambda \to x^{-1} \partial_q \lambda\; \lambda^{-1}$

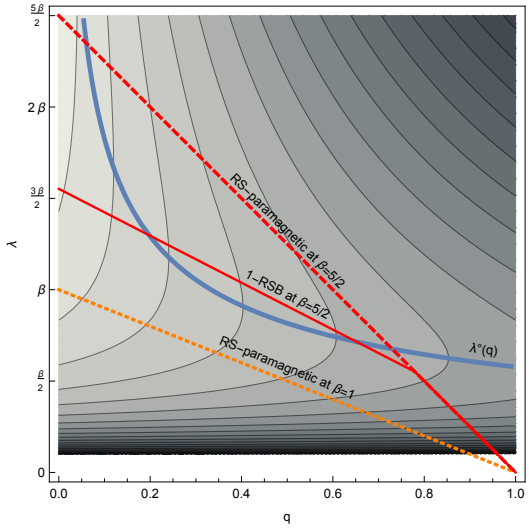

Figure 2.2: Stable solutions of the $F[\lambda(q)]$ minimization over the space of continuous concave functions $\lambda(q)$, with the Cauchy boundary conditions $\lambda(1) = 0$ and $\partial_q\lambda(1) = 1$. At $\beta = 1$ only the paramagnetic solution $\lambda(q) = (1 - q)$ is stable (orange dotted line). While at $\beta = 5/2$ both 1-RSB solution and RS are locally stable, but 1-RSB dominate.

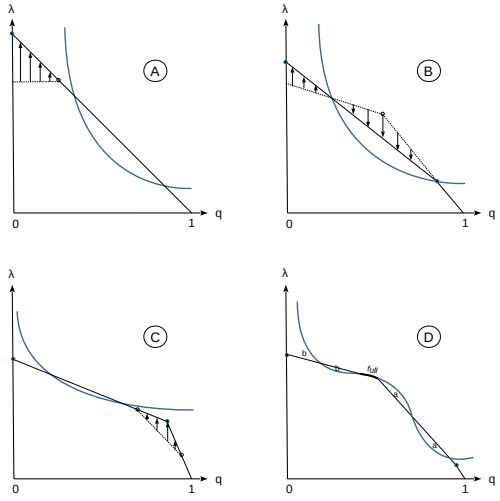

Figure 2.3: Each time a stationary solution of $\delta F/\delta\lambda = 0$ has a node of the k-RSB ansatz which lies above $\lambda^\circ(q)$ this node is unstable to small perturbations, since a further local replica step can lower the free energy. From this follows the condition for the stability of a r-node: $\lambda^*(q_r) < \lambda^\circ(q_r)$, which gives the standard stability condition for 1-RSB [CS92].

simplest possible concave solution is the paramagnetic *RS* solution ($q_0 = 0$) (see section 2.1.5), which in our functional language corresponds to $\lambda^*(q) = (1 - q) \equiv \lambda_{para}(q)$. This can be checked to be stable for any temperature, but is not always the optimal solution. The second simplest choice is the 1-RSB (with $q_0 = 0$) $\lambda(q) = \theta(1 - q)(1 - q)+\theta(q_1 - q)(q_1 - q)(1 - x)$, which bifurcates from the paramagnetic solution at T_{MCT} but remains subdominant until $T < T_K$, where it becomes the dominant one. We now show that further RSB steps do not produce stable solutions. This is a general statement each time that $\lambda^\circ(q)$ is a convex function, at most, one can have a 1-RSB stable solution [CS92]. Here we present a *graphical* proof. The first observation is that if the paramagnetic solution $\lambda_{para}(q) < \lambda^\circ(q)$ for $0 < q < 1$, since it is an upper-bound for any $\lambda^*(q)$ (from the convexity and the right border condition $\partial\lambda^*(1) = -1$), it is evident that any attempt to put nodes (RSB steps) locally increases the total free energy (see fig. 2.3 A). This reasoning can be extended to each kind of solution in the region of small q in which $\lambda^*(q) < \lambda^\circ(q)$. It also always gives the condition $q_0 = 0$, which is connected to the partitioning of the

phase space. The second statement is that if $\lambda_{para}(q)$ intersects $\lambda^{\circ}(q)$, in the region where $\lambda_{para}(q) > \lambda^{\circ}(q)$ there cannot be any node, this would be unstable (see fig. 2.3 B). This gives the generalized stability condition:

$$\lambda^{*}(q_r) < \lambda^{\circ}(q_r) \tag{2.46}$$

which when specializing to the highest overlap q_k reads:

$$(1 - q_k)^{-2} > \beta^2 f''(q_k) \tag{2.47}$$

because $\lambda_k = 1 - q_k$. This condition defines the stability of states and in the literature it also corresponds to the Plefka stability criterion [Ple82]. The last statement is that for q near 1 and larger than the left-most intersection, there can be at most one node (see fig. 2.3 C). This is a sketch of proof which can be formally characterized and it is simply extensible to any number of RSB steps with fullRSB *enclaves* (see fig. 2.3 D). Moreover, it gives a simple algorithm to find solutions that are stable: starting from high temperature and following bifurcations at the intersection of a section of $\lambda^{*}(q)$ with $\lambda^{\circ}(q)$. For example, the bifurcation point $T = T_{MCT}$ emerges exactly when it is locally stable to create a node.

We have shown that in p-spin models, in order to have at most a 1-RSB solution, the necessary condition is given by the the convexity of $\lambda^{\circ}(q)$:

$$\frac{\partial^2 \lambda^{\circ}(q)}{\partial q^2} \geq 0 \qquad \forall q \in (0, 1] \tag{2.48}$$

This is verified by both our reference models, the pure 3-spin and mixed $(3+4)$-spin. Since our main interest is to study a mean-field model that presents a RFOT and 1-RSB structure, as we will see, it is a necessary condition to have a well defined fragmentation of the phase space. For the rest of this thesis, we will restraint ourselves to models that satisfy the above convexity condition.

This formalism to study the k-RSB solution has been introduced in appendix 2 of [CS92], and has been explored in more details in a series of papers [CL04; CL06; CL07]. In this section we have revisited this formalism in what we hope to be a more intuitive presentation.

Section References

[ADG01] G. Ben Arous, A. Dembo, and A. Guionnet. "Aging of spherical spin glasses". en. In: *Probability Theory and Related Fields* 120.1 (2001).

[ASZ18] Gérard Ben Arous, Eliran Subag, and Ofer Zeitouni. "Geometry and temperature chaos in mixed spherical spin glasses at low temperature - the perturbative regime". In: *arXiv:1804.10573 [math]* (2018).

[Bar97] A. Barrat. "The p-spin spherical spin glass model". In: *arXiv:cond-mat/9701031* (1997).

[Cap+06] Barbara Capone et al. "Off-equilibrium confined dynamics in a glassy system with level-crossing states". In: *Physical Review B* 74.14 (2006).

[CC05] Tommaso Castellani and Andrea Cavagna. "Spin-Glass Theory for Pedestrians". In: *Journal of Statistical Mechanics: Theory and Experiment* 2005.05 (2005).

[CGP01] Andrea Cavagna, Irene Giardina, and Giorgio Parisi. "Role of saddles in mean-field dynamics above the glass transition". In: *Journal of Physics A: Mathematical and General* 34.26 (2001).

[CGP97a] Andrea Cavagna, Irene Giardina, and Giorgio Parisi. "An investigation of the hidden structure of states in a mean field spin glass model". In: *Journal of Physics A: Mathematical and General* 30.20 (1997).

[CGP98] Andrea Cavagna, Irene Giardina, and Giorgio Parisi. "On the stationary points of the TAP free energy". In: *Physical Review B* 57.18 (1998).

[CHS93] A. Crisanti, H. Horner, and H.-J. Sommers. "The spherical p-spin interaction spin-glass model". en. In: *Zeitschrift für Physik B Condensed Matter* 92.2 (1993).

[CL04] A. Crisanti and L. Leuzzi. "Spherical $2+p$ Spin-Glass Model: An Exactly Solvable Model for Glass to Spin-Glass Transition". In: *Physical Review Letters* 93.21 (2004).

[CL06] Andrea Crisanti and Luca Leuzzi. "The spherical 2+p spin glass model: an analytically solvable model with a glass-to-glass transition". In: *Physical Review B* 73.1 (2006).

[CL07] Andrea Crisanti and Luca Leuzzi. "Amorphous-amorphous transition and the two-step replica symmetry breaking phase". In: *Physical Review B* 76.18 (2007).

[Com+08] Pierre Comon et al. “Symmetric tensors and symmetric tensor rank”. In: *SIAM Journal on Matrix Analysis and Applications* 30.3 (2008).

[CS92] A. Crisanti and H.-J. Sommers. “The spherical p-spin interaction spin glass model: the statics”. en. In: *Zeitschrift für Physik B Condensed Matter* 87.3 (1992).

[CS95] A. Crisanti and H.-J. Sommers. “Thouless-Anderson-Palmer Approach to the Spherical p-Spin Spin Glass Model”. In: *Journal de Physique I* 5.7 (1995).

[Der80] B. Derrida. “Random-Energy Model: Limit of a Family of Disordered Models”. In: *Physical Review Letters* 45.2 (1980).

[EA75] S. F. Edwards and P. W. Anderson. “Theory of spin glasses”. en. In: *Journal of Physics F: Metal Physics* 5.5 (1975).

[FFR19] Giampaolo Folena, Silvio Franz, and Federico Ricci-Tersenghi. “Memories from the ergodic phase: the awkward dynamics of spherical mixed p-spin models”. In: *arXiv:1903.01421 [cond-mat]* (2019).

[FPV92] S. Franz, G. Parisi, and M. Virasoro. “The replica method on and off equilibrium”. In: *Journal de Physique I* 2.10 (1992).

[Gue03] Francesco Guerra. “Broken Replica Symmetry Bounds in the Mean Field Spin Glass Model”. en. In: *Communications in Mathematical Physics* 233.1 (2003).

[Hal89] Timothy Halpin-Healy. “Diverse Manifolds in Random Media”. In: *Physical Review Letters* 62.4 (1989).

[KPV93] J. Kurchan, G. Parisi, and M. Virasoro. “Barriers and metastable states as saddle points in the replica approach”. In: *Journal de Physique I* 3.8 (1993).

[KT87a] T. R. Kirkpatrick and D. Thirumalai. “Dynamics of the Structural Glass Transition and the p-Spin—Interaction Spin-Glass Model”. In: *Physical Review Letters* 58.20 (1987).

[KT87b] T. R. Kirkpatrick and D. Thirumalai. “p-spin-interaction spin-glass models: Connections with the structural glass problem”. In: *Physical Review B* 36.10 (1987).

[KZ87] Mehran Kardar and Yi-Cheng Zhang. “Scaling of Directed Polymers in Random Media”. In: *Physical Review Letters* 58.20 (1987).

[LNV18] Giacomo Livan, Marcel Novaes, and Pierpaolo Vivo. "Introduction to Random Matrices - Theory and Practice". In: *arXiv:1712.07903 [cond-mat, physics:math-ph]* 26 (2018).

[Man+19] Stefano Sarao Mannelli et al. "Passed & Spurious: Descent Algorithms and Local Minima in Spiked Matrix-Tensor Models". en. In: *International Conference on Machine Learning*. 2019.

[MP90] M. Mezard and G. Parisi. "Interfaces in a random medium and replica symmetry breaking". en. In: *Journal of Physics A: Mathematical and General* 23.23 (1990).

[Par02] Giorgio Parisi. "The physical Meaning of Replica Symmetry Breaking". In: *arXiv:cond-mat/0205387* (2002).

[Par79a] G. Parisi. "Infinite Number of Order Parameters for Spin-Glasses". In: *Physical Review Letters* 43.23 (1979).

[Par79b] G. Parisi. "Toward a mean field theory for spin glasses". en. In: *Physics Letters A* 73.3 (1979).

[Ple82] T. Plefka. "Convergence condition of the TAP equation for the infinite-ranged Ising spin glass model". en. In: *Journal of Physics A: Mathematical and General* 15.6 (1982).

[Ros+19] Valentina Ros et al. "Complex Energy Landscapes in Spiked-Tensor and Simple Glassy Models: Ruggedness, Arrangements of Local Minima, and Phase Transitions". In: *Physical Review X* 9.1 (2019).

[RTV86] R. Rammal, G. Toulouse, and M. A. Virasoro. "Ultrametricity for physicists". In: *Reviews of Modern Physics* 58.3 (1986).

[Sun+12] YiFan Sun et al. "Following states in temperature in the spherical s+p-spin glass model". In: *Journal of Statistical Mechanics: Theory and Experiment* 2012.07 (2012).

[SZ82] H. Sompolinsky and Annette Zippelius. "Relaxational dynamics of the Edwards-Anderson model and the mean-field theory of spin-glasses". In: *Physical Review B* 25.11 (1982).

2.2 Following States

In pure p-spin models there exists a bijective map that connects each minimum of the energy landscape E_{IS} with a minimum of the free energy landscape F_{min} at temperature T:

$$E_{IS} \xrightarrow{T} F_{min}(T) \tag{2.49}$$

Each energy minimum, followed in temperature, gets dressed by thermal fluctuations: $\langle E \rangle = E_{IS} + \Delta E(T)$, until it becomes unstable at a certain temperature $T_{sp}(E_{IS})$. This map is obtained by a simple manipulation of the TAP (Thouless Anderson Palmer) free energy [TAP77]. There is another complementary way of following free energy minima, starting from the ones at equilibrium in the dynamical phase ($T_k < T < T_{MCT}$):

$$F_{min}(T_{eq}) \xrightarrow{T} F_{min}(T) \tag{2.50}$$

A typical free energy minimum at the equilibrium temperature T_{eq} can also be followed to a different temperature T, by the Franz-Parisi (FP) potential [FP95]. The same kind of reasoning can be extended to mixed models, but the troubles arises. Energy minima there cannot be followed in temperature, and equilibrium configuration can only be partially followed with the FP potential. In what follows, I will show the exact matching of the two methods for pure models and highlight differences and limits of this approach in mixed models.

2.2.1 Following Energy Minima

Let's start directly from the TAP free energy that will be recovered in the dedicated appendix A.4:

$$-\beta F_\beta[m] = \frac{N}{2}\log(1-q) - \beta H[m] + \beta^2 \frac{N}{2}\big(f(1) - f(q) - (1-q)f'(q)\big) \tag{2.51}$$

where $q = \sum_i m_i^2/N$. This is the free energy of a spherical p-spin model with average magnetization per site m_i, before averaging over the quenched disorder J. We are considering a general mixed structure $H[m] = \sum_p \alpha_p J_p \bullet m^{\otimes p}$. We now rescale the magnetization as $m_i \to \sigma_i q^{1/2}$, with $\sum_i \sigma_i^2 = N$, which clarifies the connection to the zero temperature energy landscape:

$$F_\beta[m] = \sum_p \alpha_p H_p[\sigma] q^{p/2} + N R_\beta(q) \tag{2.52}$$

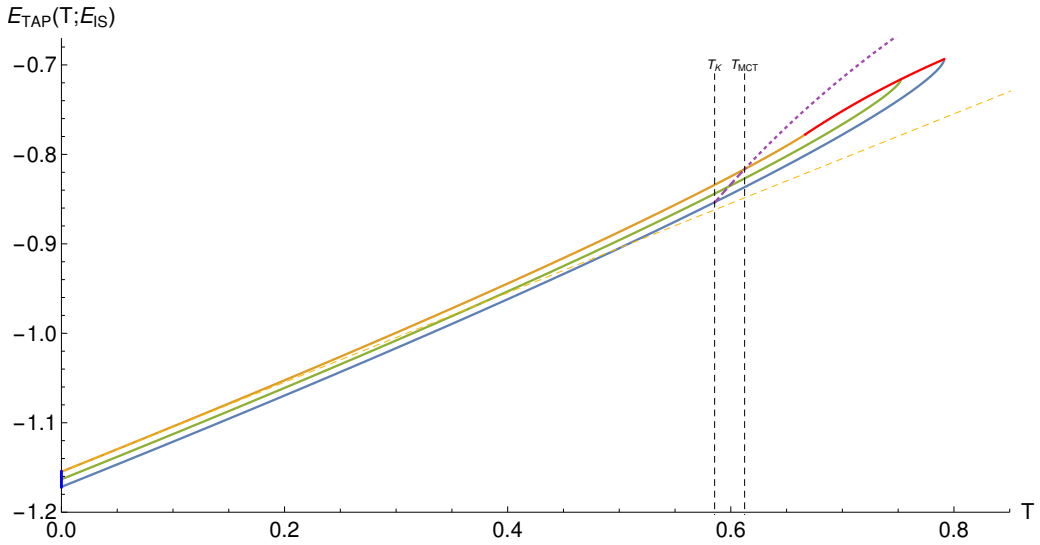

Figure 2.4: Following of TAP states in the 3-spin model. Three different energies of inherent structures ($T = 0$) are considered: $E_{IS} = E_{th}, (E_{th} + E_0)/2, E_0$. The energies of the corresponding basins are followed in temperature, until they lose their stability at $T_{sp}(E_{IS})$ (red line). The dashed violet line highlights the states which are typical at equilibrium between T_K and T_{MCT} and it coincides with the energy of the paramagnetic state.

where $H_p[\sigma] = J_p \bullet \sigma^{\otimes p}$ is the p-body interaction term in the Hamiltonian and $R_\beta(q) = -\frac{\beta^{-1}}{2}\log(1-q) - \frac{\beta}{2}\big(f(1) - f(q) - (1-q)f'(q)\big)$. Stationary points of $F_\beta[m]$ are defined by the conditions:

$$\partial_{m_i} F_\beta[m] = 0 \quad \Rightarrow \quad \begin{cases} \partial_{\sigma_i}\big(\sum_p \alpha_p q^{p/2} H_p[\sigma] + \mu\sigma^2/2\big) = 0 \\ \sum_i m_i \partial_{m_i}\big(\sum_p \alpha_p H_p[\sigma] q^{p/2} + N R_\beta(q)\big) = 0 \end{cases} \tag{2.53}$$

where μ is a Lagrange multiplier that enforces the spherical constraint $\sum_i \sigma_i^2 = N$. The second equation gives the extremization in the radial direction m_i. To have the stability in the radial direction, we need to consider a further equation:

$$\sum_{ij} m_i m_j \partial_{m_i}\partial_{m_j}\big(\sum_p \alpha_p H_p[\sigma] q^{p/2} + N R_\beta(q)\big) > 0 \tag{2.54}$$

Now we select one inherent structure σ_{IS} i.e. a configuration that corresponds to a minimum of the energy landscape:

$$\sigma_{IS} \qquad \text{s.t.} \qquad H'[\sigma_{IS}] + \mu\sigma_{IS} = \sum_p \alpha_p H_p'[\sigma_{IS}] + \mu\sigma_{IS} = 0 \tag{2.55}$$

where H' stands for $\partial_{\sigma_i} H$. The corresponding energy is $H[\sigma_{IS}] = NE_{IS}$. We wish to follow this energy minimum in temperature. In pure models ($H[\sigma] = H_p[\sigma]$) something special occurs. The homogeneity of the Hamiltonian is then such that a σ_{IS} satisfying (2.55) also satisfies the first equation of (2.53). Geometrically this means that in pure models each stationary point of $H[\sigma]$ on the sphere of radius $\sqrt{N}$ is followed radially by $F_\beta[m]$. However, this is not possible in mixed models. One could imagine to repeat the same construction at a different temperature, finding a minimum of $F_\beta[m]$ and then changing the temperature a little bit. This minimum could not be radially followed. This is sometimes related to a physical impossibility. The so-called *chaos in temperature* [RC03], i.e. the overlap between any pair of equilibrium states at different temperatures is zero. And it has been shown to hold in mixed p-spin models at low temperatures [CP17; ASZ18].

Now we concentrate on p-spin pure models and study the properties of the radially followed minima. We have a σ_{IS} of energy E_{IS}. For convenience, we define $H_{TAP}(q, E_{IS}) = E_{IS}q^{p/2}$. The spherical part of (2.53) is automatically satisfied, while for the radial part we have:

$$\partial_q\big(NH_{TAP}(q, E_{IS}) + NR_\beta(q)\big) = H'_{TAP} + R'_\beta(q) = 0 \tag{2.56}$$

This is a second order equation in inverse temperature β with a stable branch:

$$\beta_{TAP}(q, E_{IS}) = (1-q)^{-1}\big(\sqrt{H'^2_{TAP} - f''_p(q)} - H'_{TAP}\big)^{-1} \tag{2.57}$$

where $f_p(q) = 1/2q^p$ since we are specializing to pure models. The condition of stability (2.54) then reads in terms of q^*:

$$\partial_q^2\big(H_{TAP}(q, E_{IS}) + R_\beta(q)\big) > 0 \quad \Rightarrow \quad (E_{IS}^2 - 2\frac{p-1}{p})(q - \frac{p-2}{p}) < 0 \tag{2.58}$$

from which we define:

$$q_{sp} = \frac{p-2}{p} \qquad E_{th} = -\sqrt{2\frac{p-1}{p}} \tag{2.59}$$

q_{sp} is the minimal overlap when following minima of energy E_{IS} in temperature, below which they become unstable. E_{th}, as we will argue later in section 2.3.1, is the energy of highest stable stationary points (minima) of the energy landscape. The relative spinodal temperature is:

$$T_{sp}(E_{IS}) \equiv \beta^{-1}_{TAP}(q_{sp}, E_{IS}) = \sqrt{\frac{(p-2)^{p-2}}{p^p}}\left(\sqrt{E_{IS}^2 p^2 - 2p(p-1)} - E_{IS}p\right) \tag{2.60}$$

[*] $\sum_{ij} m_i m_j \partial_{m_i}\partial_{m_j} g(q) = 4\partial_q^2 g(q) q^2 + 2\partial_q g(q) q$, but $\partial_q g(q) = 0$

Given (2.57), we can follow in overlap q the free energy (2.52) of the state * with inherent structure energy E_{IS}:

$$F_{TAP}(q; E_{IS}) = E_{IS}q^{p/2} - \frac{\beta_{TAP}^{-1}}{2}\log(1-q) - \frac{\beta_{TAP}}{2}\big(f(1) - f_p(q) - (1-q)f_p'(q)\big) \quad (2.61)$$

where $\beta_{TAP} \equiv \beta_{TAP}(q_{sp}, E_{IS})$. And the relative energy of the state is†:

$$E_{TAP}(q; E_{IS}) = E_{IS}q^{p/2} - \beta_{TAP}(f(1) - f_p(q) - (1-q)f_p'(q)) \quad (2.62)$$

In figure 2.4 a parametric plot of the energy versus temperature of the followed state (changing overlap q) is shown. At $T = 0$ the state is very narrow (one configuration) and $q = 1$. Upon increasing temperature, each state opens up and q grows until the spinodal q_{sp} is reached. The deeper is the state, the later it melts in temperature, therefore, the last typical states that melt are those with the lowest inherent structure energy . As we will see in the next section, E_0 is the energy above which the number of minima of the energy landscape starts to be exponential in the size of the system i.e. $\log(\#E_0)/N = 0$. And the corresponding melting temperature $T_{TAP}(E_0)$ is the highest one at which followed states disappear.

2.2.2 Following Equilibrium States

Another way of following states in temperature is to start from the ones that are typical at equilibrium i.e. for temperatures $T_K < T < T_{MCT}$ (see fig. 2.4). To do so, we introduce the Franz-Parisi potential [FP95]. The idea is to extract a reference configuration σ_0 at equilibrium at inverse temperature β' and then evaluate the free energy (FP-potential) of a second replica σ_1 which is extracted at inverse temperature β constrained to be at a fixed overlap q_{01} from σ_0. Let's suppose that we have extracted σ_0 at β', the potential of the second reads:

$$-\beta V_J(q_{01}, \beta'; \sigma_0) = \log\Big(\int_{S_N} \mathscr{D}\sigma_1 \delta\big(\tfrac{\sigma_0\cdot\sigma_1}{N} - q_{01}\big) e^{-\beta H_J[\sigma_1]}\Big) \quad (2.63)$$

where J is a given sample of disorder. Now we suppose that the first replica is extracted at equilibrium above that Kauzmann transition temperature T_K, where the annealed calculation is valid i.e. the average over the disorder commutes with

*state, basin and free energy minimum are here used interchangeably

†$E \equiv \partial_\beta(\beta F)$

the logarithm:

$$\begin{aligned}\int dJP(J)\log\Big(\int d\sigma\frac{e^{-\beta' H_J[\sigma]}}{Z_{\beta'}}\Big) &= \log\Big(\int dJP(J)\int d\sigma\frac{e^{-\beta' H_J[\sigma]}}{Z_{\beta'}}\Big)\\ &= \log\Big(\int d\sigma\int dJP_\beta(J|\sigma)\Big)\end{aligned} \tag{2.64}$$

here $\int dJP(J) \equiv \overline{\ }$ is another way of writing the average over the disorder. $P_\beta(J|\sigma) = P(J)e^{-\beta' H_J[\sigma]}/Z_{\beta'}$ is the conditioned probability of having a quenched disorder J given the configuration σ. This way of reversing the order of conditioning is referred to as *planting* [KZ09; ZK16] and can be very useful in simulations [Cha+14b] (see section 3.3.2). In order to have a configuration that is at equilibrium, one first extracts the configuration and later the couplings (disorder) that allow the configuration to be at equilibrium. Coming back to the FP potential, we can consider the σ_0 to be a tilting field of the coupling measure $P(J)$. The disorder remains Gaussian but acquires a finite mean in the space of the Hamiltonians (compare with 2.3):

$$\begin{aligned}\overline{H[\sigma_a]}^{\sigma_0} &= N\beta' f(q_{0a})\\ \overline{H[\sigma_a]H[\sigma_b]}_C^{\sigma_0} = \overline{H[\sigma_a]H[\sigma_b]}^{\sigma_0} - \overline{H[\sigma_a]}^{\sigma_0}\overline{H[\sigma_b]}^{\sigma_0} &= Nf(q_{ab})\end{aligned} \tag{2.65}$$

the superscript σ_0 at the side of the bar indicates the planted(tilting) configuration. Thus, averaging the potential on the tilted quenched disorder and using the replica trick:

$$\begin{aligned}-\beta V_\beta(q_{01},\beta') = -\beta\overline{V_J(q_{01},\beta';\sigma_0)}^{\sigma_0} &= \lim_{n\to 0}\partial_n\overline{Z_\beta^n(q_{01})}^{\sigma_0}\\ \text{with}&\\ Z_\beta^n(q_{01}) &= \int_{S_N}\mathscr{D}^n\sigma_a\exp(-\beta\sum_{a=1}^n H[\sigma_a])\delta\big(\tfrac{\sigma_0\cdot\sigma_1}{N}-q_{01}\big)\end{aligned} \tag{2.66}$$

where $\int_{S_N}\mathscr{D}^n\sigma_a$ is the integral over all n replicas over the sphere. By construction the measure on the σ_0-tilted disorder is normalized to one i.e. $\overline{1}^{\sigma_0} = 1$. Using 2.65 we can develop the Gaussian disorder in terms of the first two cumulants:

$$-\beta V_\beta(q_{01},\beta') = \lim_{n\to 0}\partial_n\int_{S_N}\mathscr{D}^n\sigma_a\exp\Big(\sum_a^n\beta\beta' f(\tfrac{\sigma_0\cdot\sigma_a}{N}) + \frac{1}{2}\beta^2\sum_{ab}^n f(\tfrac{\sigma_a\cdot\sigma_b}{N})\Big) \tag{2.67}$$

we have omitted the $\delta\big(\frac{\sigma_0\cdot\sigma_1}{N}-q_{01}\big)$ which constrains $\sigma_0\cdot\sigma_a = Nq_{01}$, that is our constraining parameter. Here, as usual, we pass from the space of configurations σ

to the space of overlaps q which brings the volume factor $(\det \tilde{Q})^{1/2}$ (see 2.11):

$$-\beta V_\beta(q_{01},\beta') = \lim_{n\to 0}\partial_n\Big(\sum_a^n \beta\beta' f(q_{01}) + \frac{1}{2}\beta^2\sum_{ab}^n f(q_{ab}) + \frac{1}{2}\log\det\tilde{Q} + n\log S_\infty\Big) \tag{2.68}$$

To be compared with the unconstrained replicated free energy (2.13). Here $\tilde{Q}$ is the $(n+1)$-overlap matrix that also contains the overlaps with the reference configuration σ_0 (first row and column). The determinant can be rewritten in the n-subspace as:

$$\det\tilde{Q} = \det\begin{pmatrix} 1 & q_{01}^{\mathrm{T}} \\ q_{01} & q_{ab}\end{pmatrix} = \det(Q - q_{01}^2) \tag{2.69}$$

In the limit $q_{01} = 0$ the unconstrained free energy is recovered (see 2.13). We are ready to explore the following state procedure. As usual, we must set an ansatz for the overlap matrix. We take the simplest one, the Replica Symmetric matrix $q_{ab} = \delta_{ab} + (1-\delta_{ab})q$, which in the $n \to 0$ limit gives the potential:

$$\begin{aligned} -\beta V_\beta^{RS}(q_{01},\beta';q) = \beta\beta' f(q_{01}) + \frac{1}{2}\beta^2\big(f(1)-f(q)\big) \\ + \frac{1}{2}\Big(\log(1-q) + \frac{q-q_{01}^2}{1-q}\Big) + \log S_\infty \end{aligned} \tag{2.70}$$

This RS solution is replica stable as long as:

$$q > q_{RS} \qquad \text{with } q_{RS} \text{ s.t.} \qquad \beta^2 f''(q_{RS})(1-q_{RS})^2 = 1 \tag{2.71}$$

this stability condition is defined in section 2.1.5. We recall that $V_\beta^{RS}(q_{01},\beta';q)$ is the free energy of a state of overlap q at inverse temperature β which is composed of configurations that are extracted at a fixed distance (overlap q_{01}) from a typical reference configuration at β'.

To gain insight into the power of this potential, we start by looking at the simple case in which the constrained configuration is taken at the same temperature as the reference one i.e. $\beta' = \beta$. Since the reference and the constrained configuration (master and slave) are extracted at the same temperature, we expect them to have a typical overlap between each other q_{01} which is equal to the overlap of a typical equilibrium state at that temperature q (which we will check a posteriori to be true). Putting $q_{01} = q$ and $\beta' = \beta$ into (2.70) one gets the free energy:

$$-\beta V_\beta^{eq}(q) = \frac{1}{2}\beta^2\big(f(1)+f(q)\big) + \frac{1}{2}\Big(\log(1-q)+q\Big) + \log S_\infty \tag{2.72}$$

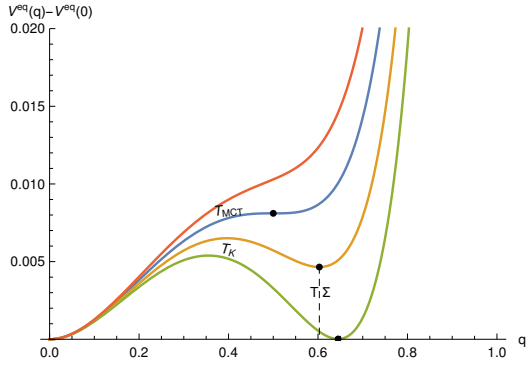

Figure 2.5: Franz-Parisi potential at equilibrium for different temperatures. Between T_k and T_{MCT} there is a metastable minimum, of which the height gives $T\Sigma$

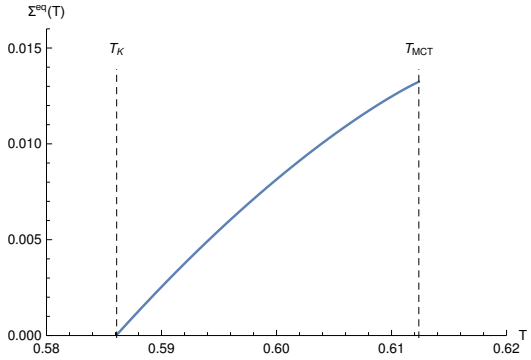

Figure 2.6: Complexity of typical equilibrium states as a function of temperature. The plot is for the 3-spin model, but mixed models have the same behavior.

In fig.2.5 the potential is shown for different temperatures for the 3-spin model, but its qualitative behavior is very robust upon changing model. Coming from high temperature a metastable minimum first appears at T_{MCT} (Mode Coupling Transition), until at T_K (Kauzmann Transition) the minimum becomes lower than the unconstrained one. At this point the RS ansatz is not valid anymore. In order to find the typical overlap q_{eq} at each temperature, we extremize this potential over q, obtaining the equation:

$$\partial_q V_\beta^{eq}(q) = 0 \qquad \Longrightarrow \qquad \beta_{eq}^2 = \frac{q_{eq}}{f'(q_{eq})(1-q_{eq})} \tag{2.73}$$

This equation relates the overlap of a typical equilibrium state to temperature *. This solution is valid as long as the minimum is locally stable, that is:

$$\partial_q^2 V_\beta^{eq}(q) > 0 \qquad \Longrightarrow \qquad \beta^2 < \beta_{mg}^2 \equiv \frac{1}{f''(q_{mg})(1-q_{mg})^2} \tag{2.74}$$

here the subscript $_{mg}$ stands for marginal, because states that respect this equality are the ones that are "marginally stable". This condition is the same that defines the stability of the RS solution i.e. $q_{mg} = q_{RS}$ (see 2.71). In view of this identity, in the following, we will sometimes interchange nomenclature. T_{MCT} is by definition the temperature at which the first stable states appear at equilibrium, therefore, such that:

$$\beta_{eq} = \beta_{mg} = \beta_{MCT} \qquad \Longrightarrow \qquad 1 - q_{MCT} = \frac{f'(q_{MCT})}{q_{MCT} f''(q_{MCT})} \tag{2.75}$$

*the same equations is retrieved by the Monasson method imposing $x = 1$ (see eq. 2.109)

and then $T_{MCT} = (1 - q_{MCT})\sqrt{f''(q_{MCT})}$. Already at this point we can see that pure models are easier, since the ratio on the right side of (2.75) simplifies to $1/(p-1)$, where p is the degree of the interaction and we can algebraically find $q_{MCT} = \frac{p-1}{p-2}$. Let's go back to the equilibrium potential. Subtracting the free energy of a single state to the free energy of the system, one obtains the logarithm of the number (complexity Σ) of states that compose the system, as a function of the equilibrium overlap q_{eq}:

$$\begin{aligned}\Sigma^{eq}(q_{eq}) &= -\beta_{eq}\big(V_\beta^{eq}(q_{eq}) - F_\beta^{an}\big) \\ &= \frac{1}{2}\beta_{eq}^2 f(q_{eq}) + \frac{1}{2}\Big(\log(1-q_{eq}) + q_{eq}\Big)\end{aligned} \tag{2.76}$$

where $F_\beta^{an} = \log S_\infty + \beta^2 f(1) = V_\beta^{eq}(0)$ is the free energy of the paramagnetic solution defined in (2.15) and it is valid since we are considering the reference configuration above T_K. This complexity is plotted in fig.2.6 for the 3-spin model. The point at which the complexity gets to zero defines T_K:

$$\Sigma^{eq}(q_{eq}) = 0 \quad \Longrightarrow \quad \frac{q_K}{f'(q_K)(1-q_K)} f(q_K) + \log(1-q_K) + q_K = 0 \tag{2.77}$$

and $T_K = \sqrt{f'(q_K)(1-q_K)/q_K}$. This concludes the equilibrium analysis.

We have defined a way of selecting equilibrium states. Now we want to follow them in temperature i.e. keeping fixed β', but changing β. The FP potential with two temperatures can be thought as describing an adiabatic annealing protocol in which the system is prepared at equilibrium and then the temperature of the bath is slowly changed till β'. The process is adiabatic since the system has the time to equilibrate in the new basin, but not enough time to cross barriers of order N. This is a "following equilibrium states protocol", which we wish to compare with the "following energy minima protocol" defined in the previous section.

In order to find the dominant states of overlap q at given q_{01}, β', β, the potential (2.70) must be extremized over q. And we must remember that in order to have the reference configuration inside an equilibrium state $\beta_{MCT} < \beta' < \beta_K$. This extremization gives the equation:

$$\partial_q V_\beta^{RS}(q_{01}, \beta'; q) = 0 \qquad \Longrightarrow \qquad \beta^2 f'(q^*) = \frac{q^* - q_{01}^2}{(1-q^*)^2} \tag{2.78}$$

Moreover, in order to have a stable state we require:

$$\partial_q^2 V_\beta^{RS}(q_{01}, \beta'; q^*) > 0 \qquad \Longrightarrow \qquad \beta^2 f''(q^*) < \frac{1}{(1-q^*)^2} + \frac{2(q^* - q_{01}^2)}{(1-q^*)^3}$$

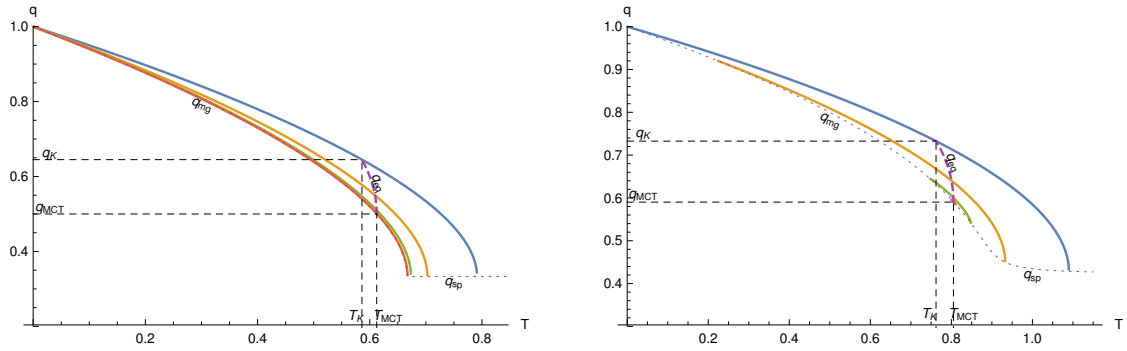

Figure 2.7: Overlap vs temperature of followed states in the 3-spin pure model (left) and 3+4-spin model (right). States at equilibrium have overlap $q_{MCT} < q_{eq} < q_K$ (dashed violet). Four following state protocols are presented starting from $q_{eq} = q_{MCT} + 0.001, q_{MCT} + 0.01, q_{MCT} + 0.05, q_K$. When heating them up, each state melts at a different temperature along q_{sp} which in pure models is $q_{sp} = (p-2)/p$. While in pure models all states can be cooled till $T = 0$, in mixed models the solution is lost at $q_{mg} < 1$.

since $q^* - q_{01}^2 = \beta^2(1-q^*)^2 f'(q^*) \geq 0$ this condition is less restrictive than the condition of stability of the RS solution $q^* > q_{RS}$ and we forget it. Plugging $q^*(q_{01}, \beta)$ back into (2.70) one gets the typical free energy of a constrained state $V_\beta^{RS}(q_{01}, \beta')$. Fixing β', this free energy has typically a double-well shape in q_{01}. One minimum is always in $q_{01} = 0$ and corresponds to the unconstrained system, thus, $V_\beta^{RS}(q_{01} = 0, \beta') = F_\beta^{RS}$. The second minimum at $q_{01} = \breve{q}_{01}$ is the interesting one, it says that there is some organization of configurations in states of overlap $\breve{q}_{01}$ around the reference configuration which is thermodynamically favorable. The minimum $\breve{q}_{01}$ is found by a further extremization of $V_\beta^{RS}(q_{01}, \beta')$ with regard to q_{01} *:

$$\partial_{q_{01}} V_\beta^{RS}(q_{01}, \beta') = 0 \qquad \Longrightarrow \qquad \beta\beta' f'(\breve{q}_{01}) = \frac{\breve{q}_{01}}{(1-q^*)} \tag{2.79}$$

And again we plug in $\breve{q}_{01}(\beta, \beta')$ into (2.70) to obtain the free energy $V_\beta^{RS}(\beta')$ of a state that is typical at temperature β but near a configuration that is typical at β'. To have a stable followed state, moreover, we require that the second derivative of the potential with regard to q_{01} is stable:

$$\partial_{q_{01}}^2 V_\beta^{RS}(\breve{q}_{01}, \beta') > 0 \implies q < q_{sp} \text{ s.t. } \breve{q}_{01}^2 > \frac{W(q_{sp})}{2}(1-q_{sp})\left(\frac{\breve{q}_{01} f''(\breve{q}_{01})}{f'(\breve{q}_{01})} - 1\right) \tag{2.80}$$
$$\text{with} \qquad W(q_{sp}) = 1 + 2\beta^2 f'(q_{sp})(1-q_{sp}) - \beta^2 f''(q_{sp})(1-q_{sp})^2$$

* $\frac{d}{dq_{01}} V_\beta^{RS}(q_{01}, \beta'; q^*(q_{01}, \beta)) = \partial_{q_{01}} V_\beta^{RS}(q_{01}, \beta'; q^*) + \partial_q V_\beta^{RS}(q_{01}, \beta'; q^*) \frac{dq^*}{dq_{01}}$ and the second term vanishes since $\partial_q V_\beta^{RS}(q_{01}, \beta'; q^*) = 0$

here $\breve{q}_{01} = \sqrt{q_{sp} - \beta^2(1-q_{sp})^2 f'(q)}$ is the solution of equation (2.78). The subscript $_{sp}$ stands for spinodal. Whenever this condition is not satisfied, the metastable secondary minimum disappears and the only stable one remains the paramagnetic $q_{01} = 0$. We say that the state melts. This is the last condition needed to follow states, at least if we want them to be RS. Resuming, we have two equations (2.78,2.79) in four variables and two stability conditions, one from the stability of the replica solution and a second from the stability of the metastable minimum.

Starting from an equilibrium state with overlap q_{eq} at β_{eq}, we now have an implicit map in temperature $q_\beta(\beta_{eq})$ which is defined over the range:

$$q_{sp}(\beta_{eq}) < q_\beta(\beta_{eq}) < q_{mg}(\beta_{eq}) \tag{2.81}$$

In fig.2.7 the following state overlap $q_{1/T}(\beta_{eq})$ of pure and mixed models is compared. In pure models (left plot) states can be followed up in temperature till $q_{sp} = (p-2)/p$, which is equivalent to the condition of stability of TAP states followed in temperature (see 2.57) and it is independent from the starting temperature β_{eq}. This is not true in mixed models, where q_{sp} has an explicit dependence on β_{eq}. In both cases, deepest states ($q_{eq} = q_K$) are the last to melt. Cooling down states, in pure models each state can be followed till $T = 0$, where it becomes a single configuration ($q = 1$) i.e. inherent structures of the energy landscape. We notice by the way, that states followed from $q_{eq} = q_{MCT}$ are always marginal, i.e. $q_\beta(\beta_{MCT}) = q_{mg}(\beta)$. Vice versa in mixed models, if the states are prepared too close to q_{MCT}, the following state solution is lost at some $q_{mq} < 1$. This condition comes from the RS stability, therefore, one can imagine to refine the calculation below this line with a 1RSB step or more (we will consider it later on). This impossibility of following states is the most intriguing difference between pure and mixed models and it has huge effects on the out-of-equilibrium dynamics.

In fig.2.8 we show the phase diagram in $T = 1/\beta$ and $T' = 1/\beta'$ for the "following equilibrium states protocol". Each protocol consists in starting from the equilibrium state (blue line $T = T'$) and going up or down to heat and cool the state at fixed T'. In mixed models the state cannot be followed up to zero temperature in the range of temperature $T_{SF} < T < T_{MCT}$.

Now let's go back to the following states equations (2.78,2.79) and recast them in a more useful format for future analysis. Instead of writing observables as a function of β and β', we use q and β as independent variables. For that we assume that the map $(q, \beta) \to (\beta', \beta)$ is bijective. Therefore, we define:

$$\begin{aligned} \breve{q}_{FP}(q,\beta) &= \sqrt{q - \beta^2(1-q)^2 f'(q)} \\ \beta'_{FP}(q,\beta) &= \frac{\breve{q}_{FP}}{\beta(1-q)f'(\breve{q}_{FP})} \end{aligned} \tag{2.82}$$

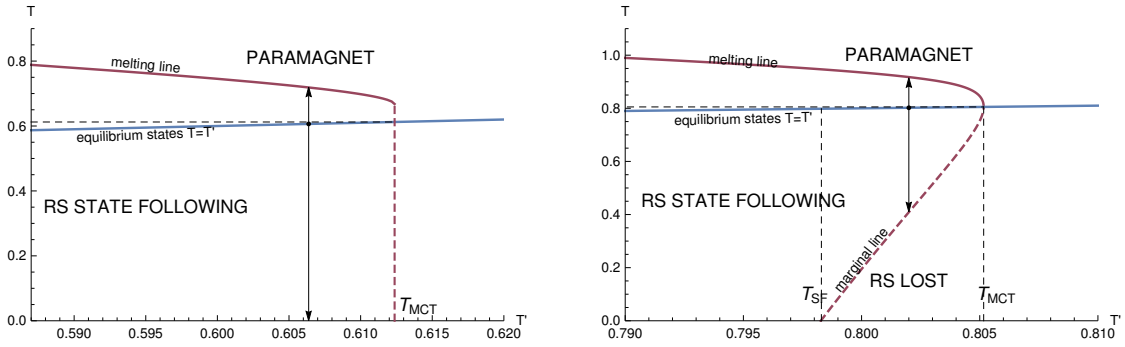

Figure 2.8: T vs T' phase diagram of the following state protocol in 3-spin pure model (left) and 3+4-spin mixed model (right). In pure models the state prepared below T_{MCT} can always be followed till zero temperature, while in mixed models states prepared between T_{SF} and T_{MCT} get lost by the RS Franz-Parisi potential

which satisfy (2.78,2.79). Now we can explicitly write the free energy and the energy of a state as a function of q and β:

$$\begin{aligned} F_{FP}(q,\beta) &= -\frac{\beta}{2}\Big(f(1)-f(q)+2\beta^{-1}\beta'_{FP}f(\breve{q}_{FP})+f'(q)(1-q)\Big)-\frac{\beta^{-1}}{2}\log(1-q) \\ E_{FP}(q,\beta) &= -\beta\big(f(1)-f(q)\big)-\beta'_{FP}f(\breve{q}_{FP}) \end{aligned} \tag{2.83}$$

These are the (free)energies of states which are dominant between all the q-states that were followed in temperature from equilibrium till temperature β, which in general, are not the same q-states that are dominant at β. The equilibrium measure is tilting the followed states.

Section References

[ASZ18] Gérard Ben Arous, Eliran Subag, and Ofer Zeitouni. "Geometry and temperature chaos in mixed spherical spin glasses at low temperature - the perturbative regime". In: *arXiv:1804.10573 [math]* (2018).

[Cha+14b] Patrick Charbonneau et al. "Hopping and the Stokes-Einstein relation breakdown in simple glass formers". In: *Proceedings of the National Academy of Sciences* 111.42 (2014).

[CP17] Wei-Kuo Chen and Dmitry Panchenko. "Temperature Chaos in Some Spherical Mixed p-Spin Models". en. In: *Journal of Statistical Physics* 166.5 (2017).

[FP95] S. Franz and G. Parisi. "Recipes for metastable states in Spin Glasses". In: *Journal de Physique I* 5.11 (1995).

[KZ09] Florent Krzakala and Lenka Zdeborová. "Hiding Quiet Solutions in Random Constraint Satisfaction Problems". In: *Physical Review Letters* 102.23 (2009).

[RC03] T. Rizzo and A. Crisanti. "Chaos in Temperature in the Sherrington-Kirkpatrick Model". In: *Physical Review Letters* 90.13 (2003).

[TAP77] D. J. Thouless, P. W. Anderson, and R. G. Palmer. "Solution of 'Solvable model of a spin glass'". In: *The Philosophical Magazine: A Journal of Theoretical Experimental and Applied Physics* 35.3 (1977).

[ZK16] Lenka Zdeborová and Florent Krzakala. "Statistical physics of inference: thresholds and algorithms". In: *Advances in Physics* 65.5 (2016).

2.3 Counting States

The energy landscape of p-spin models is full of minima. There is a region of energies for which these minima are exponential in the dimension N of the system. We will count them as a function of the energy E_{IS} of their bottom and the spectral gap $\Delta\mu$ of their spectrum, using a revised version of the Bray and More calculation [BM80]. Furthermore, in pure models, these energy minima can then be followed in temperature with a bijective map (see section 2.2). This allows us to evaluate the corresponding number of free energy minima $\mathscr{N}$ at any temperature until they melt. We will show that the same complexity ($\log \mathscr{N}$) can be obtained by directly probing the free energy landscape at a fixed temperature through a Legendre transform within the replica formalism, the so-called Monasson method [Mon95].

2.3.1 Counting Energy Minima

Let us consider the stationary points of the Hamiltonian $H[\sigma]$ on the sphere $\sum_i \sigma_i^2 = N$:

$$H'_i + \gamma\sigma_i = 0. \tag{2.84}$$

where γ is the Lagrange multiplier needed to enforce the spherical constraint. We wish to classify the stationary points of the Hamiltonian according to the energy of the bottom:

$$E_{IS} = \frac{1}{N} H[\sigma] \tag{2.85}$$

and the value of the radial reaction:

$$\mu = -\frac{1}{N}\sum_i \sigma_i H'_i \tag{2.86}$$

Contracting each side of 2.84 with σ_i we see that stationary points satisfy $\gamma = \mu$. Moreover, we will see that μ is related to the spectral gap of the stationary point.

In pure models $\mu = pE_{IS}$, while in mixed models the relation between E_{IS} and μ is not univocal and stationary points are found in a whole region of the (E_{IS}, μ) plane. Now let us consider the Hessian matrix of the stationary points:

$$M_{ij} = H''_{ij} + \mu\delta_{ij} \tag{2.87}$$

H_{ij} is a GOE random matrix with variance $\mathrm{Var}[H''_{ij}] = \frac{1}{N} f''(1)$ [CGP98; AAC10]. M has a semicircular spectral distribution with lower edge:

$$\lambda_{min} = \mu - 2\sqrt{f''(1)} = \mu - \mu_{mg} = \Delta\mu \tag{2.88}$$

where $_{mg}$ stands for marginal. Stationary points are therefore minima if $\Delta\mu > 0$ and saddles (or maxima) if $\Delta\mu < 0$. In between, $\Delta\mu = 0$ defines the manifold of minima that are marginal, which will play a crucial role in the out-of-equilibrium dynamics.

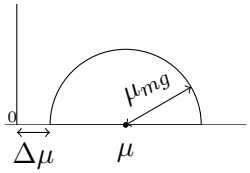

In order to characterize these minima, we count the number of stationary points of the Hamiltonian $H[\sigma]$ with fixed energy E_{IS} and radial reaction μ. Because the complexity, i.e. the logarithm of their number, is self-averaging * we can write:

$$\Sigma_0(E_{IS},\mu) = \log\left(\int_{S_N} \mathscr{D}\sigma\delta(NE_{IS}-H)\;\delta(\mu\sigma+H')\;|\det(\mu I+H'')|\right) \tag{2.89}$$

The computation of Σ_0 is standard, and can be performed in several steps. The subscript stands for zero temperature. First of all, since the matrix H'' is a GOE random matrix, the distribution of eigenvalues of $\mu I + H''$ is self-averaging and is a shifted semicircular:

$$\rho(\lambda) = \frac{2}{\pi\mu_{mg}^2}\sqrt{\mu_{mg}^2-(\lambda-\mu)^2} \tag{2.90}$$

The modulus of the determinant $|\det(\mu I + H'')|$ is self-averaging and its logarithm reads:

$$\begin{aligned} D(\mu) = \mathbf{Tr}\log(\mu I+H'') &= \int_{\Delta\mu}^{\Delta\mu+2\mu_{mg}} d\lambda\log(\lambda)\rho(\lambda) \\ &= \mathbf{Re}\Big[\frac{\mu}{\mu+\sqrt{\mu^2-\mu_{mg}^2}} + \log\left(\mu+\sqrt{\mu^2-\mu_{mg}^2}\right) - \frac{1}{2} - \log(2)\Big] \end{aligned} \tag{2.91}$$

This is valid also to evaluate the determinant of stationary points with negative gap $\Delta\mu < 0$ i.e. saddle points. The imaginary part of this expression gives the proportion of negative eigenvalues. At this point, we introduce another important observable connected to the spectrum that will be later useful, the susceptibility of an inherent structure†:

$$\begin{aligned} \chi(\mu) = \sum_i \chi_{ii} = \sum_i \frac{\partial\sigma_i}{\partial h_i} &= \mathbf{Tr}(\mu I+H'')^{-1} \\ &= \int_{\Delta\mu}^{\Delta\mu+2\mu_{mg}} d\lambda\rho(\lambda)\lambda^{-1} = \frac{\mu-\sqrt{\mu^2-\mu_{mg}}}{2f''(1)} \end{aligned} \tag{2.92}$$

*for a self-averaging observable we mean that the fluctuations induced by the quenched disorder are not thermodynamically relevant i.e. $\lim_{N\to\infty}(\overline{O^2}-\overline{O}^2)/N = 0$

†each Gaussian minimum has a cumulant generating function $C[h] = \frac{1}{2}h^T(\mu I+H'')^{-1}h$

Going back to (2.89), in order to evaluate the remaining terms, we assume that the number of minima $\mathcal{N}$ is self-averaging (further developments will be considered in section 3.2). Opening the delta functions in the Fourier basis we have:

$$\Sigma_0(E_{IS},\mu) = \log \overline{\mathcal{N}} = \log \int \mathscr{D}s \; e^{N(i\hat{\beta}E_{IS} - i\hat{\sigma}\cdot\sigma\mu)} \overline{e^{i\hat{\beta}H + i\hat{\sigma}\cdot H'}} + ND(\mu) \tag{2.93}$$

where $\int \mathscr{D}s = \int_{S_N} \mathscr{D}\sigma \int (2\pi)^{-1/2} d\hat{\beta} \int (2\pi)^{-N/2} \mathscr{D}\hat{\sigma}$ and the overline highlights the part of the integral that depends on the quenched disorder. Since the disorder is Gaussian (see 2.3):

$$\begin{aligned}\overline{e^{i\hat{\beta}H + i\hat{\sigma}\cdot H'}} &= e^{\frac{1}{2}(i\hat{\beta} + i\hat{\sigma}\cdot\partial_\sigma)(i\hat{\beta} + i\hat{\sigma}\cdot\partial_{\tilde{\sigma}}) f\left(\frac{\sigma\cdot\tilde{\sigma}}{N}\right)\Big|_{\tilde{\sigma}\to\sigma}} \\ &= \exp -\frac{N}{2}\Big(\hat{\beta}^2 f(\tfrac{\sigma\cdot\sigma}{N}) + 2\hat{\beta}\hat{\sigma}\cdot\sigma f'(\tfrac{\sigma\cdot\sigma}{N}) + (\hat{\sigma}\cdot\sigma)^2 f''(\tfrac{\sigma\cdot\sigma}{N}) + \hat{\sigma}\cdot\hat{\sigma} f'(\tfrac{\sigma\cdot\sigma}{N})\Big)\end{aligned} \tag{2.94}$$

As usual, at this point we do a change of variables from configurations σ and $\tilde{\sigma}$ to overlaps $q = \sigma\cdot\sigma/N$, $\chi = \sigma\cdot\hat{\sigma}/N$ and $r = \hat{\sigma}\cdot\hat{\sigma}/N$. The choice of using χ as an overlap variable is on order to recall the susceptibility $\chi(\mu)$ introduced in (2.92), in fact, as in Fourier transform the conjugate field $\hat{\sigma}$ acts as a derivative i.e. $\hat{\sigma}\cdot\sigma = \sum_i \partial_{h_i}\sigma_i$. The introduced change of variables brings a volume factor $\frac{1}{2}\log(qr - \chi^2)$. Putting all together we have:

$$\Sigma_0(E_{IS},\mu) = \log \int \mathscr{D}Q \; e^{NS(E_{IS},\mu,Q)} + ND(\mu) + \frac{N}{2}(\log S_\infty - \log 2\pi)$$

with

$$S(E_{IS},\mu,Q) = i(\hat{\beta}E_{IS} - \mu\chi) - \frac{1}{2}\Big(\hat{\beta}^2 f(q) + 2\hat{\beta}\chi f'(q) + \chi^2 f''(q) + r f'(q)\Big) + \frac{1}{2}\log(qr - \chi^2) \tag{2.95}$$

where Q stands for all the variables that must be extremized. $\log S_\infty = 1 + \log(2\pi)$ that comes from the volume of the sphere and $-\log 2\pi$ that comes from the Fourier transform. Now taking $S(E_{IS},\mu,Q)$ and extremizing that over $r, \chi, \hat{\beta}$ in order and putting $q = 1$ for the spherical constraint, one finally gets:

$$S(E_{IS},\mu) = -\frac{1}{2f(1)}\Big(E_{IS}^2 + \frac{\big(E_{IS}f'(1) + f(1)\mu\big)^2}{f(1)\,(f''(1) + f'(1)) - f'(1)^2}\Big) - \frac{1}{2}\big(1 + \log f'(1)\big) \tag{2.96}$$

In the case of pure models $E_{IS} = -\mu p$, the second term in the first parenthesis vanishes, and $S(E_{IS}) = -\frac{1}{2f(1)}E_{IS}^2 - \frac{1}{2}\big(1 + \log f'(1)\big)$. Finally, the general formula for

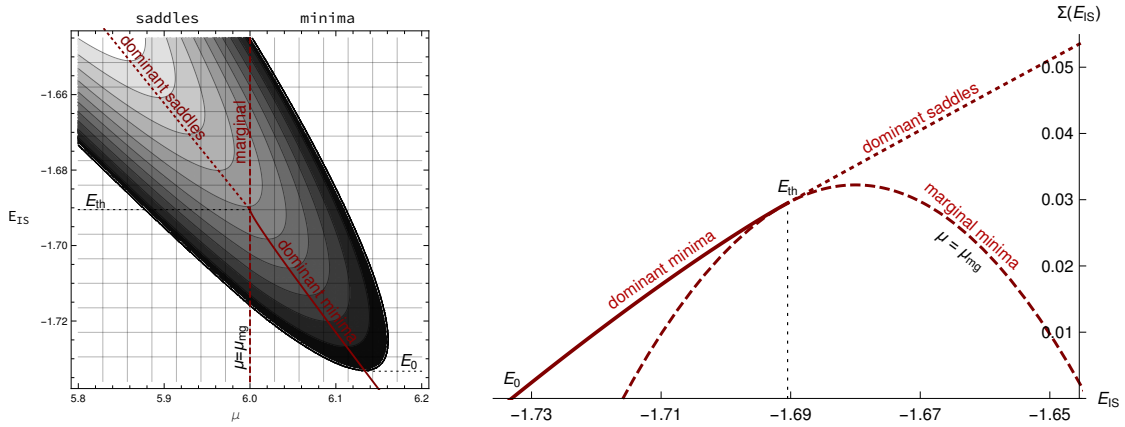

Figure 2.9: Complexity of inherent structures as a function of their energy E_{IS} in the $(3+4)$-spin mixed model. (**left**): the function $\Sigma_0(E_{IS}, \mu)$ is plotted with isoclines every 0.005. (**right**): complexity is restricted to dominant stationary points and to marginal minima.

the complexity as a function of the energy of the stationary point E_{IS} and the radial reaction μ reads:

$$\Sigma_0(E_{IS}, \mu) = \max\left\{0, \mathbf{Re}\Big[-\frac{1}{2f(1)}\Big(E_{IS}^2 + \frac{\big(E_{IS}f'(1)+f(1)\mu\big)^2}{f(1)\,(f''(1)+f'(1)) - f'(1)^2}\Big) + \frac{\mu}{\mu+\sqrt{\mu^2-4f''(1)}} + \log\Big(\mu+\sqrt{\mu^2-4f''(1)}\Big) - \frac{1}{2}\log 4f'(1)\Big]\right\} \tag{2.97}$$

The same result can be found in [ASZ18]. If then, we optimize over μ to get the dominant minima at fixed energy E_{IS}, we can define the energy of the dominant inherent structure as a function of their radial reaction:

$$E_{IS}^{dm}(\mu) = \chi(\mu)\big(f(1)-f'(1)\big) - \chi(\mu)^{-1}\frac{f(1)}{f'(1)} \tag{2.98}$$

$\chi(\mu)$ was defined in (2.92). At this point, we can define the threshold energy E_{th} from the energy landscape perspective as:

$$\begin{aligned} E_{th} \equiv E_{IS}^{dm}(\mu_{mg}) &= \chi_{mg}\big(f(1)-f'(1)\big) - \chi_{mg}^{-1}\frac{f(1)}{f'(1)} \\ \text{with} \qquad \chi_{mg} &\equiv \chi(\mu_{mg}) = f''(1)^{-1/2} \end{aligned} \tag{2.99}$$

that is the energy of the dominant minima with zero gap ($\Delta\mu = 0$). This will play a major role in the out-of-equilibrium dynamics. From the definition of dominant

minima, the dominant complexity follows:

$$\Sigma_0^{dm}(\mu) = \Sigma_0(E_{IS}^{dm}(\mu), \mu) \\ \frac{1}{2}\left(\chi(\mu)^2 f'(1) - f(1)\left(\frac{1}{\chi(\mu)f'(1)} - \chi(\mu)\right)^2 + \log\left(\frac{1}{\chi(\mu)^2 f'(1)}\right) - 1\right) \tag{2.100}$$

As we will see in the next section, this complexity is identical to that one obtained by Monasson method in the limit of zero temperature. Another important observable that will play a major role in the out-of-equilibrium dynamics is the derivative of the complexity with regard to the energy, which can be thought as an effective inverse temperature:

$$y = \frac{\Sigma_0^{dm}(E_{IS})}{\partial E_{IS}} = \frac{\partial_\chi \Sigma_0^{dm}}{\partial_\chi E_{IS}^{dm}} = \frac{1}{\chi f'(1)} - \chi \tag{2.101}$$

which for threshold minima gives:

$$y_{th} = \frac{1}{\chi_{mg} f'(1)} - \chi_{mg} = \frac{\sqrt{f''(1)}}{f'(1)} - \frac{1}{\sqrt{f''(1)}} \tag{2.102}$$

In fig. 2.9 the complexity Σ_0 in the (E, μ)-plane is shown. The locus line of dominant stationary points E_{IS}^{dm} and of marginal minima $\mu = \mu_{mg}$ is marked and reported on the right plot. We notice that, at variance to pure p-spin models, there exists a whole interval for which $\Sigma_0(E, \mu_{mg}) > 0$. The threshold energy E_{th} corresponds to the values of the energy that separates minima from saddles on the dominating line. Notice that this value does not correspond to the most numerous marginal minima, which occurs for $\mu = \mu_{mg}$ and $E > E_{th}$. To conclude, we notice that the same parabolic shape of complexity that we find here is quite a robust feature in finite size systems and is the assumption used in the PEL gaussian approximation (see section 1.2).

2.3.2 Counting with a Legendre Transform

Let's start by a brief introduction to the Monasson method (M). This method was first envisaged in 1992 [FPV92], when the idea of *real replicas* was introduced and applied to the SK model. One year later the method was explored in the p-spin case and compared to the TAP free energy [KPV93]. Eventually, the idea of using this replicated system as a general tool to study the complexity of the free energy landscape thorough a Legendre transform was established in [Mon95]. Then another paper [Méz99] remarked the importance of *cloning* the system and re-explored the

p-spin model. A pedagogical introduction to this calculation can be found in the review [Zam10]. For the latest ideas about the subject, we refer the reader to [BV15] in which the authors consider not only states, but a generic ultrametric tree and generalize the concept of complexity to arbitrary clusters. Another possible specialization of the Monasson method is to use it in an arbitrary constrained situation, and so, for example doing a Legendre transform of the Franz-Parisi potential. This allows to evaluate the complexity of constrained states [Cas06; Mor16].

Let's come back to the complexity. We wish to count the number of free energy states $\mathscr{N}(F)$ at given inverse temperature β and as a function of the bottom free energy F of the state. We decompose the partition function as a sum over the states:

$$\begin{aligned} Z_\beta &= \sum_{\sigma\in\mathscr{C}} e^{-\beta H[\sigma]} = \sum_{\alpha\in\mathscr{S}}\sum_{\sigma\in\mathscr{C}^\alpha} e^{-\beta H[\sigma]} \\ &= \sum_{\alpha\in\mathscr{S}} e^{-\beta F_\alpha} = \int dF P(F) e^{-\beta F} = \int dF e^{-\beta F+\Sigma(F)} \end{aligned} \tag{2.103}$$

where $\mathscr{C}$ is the ensemble of all configurations, $\mathscr{S}$ the ensemble of states and $\mathscr{C}^\alpha$ of configurations belonging to the state α. Here for state, we mean a free energy well, that since we are in a mean-field model, has extensive barriers ($\propto N \to \infty$). For mean-field systems, the measure concentrates on the maximum of $-\beta F + \Sigma(F)$ that gives the usual relation $\beta = \partial_F \Sigma$, which is valid at equilibrium. However, at this point we do not know either F or $\Sigma(F)$. In order to extract some information at the level of states, we need to tilt the Boltzmann measure at the level of F. For that, we introduce the conjugated variable x s.t. $x\beta = \partial_F\Sigma$ as a minimization of $-x\beta F + \Sigma(F)$. This will allow us to rebuild $\Sigma(F)$. Thus, we have the tilted partition function:

$$Z_\beta(x) = \sum_{\alpha\in\mathscr{S}} e^{-x\beta F_\alpha} = \sum_{\alpha\in\mathscr{S}} Z_\alpha^x \tag{2.104}$$

Following the replica mindset we will consider x an integer variable, the number of *clones* (copies of the system), do standard manipulation and analytically come back to real x. The n-replicated partition function of the tilted system becomes:

$$\overline{Z_\beta^n(x)} = \overline{\Big(\sum_{\alpha\in\mathscr{S}} Z_\alpha^x\Big)^n} = \overline{\Big(\sum_{\alpha\in\mathscr{S}}\Big(\sum_{\sigma\in\mathscr{C}^\alpha} e^{-\beta H[\sigma^\alpha]}\Big)^x\Big)^n} \tag{2.105}$$

the tilting field x induces a replica breaking step in the nx-overlap matrix at the level of the overlap q. At this point we come back to the p-spin model. We restrict the study to the class of models $f(q)$ whit at most a 1-RSB structure of the solution (see section 2.1.7).

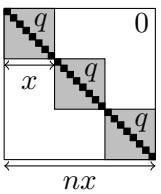

By spherical symmetry, these models always have a zero overlap between configurations belonging to different states i.e. $\sigma_{\in\mathscr{C}_\alpha}\cdot\sigma_{\in\mathscr{C}_\beta}=0$, which gives the condition $q_0=0$ (see equation 2.30). The overlap matrix has a 1-RSB structure (see 2.26) with only $q\equiv q_1$ to be minimized over:

$$\begin{aligned}\log Z_\beta(x) &= \inf_q[-x\beta F_\beta^{1RSB}(x,q)]\\ &= \frac{1}{2}\Big(x\beta^2\big(f(1)-(1-x)f(q^*)\big)+\log\frac{1-(1-x)q^*}{1-q^*}+x\log(1-q^*)\Big)\end{aligned} \tag{2.106}$$

where $q^*=q^*(x)$ is the value of q which minimizes the x-tilted free energy:

$$\partial_q\log Z_\beta(x)=0 \quad\Rightarrow\quad \beta^2 f'(q^*)=\frac{q^*}{(1-q^*)(1-(1-x)q^*)} \tag{2.107}$$

Since the states are orthogonal, the free energy 2.106 can also be thought as x times the RS free energy plus an entropic correction:

$$\log Z_\beta(x)=\inf_q[x\beta F_\beta^{RS}(q)+\log\frac{1-(1-x)q}{1-q}] \tag{2.108}$$

the entropic correction comes from the change in available volume, having fixed x clones to be in the same state. For $x>1$ a positive contribution, and negative otherwise.
At this point we notice a peculiar fact (already mentioned in [Méz99]). In building ultrametric matrices, the principle is to order the overlaps boxes. Thus $nx<x<1$ if $x<1$ and $nx<1<x$ if x is greater than 1. This second order reverts the usual structure of $1RSB$ for which the diagonal is built by ones. This to say that from the mathematical point of view, when passing $x=1$, one should be very careful. We won't spend more time on this, and we blindly accept that saddle points are analytically continuous upon changing x around 1. For more details on the Monasson analysis for $x>1$ we refer to a manuscript in preparation [Fol+20].

Let's come back to the main calculation. The solution **??** for the optimal overlap is stable as long as:

$$\partial_q^2\log Z_\beta(x)<0 \quad\Rightarrow\quad (1-x)x\Big(\frac{1-q^{*2}(1-x)}{(1-q^*)^2(1-q^*(1-x))^2}-\beta^2 f''(q^*)\Big)<0$$

This is the longitudinal stability condition (see section 2.1.5) that must be flanked by the marginal stability of the states $\beta^2 f''(q^*)-(1-q^*)^2<0$ which is ensuring

that additional steps of replica breaking are not needed (section 2.1.5 and 2.1.7). To simplify calculations, we revert the relation and write:

$$x_{M}(q,\beta) = \frac{1}{\beta^2 f'(q)(1-q)} - \frac{(1-q)}{q} \tag{2.109}$$

where the superscript * is omitted and the subscript $_M$ stands for Monasson. At each inverse temperature β and at each overlap q corresponds a typical state of free energy $F(q)$ with a tilting field $x(q) = \beta^{-1}\partial_F \Sigma(F)|_q$. At this point, we remark that the $x_M = 1$ is by construction selecting equilibrium states and gives the same equation that was obtained for equilibrium states with the FP equilibrium potential (see 2.73).

As the entropy $S(E)$ is the Legendre transform of the free energy $G(\beta) = -\beta F(\beta)$, the complexity $\Sigma(F)$ is the Legendre transform of $G(y) = \log Z_\beta(x)$ where the conjugated field is $y = \beta x$.

$$\Sigma(F^*) = \sup_y [G(y) + yF] = G(y^*) - y^* \partial_y G(y^*) = y^2 \frac{\partial}{\partial y}(y^{-1}G(y))\Big|_{y^*(F^*)} \tag{2.110}$$

with y^* s.t. $\partial_y G(y^*) = -F^*$. Thus, the free energy of a state is:

$$\begin{aligned} F_{M}(q,\beta) &= -\partial_y G(y^*) = -\beta^{-1}\partial_x \log Z_\beta(x) \\ &= -\frac{\beta}{2}\Big(f(1) - f(q) + 2x_{M} f(q) + (1-q)f'(q)\Big) - \frac{\beta^{-1}}{2}\log(1-q) \end{aligned} \tag{2.111}$$

And its energy:

$$E_{M}(q,\beta) = -\beta\big(f(1) - f(q)\big) - \beta x_{M} f(q) \tag{2.112}$$

where $x_M \equiv x_M(q,\beta)$. In pure-models this (free)energy is the same obtained by following TAP states in temperature, starting from the minima of the energy landscape (see section 2.2). For what concerns the complexity, using (2.110) we have:

$$\begin{aligned} \Sigma_{M}(q,\beta) &= x^2 \frac{\partial}{\partial x}(x^{-1}\log Z_\beta(x))\Big|_{y^*} \\ &= \frac{1}{2}\Big(- \beta^2 x_{M}^2 f(q) - \frac{q x_{M}}{1-(1-x_{M})q} + \log\frac{1-(1-x_{M})q}{1-q}\Big) \end{aligned} \tag{2.113}$$

We notice, that for any temperature $\beta > \beta_K$, taking states that have zero complexity $\Sigma_M(q,\beta) = 0$, corresponds to selecting the condensed $1RSB$ states that dominate the partition function (found in 2.1.6). Thanks to the Monasson method, we have evaluated x_M, F_M, E_M, Σ_M as a function of q and β. We go back to the complexity

of dominant minima of the energy landscape $\Sigma^{dm}(\mu)$ defined in the previous section (2.100) and compare it with $\Sigma_{M}(q, \beta \to \infty)$. Using the change of variables $q \to 1 - \chi\beta^{-1}$ and taking the limit $\beta \to \infty$ we obtain the complexity:

$$\Sigma_{M}(\chi) = \frac{1}{2}\left(\chi^2 f'(1) - f(1)\left(\frac{1}{\chi f'(1)} - \chi\right)^2 + \log\left(\frac{1}{\chi^2 f'(1)}\right) - 1\right) \tag{2.114}$$

which is exactly the complexity of dominant inherent structure $\Sigma^{dm}(\mu)$ written in terms of χ.

2.3.3 Universal Complexity

In this small section, we wish to introduce a way of writing the complexity that directly matches the three complexities introduced so far: Franz-Parisi equilibrium complexity $\Sigma^{eq}_{FP}(q_{eq})$, Monasson complexity $\Sigma_{M}(q, \beta)$ and zero temperature dominant complexity $\Sigma^{dm}_{0}(\mu)$. Let's introduce the Universal Complexity:

$$\Sigma_{UN}(K, q) = \frac{1}{2}\left(-\frac{(1-K)^2}{K}\frac{f(q)}{qf'(q)} + K - \log(K) - 1\right) \tag{2.115}$$

Though different choices of the variable K we recover the three different complexities. The M complexity at general β:

$$K_{M} = \frac{\beta^2 f'(q)(1-q)^2}{q} \qquad \Longrightarrow \qquad \Sigma_{UN}(K_{M}, q) \equiv \Sigma_{M}(q, \beta) \tag{2.116}$$

The FP complexity at equilibrium:

$$K_{eq} = 1 - q_{eq} \qquad \Longrightarrow \qquad \Sigma_{UN}(K_{eq}, q_{eq}) \equiv \Sigma^{eq}_{FP}(q_{eq}) \tag{2.117}$$

The dominant complexity at $T = 0$:

$$K_0 = \chi^2 f'(1) \qquad \Longrightarrow \qquad \Sigma_{UN}(K_0, 1) \equiv \Sigma^{dm}_{0}(\chi) \tag{2.118}$$

Section References

[AAC10] A. Auffinger, G. Ben Arous, and J. Cerny. "Random Matrices and complexity of Spin Glasses". In: *arXiv:1003.1129 [math-ph]* (2010).

[ASZ18] Gérard Ben Arous, Eliran Subag, and Ofer Zeitouni. "Geometry and temperature chaos in mixed spherical spin glasses at low temperature - the perturbative regime". In: *arXiv:1804.10573 [math]* (2018).

[BM80] A. J. Bray and M. A. Moore. "Metastable states in spin glasses". en. In: *Journal of Physics C: Solid State Physics* 13.19 (1980).

[BV15] R. Baviera and M. A. Virasoro. "A method that reveals the multi-level ultrametric tree hidden in p-spin glass like systems". In: *Journal of Statistical Mechanics: Theory and Experiment* 2015.12 (2015).

[Cas06] Tommaso Castellani. "The multi p-spin model: comparing tap states and out-of-equilibrium dynamics". PhD thesis. 2006.

[CGP98] Andrea Cavagna, Irene Giardina, and Giorgio Parisi. "On the stationary points of the TAP free energy". In: *Physical Review B* 57.18 (1998).

[Fol+20] G. Folena et al. "manuscript in preparation". In: (2020).

[FPV92] S. Franz, G. Parisi, and M. Virasoro. "The replica method on and off equilibrium". In: *Journal de Physique I* 2.10 (1992).

[KPV93] J. Kurchan, G. Parisi, and M. Virasoro. "Barriers and metastable states as saddle points in the replica approach". In: *Journal de Physique I* 3.8 (1993).

[Méz99] Marc Mézard. "How to compute the thermodynamics of a glass using a cloned liquid". In: *Physica A: Statistical Mechanics and its Applications* 265.3 (1999).

[Mon95] R. Monasson. "The structural glass transition and the entropy of the metastable states". In: *Physical Review Letters* 75.15 (1995).

[Mor16] Sebastian Morel-Balbi. "Multi-replica effective potential for state following in disordered systems". PhD thesis. 2016.

[Zam10] Francesco Zamponi. "Mean field theory of spin glasses". In: *arXiv:1008.4844 [cond-mat]* (2010).

2.4 Three ways of Selecting States

In this section, I will try to put forward the analogies and differences between three methods of selecting states: the Thouless-Anderson-Palmer (TAP) approach from zero temperature, the Monasson (M) approach from fixed temperature and the Franz-Parisi (FP) approach from equilibrium. The three methods turn out to select the same states in pure models, while in mixed models the situation is much more complex. Temperature chaos does not allow to follow energy minima. Moreover the FP and M methods select different states at a same condition. In particular FP selects a sub-portion of all available states identified by M at low temperature.

2.4.1 Pure Models: Perfect Matching

As we have seen in section 2.2, in pure models, one can follow minima of the free energy landscape from zero temperature until they melt; deeper minima do so at higher temperatures. Each minimum is identified by its inherent structure energy E_{IS} and by the free energy of its basin $F_{TAP}(E_{IS}, \beta)$. The E_{IS} ranges between E_0, the energy of the lowest lying minima, which are extensive in number, and E_{th}, the energy of the highest stable minima (see section 2.3), which are also the most numerous. The peculiar fact about pure models is that the only marginal states of the free energy landscape (with zero gap spectrum) are the threshold ones (the highest and most numerous stable minima). The same map that allows to follow minima by heating them up, can be also built from the equilibrium measure through the FP construction. The so built potential can be considered as the analytical equivalent of a slow annealing in temperature, which takes a state at equilibrium and brings it to a second temperature. The third way of analyzing the free energy landscape is to directly fix a temperature and select the states based on their energies. It turns out that at each temperature, typical states of given energy are the same as those which are typical at zero temperature or at equilibrium followed with their multiplicity.

A simple way of resuming this equivalence is to imagine each following minima protocol as a rope in free energy, which can be indexed by the value of its zero temperature inherent structure minima E_{IS} (TAP), or by the temperature at which the state is at equilibrium β' (FP). The number of ropes can then be counted at each temperature, giving the same result (M).

To further clarify the formal equivalence between the three methods, let's consider the energy of a state at inverse temperature β and with overlap q (see eqs. (2.62),

(2.83) and (2.112)):

$$\begin{aligned} E_{M}(q,\beta) &= -\beta\big(f(1)-f(q)\big) - \beta x_{M} f(q) \\ E_{FP}(q,\beta) &= -\beta\big(f(1)-f(q)\big) - \beta'_{FP} f(\mathring{q}_{FP}) \\ E_{TAP}(q,E_{IS}) &= -\beta\left(f(1)-f(q)\right) + E_{IS}\, q^{p/2} - \beta f'(q)(1-q) \end{aligned} \tag{2.119}$$

where $E_{TAP}(q,E_{IS})$ is by definition valid only for pure models i.e. $f(q)=q^p/2$. Let's start by comparing $E_{M}(q,\beta)$ and $E_{FP}(q,\beta)$, which are equivalent if:

$$\beta x_{M} f(q) = \beta'_{FP} f(\mathring{q}_{FP}) \tag{2.120}$$

recalling the definitions eqs. (2.82) and (2.109) we obtain the condition:

$$\frac{f(q)}{q f'(q)} = \frac{f(\mathring{q}_{FP})}{\mathring{q}_{FP} f'(\mathring{q}_{FP})} \tag{2.121}$$

which is identically satisfied only for pure models. This means that selecting states by M or FP is equivalent in pure models, where also the TAP free energy protocol is well defined. In order to find the connection between E_{FP} and E_{TAP} we look at equilibrium states. These, in the M construction, are defined by the condition $x_{M}=1$ and in FP by $\partial_q V_\beta^{eq}(q)=0$. The equation that relates their overlap and the temperature at which they are at equilibrium is:

$$\beta_{eq}(q_{eq}) = \sqrt{\frac{q_{eq}}{(1-q_{eq})f'(q_{eq})}} \qquad \text{with} \qquad q_{K} < q_{eq} < q_{MCT} \tag{2.122}$$

where q_{MCT} is the overlap above which equilibrium states become unstable, and q_{K} is the overlap below which their number of them becomes sub-extensive. The corresponding energy of equilibrium states is:

$$E_{M}(q_{eq}) = E_{FP}(q_{eq}) = -\beta_{eq}(q_{eq}) f(1) \tag{2.123}$$

which is the paramagnetic energy in the region $T_{K} < T < T_{MCT}$ where the paramagnetic state is partitioned in an exponential (in N) number of states. In pure models, for each β between β_{MCT} and β_{K} the equilibrium state can also be reached following the TAP energy up to β. This maps inherent structures to equilibrium states. And in particular, labeling equilibrium states by their equilibrium overlap q_{eq} and inherent structures by their energy E_{IS}:

$$\begin{aligned} &E_{TAP}(q_{eq},E_{IS}) = E_{FP}(q_{eq},\beta_{eq}) \\ &\qquad \Rightarrow E_{IS}(q_{eq}) = -\frac{\beta_{eq} f(q_{eq}) - \beta_{eq} f'(q_{eq})(1-q_{eq})}{q_{eq}^{p/2}} \end{aligned} \tag{2.124}$$

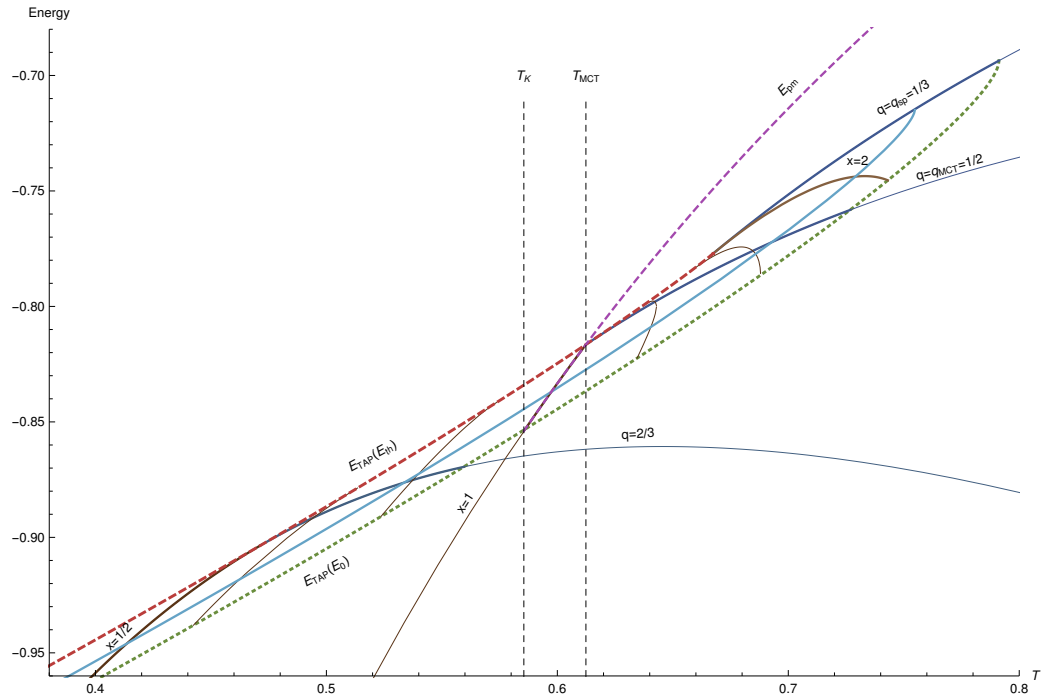

Figure 2.10: Following of states in energy in the 3-spin model. TAP states followed from $T = 0$, FP states followed from $T = T_{eq}$ and M states sampled for each temperature. In pure models the three methods coincides. Heating the systems threshold states E_{th} are the first to melt, while deepest states E_0 are the last. Isocline at constant x and constant q are shown.

where $\beta_{eq} \equiv \beta_{eq}(q_{eq})$. If now one evaluates the complexity of equilibrium states as a function of the overlap q_{eq} (see 2.76) and compares it with the complexity of energy minima in pure models through the map (2.124), the following identity is obtained:

$$\Sigma_{FP}(q_{eq}) = \Sigma_0^{dm}(E_{IS}(q_{eq})) \tag{2.125}$$

One can further take any followed state by TAP or by FP at any temperature and compare its complexity with that obtained by M, obtaining:

$$\Sigma_{FP}(q, \beta) = \Sigma_M(q, \beta) \tag{2.126}$$

In 2.10 the energy of the states versus temperature is shown for the three different methods. As we have shown, by fixing (q, β) we have unambiguously defined the state, no matter what method is used to select it.

Finally, we notice that there is a region above T_{MCT} within which, given the temperature, there exists two different overlap q_a and q_b with the same x. This

means that the configurational entropy is non concave with regard to the free energy of the basin. This could be interesting if read in correspondence to finite dimensional system, since it is signaling a phase transition in free energy of basins. It could be that the mean-field counterpart of the developing of two different length scales in the diffusion processes.

2.4.2 Mixed Models: which States are Selected?

The three methods of selecting states (TAP,FP and M) are not identical in mixed ones. Here we remark, once again, that many properties of pure models are very singular. It would suffice to slightly perturb their Hamiltonian with a small field to lose all the correspondences we have described in the previous section. We have seen (section 2.2) that in pure models, following TAP states in temperature is equivalent to finding Hamiltonian minima on the N-dimensional sphere and follow them radially. This is not valid in mixed models and, for which, until now, there is no analytical way to follow their TAP states in temperature. And moreover, in some energy regions this is a physical impossibility, since there is *chaos in temperature*.

It's however still possible to follow an equilibrium state, using the FP potential. Even though there are fundamental differences with pure models, many qualitative features remain true. As we already noted, in mixed models, states prepared near T_{MCT} are very simple to lose, upon both heating them and cooling them (see bottom inset fig. 2.11). In particular, at low temperature there is a range of followed states which are lost and there has been, untill now, no analytical way to follow them further. The interesting thing is that there are some regions in which following the states would anyhow be impossible, due to the aforementioned chaos in temperature.

The last way to select states is by tilting the measure, which inflates the free energy of some states more than others. This is the Monasson method. This method cannot follow states. What it does is to scan the landscape of states at any given temperature, counting and weighting them. In pure models, selecting *dominant* states of given overlap q at temperature T is equivalent to looking at *followed* states of overlap q at temperature T. It is not true in mixed models. This can be seen in figure 2.11:TOP, where the region of possible energies of followed states (FP: purple) is compared to the the region of possible energy of selected states (M: green). Only on the equilibrium line $x = 1$ between T_K and T_{MCT} do the two methods agree, by definition. The FP region is defined by the locus of energies compatible with states followed from equilibrium. While the M region is defined by the condition of positive complexity $\Sigma_M(q, \beta) > 0$. Going down in temperature, the FP-region shrinks and the number of states diminishes with regard to the M region. Going up in temperature,

followed states are more numerous than typical ones, to the point that some followed states exist where no states are typically selected by M method. This phenomenology is highlighted in figure 2.11:BOTTOM, where complexity as a function of the energy of the state $\Sigma(E)$ is shown for both methods at different temperatures.

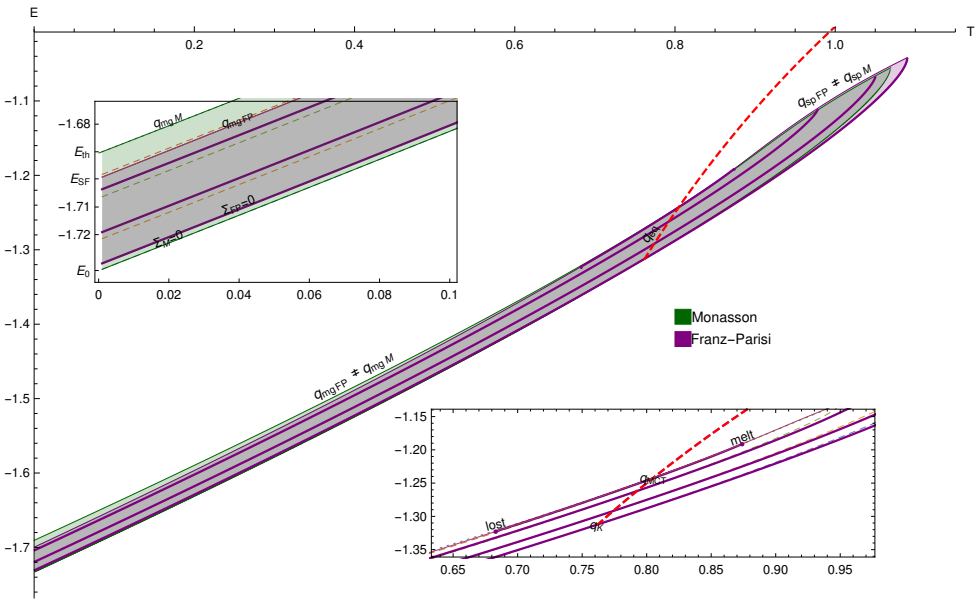

Figure 2.11: Franz-Parisi vs Monasson, two different methods to select states in the mixed (3+4)-spin model. (**TOP**): The region of possible energies for the states are plotted as a function of temperature. Thick purple lines show the energy of four states followed with FP. (**bottom inset**): a zoom around T_{MCT}. The state prepared close to T_{MCT} presents a melting point and a "lost" point. (**top inset**): a zoom around $T = 0$. There is a range of energies between E_{SF} and E_{th} where FP followed states do not exist. (**BOTTOM**): complexity of FP states $\Sigma_{FP}(E_{FP})$ and of M states $\Sigma_M(E_M)$ at different temperatures. Underneath the gaps between the support of the two complexities. Below T_K the support of the M-region is larger than that of the FP-region, while above T_{MCT} the opposite is true. Moreover, contrary to intuition, followed states at temperatures above T_{MCT} are more than typical states of the same energy.

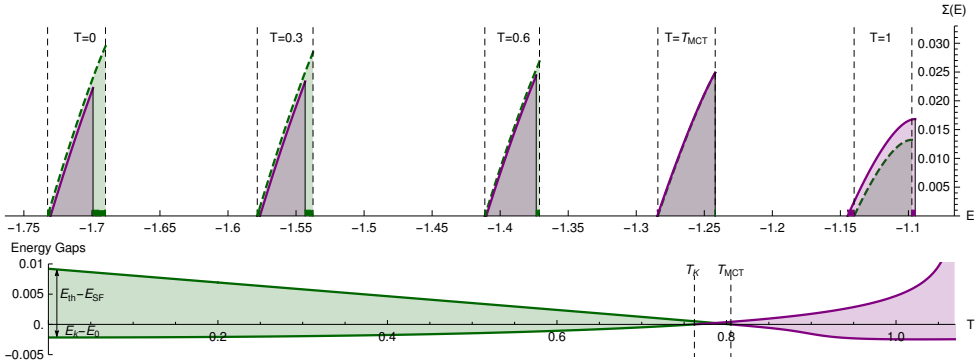

2.5 Mean Field Dynamical Equations with Cavity Method

The Langevin dynamics of a mean-field model can be translated into a single component dynamics with colored noise and a memory kernel. This is a general result obtained each time a Markovian dynamics is projected onto a subspace of the original space (see chapter 8 [Zwa01]). Here, in order to derive this effective equation of motion, we use the so-called cavity method [MPV87]. For another mean-field model, the so obtained equation was shown to be equal with the one obtained through the Martin-Siggia-Rose-Jensen-De Dominicis (MSRJD) path-integral method [Ago+17]. A similar derivation to the one here presented can be found in the appendix of [FM94]. Given the system of N spins, the spin σ_0 is added and its dynamics is evaluated self-consistently. Two main contributions arise: a cavity field generated by all the other N spins (colored noise $\Xi(t)$) and a self-reaction field induced by σ_0 through all the other spins (memory kernel $M(t,t')$):

$$\dot{\sigma}_0(t) = -\mu\sigma_0(t) + \Xi(t) + \int^t dt' M(t,t')\sigma_0(t') \tag{2.127}$$

where μ enforces the spherical constraint. The goal is to evaluate $\Xi(t)$ and $M(t,t')$ for the mixed p-spin spherical model. Let's start by recalling the Langevin equation for the system:

$$\dot{\sigma}_i(t) = -\mu\sigma_i(t) - H_i'(t) + \xi_i(t) \tag{2.128}$$

where $i = 1...N$, $H_i'(t)$ stands for $\partial_{\sigma_i} H[\sigma(t)]$ and ξ is a white noise with variance $2T$ i.e. $\langle \xi_i(t)\xi_j(s)\rangle = 2T\delta_{ij}\delta(t-t')$. Given an observable O, its linear response to a small time dependent perturbation of the Hamiltonian $\delta H(t)$ can be written as:

$$\delta O(t) = \int^t ds \frac{\delta O(t)}{\delta H_j'(s)} \delta H_j'(s)$$

We have decomposed the perturbation induced on O by δH in terms of the linear response fields $\delta H_j'(s)$, since these are the ones that directly influence the Langevin dynamics of the spins σ_j.

At this point, we start the cavity calculation. We introduce a new spin σ_0 with the relative couplings, that induces a small perturbation of the Hamiltonian $\delta H = H_0'\sigma_0$, which linearly perturbs the dynamics of the other N spins $\sigma_i(t) \to \sigma_i(t) + \delta\sigma_i(t)$:

$$\delta\sigma_i(t) = \int^t ds \frac{\delta\sigma_i(t)}{\delta H_j'(s)} \frac{\delta H_j'(s)}{\delta\sigma_0(s)} \sigma_0(s) = \int^t ds R_{ij}(t,s) H_{j0}''(s)\sigma_0(s) \tag{2.129}$$

where $H''_{i0} \equiv \partial_{\sigma_0} H'_i$ is a row of the Hessian and $R_{ij}(t,s) \equiv \frac{\delta \sigma_i(t)}{\delta H'_j(s)}$ is the response of the system. Given the perturbed $\sigma_i(t) + \delta\sigma_i(t)$, the equation of motion for σ_0 reads:

$$\begin{aligned}\dot{\sigma}_0(t) &= -\mu\sigma_0(t) - H'_0[\{\sigma_i(t) + \delta\sigma_i(t)\}] + \xi_0(t) \\ &\approx -\mu\sigma_0(t) - H'_0[\{\sigma_i(t)\}] + \int^t ds H''_{0i}(t) R_{ij}(t,s) H''_{j0}(s)\sigma_0(s) + \xi_0(t)\end{aligned} \tag{2.130}$$

where $H'_0[\{\sigma_i(t)\}]$ depends on the unperturbed spins $\sigma_i(t)$ which are uncorrelated and therefore, they all give independent contributions. Doing a direct comparison with (2.127) we have the colored noise:

$$\Xi(t) = -H'_0[\{\sigma_i(t)\}] + \xi_0(t) \tag{2.131}$$

And the memory kernel:

$$M(t,s) = H''_{0i}(t) R_{ij}(t,s) H''_{j0}(s) \tag{2.132}$$

Now let's average (2.130) over the quenched disorder. We recall that at the leading order in N, we have $\overline{H'_i[\sigma]H'_j[\tau]} = \delta_{ij} f'(\sigma\cdot\tau/N)$ and $\overline{H''_{ij}[\sigma]H''_{kl}[\tau]} = N^{-1}\delta_{(ij)(kl)} f''(\sigma\cdot\tau/N)$ (see appendix A.1). Therefore, the memory part of the colored noise gets:

$$\overline{\langle H'_0[\{\sigma_i(t)\}] H'_0[\{\sigma_i(s)\}]\rangle} = \langle \delta_{00} f'(\frac{\sigma(t)\cdot\sigma(s)}{N})\rangle = f'(C(t,s)) \tag{2.133}$$

where we have defined the correlation function $C(t,s) \equiv \lim_{N\to\infty}\langle\sigma(t)\cdot\sigma(s)\rangle/N$. The equality must be read in the thermodynamic limit $N \to \infty$. The second equality comes from the concentration of the correlation in the thermodynamic limit, i.e. $\langle f'()\rangle = f'(\langle\rangle)$. For the memory kernel we have:

$$\begin{aligned}M(t,s) &= \overline{\langle H''_{0i}(t)\frac{\delta\sigma_i(t)}{\delta H'_i(s)} H''_{i0}(s)\rangle} \\ &= \langle f''(\frac{\sigma(t)\cdot\sigma(s)}{N})\rangle\langle\sum_i^N \frac{\delta\sigma_i(t)}{\delta H'_i(s)}/N\rangle \\ &= f''(C(t,s))R(t,s)\end{aligned} \tag{2.134}$$

where $R(t,s) \equiv \langle\sum_i^N \frac{\delta\sigma_i(t)}{\delta H'_i(s)}/N\rangle$ is the local response function. The fact that we have taken only the diagonal terms $i = j$ in the response is because all non diagonal terms are suppressed by N^{-1} in the thermodynamic limit. This can directly be seen in the correlation of gradients $H'_i[\sigma]H'_j[\tau] = \delta_{ij} f'(\sigma\cdot\tau/N) + O(N^{-1})$ (appendix A.1).

We remark that the parameter μ must enforce the spherical constraint at every time, so in general it has a time dependency that can be fixed a posteriori such that $\lim_{t\to t'} C(t,t') = 1$.

Rewriting all terms together, we get the stochastic equation with memory:

$$\begin{aligned} \dot{\sigma}(t) &= -\mu\sigma(t) - \int^t ds f''(C(t,s))R(t,s)\sigma(s) + \Xi(t) \\ \langle \Xi(t)\Xi(s)\rangle &= 2T\delta(t-s) + f'(C(t,s)) \end{aligned} \tag{2.135}$$

This equation describes the dynamics of a generic component i of the spin σ and will be our point of departure for equilibrium and out-of-equilibrium computations.

2.5.1 Equilibrium Equations

At equilibrium the dynamics follows two general laws: time translation invariance (TTI) of two-times observables and the fluctuation dissipation theorem (FDT). The first gives that the correlation and the response depend on the time differences:

$$\begin{aligned} C(t,t') &\overset{TTI}{\Longrightarrow} C(t-t') \\ R(t,t') &\overset{TTI}{\Longrightarrow} R(t-t') \end{aligned} \tag{2.136}$$

And FDT relates the correlation and the response of the system through the temperature of the thermal bath β^{-1}:

$$\beta\partial_{t'} C(t,t') \overset{FDT}{=} R(t,t') \tag{2.137}$$

We are ready to look at the equilibrium dynamics of the mixed p-spin spherical model. Putting together 2.127,2.133,2.134 and using TTI and FDT we get:

$$\begin{aligned} \dot{\sigma}(\tau) &= -\mu\sigma(\tau) + \Xi(\tau) - \beta\int_0^\tau ds f'(C(\tau-s))\dot{\sigma}(s) \\ \langle \Xi(\tau)\Xi(0)\rangle &= 2T\delta(\tau) + f'(C(\tau)) \end{aligned} \tag{2.138}$$

where we have used integration by parts and have omitted the subscript $_0$, because all the spins are equivalent after averaging over the quenched disorder. This is the stochastic equation of motion that describes the dynamics of a typical spin in equilibrium at β.

2.5.2 Equations for Correlation and Response

Given the dynamical equations just defined in 2.135, we write the corresponding equations for the correlation $C(t,t')$ and the response $R(t,t')$. This is possible since the noise $\Xi(t)$ is Gaussian, and therefore, all correlations can be decomposed in two-points correlations, the so-called Wick theorem (see first chapter [Zin02]). To obtain the equation for $C(t,t') \equiv \langle \sigma(t)\sigma(t') \rangle$, we multiply both sides of (2.135) by $\sigma(t')$ and average over the colored noise Ξ.

$$(\partial_t + \mu)\langle \sigma(t)\sigma(t') \rangle = -\int^t ds f''(C(t,s))R(t,s)\langle \sigma(s)\sigma(t') \rangle + \langle \Xi(t)\sigma(t') \rangle \tag{2.139}$$

Using Wick theorem the last term becomes:

$$\langle \Xi(t)\sigma(t') \rangle = \int ds \langle \Xi(t)\Xi(s) \rangle \langle \frac{\delta \sigma(t')}{\delta \Xi(s)} \rangle = \Big(2T\delta(t-s) + f'(C(t,s)) \Big) R(t',s) \tag{2.140}$$

where we used the fact that the noise Ξ acts as an external field h, and thus $\langle \frac{\delta \sigma(t')}{\Xi(s)} \rangle = \langle \frac{\delta \sigma(t')}{h(s)} \rangle \equiv R(t',s)$. This term gives non-null contributions only for $s < t'$, due to the causality of the response. For the equation of motion of the response $R(t,t')$ we differentiate both sides of (2.135) by $h(t')$, obtaining:

$$(\partial_t + \mu)\langle \frac{\delta \sigma(t)}{\delta h(t')} \rangle = -\int^t ds f''(C(t,s))R(t,s)\langle \frac{\delta \sigma(s)}{\delta h(t')} \rangle + \langle \frac{\delta \Xi(t)}{\delta h(t')} \rangle \tag{2.141}$$

where $\langle \frac{\delta \Xi(t')}{\delta h(t)} \rangle = \delta(t-t')$.
For future reference we also give the formula for the energy:

$$E(t) \equiv \overline{\langle H[\sigma(t)] \rangle} = -\int^t f'(C(t,s))R(t,s)ds \tag{2.142}$$

To close the section, let's discuss the starting condition, which we omitted so far. Let's suppose that the system is at equilibrium at inverse temperature β' until time $t = 0$. Then, both TTI and FDT are satisfied for $t < 0$, and the first part of the integral in (2.139) reads:

$$\begin{aligned} \int_{-\infty}^0 ds f''(C(t,s))R(t,s)C(s,t') &= \beta' \int_{-\infty}^0 ds \partial_s f'(C(t,s))C(s,t') \\ &= \beta' f'(C(t,0))C(0,t') \end{aligned} \tag{2.143}$$

which gives the contribution of the initial β'-equilibrium to the evolution of $C(t,t')$.

2.5.3 Out-of-equilibrium: two Temperature Protocol

In this section we write down the mean-field dynamical equations (MFDE) for the two-temperature protocol, i.e. the system is initially at equilibrium at T', and suddenly at time $t = 0$ a quench brings the thermal bath to the temperature T, at which the system relaxes. We just report (2.139) and (2.141) together with the initial condition (2.143)*:

$$\begin{aligned}\partial_t C_{tt'} =& -\mu_t C_{tt'} + \int_{t'}^{t} f''(C_{ts}) R_{ts} C_{st'} ds \\ &+ \int_0^{t'} \big(f''(C_{ts}) R_{ts} C_{t's} ds + f'(C_{ts}) R_{t's} \big) ds + \beta' f'(C_{t0}) C_{t'0} \\ \partial_t R_{tt'} =& \delta_{tt'} - \mu_t R_{tt'} + \int_{t'}^{t} f''(C_{ts}) R_{ts} R_{st'} ds\end{aligned} \tag{2.144}$$

where $\mu_t = T + \int_0^t \big(f''(C_{ts}) R_{ts} C_{ts} ds + f'(C_{ts}) R_{ts} \big) ds + \beta' f'(C_{t0}) C_{t0}$, in order to enforce the spherical constraint. $\delta_{tt'}$ is the Dirac delta. These equations have a hidden arbitrary time scale, but for simplicity we have chosen to fix it with the normalization $\lim_{t \to t'} \partial_t C_{tt'} = -T$.

These equations where first reported in [FP95] in the context of state following. Initiating the system at infinite temperature ($\beta' = 0$), one retrieves the MFDE from random initial condition studied in [CHS93; CK93].

This closed set of integro-differential equations in C and R can be integrated numerically and studied analytically in different asymptotic regimes.

*here we change the notation from (s,t) to $_{st}$ for compactness

Section References

[Ago+17] Elisabeth Agoritsas et al. "Out-of-equilibrium dynamical mean-field equations for the perceptron model". In: *arXiv:1710.04894 [cond-mat]* (2017).

[CHS93] A. Crisanti, H. Horner, and H.-J. Sommers. "The spherical p-spin interaction spin-glass model". en. In: *Zeitschrift für Physik B Condensed Matter* 92.2 (1993).

[CK93] L. F. Cugliandolo and J. Kurchan. "Analytical Solution of the Off-Equilibrium Dynamics of a Long Range Spin-Glass Model". In: *Physical Review Letters* 71.1 (1993).

[FM94] Silvio Franz and Marc Mézard. "On mean field glassy dynamics out of equilibrium". en. In: *Physica A: Statistical Mechanics and its Applications* 210.1 (1994).

[FP95] S. Franz and G. Parisi. "Recipes for metastable states in Spin Glasses". In: *Journal de Physique I* 5.11 (1995).

[MPV87] M. Mezard, G. Parisi, and M. Virasoro. *Spin Glass Theory and Beyond: An Introduction to the Replica Method and Its Applications*. en. World Scientific Publishing Company, 1987.

[Zin02] Jean Zinn-Justin. *Quantum Field Theory and Critical Phenomena*. en. Clarendon Press, 2002.

[Zwa01] Robert Zwanzig. *Nonequilibrium Statistical Mechanics*. en. Oxford University Press, 2001.

2.6 Equilibrium Dynamics

In this section, we focus on the equilibrium dynamics of p-spin spherical models. In equilibrium, pure and mixed models do not show any substantial difference. As it has been already remarked in the first chapter, the p-spin spherical model was indeed introduced in the attempt to build a static interpretation of the Mode-Coupling theory [KT87a]. A comprehensive treatment of the equilibrium dynamics of the pure p-spin model can be found in [CHS93]. The equation of motion for correlation of spins has exactly the form of a *schematic* MCT:

$$\dot{C}(\tau) = -TC(\tau) - \beta \int_0^\tau ds f'(C(\tau - s))\dot{C}(s) \tag{2.145}$$

where $\dot{C}(\tau) \equiv \partial_\tau C(\tau)$. This is a 1-dimensional time equation with memory kernel. The only difference with the schematic MCT is in the choice of an overdamped dynamics instead of an inertial one, that is the free propagator, which influences only the short time dynamics. In the following, we will illustrate the major features derived in MCT, illustrating them through the p-spin model. The major aspect of this 1-dimensional equation with memory kernel is the presence of a phase transition by tuning the temperature T. This can be simply understood by taking the $\tau \to \infty$ limit of 2.145 imposing a final overlap $C(\tau \to \infty) = q$:

$$\begin{aligned} \dot{C}(\tau \to \infty) = & -Tq + \beta f(q)(1-q) \\ & - \beta \int_0^\infty ds \big(f'(C(\infty - s)) - f'(q)\big)\dot{C}(s) \end{aligned} \tag{2.146}$$

this is obtained by adding and subtracting the term $\int_0^\tau ds f'(C(\tau))\dot{C}(s)$. The lhs term goes to zero, since the correlation is monotonously decreasing and low bounded. The last term on the rhs goes to zero, since it is a convolution of two monotonously fast decreasing functions with lower bound 0. Thus, we obtain $Tq = \beta f(q)(1-q)$,which is exactly the equation found from static calculation of the equilibrium overlap inside a state, both with the Franz-Parisi method (2.73) and with the Monasson method for $x = 1$ (2.109), with a coupling transition temperature T_{MCT} above which the system is ergodic, and below which it partitions in an exponential (in N) number of states (see fig. 2.6). All curves shown are obtained by numerical integration of (2.145) using the rescaling-time method presented in appendix A.6. The development of the plateau corresponds to the slowing down dynamics of supercooled liquid, and it has some very remarkable algebraic properties that can be obtained by Laplace transforming

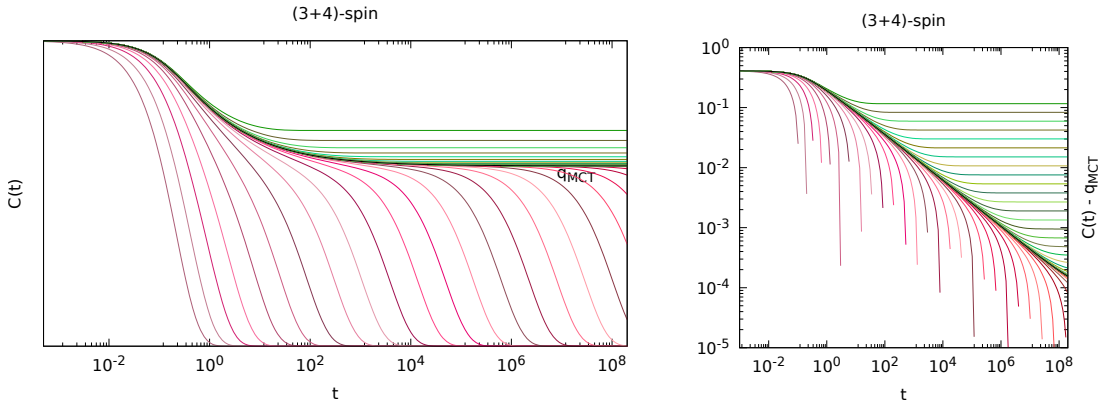

Figure 2.12: Slowing down of the dynamics near T_{MCT}. Correlation C(τ) vs time, both in the ergodic phase (red curves) and in the partitioned phase (green curves). Temperatures are taken as $(T - T_{MCT})/T_{MCT} = \pm 1/2^k$

equation 2.145:

$$(z\widetilde{C}(z) - C(0)) = -\beta^{-1}\widetilde{C}(z) - \beta\widetilde{f}'(z)(z\widetilde{C}(z) - C(0)) \tag{2.147}$$

where $\widetilde{C}(z) = \int_0^\infty dt C(t)e^{-zt}$ is the Laplace transform, of the correlation and $\widetilde{f}'(z) = \int_0^\infty dt f'(C(t))e^{-zt}$ is the Laplace transform of the kernel function. And we have used standard properties of Laplace transform. We then notice that upon defining a time scale τ_0, the previous equation shows an explicit dependence on it:

$$(z\widetilde{C}(z) - 1)(1 + \beta\widetilde{f}'(z)\tau_0) = -\beta^{-1}\widetilde{C}(z)\tau_0 \tag{2.148}$$

we also used the identity $C(0) = 1$. In the limit of small times $\tau_0 \to 0$ or equivalently large temperature T ($\beta \to 0$) the system shows an exponential relaxation:

$$\widetilde{C}(z) = \frac{1}{(z + \beta^{-1}\tau_0)} \qquad \Rightarrow \qquad C(t) = \exp(-z^*) \qquad z^**= \beta^{-1}\tau_0 \tag{2.149}$$

which corresponds to a simple pole z^* in the negative z-axis. Each pole in the Laplace transformed functions corresponds to a specific time scale. And a pole that touches $z = 0$ axis, defines a diverging time scale. How the poles approach $z = 0$ defines the critical dynamics, a little bit in the same sense as in critical static transition. The main goal is to find the dependence of each pole z^* of $\widetilde{C}(z)$ on external parameters, which in our case are the temperature and the same form of the kernel f' (polynomial coefficients). Here, we concentrate on the critical dynamics of a single plateau (for

multiple see [CLP11]) and expose the results that where originally obtained in two capital papers of MCT [Leu84; BGS84], in which it was shown that this critical dynamics exhibits a simple relation, connecting power law exponents, approaching and leaving the plateau.
When one takes $\tau_0 \to \infty$, it is as if observing the system at long time scales, and equation 2.148 becomes:

$$\begin{aligned} \beta^2 \widetilde{f}'(z) &= \frac{\widetilde{C}(z)}{(1 - z\widetilde{C}(z))} \\ &= \frac{1}{z}\big((1 - z\widetilde{C}(z))^{-1} - 1\big) \end{aligned} \tag{2.150}$$

At this point we consider the correlation $C(t)$ near criticality, when it has developed a 'well defined' plateau of value q^*:

$$C(t) = q^* + \delta C(t) \Longrightarrow \widetilde{C}(z) = q^*/z + \widetilde{\delta C}(z) \tag{2.151}$$

where $\delta C(t)$ are small deviations from the plateau and $\widetilde{\delta C}(z)$ its transformed counterpart. While for the kernel function:

$$\begin{aligned} f'(C(t)) = f'(q^*) + \delta f'(t) \Longrightarrow \widetilde{f}'(z) &= \frac{f'(q^*)/z}{z} + \widetilde{\delta f}'(z) \\ &= \frac{f'(q^*)/z+}{z} + \frac{1}{z}\sum_{k=1}^{\infty} \frac{f^{(k+1)}(q^*)}{k!} z^k \widetilde{\delta C^k}(z) \end{aligned} \tag{2.152}$$

where $\widetilde{\delta C^k}(z) = \int_0^\infty ds \delta C(t)^k e^{-zt}$. This allows us to rewrite (2.150) as:

$$\begin{aligned} \beta^2\Big(\frac{f'(q^*)}{z} + \widetilde{\delta f}'(z)\Big) &= \frac{1}{z}\Big(\frac{1}{(1-q)(1 - \frac{z\widetilde{\delta C}(z)}{(1-q)})} - 1\Big) \\ \beta^2\Big(\frac{f'(q^*)}{z} + \sum_{k=1}^{\infty} \frac{f^{(k+1)}(q^*)}{k!} z^k \widetilde{\delta C^k}(z)\Big) &= \frac{1}{z}\Big((1-q)\big(\sum_{k=0}^{\infty}(\frac{z\widetilde{\delta C}(z)}{1-q})^k\big) - 1\Big) \end{aligned} \tag{2.153}$$

Both sides of this equation can be compared order by order in z. The order z^{-1} corresponds to poles and gives the usual equation for the equilibrium overlap already found at (2.146):

$$\beta^2 f'(q^*) = q^*/(1 - q^*) \tag{2.154}$$

The order z^0 gives the equation:

$$\beta^2 f''(q^*)\widetilde{\delta C}(0^+) = (1 - q^*)^{-2}\widetilde{\delta C}(0^+) \tag{2.155}$$

which is the marginal condition. Thus, we see that small fluctuations around the plateau are possible for arbitrary $\widetilde{\delta C}$, whenever the dynamics is marginal. Thus, the two smallest orders in z have fixed the dynamics to have the mode-coupling overlap q_{MCT} (see section 2.2.2). Finally, if we look at the order z^1 we obtain the equation:

$$\beta^2 \frac{f'''(q_{MCT})}{2} \widetilde{\delta C^2}(0^+) = (1 - q_{MCT})^{-3} \widetilde{\delta C}^2(0^+) \tag{2.156}$$

This defines a relation between the Laplace transform of the first and second moment of the correlation fluctuation $\delta C(t)$. In the literature $\lambda \equiv \widetilde{\delta C}^2(0^+)/\widetilde{\delta C^2}(0^+)$ is the exponent parameter. The critical behavior (diverging plateau) suggests a power-law ansatz for the relaxation to the plateau $\delta C(t) \propto t^{-a}$ with $a > 0$, both above and below T_{MCT} and a second power law $\delta C(t) \propto -t^b$ with $b > 0$, in the ergodic phase. Doing the Legendre transform of these power laws, we find the exponent parameter:

$$\lambda = \frac{\widetilde{\delta C}^2(0^+)}{\widetilde{\delta C^2}(0^+)} = \frac{\Gamma(1-a)^2}{\Gamma(1-2a)} = \frac{\Gamma(1+b)^2}{\Gamma(1+2b)} \tag{2.157}$$

On the other side, using the value of λ is defined by the model as (see 2.156):

$$\lambda_f = \frac{1}{2\beta} \frac{f'''(q_{MCT})}{f''(q_{MCT})^{3/2}} = \frac{f'''(q_{MCT}) f'(q_{MCT})}{2 q_{MCT} f''(q_{MCT})^2} \tag{2.158}$$

where the subscript $_f$ recalls the dependence on the model. In fig. 2.6 the implicit evaluation of a, b for different models are shown. We notice, by the way, that the initial declaration of this section, remarking that the equilibrium dynamics do not show substantial difference between mixed and pure models, is not completely true. In fact, for pure models $q_{MCT} = \frac{p-1}{p-2}$ (see section 2.2.2) which plugged in (2.158) gives $\lambda_p = 1/2$ for every number of p-body interactions. This gives two universal (in pure models) exponents $a_p = 0.395(2)$ and $b_p = 1$. Vice versa in mixed models, these two coefficients depend explicitly on the chosen model and satisfy the bounds $a_m < 0.395(2)$ and $b_m < 1$. In fig. 2.6 we show a direct comparison of the analytic results and the numeric integrations, both in pure 3-spin and in mixed 3+4-spin models. Other two power laws directly connected with a, b come from the divergence, by changing the temperature of the time scale to get to the plateau $\tau_a = (T - T_{MCT})^{-\gamma_a}$, and to get out of it $\tau_b = (T - T_{MCT})^{-\gamma_b}$. The first exponent is found by a simple argument. Near the plateau we have that $\delta C \propto t^{-a}$, but from (2.154) one can also see that a change in $\delta\beta$ around β_{MCT} causes a change in the plateau's height $\delta q \propto \delta\beta^{1/2}$. Comparing δC and δq we find the relation $\gamma_a = \frac{1}{2a}$. The second one

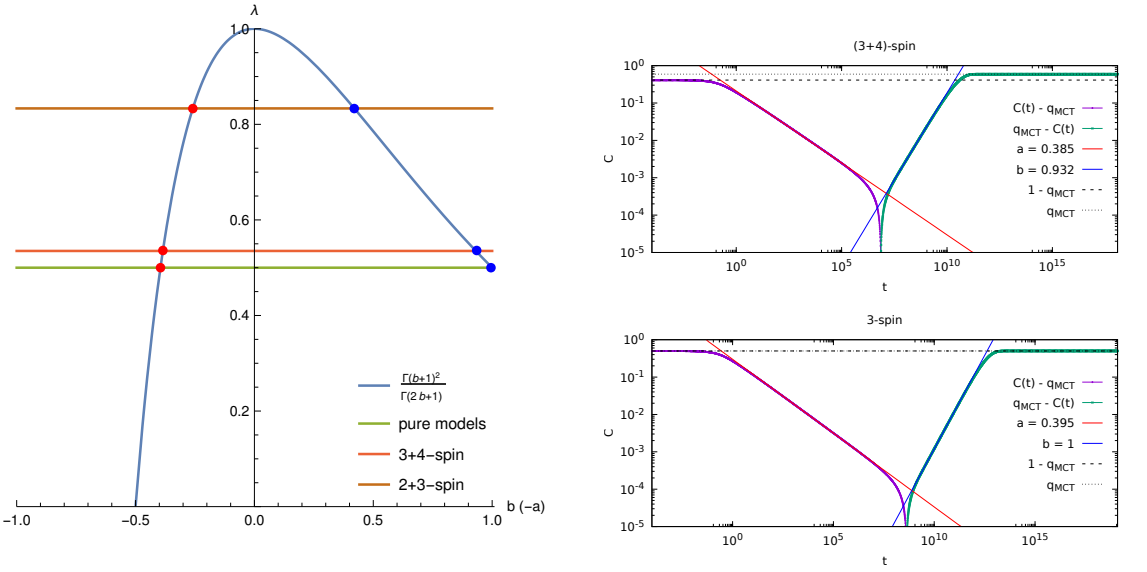

Figure 2.13: On the left side the theoretical prediction of power law exponents has the intersection of the universal function $\frac{\Gamma(1+x)^2}{\Gamma(1+2x)}$ and the exponent parameter of different models: $\lambda_p, \lambda_{3+4}, \lambda_{2+3}$. On the right, side the comparison of the theoretical predicted exponent with the numerically integrated dynamics for 3 and 3+4 models.

can be found to be $\gamma_b = \frac{1}{2a} + \frac{1}{2b}$ (see [Leu84; BGS84] for a proof). To resume, the equilibrium dynamics presents critical points that correspond to 0-poles of the Laplace transformed correlation. In 1RSB models there is only one possible critical point that is by definition at T_{MCT}. Near criticality from the ergodic phase, the correlation function presents four regimes. One initial exponential relaxation from the initial configuration, which defines the microscopic scale of the dynamics. Then a long power law approach to the overlap $\approx q_{MCT}$ of a quasi-state with a power law t^{-a}. After that, it finds a small path to decorrelate and a second power law relaxation $-t^b$ from the plateau begins. Finally, the system reaches a timescale for which the dynamics is ergodic and the relaxation is again exponential. Let's point out that also for the plateau development, there is a correspondence between dynamics and static. It was found in [Cal+12] that near T_{MCT} and around states of overlap q_{MCT} the fluctuations in the replicon sector (see section 2.1.5) give the long time fluctuations around the plateau and λ is statically defined in the replica space as the ratio between third moments [Fer+12]:

$$\lambda_{static} = \frac{(\sum_{ab} \delta^R q_{ab})^3}{\sum_{ab} \delta^R q_{ab}^3} \quad \Longleftrightarrow \quad \lambda_{dynamics} = \frac{\widetilde{\delta C}^2(0^+)}{\widetilde{\delta C^2}(0^+)} \tag{2.159}$$

This is another important step in the static-dynamics connection. To conclude a final remark, all the dynamical analysis presented here, were already carried out in the MCT papers [Leu84; BGS84] for an equation of motion that is exactly that of the 3-spin spherical model, even though the p-spin spherical model had not yet been introduced!

Section References

[BGS84] U. Bengtzelius, W. Gotze, and A. Sjolander. "Dynamics of supercooled liquids and the glass transition". en. In: *Journal of Physics C: Solid State Physics* 17.33 (1984).

[Cal+12] F. Caltagirone et al. "Critical Slowing Down Exponents of Mode Coupling Theory". In: *Physical Review Letters* 108.8 (2012).

[CHS93] A. Crisanti, H. Horner, and H.-J. Sommers. "The spherical p-spin interaction spin-glass model". en. In: *Zeitschrift für Physik B Condensed Matter* 92.2 (1993).

[CLP11] Andrea Crisanti, Luca Leuzzi, and Matteo Paoluzzi. "Statistical mechanical approach to secondary processes and structural relaxation in glasses and glass formers". In: *The European Physical Journal E* 34.9 (2011).

[Fer+12] U. Ferrari et al. "Two-step relaxation next to dynamic arrest in mean-field glasses: Spherical and Ising p-spin model". In: *Physical Review B* 86.1 (2012).

[KT87a] T. R. Kirkpatrick and D. Thirumalai. "Dynamics of the Structural Glass Transition and the p-Spin—Interaction Spin-Glass Model". In: *Physical Review Letters* 58.20 (1987).

[Leu84] E. Leutheusser. "Dynamical model of the liquid-glass transition". In: *Physical Review A* 29.5 (1984).

2.7 Out of Equilibrium Dynamics

In this section, we consider the out-of-equilibrium dynamics, which is probably the only convenient way to describe most amorphous materials. In the previous sections we have seen how to write the mean-field dynamical equations (MFDE) for the correlation and response and use them to study the equilibrium dynamics of the model. Here instead, we consider one particular kind of out-of-equilibrium dynamics, the two temperature protocol dynamics. The system is prepared at a *parent* temperature T', and after a sudden change of temperature, it relaxes at the *bath* temperature T. We focus on the overdamped Langevin dynamics, but similar results are expected to hold for different short time dynamics. As we have seen in section 2.2, it is possible to define a static free energy (Franz-Parisi potential) which, with a quasi equilibrium approach, is capable of *following states* from equilibrium, to some other temperature. The dynamics we are now considering reflects the same preparation protocol. Let's start by considering a system prepared in a state with $T_K < T < T_{MCT}$. Whenever the temperature jump is small enough, the dynamics will quickly relax to a new equilibrium inside the initial state, following exactly the previsions of the FP potential. However, if the temperature jump is big enough, the initial state can be forgotten. There are two main possibilities: increasing or decreasing temperature. In the first case, the system melts into the paramagnetic state. This case is simple in the sense that the paramagnetic state is one and the melting point is just a standard spinodal point. In the latter case, the state can be lost in the sense that we do not have the right tools to describe its asymptotic dynamics. If now we consider a system that is initially equilibrated in the ergodic phase $T' > T_{MCT}$, it will quickly relax if the second temperature remains greater than T_{MCT}, and if $T < T_{MCT}$, it will have a very slow dynamics, showing *aging* behavior.

2.7.1 Two Temperature Protocol: Following States

Our point of departure is the two temperature mean-field dynamical equation (MFDE) (2.144). We wish to understand where the system goes, after a small temperature jump. For that we have two paths, the analytic search for the asymptotic dynamics as in the equilibrium case, and the direct integration of the MFDE. Let's start by the analytical search. The system is prepared in equilibrium inside a state between T_K and T_{MCT} and relaxed at the second temperature T which is not 'too far' from the original one. Since the perturbation is 'small' - later on we will see that this works also for large perturbations in many cases - we assume that there will be a fast transient dynamics to a new equilibrium inside the state. Acthung, the so reached

state is not a typical equilibrium state at temperature T, but it is just a *followed state* typical at T'. In terms of dynamics, the system gets fast (time $\approx \delta t$) to a new stationary regime which respects the local equilibrium assumption of fluctuation dissipation theorem (FDT), i.e. $R_{tt'} = \beta \partial_{t'} C_{tt'}$. Therefore, from (2.144) we obtain one single equation of motion for the correlation:

$$\begin{aligned} \partial_t C_{tt'} = &- \mu_t C_{tt'} + \beta \int_{t'}^{t} f''(C_{ts}) \partial_s C_{ts} C_{st'} ds \\ &+ \beta \int_{\delta t}^{t'} \big(f''(C_{ts}) \partial_s C_{ts} C_{t's} ds + f'(C_{ts}) \partial_s C_{t's} \big) ds + \beta' f'(C_{t0}) C_{t'0} \end{aligned} \tag{2.160}$$

and $\mu_t = T + \beta \int_{\delta t}^{t} \big(f''(C_{ts}) \partial_s C_{ts} C_{ts} ds + f'(C_{ts}) \partial_s C_{ts} \big) ds + \beta' f'(C_{t0}) C_{t0}$. We have neglected any contribution to the integrals coming from transient dynamics, i.e. from times smaller than δt, and we have used FDT from time δt. Going on with one partial integration and recognizing some exact differentials:

$$\begin{aligned} \partial_t C_{tt'} = &- \mu_t C_{tt'} + \beta f'(C_{ts}) C_{t's} \big|_{t'}^{t} - \beta \int_{t'}^{t} f'(C_{ts}) \partial_s C_{st'} ds \\ &+ \beta f'(C_{ts}) C_{t's} \big|_{\delta t}^{t'} + \beta' f'(C_{t0}) C_{t'0} \end{aligned} \tag{2.161}$$

with $\mu_t = T + \beta f'(C_{ts}) C_{ts} \big|_{\delta t}^{t} + \beta' f'(C_{t0}) C_{t0}$. We finally define the asymptotic correlation:

$$\lim_{\substack{t,t' \to \infty \\ t - t' = \tau}} C_{tt'} = C_\tau \tag{2.162}$$

together with the limiting values $\lim_{t\to\infty} C_{t0} = p$, which defines the average overlap between the asymptotic configuration and starting configuration which sampled at temperature T' and $\lim_{\tau\to\infty} C_\tau = q$ which defines the equilibrium overlap inside the *followed state*.

$$\partial_\tau C_\tau = - T C_\tau + \big(\beta' f'(p) p - \beta f(q) q \big)(1 - C_\tau) - \beta \int_0^\tau f'(C_{\tau - s}) \partial_s C_s ds \tag{2.163}$$

where we have used $\lim_{t\to\infty} \mu_t = T + \beta f(1) 1 - \beta f(q) q + \beta' f(p) p$. We note the resemblance with the equilibrium equation (2.145). There is one additional term $\big(\beta' f'(p) p - \beta f(q) q \big)(1 - C_\tau)$ which couples the dynamics with the starting configuration. With the same add-subtract trick used for the equilibrium dynamics, we can evaluate the asymptotic limit:

$$\begin{aligned} \lim_{\tau\to\infty} (2.163) \qquad \Longrightarrow \qquad & T q = \big(\beta' f'(p) p - \beta f(q) q \big)(1 - q) - \beta f'(q)(1 - q) \\ & \frac{T}{1 - q} = \mu_{ag} \end{aligned} \tag{2.164}$$

where we have introduced the *aging* parameter:

$$\mu_{ag} \equiv \lim_{t\to\infty} \mu_t - \beta f'(C_{ts})|_{\delta t}^{t} = T + \beta f(q)(1-q) + \beta' f'(p)p \tag{2.165}$$

which will have a clear interpretation in the aging dynamics (next section). Still, we need to have another equation to find both p and q. This comes directly from the definition of $p = \lim_{t\to\infty} C_{t0}$. The equation (2.160) for the correlation with the starting configuration reads:

$$\begin{aligned}\partial_t C_{t0} =& -\mu_t C_{t0} + \beta \int_{\delta t}^{t} f''(C_{ts})\partial_s C_{ts} C_{s0} ds + \beta' f'(C_{t0}) C_{00} \\ =& -\mu_t C_{t0} + \beta f'(C_{ts})|_{\delta t}^{t} C_{t0} + \beta' f'(C_{t0}) \\ \approx& -\mu_{ag} C_{t0} + \beta' f'(C_{t0})\end{aligned} \tag{2.166}$$

where the second line is obtained by using the add-subtract trick:

$$\int_{\delta t}^{t} f''(C_{ts})\partial_s C_{ts}\big(C_{s0} - C_{t0}\big) ds + \beta f'(C_{ts})|_{\delta t}^{t} C_{t0}$$

and considering again that both $\lim_{s\to t}(C_{s0} - C_{t0})$ and $\lim_{s\to 0} f''(C_{ts})\partial_s C_{ts}$ go to zero fast enough. Evaluating the asymptotic limit we get:

$$\lim_{\tau\to\infty}(2.166) \qquad \Longrightarrow \qquad \mu_{ag} p = \beta' f'(p) \tag{2.167}$$

We finally have two equations, (2.164) and (2.167). These two equations define implicitly q and p for any given β and β', but more incredibly they are equivalent to the equations found by the static computation of the constrained FP free energy. Thus, the FP construction is not only capable of selecting equilibrium states, but also, to follow them in temperature.

To support this calculations, it is possible to directly integrate numerically the equations (2.144). I have used two different algorithms, that can reach times of the order of 10^3 (in normal time units) to be confronted with 10^{10} or more, reachable with the equilibrium algorithm (for more details see appendix A.7). Both algorithms agree on the results and the time scale reached is large enough to observe the fast relaxing dynamics we are considered here. Since the equations that define followed states have been already studied in section 2.2, let's bring back the so obtained temperature phase diagram for the 3+4 model, shown for convenience in fig. 2.14. And we focus on following states initially thermalized at $T = 0.802$. In the figure, the integrated energies and the correlations are shown for different final temperatures T. In the following state region they perfectly match analytical asymptotic limits. Moreover, the temperature at which the minima are lost (marginal condition), corresponds to a critical dynamics (power-law) as shown in the log-log inset on the right. The same integration check was firstly performed in [FP95], and confirmed in [BBM96].

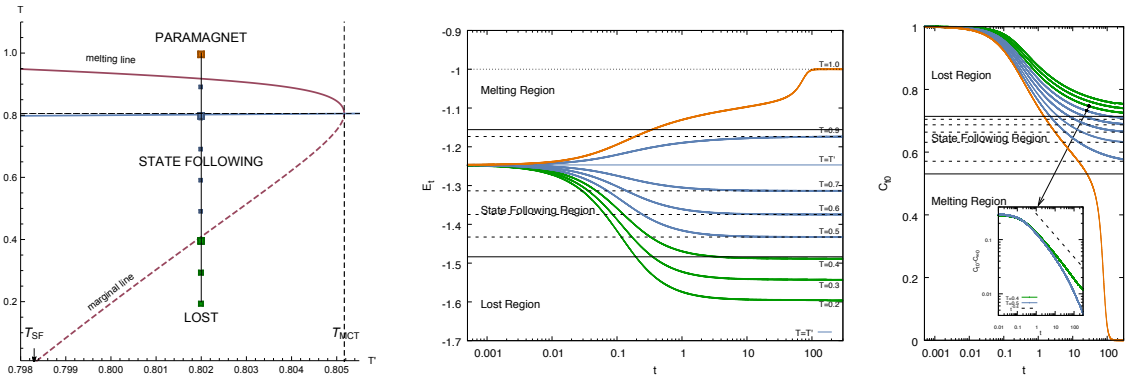

Figure 2.14: Following states in the mixed (3+4)-spin model. Comparison between asymptotic calculation (or FP potential) and numerical integration. Different protocol with the same parental temperature $T' = 0.802$ are considered. (**left**): phase diagram in the (T', T) plane. (**center**): time evolution of the energy for different bath temperatures T. The dashed lines corresponds to analytical results. (**right**): correlation with the starting configuration versus time. The inset shows the power law behavior near the marginal bound.

2.7.2 Two Temperature Protocol: Aging

In this section, we consider the asymptotic dynamics in the aging regime, i.e. for parent temperature $T' > T_{MCT}$ and bath temperature $T < T_{MCT}$. The particular case of random initial condition ($T' = \infty$) in the pure p-spin model was successfully analyzed by L.F.Cugliandolo and J.Kurchan in 1993 [CK93], fixing the first milestone in the analytical treatment of out-of-equilibrium dynamics. Here, we revisit their calculation by introducing the parent temperature T'. Again, our starting points are the equations for the correlation and the response (2.144). In order to understand how these equations behave in the long-time limit, we re-parametrize this time in terms of the correlation [CK94; CK95]. This method directly forecasts the asymptotic overlaps. To understand the idea, we start by a simple asymptotic calculation for the energy (see 2.142):

$$\begin{aligned} \lim_{t\to\infty} E_t &= \lim_{t\to\infty} -\int_0^t f'(C_{ts}) R_{ts} ds - \beta' f(C_{t0}) \\ &= -\beta \int_p^1 dC X(C) \partial_C [f(C)] - \beta' f(p) \end{aligned} \tag{2.168}$$

the first line is simply the definition of energy given in (2.142). The second line shows the re-parametrization $t \to C$. Behind it there is the generalization of the fluctuation-dissipation theorem to different time sectors:

$$\chi_{tt'} = \beta X(C_{tt'}) C_{tt'} \tag{2.169}$$

where $\chi_{tt'} = -\int_{t'}^{t} ds R_{ts}$ is the integrated response and X is the so called fluctuation dissipation ratio (FDR). The fact that X depends on times t, t' only through the correlation C is true in the asymptotic limit $t, t' \to \infty$. The way the two times are diverging, one regarding the other, defines the *time sector* (TS) that we are considering.

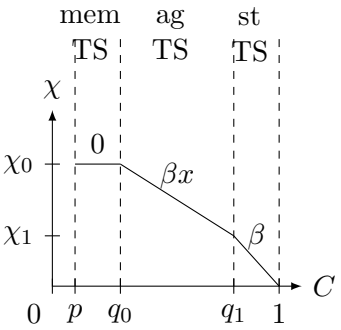

For example the *stationary TS* (stTS) for the correlation reads:

$$\lim_{\substack{t,t'\to\infty \\ t-t'=\tau}} C_{tt'} = C_\tau \qquad X(C_\tau) = 1 \qquad q_1 < C_\tau < 1 \tag{2.170}$$

$q_1 \equiv \lim_{\tau\to\infty} C_\tau$ defines the asymptotic limit within the stationary TS. This is the FDT regime that we already considered in the previous section for the following state construction, but now it is just one of the many possible TSs. Then we consider the *aging TS* (agTS):

$$\lim_{\substack{t,t'\to\infty \\ t/t'=\lambda}} C_{tt'} = C_\lambda \qquad X(C_\lambda) = x < 1 \qquad q_0 < C_\lambda < q_1 \tag{2.171}$$

where $q_1 = \lim_{t/t'\to 1} C_\lambda$ and $q_0 = \lim_{t/t'\to\infty} C_\lambda$ are the correlation bounds in this TS. The fluctuation dissipation ratio x which gives an effective temperature $T_{eff} = 1/(\beta x)$ greater than the bath temperature. We finally introduce the *memory TS* (memTS) which considers the asymptotic correlation with the initial configuration:

$$\lim_{t\to\infty} C_{tt'} = C_{\infty t'} \qquad X(C_{\infty t'}) = 0 \qquad p < C_{\infty t'} < q_0 \tag{2.172}$$

with $p = \lim_{t'\to\infty} C_{\infty t'}$. In general, there can be many TSs and even an infinity [CK94] , but our focus will only be on three, which is believed to be the right ansatz for a RFOT model. Within these three TS construction we can finally rewrite the energy (2.168) as:

$$\lim_{t\to\infty} E_t = -\beta\big(f(1) - f(q_1)\big) - \beta x\big(f(q_1) - f(q_0)\big) - \beta' f(p) \tag{2.173}$$

The same asymptotic limit can be taken for the Lagrange multiplier:

$$\begin{aligned} \mu_\infty &= \lim_{t\to\infty} \Big(T + \int_0^t f''(C_{ts}) R_{ts} C_{ts} ds + \int_0^t f'(C_{ts}) R_{ts} ds + \beta' f'(C_{t0}) C_{t0} \Big) \\ &= T + \beta \int_p^1 dC X(C) \partial_C [f'(C) C] + \beta' f'(p) p \\ &= T + \beta\big(f'(1) - f'(q_1) q_1\big) + \beta x\big(f'(q_1) q_1 - f'(q_0) q_0\big) + \beta' f'(p) p \end{aligned} \tag{2.174}$$

Now we consider to the asymptotic behavior of the correlation C. The idea is to recast the equation from times (t, t', s) to correlations (C, C', C''), and then to study the different TSs. Each TS has its own equations of motion and its own lower and upper bound. Each bound of each TS must match the bounds of the nearby TSs, which defines a cascade of equations to fix all free parameters. To clarify, let's focus on the RFOT for which we assume a three TS ansatz. There will be four equations which fix the four parameters q_1, q_0, p, x: One equation comes from the $\lim_{\tau\to\infty} C_\tau$ in the stationary TS, one from $\lim_{t/t'\to\infty} C_{t/t'}$ in the aging TS, one from the memory TS $\lim_{t'\to 0} C_{\infty t'}$. The last equation will come from the equation for the response R. In the following, we will write the equations of motions in these three TSs and retrieve all the aforementioned asymptotic equations. We first recast the equation for the correlation (2.144):

$$\begin{aligned}
\partial_t C_{tt'} =& -\mu_t C_{tt'} + \beta' f'(C_{t0}) C_{t'0} \\
&+ \int_0^{t'} (f''(C_{ts}) R_{ts} C_{t's} ds + f'(C_{ts}) R_{t's}) ds \\
&+ \int_{t'}^{t} f''(C_{ts}) R_{ts} C_{st'} ds \\
\lim_{t,t'\to\infty} & \\
dC =& -\mu_\infty C + \beta' f'(p) p \\
&+ \beta \int_p^C (f''(C') X(C') C''(C,C') + f'(C') X(C''(C,C')) \frac{dC''}{dC'}) dC' \\
&+ \beta \int_C^1 f''(C') X(C') C''(C,C') dC'
\end{aligned} \tag{2.175}$$

where we used the following substitutions:

$$C_{tt'} \to C \qquad C_{ts} \to C' \qquad C_{t's} \to C''$$

$C''(C, C') = \lim_{t,t',s\to\infty} C_{t's}(C_{tt'}, C_{ts})$, is the asymptotic limit of a map that, given the correlation $C_{tt'}$ and C_{ts}, returns the correlation $C_{t's}$. This is a formal way of eliminating the time dependence. It can be shown that this limit is well defined and it has an ultrametric structure in the correlation [CK94], which in formula:

$$C''(C, C') = \min(C, C') \qquad \Longleftrightarrow \qquad \underset{\text{belongs to different TSs}}{C \text{ and } C'} \tag{2.176}$$

This is the decoupling of TSs and it physically means that faster degrees of freedom see the slower ones as quenched (Heisenberg decoupling electron-nucleus dynamics). Let's analyze one by one the three TSs.

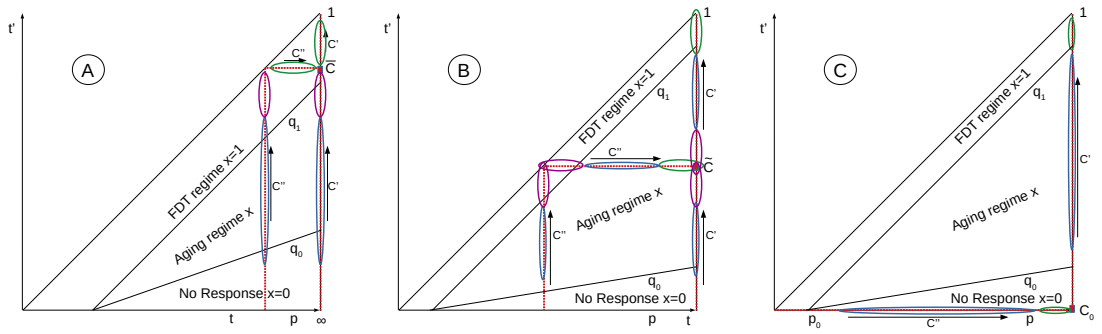

Figure 2.15: Schematic representation of the decoupling approximations in the integration that leads to specific asymptotic equations in each time sector (TS). On the axis the time t, on the y-axis the waiting time t'. The dotted red lines mark the integration path. The right-most line is over $C_{ts} = C'$, while the left-most is over $C_{t's} = C''$. (**A**): Stationary TS, $q_1 < \bar{C} < 1$. (**B**): Aging TS, $q_0 < \tilde{C} < q_1$. (**C**): Memory TS, $p < \tilde{C} < p_0$

.

A) Stationary Time Sector $q_1 < \bar{C} < 1$, $X(\bar{C}) = 1$

$$d\bar{C} = \begin{cases} -\mu_\infty \bar{C} \\ \beta' f'(p) p \\ \beta \int_p^{q_0} (f''(C')X(C')C'' + f'(C')X(C'')\frac{dC''}{dC'})dC' \approx 0 \\ \beta x \int_{q_0}^{q_1} \partial_{C'}[f'(C')C']dC' = \beta x\big(f'(q_1)q_1 - f'(q_0)q_0\big) \\ \beta \int_{q_1}^{1} \partial_{C'}[f'(C')C'']dC' = \beta\big(f'(1)\bar{C} - f'(q_1)q_1\big) \\ -\beta \int_{\bar{C}}^{1} f'(C')\frac{dC''}{dC'}dC' \end{cases} \tag{2.177}$$

in the third line the assumption is that the memory TS have a FDR $X = 0$, which means no long time response. In the fourth line we used the fact that $\bar{C}$ and C' belong to two different TSs (2.176) and we considers integrating in the aging TS $X(C) = x$. This part of the integration is underlined by a blue ellipse in fig. 2.15 plot A. The part of the integration in the fifth line has the three correlations $\bar{C}, C', C''$ in the same stationary TS where FDT holds, thus $x(C) = 1$. And $C''(\bar{C}, 1) = \bar{C}$ and $C''(\bar{C}, q_1) = q_1$. We have that the evolution of the correlation in the stationary TS reads:

$$d\bar{C} = -T + (\mu_\infty - \beta f'(1))(1 - \bar{C}) - \beta \int_{\bar{C}}^{1} f'(C')\frac{dC''}{dC'}dC' \tag{2.178}$$

Now we look at the asymptotic limit $\bar{C} \to q_1$. Reusing the add-subtract trick (see 2.146) we obtain:

$$T = (\mu_\infty - \beta f'(1) + \beta f(q_1))(1 - q_1) \tag{2.179}$$

which is the first equation of the four needed to fix q_0, q_1, p, x. We recall the definition of $\mu_{ag} = \mu_\infty - \beta f'(q)|_{q_1}^{q_0}$ (given in 2.165) and see that again the stationary regime follows the same law $\mu_{ag} = T/(1-q)$.

B) Aging Time Sector $q_0 < \tilde{C} < q_1$, $X(\tilde{C}) = x$:

$$d\tilde{C} = \begin{cases} -\mu_\infty \tilde{C} \\ \beta' f'(p) p \\ \beta \int_p^{q_0} (f''(C')X(C')C'' + f'(C')X(C'')\frac{dC''}{dC'})dC' \approx 0 \\ \beta x \int_{q_0}^{q_1} \partial_{C'}[f'(C')C'']dC' = \beta x\big(f'(q_1)\tilde{C} - f'(q_0)q_0\big) \\ \beta \int_{q_1}^{1} f''(C')dC'C''[\tilde{C}, C'] \approx \beta\big(f'(1) - f'(q_1)\big)\tilde{C} \\ \beta f'(\tilde{C}) \int_{\tilde{C}-\delta\tilde{C}_{FDT}}^{\tilde{C}} C''[\tilde{C}, C']dC' \approx \beta f'(\tilde{C})\big(1 - q_1\big) \\ -\beta x \int_{\tilde{C}}^{q_1} f'(C')\frac{dC''}{dC'}dC' \end{cases} \tag{2.180}$$

in the third line we assume again FDR $X = 0$ in the memory TS. In the fourth line we are considering the entire aging TS (blue ellipses in plot B of fig.2.15). This is an exact differential. The fifth an sixth lines are approximations given by the decoupling of TS. The slowest are fixed and the fastest one integrated. The equation of motion for the correlation in the aging TS reads:

$$\begin{aligned} d\tilde{C} = &- \Big(\mu_{ag} - \beta x\big(f'(q_1) - f'(q_0)\big)\Big)\tilde{C} + \beta f'(\tilde{C})(1 - q_1) \\ &+ \beta x f'(q_0)(q_1 - q_0) + \beta' p f'(p) \\ &- \beta x \int_{\tilde{C}}^{q_1} (f'(C') - f(q_0))\frac{dC''}{dC'}dC' \end{aligned} \tag{2.181}$$

where we used the definition of μ_{ag} and the add-subtract trick. Evaluating the lowest bound $\tilde{C} \to q_0$:

$$\mu_{ag} q_0 = \beta x\big(f'(q_1) - f'(q_0)\big)q_0 + \beta f'(q_0)(1 - q_1) + \beta x f'(q_0)(q_1 - q_0) + \beta' p f'(p) \tag{2.182}$$

On the other side, the limit $\tilde{C} \to q_1$ gives the equation:

$$\mu_{ag} q_1 = \beta f'(q_1)(1 - q_1) + \beta x\big(f'(q_1)q_1 - f'(q_0)q_0\big) + \beta' p f'(p) \tag{2.183}$$

which is equivalent to equation (2.179). This is just a confirmation that the decoupling of TS is working as it should, i.e. different TSs match at the borders.

C) Memory Time Sector $p < C_0 < q_0$, $X(C_0) = 0$:

This time sector connect the asymptotic dynamics with the initial condition. Thus, in a way it is the most important part in order to understand the long time behavior. To simplify the treatment, we directly explore the bound $C_0 \to p$ from the other side, i.e. $\lim_{t\to\infty} C_{t0} = p$. We rewrite the equation for the correlation:

$$\partial_t C_{t0} = -\mu_t C_{t0} + \beta' f'(C_{t0}) + \int_0^t f''(C_{ts}) R_{ts} C_{s0} ds \tag{2.184}$$

The result in the asymptotic limit reads:

$$0 = -\mu_\infty p + \beta' f'(p) + \beta \int_p^1 f''(C') X(C') C''(C_0, C') dC' \tag{2.185}$$

we obtain:

$$0 = \begin{cases} -\mu_\infty p \\ \beta' f'(p) \\ \beta \int_p^{q_0} f''(C') X(C') C'' dC' \approx 0 \\ \beta x \int_{q_0}^{q_1} \partial_{C'} [f'(C') C''] dC' = \beta x \big(f'(q_1) C''(p, q_1) - f'(q_0) C''(p, q_0) \big) \\ \beta \int_{q_1}^1 f''(C') dC' C''[\tilde{C}, C'] \approx \beta \big(f'(1) - f'(q_1) \big) C_0 \\ -\beta x \int_{q_0}^{q_1} f'(C') \frac{dC''}{dC'} dC' \end{cases} \tag{2.186}$$

the third line comes from assumption $X = 0$ in the memory TS. The fourth line is a exact differential that comes from a partial integration in the aging TS (blue ellipse in fig. 2.15 plot C), and it comes together with line six. The sixth line is the coupling with the stationary TS (violet ellipse). Putting all together we have:

$$\mu_{ag} p = \beta x \big(f'(q_1) p - f'(q_0) p_0 \big) - \beta x f'(q_0)(p - p_0) + \beta' f'(p) \tag{2.187}$$

where we have defined $p_0 \equiv C''(p, q_0)$. In all previous computations the p_0 term has been put to equal to p. In here, we want to precociously let it undefined, because there is no clear argument for this equality. This is the third of four equations to characterize the asymptotic dynamics (if $p = p_0$). We will come back to a possible ansatz for p_0 in the gradient descent dynamics in section 3.1.4.

D) Response in the Aging TS $q_0 < \tilde{C} < q_1$, $X(\tilde{C}) = x$:

We take back the equation for the response (2.144) and rewrite it for the integrate response $\chi_{tt'} = -\int_{t'}^{t} ds R_{ts}$.

$$\begin{aligned} \partial_t \chi_{tt'} =& -\mu_t \chi_{tt'} + \int_{t'}^{t} f''(C_{ts}) \partial_s \chi_{ts} \chi_{ts} ds \\ & \lim_{t,t' \to \infty} \\ \beta x d\tilde{C}_{R} =& -\mu_\infty \beta x \tilde{C}_{R} + \beta^2 \int_{\tilde{C}_R}^{1} f''(C') X(C') X(C'') C''(C, C') dC' \end{aligned} \tag{2.188}$$

where we have used the FDR in the integral form: $\chi = \beta X(C) C$. Evaluating it in the aging TS:

$$d\tilde{C}_{R} = \begin{cases} -\mu_\infty \tilde{C}_{R} \\ \beta x \int_{\tilde{C}_R}^{q_1} \partial_{C'} [f'(C') C''] dC' = \beta x \big(f'(q_1) \tilde{C}_{R} - f'(\tilde{C}_{R}) q_1 \big) \\ \beta \int_{q_1}^{1} f''(C') dC' C''[\tilde{C}_{R}, C'] \approx \beta \big(f'(1) - f'(q_1) \big) \tilde{C}_{R} \\ \beta f''(\tilde{C}_{R}) \tilde{C}_{R} \int_{\tilde{C}_R}^{\tilde{C}_R + \delta \tilde{C}_{RFDT}} dC' \partial_{C'} C''[\tilde{C}_{R}, C'] \approx \beta f''(\tilde{C}_{R}) \tilde{C}_{R} \big(1 - q_1 \big) \\ -\beta x \int_{\tilde{C}_R}^{q_1} f'(C') \frac{dC''}{dC'} dC' \end{cases} \tag{2.189}$$

we have every term by βx. The second line is the exact differential and comes together with the last line. The third and fourth lines come from decoupling of stationary and aging TSs. We finally end with the equation:

$$\begin{aligned} d\tilde{C}_{R} =& -\mu_{ag} \tilde{C}_{R} + \beta f''(\tilde{C}_{R}) \big(1 - q_1 \big) \\ & \beta x \big(f'(q_1) \tilde{C}_{R} - f'(\tilde{C}_{R}) q_1 \big) - \beta x \int_{\tilde{C}_R}^{q_1} (f'(C') - f(q_0)) \frac{dC''}{dC'} dC' \end{aligned} \tag{2.190}$$

This equation in the limit $\tilde{C}_{R} \to q_1$ gives the very "famous" marginal condition:

$$\mu_{ag} = \beta f''(q_1) \big(1 - q_1 \big) \tag{2.191}$$

recalling that $\mu_{ag} = T/(1 - q_1)$. This is not a coincidence, and it comes from the connection between the stationary and the aging TS for the response. Here, we recall that statically, the marginal condition is the one that defines the rupture of a state, which cannot be followed anymore. It comes out in replica calculations as the bound for the stability of the replicon eigenvalue. While dynamically it connects the two TSs. This is the last of the four equations (2.177,2.180,2.184,2.191) necessary to fix all the free parameters p, q_0, q_1, x, which describe the asymptotic dynamics. In the next section, we will describe how the solutions to this equations are found from a static calculation.

2.7.3 Two Temperature Protocol: Static *vs* Dynamics

From the calculation of the previous section, it follows that the asymptotic dynamics of a general two temperature protocol $T' \to T$ can be described by the set of equations:

$$\begin{cases} \frac{1}{\beta(1-q_1)} = T + \beta\big(f'(1) - f'(q_1)q_1\big) + \beta x\big(f'(q_1)q_1 - f'(q_0)q_0\big) + \beta' f'(p)p - \beta\big(f'(1) - f(q_1)\big) \\ \frac{q_0}{\beta(1-q_1)} = \beta x\big(f'(q_1) - f'(q_0)\big)q_0 + \beta f'(q_0)(1-q_1) + \beta x f'(q_0)(q_1 - q_0) + \beta' p f'(p) \\ \frac{p}{\beta(1-q_1)} = \beta x\big(f'(q_1)p - f'(q_0)p_0\big) - \beta x f'(q_0)(p - p_0) + \beta' f'(p) \\ \frac{1}{\beta(1-q_1)} = \beta f''(q_1)\big(1 - q_1\big) \end{cases} \tag{2.192}$$

Where the first line describes the lowest (in correlation) bound of the stationary TS. The second line the lowest bound of the aging TS. The third line the asymptotic memory of the initial condition. And the last is the marginal condition which comes from the response in between stationary and aging TS. These equations (fixing $p_0 = p$) were first introduced by A.Barrat, S. Franz, G. Parisi [Bar97]* with the idea of extending the parallelism between static and dynamics, already introduced with the FP potential [FP95]. The idea was to extend the FP potential from RS to 1RSB to take into account the rupture of the states when followed. The same set of equations (2.192) is then retrieved by minimizing this 1RSB potential with regard to p, q_0, q_1 and to add the marginal condition in order to fix the last parameter x. The same analysis was re-explored later in [Cap+06; Sun+12]. Here, we just want to say that although this correspondence between static and dynamics through the FP potential is rather appealing and it strengthens the approximations in the asymptotic analysis the results only partially match numerical integrations. Thus, we prefer to focus on the results that are "safe" and to postpone the discussion of open problems to the next chapter in which we will focus on $T = 0$ protocols, i.e. gradient descent dynamics.

2.7.4 Two Temperature Protocol: "Classical" Aging

To conclude this section, we focus on the "classical" aging solution, given by L.F.Cugliandolo and J.Kurchan. They have considered random initial conditions that correspond to put $\beta' = 0$ in (2.192). Moreover, they assumed the loss of memory of the initial condition $p = 0$ and what they have named *weak ergodicity breaking*, which stands that for every fixed waiting time t', the system ultimately decorrelates:

$$\lim_{t \to \infty} C_{tt'} = 0 \qquad \forall t' \tag{2.193}$$

*in this paper there is a mistake in the equation for q_0

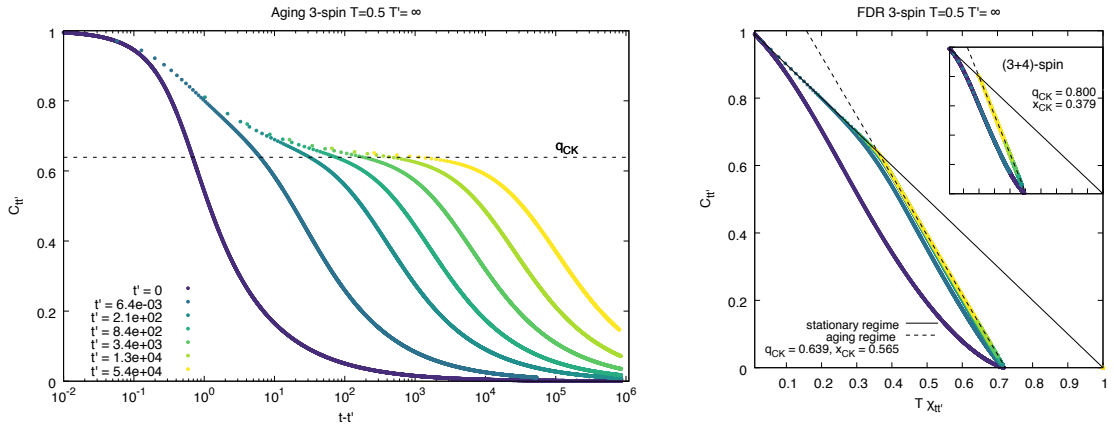

Figure 2.16: (**left**): correlation $C_{tt'}$ plotted versus $t - t'$ for different waiting times t'. More the time passes, more the system gets stuck, showing *aging* behavior. (**right**): violation of the fluctuation dissipation theorem, with the presence of another effective inverse temperature βx which characterize the long relaxation dynamics. The theoretical predictions agrees perfectly with the integration.

that fixes $q_0 = 0$. The system of equation then greatly simplifies:

$$\begin{cases} \frac{1}{\beta(1-q_{CK})} = \beta^{-1} + \beta f'(q_{CK})(1 - q_{CK}) + \beta x_{CK} f'(q_{CK}) q_{CK} \\ \frac{1}{\beta(1-q_{CK})} = \beta f''(q_{CK})\big(1 - q_{CK}\big) \end{cases} \tag{2.194}$$

where we have renamed (q_1, x) as (q_{CK}, x_{CK}) in reference to the authors. In figure 2.16 the integration of the MFDE (2.144) is shown for a thermal bath at $T = 0.5$, starting from a random configuration. The overlap of the asymptotic stationary dynamics q_{CK}, i.e. the plateau that is diverging, is exactly that obtained by the asymptotic calculation. On the right plot the FDR is shown for the same dynamics and the expected x_{CK} is confirmed (in the inset also for the 3+4 model). The two regimes in the FDR plot appear well defined already for small waiting times, indicating that the two TS decouple is rather quickly. Here we note that:

$$x_{CK}(\beta) = x_M(q_{mg}, \beta) \tag{2.195}$$

where x_M is the Monasson parameter defined in (2.109). This is not a coincidence, since we have seen that the asymptotic dynamics can be mapped in the 1RSB FP potential. Which in the case of zero constraint with the reference configuration ($p = 0$) is equivalent to the Monasson construction. Physically, it is saying that the dynamics from random initial condition is going towards the most numerous stable

state at temperature T. In pure models the scenario is further simplified, because the most numerous stable states remain the same at every temperature and corresponds to the inherent structure with energy E_{IS} (see section 2.2). By contrast in mixed models, quenching to different temperatures T selects different asymptotic states. What is even more interesting is that $\beta x_{M} = d\Sigma(f)/df$, i.e. it is the derivative of the complexity by the free energy of the states. This confirms the role of $1/(\beta x)$ as an effective temperature, both statically, as the derivative of an entropy (of states) and dynamically as a fluctuation dissipation ratio:

$$\frac{\tilde{\chi}}{\tilde{C}} = \beta x = \frac{d\Sigma}{df} \tag{2.196}$$

Section References

[Bar97] A. Barrat. "The p-spin spherical spin glass model". In: *arXiv:cond-mat/9701031* (1997).

[BBM96] A. Barrat, R. Burioni, and M. Mézard. "Dynamics within metastable states in a mean-field spin glass". In: *Journal of Physics A: Mathematical and General* 29.5 (1996).

[Cap+06] Barbara Capone et al. "Off-equilibrium confined dynamics in a glassy system with level-crossing states". In: *Physical Review B* 74.14 (2006).

[CK93] L. F. Cugliandolo and J. Kurchan. "Analytical Solution of the Off-Equilibrium Dynamics of a Long Range Spin-Glass Model". In: *Physical Review Letters* 71.1 (1993).

[CK94] L. F. Cugliandolo and J. Kurchan. "On the Out of Equilibrium Relaxation of the Sherrington - Kirkpatrick model". In: *Journal of Physics A: Mathematical and General* 27.17 (1994).

[CK95] L. F. Cugliandolo and J. Kurchan. "Weak-ergodicity breaking in mean-field spin-glass models". In: *Philosophical Magazine B* 71.4 (1995).

[FP95] S. Franz and G. Parisi. "Recipes for metastable states in Spin Glasses". In: *Journal de Physique I* 5.11 (1995).

[Sun+12] YiFan Sun et al. "Following states in temperature in the spherical s+p-spin glass model". In: *Journal of Statistical Mechanics: Theory and Experiment* 2012.07 (2012).

3

Exploring the Landscape through Gradient Descent

3.1 Numerical Integration

This chapter is the most crucial part of this thesis, in here we present the new facts about the dynamics of mixed p-spin models. Throughout all the second chapter, we have explored the major achievements in the analytic analysis of p-spin spherical models, and we have strongly remarked that pure models due to their homogeneity do no represent the general case, but a rather singular subclass of RFOT mean-field models. In particular, the possibility of following states in temperature is not guaranteed in mixed-models: states can be *lost* upon cooling them. Moreover, if the system is prepared in the ergodic phase and relaxed at a low temperature, in pure models the inherent structure energy does not depend on the initial temperature, while in mixed ones it does. Therefore, mixed models can also describe what was often been considered a feature of finite size systems, having *memory* of the ergodic phase.

To gather insight in the importance of mixed models as a mean-field prototype of super-cooled liquid, here we consider an extreme case dynamics, the GD dynamics in the energy landscape. This dynamics is theoretically important, because it is directly connected to the search of IS of the energy landscape. Thus, we do the inverse of the usual reasoning. To gather information about the landscape, we explore the dynamics. In the following, we fully characterize this gradient descent (GD) dynamics, which is studied by integrating MFDE at zero temperature T of the bath and then varying the parent temperature T'. We obtain that, by contrast to pure models, mixed models present the emergence of a new phase that presents memories

of the initial condition together with aging effects.

3.1.1 Under-threshold Dynamics

Let's start by what has been the initial 'bizarre' observation in this research project, the fact that in the 3+4-model, equilibrating the system above T_{MCT} and doing a GD dynamics, i.e. MFDE integrated at $T = 0$, the energy relaxes below what was considered - by us and in general by the community - the threshold energy E_{th}. In section 2.3, we have seen how E_{th} is statically characterized as the energy at which typical minima of the energy landscape become saddles. Since the work of L.F.Cugliandolo and J.Kurchan [CK93] on the out of equilibrium dynamics of pure p-spin models, the threshold energy has enforced its role as a theoretical lower bound in every mean-field dynamics starting at high energies (section 2.3). Specializing to GD dynamics, the picture is the following: starting from high temperature, the system surfs between saddles until it meets the highest energy minima, which are also the most numerous ones, and it asymptotically tends to them, aging on a marginal manifold. This is valid for any starting temperature above T_{MCT}. In terms of IS this corresponds to saying that $E_{IS} = E_{th}$ for any $T' > T_{MCT}$ (see inset fig. 3.1 and top right plot). In mixed models the situation is quite different. We again consider a system prepared above T_{MCT} and we observe two distinct behaviors. If the parent temperature T' is high, the system asymptotically tends to the theoretical energy E_{th}, while if T' is above but close to T_{MCT}, the dynamics goes under-threshold, i.e. $E_{IS} < E_{th}$ (see 3.1). This is an important observation, because it breaks a 'strong' prejudice of the impossibility of describing the complex behavior of glassy dynamics with mean-field models, opening a new revival in mean-field out of equilibrium analysis. Crossing T_{MCT} - at which the ergodicity is broken - and looking at the asymptotic energy (see fig. 3.4 bottom right), there is not a clear signature of T_{MCT}, which passes unnoticed by the E_{IS}. By contrast in pure models T_{MCT} is not only an equilibrium temperature but it also marks a change in the typical IS energy landscape. In the state following computation (section 2.7.1), we have already seen that there is a range of parent temperatures $T_{SF} < T' < T_{MCT}$ for which the state could not be followed down to zero temperature. Preparing a system below T_{SF}, a fast relaxation occurs to the bottom of the basin, as we have largely discussed in previous sections. In summary, we have three GD phases or IS types of minima:

$T' < T_{SF}$ the dynamics is of fast relaxation to the bottom of the basin. State following solution.

$T_{SF} < T' < T_{onset}$ the dynamics presents aging and memory of the initial condition.

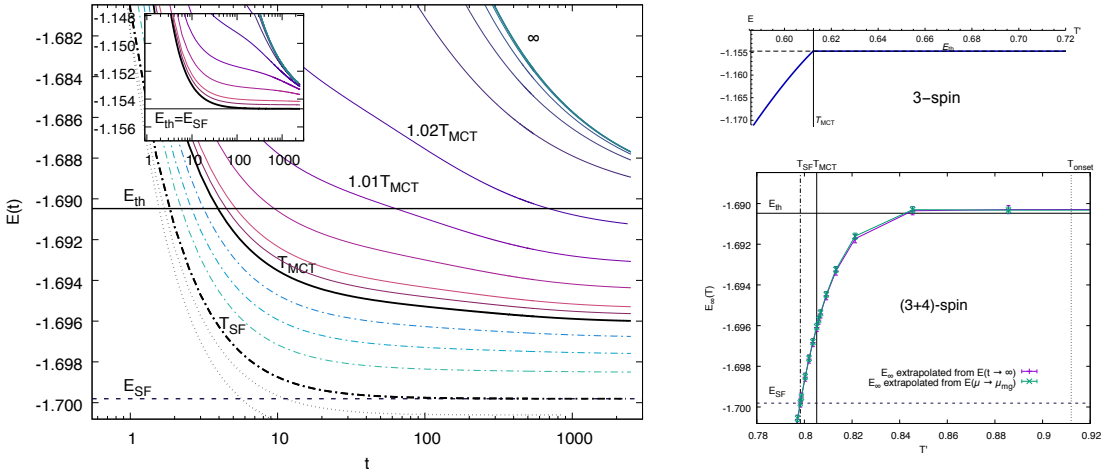

Figure 3.1: (**left**): under-threshold relaxation of the energy $E(t)$ for the GD dynamics in the (3+4)-spin, for parent temperatures both above and below T_{MCT}. In the inset, the same dynamics in the pure 3-spin model were the threshold is "well defined". (**right,bottom**): two different asymptotic extrapolations of the energy for different parent temperatures T', which correspond to the E_{IS}. (**right,top**): the E_{IS} dependence on parental temperature in the pure 3-spin model.

No analytical treatment.

$T_{onset} < T'$ the dynamics follows the 'standard' aging to the threshold manifold. Full asymptotic solution.

Here T_{onset} is not necessarily a well defined temperature, it could be a transition range. In the following sections, we will characterize the new phase that emerges in mixed models between T_{SF} and T_{onset}. Recall that, T_{on} was first described in a famous paper of S. Sastry, P.G. Debenedetti, F.H. Stillinger [SDS98] in which the correspondence between slowing down of the equilibrium dynamics and the dependence of the E_{IS} on the parent temperature was numerically found for Lennard-Jones binary mixtures (see section 1.1.2).

3.1.2 Relaxing on a Marginal Manifold

Here, we concentrate on the new phase. As we have already remarked, the asymptotic limit of the GD dynamics corresponds to a search for the ISs in the energy landscape. This one-to-one correspondence can be explored by looking at two dy-

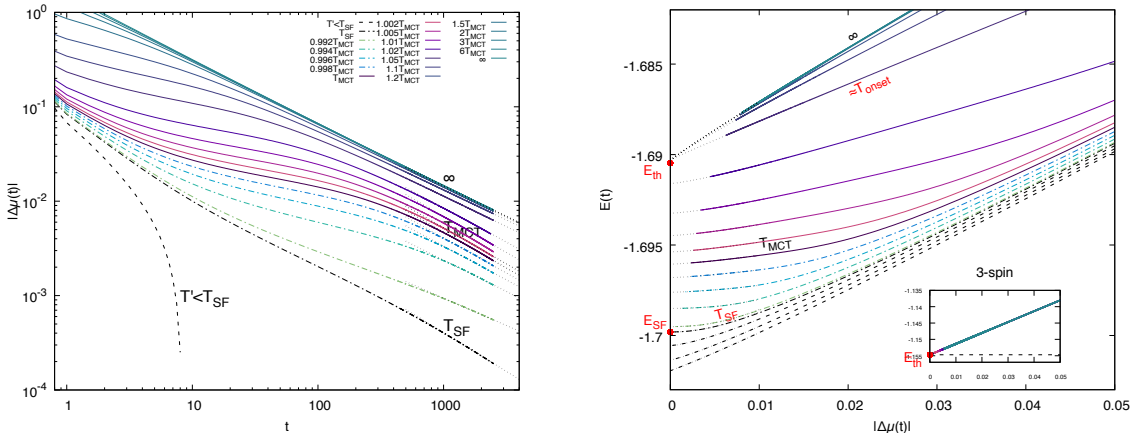

Figure 3.2: In the (3+4)-spin model. (**left**): the spectral gap $\Delta\mu(t)$ versus time. The system gets towards the marginal manifold $\Delta\mu = 0$ for every parent temperature $T' > T_{SF}$. (**right**): parametric plot $E(t)$ vs $\Delta\mu(t)$. For $T > T_{onset}$ the system gets marginal $\Delta\mu = 0$ at E_{th}. Between T_{SF} and T_{onset} it is still marginal, but under-threshold. Below T_{SF} it gets to a 'well defined' minimum. In the inset, the same plot in the pure 3-spin model. All lines are superimposed and tend to E_{th}.

namical observables (see section 2.7.2), the energy:

$$E_{T'}(t) \;\; = -\int_0^t f'(C_{ts})R_{ts}ds - \beta' f(C_{t0}) \tag{3.1}$$

and the spectral gap:

$$\Delta\mu_{T'}(t) = \int_0^t ds f''(C_{ts})R_{ts}C_{ts} + \int_0^t ds f'(C_{ts})R_{ts} + \beta' f'(C_{t0})C_{t0} - 2f''(1)^{-1/2} \tag{3.2}$$

where $_{T'}$ denotes for the parent temperature dependence $T' = 1/\beta'$. In the asymptotic limit $t \to \infty$:

$$E_{IS}(T') \equiv \lim_{t\to\infty} E_{T'}(t) \qquad \Delta\mu_{IS}(T') \equiv \lim_{t\to\infty} \Delta\mu_{T'}(t) \tag{3.3}$$

These are our definitions of energy and spectral gap of IS for a given parent temperature T'. Here we recall that, a positive $\Delta\mu_{IS}$ signals that the IS is in a well-defined minimum of the energy landscape, while $\Delta\mu_{IS} = 0$ defines the so-called *marginal manifold*, i.e. the ensemble of minima that have almost flat directions. Remember that in the p-spin model the typical spectrum is a Wigner semi-circle law [LNV18], with possible isolated eigenvalues [Ros+19]. A direct look at the time evolution of the spectral gap (fig. 3.2 left) shows that for parent temperature $T' > T_{SF}$ the system tends towards the marginal manifold, while for $T' < T_{SF}$ the system is typically in

a well-defined minimum and $\Delta\mu_{IS} > 0$. Now we look at the parametric plot $E(t)$ vs $\mu(t)$ presented on the right side of figure 3.2.

Here, the distinction between the three phases is noticeable. At high parent temperature, the system tends towards the marginal manifold $\Delta\mu_{IS} = 0$ that lies at the threshold energy $E_{IS} = E_{th}$. Going below T_{onset} (temperature or range of temperatures) the system dynamics remains asymptotically marginal $\Delta\mu_{IS} = 0$, but it starts to surf under-threshold $E_{IS} < E_{th}$, finally for parent temperature smaller than T_{SF} the system can be followed $E_{IS} \leq E_{SF}$ and minima are well defined $\Delta\mu_{IS} > 0$. Both E_{th} and E_{SF} are statically defined quantities, the first from energy landscape computations (section 2.3) and the second from state following computations (section 2.2). In the inset, the same plot is shown for the 3-spin pure model and all lines are superimposed. This comes directly from the homogeneity of the Hamiltonian*, which implies $E(t) - E_{th} = -\Delta\mu(t)$ (see 3.1 and 3.2). In terms of energy landscape, this is related to the fact that in pure models, given a stationary point of definite spectral gap $\Delta\mu_{IS}$, its typical energy is univocal $E_{IS}(\Delta\mu_{IS})$ and in particular $E_{th} = E_{IS}(\Delta\mu_{IS} = 0)$, while in mixed models there is no bijective map, and, given $\Delta\mu_{IS}$, there is a whole region of possible E_{IS}.

3.1.3 Aging in a Confined Space

Now we further explore the dynamics, looking at two times observables. The system shows aging, whenever it tends towards the marginal manifold $\Delta\mu_{IS} = 0$, thus, for every $T' > T_{SF}$. If we assume a 1-RSB scheme for the aging solution of the asymptotic dynamics, the correlation C and the fluctuation-dissipation ratio X take the form (section 2.7.2):

$$\begin{cases} 1 - T\chi < C < 1 \quad X = 1 & \text{st TS} \\ q_1 < C < 1 - T\chi \quad X = Ty & \text{ag TS} \\ p < C < q_1 \quad X = 0 & \text{mem TS} \end{cases} \tag{3.4}$$

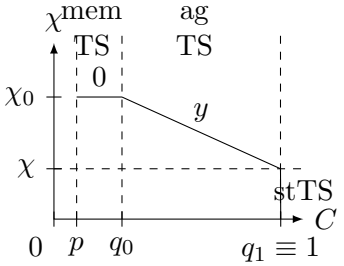

where $y \equiv \lim_{T\to 0} x/T$. Here we are considering a small T expansion, which corresponds to GD dynamics. Using this ansatz, we can write the asymptotic energy as (2.173):

$$E^{as}(T') = [-f'(1)\chi - yf(1)] + yf(q_0) - \beta' f(p) \tag{3.5}$$

*$qf'(q) = pf(q)$ in p-spin , analogously for further derivatives

where we just expanded in small T using $q_1 = 1 - \chi T$. The suffix ^{as} stands for asymptotic approximation, to which we would like to match the true $E_{IS}(T')$. The same can be done for the spectral gap:

$$\Delta\mu^{as}(T') = [(f'(1) + f''(1))\chi + yf'(1)] - yf'(q_0)q_0 + \beta' f'(p)p - 2f''(1)^{-1/2} \quad (3.6)$$

First of all let's study the high T' regime, where the memory-less Cugliandolo-Kurchan solution holds. This implies $p = 0, q_1 = 0$, which give:

$$\begin{aligned} E^{CK}(T') &= -f'(1)\chi_{CK} - y_{CK}f(1) = E_{th} \\ \Delta\mu^{CK}(T') &= (f'(1) + f''(1))\chi_{CK} + y_{CK}f'(1) - 2f''(1)^{-1/2} = 0 \end{aligned} \quad (3.7)$$

where we have used $\chi_{CK} = f''(1)^{-1/2}$ and $y_{CK} = 1/(\chi_{CK}f'(1)) - \chi_{CK} = y_{th}$ solution of (2.194) at $T = 0$. Both E_{th} and $y_{th} = \partial_E \Sigma_0^{dm}$ where found in the analysis of the energy landscape. Until here the matching between energy landscape and asymptotic dynamics is clear. Aging occurs on a *marginal manifold* at the threshold energy, and the effective temperature is exactly the derivative of the complexity of dominant stationary point at the threshold.

Now let's study the *under-threshold* regime, i.e. $T < T_{on}$. In this regime the dynamics has memory of the initial condition. This is already clear from the fact that the asymptotic energy remembers the initial temperature. It is confirmed by the correlation with the initial condition $C(t, 0)$, which in the under-threshold regime does not tend to zero (see fig. 3.3). Unfortunately the largest integration time is not large enough to have a 'fair' extrapolation of the asymptotic values. However, a difference regarding the pure case is evident. We also look at the aging phenomenon by looking at the correlation $C(t, s)$ versus $t - s$ for different t. This directly answers the question, given a configuration at time t which is the typical with its passed dynamics. It is found (fig. 3.3:right) that there is a strong memory until a time s, which corresponds to a fast drop from $q_0(t)$ to $C(t, 0)$. This is true in pure and mixed models, with the difference that in pure models it drops asymptotically to zero ($\lim_{t\to\infty} C(t, 0) = 0$), while it does not in mixed models at temperature below T_{on}. We say that the system at time t remembers the initial condition with overlap $C(t, 0)$ and remembers its 'far-away' past with overlap $q_0(t)$. These two overlap scales in the asymptotic limit tend to:

$$\lim_{t\to\infty} C(t, 0) = p \qquad \text{and} \qquad \lim_{t\to\infty} q_0(t) = q_0 \quad (3.8)$$

We now back to the asymptotic analysis. Because the dynamics goes under-threshold, we need another solution compatible with this observation. If the 1-RSB

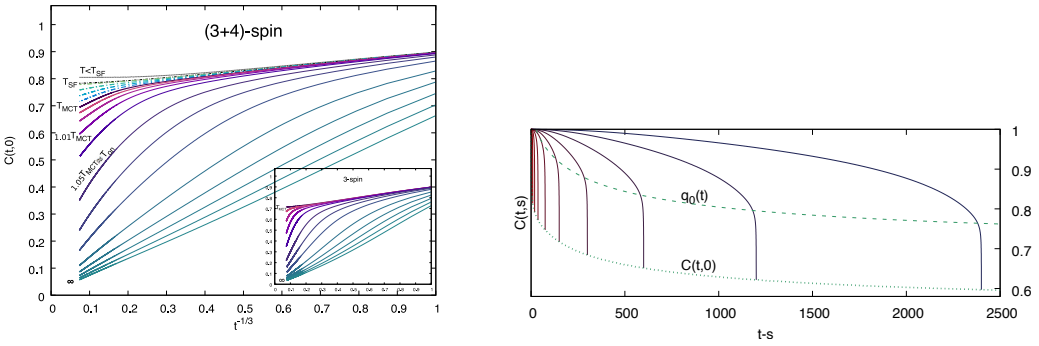

Figure 3.3: (**left**): time evolution of the correlation with the initial configuration $C(t,0)$ in the GD dynamics of the mixed $(3+4)$-spin model. The time is rescaled with a power-law $t^{-1/3}$, which is the one followed starting from infinite temperature $T'=\infty$ (lower curve). For $T'>T_{on}$ the correlation seems to tend to a finite value $C(t,0)>0$, thus the system remembers its initial condition. In the inset, the same plot for the pure 3-spin model, where no memory is present. (**right**): aging in the $(3+4)$ at $T'=1.01T_{MCT}$, the correlation $C(t,s)$ with the past, having fixed the actual time t $(2400/2^n)$. For every t two regimes are presented, the slow relaxation with aging features till an overlap $q_0(t)$ and a quick drop between $q_0(t)$ and $C(t,0)$, which corresponds to the earliest dynamics.

asymptotic equations (2.192) were 'correct', one could find χ, q_0, p, y and deduce $E^{as}(T')$ and $\Delta\mu^{as}(T')$. However, comparing with asymptotic values extrapolated from numerical integration, we found that they do not give the 'right' answer. The strange thing about this 'new' aging regime is that it seems to have a FDR $y \approx y_{th}$, the one defined by the threshold energy. This is shown on (fig.3.4:left) by dashed lines and seems not to depend on the temperature. The dynamics goes under-threshold, but with an effective temperature, compatible with the threshold. While the solution given by the 1-RSB ansatz (fig.3.4:right) gives an y too small. This highlights vividly, the 'non-correctness' of the solution. Moreover, the 1-RSB solution disappears at a temperature below $T_0 < T_{MCT}$ and the extrapolated p does not match this solution even below T_0. The possibility that further RSB steps can give better results remains open. My belief is that the incoherency in the asymptotic solution comes from short-time contributions that are not properly considered.

In the actual impossibility of finding an exact solution, we propose a semi-empirical ansatz which seems to fit 'properly' the long time dynamics, as it is shown in fig.3.4:right for q, p, q_0. In the next section, we present this approximation.

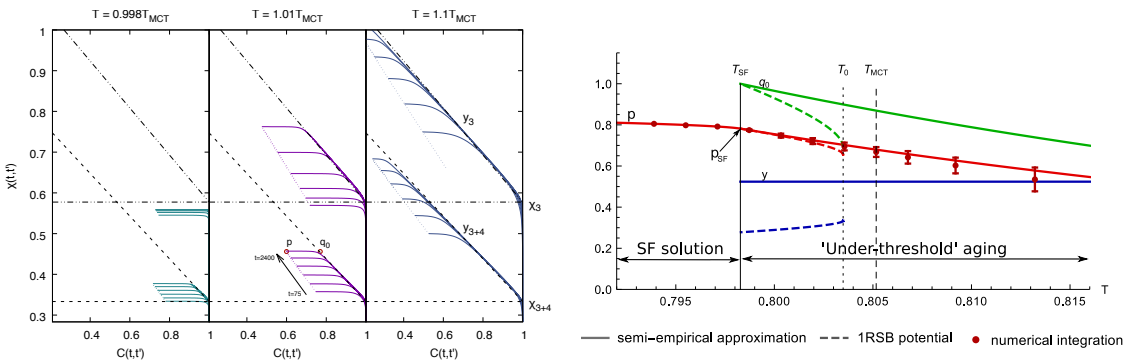

Figure 3.4: (**left**): the generalized fluctuation dissipatio ratio is presented through a plot of $\chi(t,s)$ vs $C(t,s)$. For three different temperatures both the $(3+4)$-spin (bottom) and 3-spin are presented (top). Each line corresponds to a fix t and a varying s, as in fig. 3.3:right. The fast stationary TS corresponds to a vertical line till $\chi_{34}(\chi_3) = \chi_{mg}$, the aging TS corresponds to the $y_{34}(y_3) = y_{th}$ fluctuation dissipation ratio, which seems independent on the parental temperature (**right**): comparison between parameters evaluated from the integration of the dynamics and from the 1-RSB ansatz on the asymptotic analysis. The two clearly do not match.

3.1.4 Onset Temperature a Semi-empirical Law

The basic assumptions for the approximation that we will introduce in this section, come directly from the observation of the FDR plot for different temperatures fig. 3.5. There exist two master curves, both in mixed and pure models, that envelop the aging curves. These are shown by dashed lines in the plots. The upper one corresponds to the CK solution of the asymptotic dynamics, while the lower one is given by a non trivial use of state-following solution. These curves do not depend on temperature. In pure models for long times the aging dynamics explore all the upper curve. By contrast in mixed models, if the parent temperature $T' < T_{on}$, at a certain point, the dynamics that was following the CK solution discovers the limitedness of the basin and stops exploring further. This corresponds to a finite q_0, p.

Let's assume that the aging dynamics is exploring a marginal manifold. This fixes two conditions:

$$\chi = \chi_{mg} \qquad \text{and} \qquad \Delta\mu^{as}(T') = 0 \tag{3.9}$$

Moreover, we have seen that $y \approx y_{th}$. Using both y_{th} and χ_{mg} corresponds to using the CK solution, but without fixing q_0 and p to 0. Therefore, we have the energy and the spectral gap:

$$\begin{aligned} E^{as}(T') &= E_{th} + y_{th} f(q_0) - \beta' f(p) \\ \Delta\mu^{as}(T') &= -y_{th} f'(q_0) q_0 + \beta' f'(p) p = 0 \end{aligned} \tag{3.10}$$

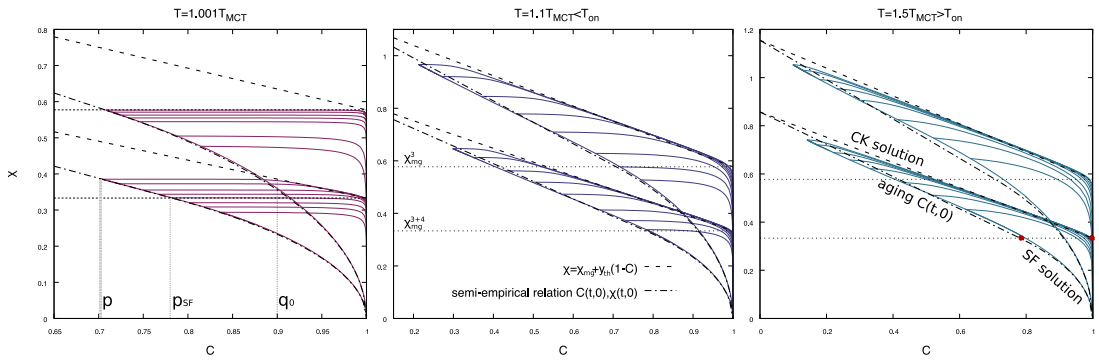

Figure 3.5: The semi-empirical approximation of the long time dynamics stems from the observation that there exist two master curves which are independent on the temperature and envelope the aging curves. The upper one (dashed line) comes from the standard Cugliandolo-Kurchan solution, while the lower one (dashed-dotted), which corresponds to the curve $\chi(t,0)$ vs $C(t,0)$, is given by a state following approximation of the short time dynamics. These two curves together with the marginal condition $\Delta\mu = 0$, define the asymptotic behavior, and thus the presence of T_{on}.

We thus have two unknowns q_0, p and one equation. We need another, for which we will use the lower master curve, which approximates 'properly' the behavior of $\chi(t,0)$ vs $C(t,0)$. This master curve is defined by two parts: for $\chi(t,0) \geq \chi_{mg}$ we assume a linear behavior, which corresponds to the "aging $C(t,0)$" part , while in the regime $\chi(t,0) < \chi_{mg}$ we assume a "SF solution" (fig. 3.5:right). These two behaviors correspond to two different time sectors. At the short times, the dynamics of $C(t,0)$ and $\chi(t,0)$ almost exactly follows the state following solution, which corresponds to the relaxation inside a modified state. At the start, the dynamics sees only fast relaxation modes, and relaxes as if the state were stable, until it finds out that it is not and it starts surfing into other basins, through saddle points. This long time behavior takes place on an almost marginal manifold ($\Delta\mu^{as}(T') = 0$). We will provide more details of these two relaxation regimes in the next section. For what concern the SF solution, we just take the first equation of the FP solution (2.82). The lower curve (dashed-dotted) is thus given by:

$$\begin{cases} \chi(t,0) &= \chi_{mg} + y_{th} - C(t,0)\frac{y_{th}}{p_{SF}} \qquad C(t,0) \in [0, p_{SF}] \quad (\chi(t,0) \geq \chi_{mg}) \\ \chi(t,0) &= \sqrt{\frac{1-C(t,0)^2}{f'(1)}} \qquad\qquad\qquad C(t,0) \in [p_{SF}, 1] \quad (\chi(t,0) < \chi_{mg}) \end{cases} \tag{3.11}$$

where

$$p_{SF} = \sqrt{1 - \chi_{mg}^2 f'(1)} = \sqrt{1 - \frac{f'(1)}{f''(1)}}$$

This is the value of the minimal overlap with the initial configuration within the SF solution, and corresponds to the temperature T_{SF}. We notice that this curve has a continuous first derivative at the point (p_{SF}, χ_{mg}), as it can be easily checked by taking derivatives. Our asymptotic ansatz thus implies a very simple relation between the overlaps, describing the asymptotic aging regime, namely:

$$p = p_{SF} q_0 \tag{3.12}$$

Plugging this relation into the condition of gap-less spectrum (3.10), it is easy to find that a solution with $p > 0$ can exist only if:

$$T < T_{on} \equiv \frac{p_{SF}^k}{y_0} = \frac{f'(1)[f''(1) - f'(1)]^{\frac{k}{2}-1}}{f''(1)^{\frac{k-1}{2}}} , \tag{3.13}$$

where k is defined by $f(q) \propto q^k$ for $q \to 0$ (in the 3+4-model $k = 3$ and $T_{on} = 0.91$). This approximation seems to do a very good job in the vicinity of T_{MCT} (fig. 3.4). Despite not being an exact solution of the asymptotic equations, it is a strong indication that there is a phase transition between a memoryless phase, where dynamics decorrelate from the initial condition and falls over the 'usual' threshold states with $E = E_{th}$ and a phase in which aging takes place in a confined space, with an asymptotic energy below threshold and depending on β.

3.1.5 Two Time Scales for Two Power Laws

In this section, we give a theoretical justification to two power laws that arise in GD dynamics, both in pure and in mixed models. The relaxation of the energy to its asymptotic values in the (3+4)-model is shown in fig. 3.1.5. If T' is high, the energy goes as $t^{-2/3}$, while if $T' \approx T_{SF}$ it goes as $t^{-3/2}$. For temperatures in between, there is a mixing of the two trends, for small time $t^{-3/2}$ and for large time $t^{-2/3}$. The same behavior holds also in the pure 3-spin model (inset), where now the energy is always getting to E_{th} and T_{SF} is substituted by T_{MCT}. To justify these power-law behaviors, we first observe that the typical spectrum of the Hessian during the GD dynamics is a semi-circle law * of radius μ_{mg} and spectral gap $\Delta\mu(t) = \mu(t) - \mu_{mg}$. This spectrum is moving towards its asymptotic limit: $\lim_{t\to 0} \Delta\mu(t) = 0$ for the aging dynamics ($T' > T_{SF}$) and $\lim_{t\to 0} \Delta\mu(t) > 0$ for the relaxations inside a state ($T' < T_{SF}$). Now let's approach T_{SF} from below. The corresponding typical IS is a minimum and, therefore, the long-time relaxation dynamics around it can simply be written as:

*here isolated eigenvalues are neglected

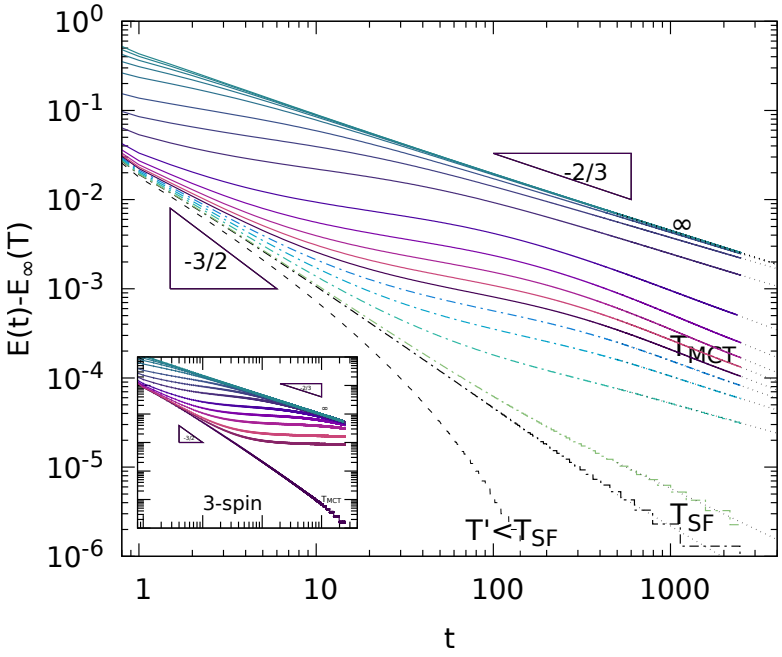

Figure 3.6: Power law behavior of the energy relaxation in the GD dynamics in the $(3+4)$-spin model. The asymptotic extrapolated energy $E_\infty(T')$ is subtracted. Starting from high T' (upper curves) the relaxation follows the "saddle to saddle" power law $t^{-2/3}$, while near T_{SF} it is almost "trapped in a state" and shows a $t^{-2/3}$ power law. In between a transition from a short time $t^{-3/2}$ to a long time $t^{-2/3}$. Bot h power law are connected to the lower edge of the typical Hessian spectrum. In the inset the same behavior is found in the 3-spin model, with $T_{SF} = T_{MCT}$

$$\delta\sigma_i(t) = \sum_\lambda P_\lambda \delta\sigma_i(0) e^{-\lambda t} = \int_{\Delta\mu_{IS}}^{\Delta\mu_{IS}+2\mu_{mg}} d\lambda \rho(\lambda)\ P_0(\lambda) e^{-\lambda t} \tag{3.14}$$

where P_λ is the projector on the λ eigenspace of the Hessian and $\delta\sigma_i(0)$ is $\sigma_i(0) - \sigma_i^{IS}$. $\rho(\lambda)$ is the semi-circle spectrum defined in (2.90) and $P_0(\lambda)$ the projected initial condition. We have just decomposed the evolution of $\delta\sigma_i(0)$ into its normal modes, each one with its typical time scale λ^{-1}. For what concerns the energy:

$$E(t) = E_{IS} + \frac{1}{2} H''_{ij} \delta\sigma_j(t) \delta\sigma_i(t) = E_{IS} + \int_{\Delta\mu_{IS}}^{\Delta\mu_{IS}+2\mu_{mg}} d\lambda \rho(\lambda)\ \lambda P_0(\lambda)^2 e^{-2\lambda t} \tag{3.15}$$

The lowest relaxation modes ($\Delta\mu_{IS}$) dominate the long time dynamics independently on the initial condition $P_0(\lambda)$ *. We then expect the energy to have a characteristic time scale $\tau = -1/2\Delta\mu_{IS}$. If now $T' \to T_{SF}$, the gap goes towards zero and we assume a power-law behavior which is strictly connected to the left shape $\propto \lambda^{1/2}$ of the Hessian spectrum:

$$E(t) - E_{IS} \propto \int_0^{2\mu_{mg}} d\lambda\ \lambda^{1/2} P_0(\lambda)^2 e^{-2\lambda t} \propto t^{-3/2} \tag{3.16}$$

Which is the observed power-law both in 3-spin at T_{MCT} and (3+4)-spin at T_{SF}. The same power-law is observed also for the highest parent temperatures in the short-time regime (short but macroscopic). This is given by the relaxation of slow modes of a nearly marginal spectrum. And more generally, the slow modes of a quasi-equilibrium structure reflects the FDT regime, with again the same $t^{-3/2}$ power [KL95]. In the following, we want to argue that the shape of the spectrum not only gives - by its quasi-equilibrium relaxation - the short time power law $t^{-3/2}$ relaxation, but - by a stochastic mechanism - it also gives the long time aging power law $t^{-2/3}$. Both of these powers depend on the lower part of the spectrum. The aging relaxation is governed by the random exploration of the gradient upon the Hessian eigenstates at long times. The typical picture is the following. At the beginning, the gradient has a direction that is completely independent from the Hessian eigenspaces so that each eigenstate is equally populated. Then, in the short time dynamics there is an exponential deflation of the positive part of the spectrum, which we have already described. At the same time another process is going on, namely the discovery of new saddles in the negative part of the spectrum. The process is essentially different, since the negative part of the Hessian corresponds to unstable directions. Each time the system gets in a negative direction it must find another saddle or a final minimum. This jumping from saddle to saddle gives the shift of the spectrum with time. The Hessian has been shown to behave very chaotically [KL95] in the sense that its eigenstates turn very rapidly. Thus, the gradient that for long times is almost all along flat directions $\lambda \approx 0$, finds itself in a new direction regarding of the Hessian eigenspaces every time. But the only contribution to the probability of exploration of new saddles $P_{saddles}$, so to the long time relaxation, comes from the proportion of times in which the new pointed eigenspace is negative. This is given

*if non-null everywhere in the spectrum support

by the integral of the spectrum on negative directions:

$$P_{saddles}(t) \propto \int_{\Delta\mu(t)}^{0} d\lambda\ \rho(\lambda) \approx \Delta\mu(t)^{3/2} \tag{3.17}$$

which is inversely proportional to the time to escape a saddle, thus:

$$\Delta\mu(t) \propto t^{-2/3} \tag{3.18}$$

which gives long-time power-law behavior of the spectral gap. In the pure p-spin this gives directly the power law for $E(t) - E_{th}$. In the mixed case the asymptotic power law for the energy is not obvious , but from the paramagnetic plot in fig. 3.2 it seems that there is a linear relation between $E(t) - E_{IS}(T)$ and $\Delta\mu(t)$, implying the same power law for the energy.
This was not intended to be a proof, but a hint of what could be the mechanism behind a law that seems quite robust. Other pure and mixed models show the same short and long time behavior. And it is interesting to observe that both regimes are defined by the lower bound of the moving spectrum.

3.2 Constrained Complexity

In this section, we ask if we can understand the attractors of the dynamics in terms of typical marginal saddles and minima that lie close to the initial configuration. The idea is to count stationary points as we have done in section 2.3, but with an additional constraint q_{01}, which is the overlap to a reference σ_0 configuration typical at temperature T'. This constrained calculation is directly inspired by the analogy with the FP-potential. Let us consider the stationary points of the Hamiltonian $H[\sigma]$ on the sphere $\sum_i \sigma_i^2 = N$:

$$H'_i + \mu\sigma_i = 0. \tag{3.19}$$

We wish to classify the stationary points according to their energy $E_{IS} = \frac{1}{N}H[\sigma]$, their spectral gap $\mu = -\frac{1}{N}\sum_i \sigma_i H'_i$ and the value of their overlap $q_{01} = \frac{1}{N}\sigma_0 \cdot \sigma$, with the reference configuration σ_0 sampled at T'. We remind the reader that in mixed models, the relation between E_{IS} and μ is not univocal and stationary points are found over a whole region of the (E_{IS}, μ) plane. Since the complexity, i.e. the logarithm of their number is self-averaging, we write:

$$\begin{aligned}\Sigma(E_{IS}, \mu, q_{01}, \beta) = &\int_{S_N} \mathscr{D}\sigma_0 \, \frac{e^{-\beta H[\sigma_0]}}{Z_\beta} \\ &\log\Big(\int_S \mathscr{D}\sigma \delta(Nq_{01} - \sigma_0 \cdot \sigma)\, \delta(NE_{IS} - H)\, \delta(\mu\sigma + H')\, |\det(\mu I + H'')|\Big)\end{aligned} \tag{3.20}$$

The computation of Σ is standard, and can be performed in several steps. Since the matrix H'' is a GOE random matrix, the distribution of eigenvalues of $\mu I + H''$ is self-averaging and is a shifted semicircular. The logarithm of the modulus of its determinant reads (eq. 2.91):

$$D(\mu) = \mathbf{Re}\Big[\frac{\mu}{\mu + \sqrt{\mu^2 - \mu_{mg}^2}} + \log\Big(\mu + \sqrt{\mu^2 - \mu_{mg}^2}\Big) - \frac{1}{2} - \log(2)\Big]$$

which only depends on μ and $\mu_{mg} = 2\sqrt{f''(1)}$. To evaluate the remaining terms, we use replicas and write $\Sigma \equiv \overline{\log(\mathcal{N})} = \lim_{n\to 0} \frac{\overline{\mathcal{N}^n} - 1}{n}$. We concentrate on the case of temperatures greater than the static transition temperature ($T > T_K$) of the model, where the partition function appearing in the denominator of (2.89) is self-averaging and takes its annealed value $\overline{Z_\beta} = e^{\frac{N}{2}\beta^2 f(1)}$. One can then average over the disorder and the configuration σ_0 at the same time. Opening the delta function in the Fourier

basis,

$$\Sigma(E_{IS},\mu,p,\beta)=\lim_{n\to 0}\frac{1}{n}\Big(e^{-\frac{1}{2}\beta^2 f(1)}\int \mathscr{D}s\; e^{\sum_a^n N(i\hat{\beta}_a E_{IS}-i\hat{\sigma}_a\cdot\sigma_a\mu)} \\ \delta(Nq_{01}-\sigma_a\cdot\sigma_0)\;\overline{e^{-\beta H_0}\; e^{\sum_a^n(i\hat{\beta}_a+i\hat{\sigma}_a\cdot\nabla)H_a}}\Big)+ND(\mu) \quad (3.21)$$

where $\int \mathscr{D}s=\int_S \mathscr{D}\sigma_0\prod_a\Big(\int_S\mathscr{D}\sigma_a\int\mathscr{D}\hat{\sigma}_a\int\hat{\beta}_a\Big)$.

And because the disorder is Gaussian (see appendix A.1):

$$\overline{e^{-\beta H_0}\quad e^{\sum_a^n(i\hat{\beta}_a+i\hat{\sigma}_a\cdot\nabla)H_a}}= \\ e^{\frac{1}{2}\Big(\beta^2 f\left(\frac{\sigma_0\cdot\sigma_0}{N}\right)+2\beta\sum_a(i\hat{\beta}_a+i\hat{\sigma}_a\cdot\nabla^a)f\left(\frac{\sigma_a\cdot\sigma_0}{N}\right)+\sum_{ab}(i\hat{\beta}_a+i\hat{\sigma}_a\cdot\nabla^a)(i\hat{\beta}_b+i\hat{\sigma}_b\cdot\tilde{\nabla}^b)f\left(\frac{\sigma_a\cdot\tilde{\sigma}_b}{N}\right)\Big|_{\tilde{\sigma}\to\sigma}\Big)}$$

Now we define overlap variables $NQ_{ab}=\sigma_a\cdot\sigma_b$, $N\chi_{ab}=i\sigma_a\cdot\hat{\sigma}_b$ and $NV_{ab}=-\hat{\sigma}_a\cdot\hat{\sigma}_b$, and the overlaps with the reference configuration $Nq_{01}=\sigma_a\cdot\sigma_0$, $N\chi_p=i\hat{\sigma}_a\cdot\sigma_0$. This change of variables defines a matrix:

$$\mathscr{Q}\equiv\begin{pmatrix}1 & q_{01} & -i\chi_p\\ q_{01} & Q_{ab} & -i\chi_{ab}\\ -i\chi_p & -i\chi_{ab} & -V_{ab}\end{pmatrix}$$

where $Q_{aa}=1$ by spherical constraint. From the equivalence between replicas, we fix $i\hat{\beta}_a=y$ and $\chi_{aa}=\chi\;\forall a$. With this change of variables eq. (3.21) becomes:

$$\Sigma=(yE_{IS}-\mu\chi)+\beta\left(yf(q_{01})+\chi_p f'(q_{01})\right)+\lim_{n\to0}\frac{1}{n}\left(\frac{1}{2}\log(\det\mathscr{Q})\right)+D(\mu) \\ +\lim_{n\to0}\frac{1}{n}\left(\frac{1}{2}\sum_{ab}[y^2f(Q_{ab})+2yf'(Q_{ab})\chi_{ab}+f'(Q_{ab})V_{ab}+f''(Q_{ab})(\chi_{ab})^2]\right) \quad (3.22)$$

where $\frac{1}{2}\log(\det\mathscr{Q})$ is the volume factor that comes from the change of variables from spins to overlaps. To get the leading N contribution we must extremize the system regarding all the overlap parameters $\mathscr{Q}$ and y. We notice that a further simplification of the expression (3.22) can be obtained by first extremizing with regard to V_{ab}. Assuming a replica symmetric ansatz for the overlap matrices Q and

χ, i.e. $Q = \delta_{ab} + (1-\delta_{ab})q_0$ and $\chi_{ab} = \delta_{ab}\chi + (1-\delta_{ab})\chi_1$ we get, in the limit $n \to 0$:

$$\begin{aligned}\Sigma(E_{IS},\mu, q_{01}, \beta; y, \chi, \chi_1, \chi_p, q_0) = \\ &+ yE_{IS} - \mu\chi + \beta[yf(q_{01}) + \chi_p f'(q_{01})] \\ &+ \frac{1}{2}[y^2(f(1) - f(q_0)) + 2y(f'(1)\chi + f'(q_0)\chi_1) + \mathscr{R} + (\chi^2 f''(1) - \chi_1^2 f''(q_0))] \\ &+ \frac{1}{2}(\log(1-q_0) + \frac{q_0 - q_{01}^2}{1-q_0} - \log(f'(1) - f'(q_0)) - \frac{f'(q_0)}{f'(1) - f'(q_0)} + D(\mu)\end{aligned} \tag{3.23}$$

where

$$\mathscr{R} \equiv 1 + f'(1)\big(\tfrac{\chi-\chi_1}{1-q_0}(\chi - \chi_1)\big) + \big(f'(1) - f'(q_0)\big)\big(\chi_p^2 + \tfrac{\chi-\chi_1}{1-q_0}(2(\chi_1 - p\chi_p) - \tfrac{q_0-q_{01}^2}{1-q_0})\big)$$

This can be extremized explicitly with regard to y, χ, χ_1, χ_p, while q_0-extremization has to be done numerically. For $q_{01} = 0$ the solution is $q_0 = 0$ and we recover the unconstrained complexity (2.97) as found in [ASZ18]. A similar 1-RSB calculation of the complexity in p-spin models, with some external field breaking the spherical symmetry, can be found in [CGG99; Ros+19].

As we have already seen in mixed models there is a full range of marginal minima, here we are extending this concept to the constrained case $q_{01} > 0$. Fixing T' for each q_{01} there is a range of marginal minima. Extremizing the constrained complexity over the spectral gap, one obtains the dominant stationary points $\Sigma_{dm}(E_{IS}; q_{01}, T')$. This is shown in 3.7 for $T' = T_{MCT}$. For each different q_{01} we can define the *threshold* energy $E_{th}(q_{01}; T')$, as the energy at which dominant stationary points pass from minima to saddle changes. This threshold energy shows a clear dependence on q_{01}:

$$E_{th}(q_a; T') < E_{th}(q_b; T') \qquad \forall \quad q_a > q_b \tag{3.24}$$

This result is in the correct direction regarding the dynamics, since it is saying that the more the space around the reference configuration is confined, the more the system finds deeper minima. And this is exactly what is observed in the aging dynamics below T_{on}. The so found range of variation of E_{th} is compatible with the dynamics, while the range of energies with a positive complexity is very large in comparison. Unfortunately, however, we could not find an exact solution to the asymptotic dynamics by looking at the constrained energy landscape. On the right plot, green ellipses represent our best estimate for the large time limit of the actual dynamics solved numerically. While the energy can be very well estimated, the limit of $C(t, 0)$ is plagued by a large uncertainty due to its slow convergence. From this plot one is tempted to conjecture that the dynamics converges to marginal states

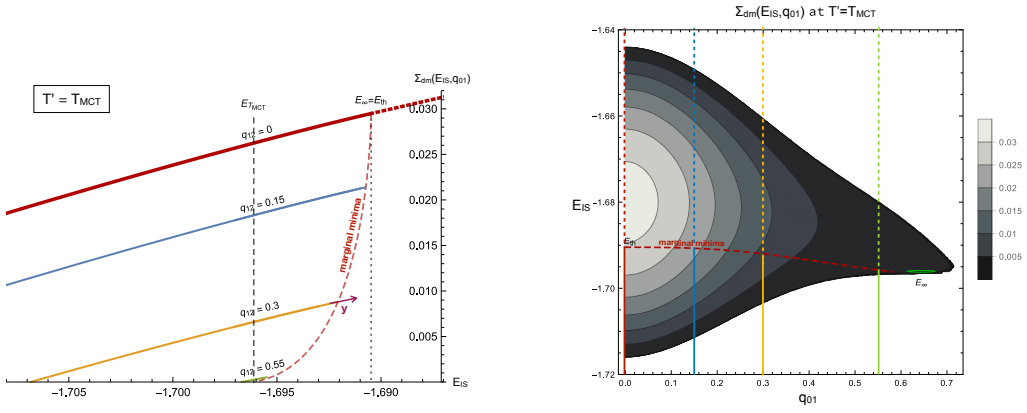

Figure 3.7: (**left**): complexity constraining the system at a fixed overlap q_{01} from a reference configuration sampled at temperature $T = T_{MCT}$. Vertical lines mark energy values E_{th} and $E_{T_{MCT}}$ corresponding to extrapolated asymptotic energies reached by the dynamics starting respectively from $T = \infty$ and $T = T_{MCT}$. The dynamics starting from a random configuration goes to the *most numerous marginal minima* ($E_\infty = E_{th}$), while starting near T_{MCT} the dynamics goes below E_{th}. Constraining to an overlap $q_{01} > 0$ from the initial configuration provides a qualitatively correct explanation: the energy of the most numerous marginal minima decreases. (**right**): the same complexity shown on the 2-dimensional plane (E, q_{01}). Vertical colored lines mark the same curves of the left plot. The red curve marks the energy of marginal states varying overlap with the reference configuration $E_{mg}(q_{01})$. The green ellipses is our best estimate for the the large time limit of the gradient descent dynamics, obtained from the numerical integration.

with a threshold energy $E_{th}(q_{01})$. However, we have not found any principle to fix the value of q_{01} solely from the complexity curve, and further studies are needed to better match the large-time limit of the dynamics to the energy landscape.

Assuming that at large times the relaxation dynamics converges to the manifold of marginal states belonging to the curve $E_{th}(q_{01})$ one could estimate the point reached by the dynamics by extrapolating the asymptotic energy $E_\infty(T)$ and estimating q_{01} from the equality $E_{th}(q_{01}) = E_\infty$. Having fixed the values of E and q_{01}, one can proceed by estimating the remaining parameters of the asymptotic aging dynamics, q_0 and $y = \partial_E \Sigma$. The result of this computation is shown in fig.3.8 with full lines, and compared to the (very uncertain) extrapolation of $C(\infty, 0)$, shown by red points with errors. We clearly see that, while the estimate of q_{01} is compatible with the actual dynamics, the other two parameters are far from the values measured in the numerical solution of the dynamics. Indeed q_0 becomes smaller than q_{01} while in the actual dynamics the inequality $q_{01} < q_0$ is always satisfied, and y becomes much smaller than y_{th} (dotted horizontal line), which is a good descriptor of the actual aging in the whole temperature range studied. So, we believe the present computation of the

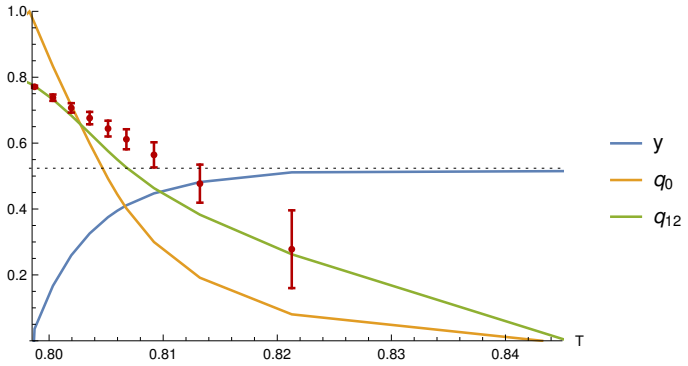

Figure 3.8: Assuming the dynamics relaxes on the marginal manifold with energy $E_{th}(q_{01})$ and fixing the energy from the large time extrapolation of the numerical data, which in its turn fixes the value for q_{01}, we can compute analytical values for the remaining aging parameters, namely q_0 and $y = \partial_E \Sigma$. While the estimate of q_{01} is compatible with the large time extrapolation of $C(t, 0)$ (red points with error in the figure), the other aging parameters are far from those measured in the actual dynamics.

constrained complexity of the energy function in mixed p-spin models is not the end of the story. Much more work will be required to relate the large time aging dynamics to the properties of the energy landscape. For instance basins of attractions are likely to play an important role, but are absent until now in the computation.

3.3 Numerical Simulation

In this section, I would like to support the analytical results of the gradient descent dynamics in p-spin spherical models by numerical simulation of finite size systems. By contrast to the enormous amount of analytical results, in the literature direct numerical simulations of fully-connected disordered models are quite rare. In particular for the out-of-equilibrium p-spin dynamics, for what I am aware of, only one paper briefly relates to it [KL95]. Here, I will try to introduce the numerical tricks and details, in order to simulate a p-spin fully connected model up to 4-body interaction and present the results that confirm and enlarge the out-of-equilibrium scenario, presented in previous sections.

3.3.1 Dilution

The system that we wish to simulate is a p-spin spherical model (pure or mixed) up to 4-body interaction. It is a fully connected model, thus, there are $\binom{N}{4}$ couplings which means that already with $N = 400$ we need to allocate $2^{30}(double)$ which corresponds to 8 Gb of memory. And from preliminary simulations of the dynamics comes that for values smaller than $N = 400$ finite-size effects are too large to deduce the thermodynamic behavior. Therefore, the need to find a modified system that has the same thermodynamic properties, but fewer couplings at any given N. The so diluted system will have different behaviors at any finite size, but it is build in such a way that in the $N \to \infty$ limit the expected analytical results are recovered. This process is called dilution and its is based on the idea that the only thermodynamically meaningful disorder quantity is the variance of the Hamiltonian fluctuations $\overline{H[\sigma]H[\tau]} = Nf(q)$ (see 2.3). To maintain it fixed, while we take a fraction d_p of the original $\binom{N}{p}$ couplings, we rescale the remaining ones by the inverse factor $1/d_p$. In principle, this procedure can be used independently for each p-body interaction, however, to simplify the analysis we will consider a global dilution parameter d. If the parameter d gets larger than the condensation value $d_p^c(N)$, which depends on N and on the number of interactions p, the remaining couplings are too few and the system condensates, i.e. the minima of the energy landscapes get concentrated on a few spin components $\sigma_{i\in\partial J_{max}}$, which are those that interact through the strongest of the remaining couplings J_{max}. This $d^c(N)$ can be estimated by a naive extreme value analysis (see [Bov05] for a pedagogical introduction). The energy of the condensed p-tuple is given by:

$$NE_c = -J_{max}(\sigma_c)^p \qquad \text{with} \qquad \sigma_c = \sqrt{N/p} \tag{3.25}$$

that comes directly from the fact that in a condensed state the total radius $\sqrt{N}$ is decomposed onto p components. Fg.3.9 shows, for different dilutions, the relative distribution of condensed energies. Now let's evaluate the average value of J_{max}, which is the maximal value over the extraction of $N_p^J(d) = \binom{N}{p}d$ couplings from a Gaussian distribution of variance $\overline{J_p^2}(d) = \frac{1}{2}N/\binom{N}{p}/d$, in our dilute system. J_{max} follows a Gumbel distribution with mode*:

$$\hat{J}_{max} = \sqrt{\overline{J^2}_p(d)^2}\sqrt{2\log(N_p^J(d))} \approx \sqrt{p!/d\ N^{1-p}\log(N^p)} \tag{3.26}$$

The standard deviation std(J_{max}) scales as the mode $\hat{J}_{max}$ at the leading order in N. The modal energy of the condensate, i.e. the energy of the pick of the distribution is approximately:

$$\hat{E}_c = -\frac{\hat{J}_{max}(\sigma_c)^p}{N} \approx -\sqrt{\frac{1}{d}\ \frac{(p-1)!}{p^{p-2}}\ \frac{\log(N)}{N}} \tag{3.27}$$

The system condensates whenever the energy of the condensate E_c gets lower than the typical thermal energy $\langle E\rangle$. To have a crude estimate of the gain in diluting the system, we simply take for the thermal energy the MCT energy $E_{MCT} = -\sqrt{(p-1)^{p-1}/(p-2)^{p-2}/2p}$ and for the energy of the condensate, that of the pick $\hat{E}_c$, obtaining the limiting dilution:

$$d_p^c(N) = \frac{1}{E_{MCT}^2}\frac{(p-1)!}{p^{p-2}}\frac{\log N}{N} = 2p\Big(\frac{p-2}{p(p-1)}\Big)^{p-2}(p-2)!\frac{\log N}{N} \tag{3.28}$$

We see that the maximal possible dilution (minimal $d_p^c(N)$) increases with p so if we want to take a global dilution in a mixed model, we need to optimize it for the lowest p. Defining the maximum diluted system as the one for which we take $d_p \equiv d_{p_{min}}^c$ we see that dilution allows to rescale the total number of couplings by a factor $N\log N$ without condensation. So, for example, taking a $3+4$, model we get a maximal dilution with a total number of 4-body couplings $N_4^J(d_3^c) \approx N^3\log N/4!$. Therefore, it is now possible to simulate with the same 8 Gb the same system up to $N = 1500$ (to be compared with $N = 400$). On the right plot of figure 3.9 we can see that as long as the dilution energy E_c is low enough with respect to the equilibrium energy E_{eq}, the system has always the same distribution of energies, independently of the dilution (inset). Thus, we will always consider the smallest dilution possible, which is given by 3.28.

*given n extraction from a Normal pdf, the maximum is distributed according to a Gumbel pdf of mode $\mu = \frac{4\log(n)-\log(4\pi\log(n))}{2\sqrt{2}\sqrt{\log(n)}} \approx \sqrt{2\log(n)}$ and $\beta = \sqrt{2\log(n)}$

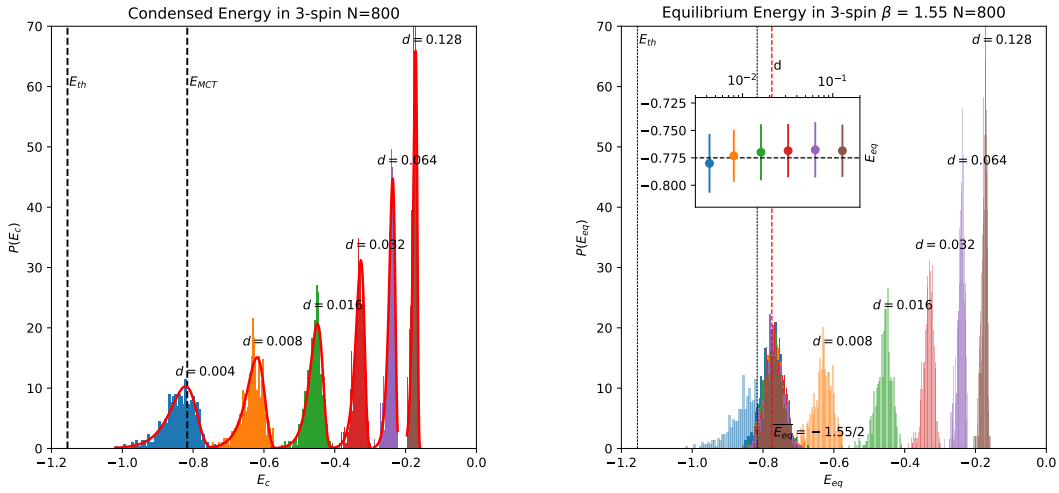

Figure 3.9: (**left**): the distribution of condensed energies E_c in the 3-spin model with $N = 800$ for different dilutions d of the system. The maximal possible dilution to avoid condensation depends on the typical energy at which the system need to be simulated. (**right**): the effect of condensed states on the equilibrium energy of the system at $\beta = 1.55$. In the inset, the average energy as a function of the dilution.

3.3.2 Annealing *vs* Planting

Recall that our gradient descent protocol starts at equilibrium at temperature β'. To equilibrate the system, we compare two different methods: the Monte Carlo annealing in temperature and the more clever, but more dangerous, planting. The equilibration through annealing is at a constant rate of inverse temperature change $v = \Delta\beta/\mathrm{MC}_{step}$, where each Monte Carlo step (MC_{step}) is defined by $N(N-1)/2$ Metropolis steps in configuration space, each one consisting of a random rotation α between a couple of randomly chosen spin components (i, j), with probability:

$$P(\Delta E_{ij}) = \max\{1, \exp(-\beta\Delta E)\} \tag{3.29}$$

where $\Delta E_{ij} = E[\sigma^f] - E[\sigma^{in}]$ with $\sigma_i^f = \sigma_i^{in}\cos(\alpha)$ and $\sigma_j^f = \sigma_j^{in}\sin(\alpha)$. This allows a local Metropolis-move on the sphere. The system is initialized at a random configuration, at initial inverse temperature $\beta_{in} < \beta_{MCT}$. Then the annealing proceeds until the final equilibrium temperature β'. This procedure has the advantage of reflecting a real cooling of the system, but it is numerically very expensive. In figure 3.10 for three different cooling rates, 20 different protocols for the pure 3-spin model

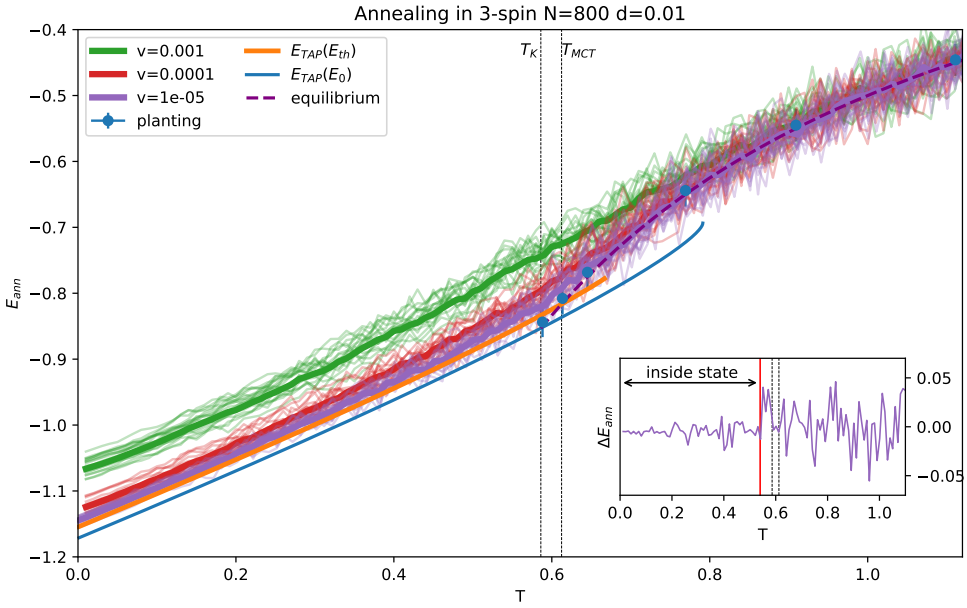

Figure 3.10: The energy versus temperature in the annealing protocol for three different cooling rates. Thick lines are average over 40 trajectories, while thin lines are single cooling schedules, over different systems. These are compared with the thermodynamic following states (section 2.2). Full points represent average energies from the planting procedure. The inset shows fluctuations over a single trajectory with $v = 10^{-5}$.

with $N = 800$ are shown. Decreasing the cooling rate v, the protocol gets closer to the thermodynamic curve of marginal states, but the two curves do not show the same kind of states. In finite N simulations, the annealing protocol allows the dynamics to jump from one state to another until temperatures lower than T_{MCT}. This is evident in the inset, where the energy of a single cooling is considered. The so obtained final state has a gapped spectrum. While in the thermodynamic limit, one expects the system to anneal on a marginal manifold below T_{MCT} and thus, to have a gapless spectrum.

Another way of preparing the system is to consider the planting procedure (see section 2.2.2), which is valid above T_K. One configuration σ^* is randomly picked on

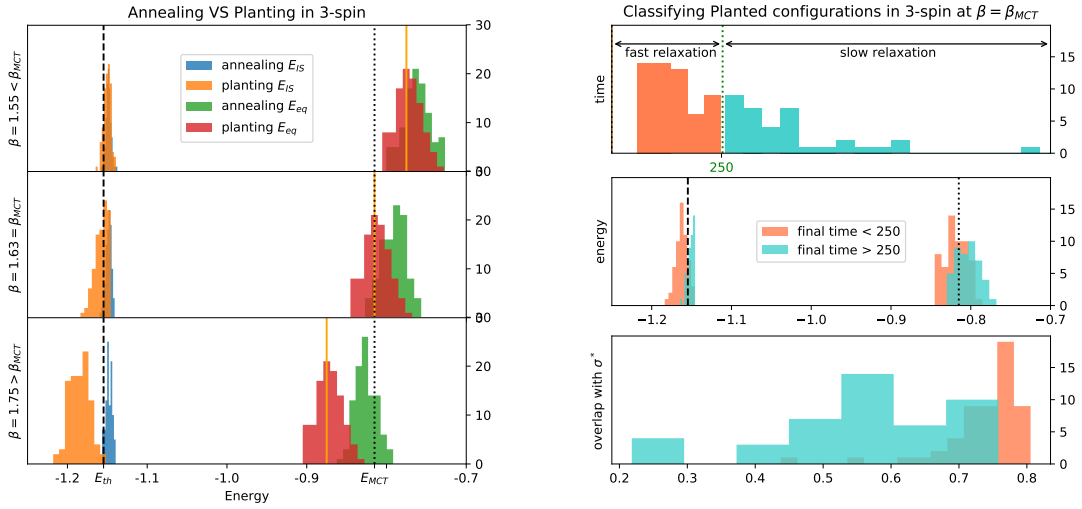

Figure 3.11: (**left**): panel pdf of equilibrium energies E_{eq} and energies of inherent structures E_{IS} for three different temperatures, both with annealing preparation and planting preparation. (**right**): a simple classification of equilibrium configurations based on the time needed to search for the inherent structure, allowing to distinguish between pure states (fast relaxation) and marginal states (slow relaxation).

the sphere and the couplings are generated according to the Gaussian distribution:

$$P(J_{ijk}) \propto \exp(-\frac{1}{2}\frac{J_{ijk}^2}{\overline{J_3^2}(d)} + \beta' \sigma_i^* \sigma_j^* \sigma_k^*) \tag{3.30}$$

for the 3-spin model, where $\overline{J_3^2}(d) = \frac{1}{2}N/\binom{N}{3}/d$, and analogously for any p. *Planting* allows to build a system for which the starting σ configuration is already inside an equilibrium state. This is a very fast and precise procedure in order to initialize a system at equilibrium between T_K and T_{MCT}. In figure 3.10 the average energy of a planting preparation for different temperatures are shown (blue dots). There are, however, two drawbacks. First, since the system is prepared around one specific configuration, we cannot compare multiple equilibrium states, unless we prepare them with another procedure. Second, the system is prepared within a non-smooth protocol, in the sense that finite size fluctuations can induce a given system, prepared at a temperature near T_{MCT}, to be either in the paramagnetic state or inside a confined state $q \neq 0$. Thus, giving very different prepared samples. This can be appreciated in figure 3.11, where a direct comparison of annealing and planting is reported for

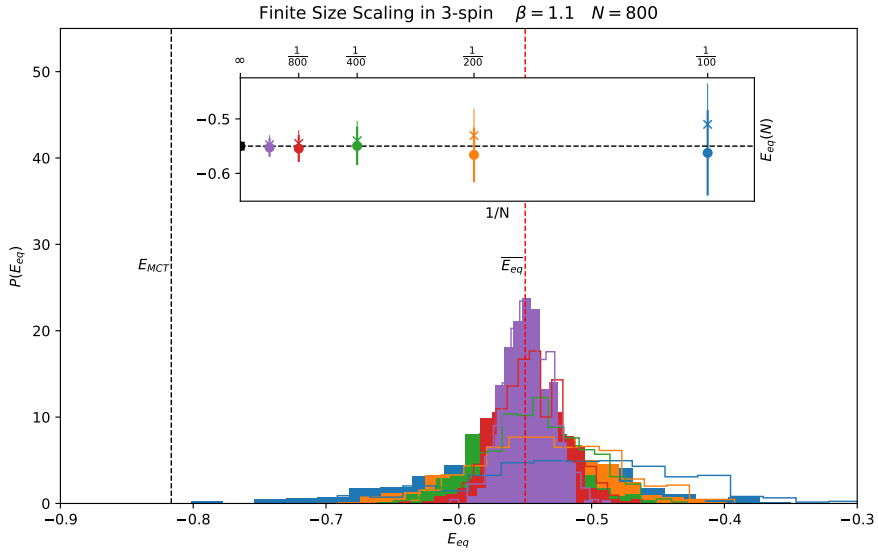

Figure 3.12: Distribution of equilibrium energies in 3-spin model at temperature well above T_{MCT}, both as obtained by the planting method (empty boxes) and by the annealing procedure (filled boxes) for different sizes of the system. In the inset, the average and the dispersion of the same distributions as a function of $1/N$; crosses for planting and circles for annealing. We notice an $1/N$ bias in the planting averages.

a system of $N = 800$ ($d = 0.01$). In the left plot, for three different temperatures, the pdf of the starting equilibrium energy E_{eq} is shown together with the pdf of the energy of corresponding inherent structures E_{IS}. This last quantity is evaluated by a gradient descent dynamics in the energy landscape, that will be described in details in the next section. From this plot it can be deduced that, planting near T_{MCT} is selecting states that give the same typical energy of equilibrium states E_{eq}, while annealing selects only states that are near the marginal manifold i.e. which have $E_{IS} \approx E_{th}$. Planting is thus selecting states arbitrary far from the marginal manifold. The right panel focuses on planting for $\beta = 1.63$ and it is shown that the so selected states can be (somehow arbitrary) divided in two classes: those for which the search of the inherent structure minimum is fast (time > 250), which turn out to have greater overlap with the reference configuration σ^* and correspond to a situation for which the system is prepared in a *pure* state. And those for which the search for the inherent structure is slow and corresponds to states that have a lower overlap with σ^* and for which the inherent structure energy is almost E_{th}. Therefore,

doing planting and annealing are sampling states that, while in the thermodynamic limit are expected to have the same properties, in any finite size system can give very different results, in particular near the mode coupling transition T_{MCT}.

For what concerns finite size scaling (FSS) effects, the plating procedure gives a broader distribution of energies and a $1/N$ systematic bias of the energies. This can be clearly seen in figure 3.12. In order to get less biased results, while using the planting procedure, we will first plant the configuration and then relax it with a number of MC steps of the order of the relaxation time inside the basin. The obtained result perfectly agree with the annealed ones, again, if we are not too close to T_{MCT}.

3.3.3 Simulation *vs* Integration

In this section, we will show how the simulations give results in agreement with those obtained from numerical integration of MFDE. We will focus on the gradient descent dynamics of the $(3+4)$-spin model for system sizes $N = 1600, 800, 400$ and dilution parameters $d = 0.0025, 0.005, 0.01$ respectively . The system is initialized with a planting procedure and a successive Monte Carlo relaxation dynamics inside the basin. As we have seen, the planting procedure can be 'dangerous' near T_{MCT}, since the system can find itself confined in a state, incapable to age outside. In order to reduce possible fluctuations in the average dynamics, due to the width of the initial energy distribution, we label each trajectory by its starting energy E', instead of its parent temperature T' (microcanonical sampling). So, in a few words, each configuration is planted at T', relaxed at T' and then labeled by its own energy E'. All averages are done by considering a small range $\Delta E'/E' = 0.005$ of the trajectories' energy around E'.

Let's look at the result from a parent temperature $T' \approx T_{MCT}$, that is $E' \approx -1/T_{MCT} = -1.24$. Let's consider a single sample of quenched disorder. In fig. 3.13:left are shown the energy relaxations of one GD trajectory from $E' = -1.24$, and four GD trajectories from $E' = -1/T' = 0$, i.e. from random configurations. As a general behavior of the single trajectory, we notice that there seems to be a length scale $\tau(N)$ depending on the size of the system. For times smaller than $\tau_{FSS}(N)$ the single GD trajectory shows self-averaging behavior, while for times greater than $\tau_{FSS}(N)$ there is a net separation of single trajectory behavior. It would be interesting to explore this dynamical FSS in more details. Here, we just want to give support to the picture built from the numerical integration. In the plot on center,top of fig. 3.13 the same sample is shown in the usual plane $\Delta\mu, E$. also at the level of the single sample the distinction of the aging dynamics between random and T_{MCT}

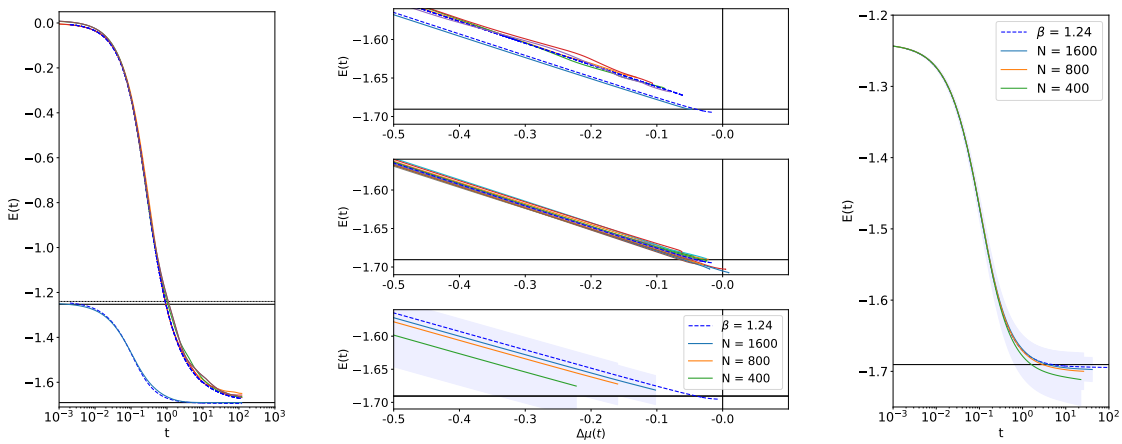

Figure 3.13: Simulation of the gradient descent dynamics in the mixed p-spin model with N=1600. Blue dashed lines show the results from the numerical integration. (**left**): energy relaxation along one GD trajectory from $T' \approx T_{MCT}$ and four trajectories from $T' = \infty$ with the same quenched disorder. (**center**): the three plots present the evolution of the energy E vs the spectral-gap $\Delta\mu$ at $T' \approx T_{MCT}$. On top, the same trajectory presented on the left plot. In the middle, many trajectories with different disorder. In the bottom, averages over 100 samples of disorder, for different sizes of the system. (**right**): relaxation energy averaged as a function of time over 100 sample of disorder. The same data used in (center):bottom plot.

configurations in net. The dynamics goes on in parallel, in the landscape of saddles. The figure below shows many trajectories from many different samples prepared at T_{MCT}. Below, the energies averaged over the 100 samples, as a function of $\Delta\mu$, for three different sizes of the system are shown. Finally on the right, the averages are evaluated as a function of the time. All plots also present the mean-field integrated dynamics (blue-dashed line). These plots confirm that an almost marginal dynamics over the single trajectory is taking place, and that this dynamics is going on under-threshold for $T' \approx T_{MCT}$. It is important to remark the new important point given by the simulation, the under-threshold aging, is observed over the single trajectory.

Now let's look at the correlation with the initial configuration, averages over different 100 samples are shown in fig. 3.14. Again the mean-field behavior is confirmed, but the time reached is too small to say anything more about the "confined" dynamics. Finally, we look at the energy of the 3-spin part E_3, and separately of the 4-spin part E_4. In figure 3.14 the single trajectories and their average are shown. Here, we want to comment on the strange behavior that follows E_3, which is not monotonously decreasing. One possible explanation is the following. The 3-spin interactions are less in number and easier to relax, thus, at the beginning of the GD dynamics they

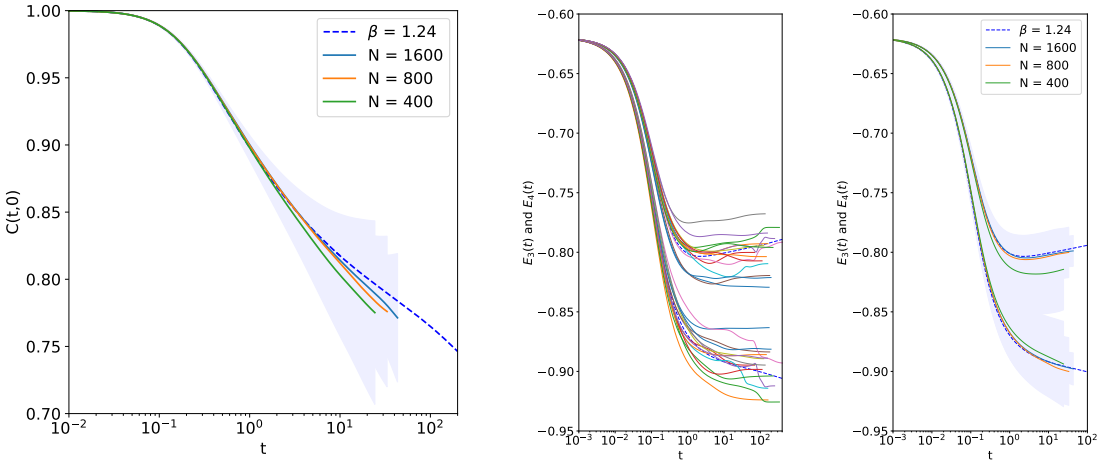

Figure 3.14: Simulation of the gradient descent dynamics in the mixed p-spin model with N=1600. Blue dashed lines show the results from the numerical integration. (**left**): correlation with the starting configuration averaged over 100 samples of disorder for different system sizes at $T' \approx T_{MCT}$. (**center**): energy relaxation of the 3-spin E_3 part and of the 4-spin E_4 for many trajectories with different disorder at $T' \approx T_{MCT}$. We observe that the 3-spin part is not monotonous in time. (**right**): E_3 and E_4 averaged over 100 samples of disorder for different sizes of the system.

find optimal (in E_3) configurations, on the other hand 4-spin interactions are slower to relax in relative scale *, but since they are more and so have more 'inertia', in order to further relax, they exchange energy to the E_3 part, which goes up. The interesting aspect is that this mechanism is connected to the under-threshold dynamics. Both E_3 and E_4 have a CK threshold value $E_{3,th} = -16/21$ $E_{4,th} = -13/14$, which they attain, starting from high parent temperature. It is around T_{on} that E_3 start to become non monotonously decreasing. And both E_3 and E_4 start to asymptotically deviate from their threshold values $E_{3,th}, E_{4,th}$.This mechanism is general in mixed models, where the part of the energy which corresponds to fewer spins, relaxes the fastest. The greater is the gap in number of interactions, the greater is the effect of this mechanism, and thus, the greater the under-threshold range. This gives a simple predictive intuition about what happens if taking for example the $3+6$ model, since the difference in time scales of relaxation will be greater, the under-threshold range will be greater than in the $3+4$ model. To conclude, I restate the main conjecture. In mixed models, the onset temperature T_{on} is connected to the non monotonous behavior of the fastest relaxing modes.

*for relative scale we mean that both E_3 and E_4 are considered to relax between 0 at time 0 and -1 at time ∞

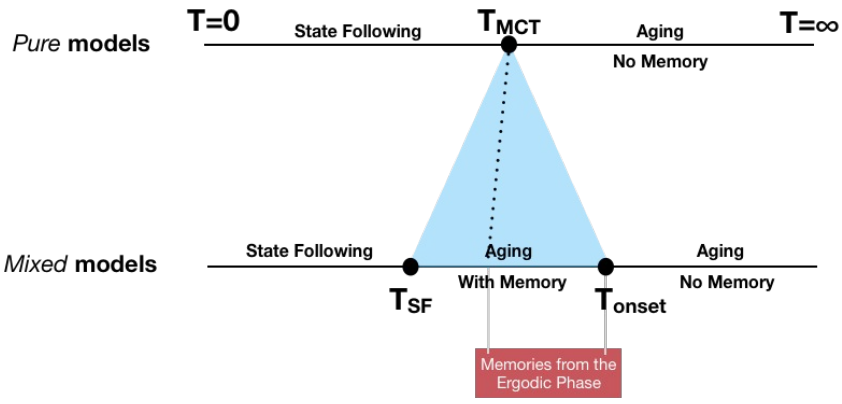

Figure 3.15: Sketch of the different out-of-equilibrium dynamical phases in the gradient descent dynamics for pure and mixed models.

3.4 The Emergence of a New Phase

All the results exposed in this chapter invite to rethink the out-of-equilibrium dynamics of mean-field models. The main ideas were developed on the result obtained looking at the pure p-spin spherical model, which has a rather trivial and pathological energy landscape. Whenever looking at mixed models, the scenario complexifies at the point that we are not anymore able to predict the asymptotic dynamics. This is directly related to the existence of a full range of marginal manifolds, possible candidates for the aging dynamics. The main obtained result is that there exists a range of parent temperature between T_{SF} and T_{on}, between which the GD dynamics show aging together with memories of the starting condition. In this picture T_{MCT} does not seem to have any interesting role. At equilibrium it is the temperature at which ergodicity is broken, but out-of-equilibrium, it is just one of the many temperatures. It is only in pure models where $T_{SF} = T_{MCT}$ that there it acquires a double role. The whole picture is summarized in figure 3.15 and firstly presented in "Memories of the ergodic phase" written by me, and my two advisors Silvio Franz and Federico Ricci-Tersenghi [FFR19].

The question that naturally follows, is how does the dynamics behave if instead of considering GD dynamics, we consider a finite temperature bath at T? Let's refer to figure 3.16. As we have seen from the state following procedure, there is a line at which states are lost $T_{lost}(T')$ at which the dynamics become critical. This line terminates down at $T_{lost}(0) = T_{SF}$ and up at $T_{lost}(T_{MCT}) = T_{MCT}$. This marks the

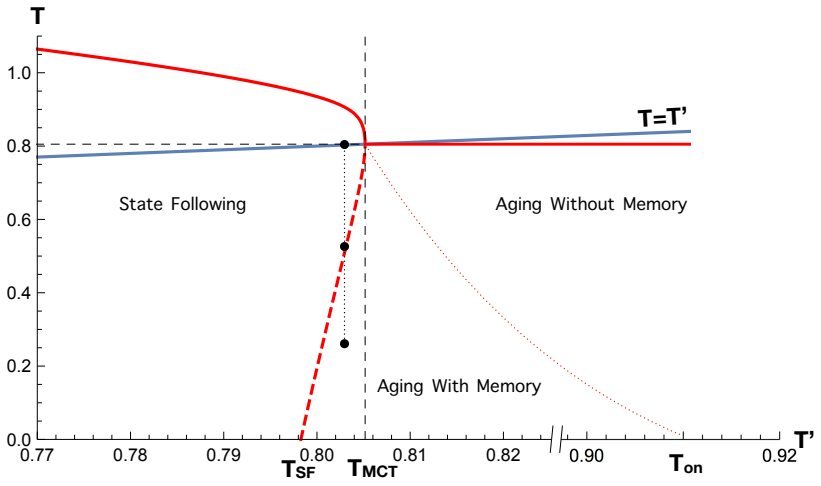

Figure 3.16: The two-temperature protocol phase diagram for the (3+4)-model with the new emerging phase: "Aging with Memory". The thin pointed line is here conjectured and could also corresponds to a crossover.

entrance into an out-of-equilibrium phase which, from preliminary studies and from continuity with the $T = 0$ case, shows aging in a confined space, which we define "aging with memory". On the other side, there is the onset of this new phase, that is not clear yet whether it is a sharp transition or a crossover, which is shown as a temperature band.

The conjecture is that in the two temperature protocol of mixed p-spin models a new phase emerges, between the state following phase at low temperature parent temperature and the threshold aging for high-parent temperature, for any temperature of the thermal bath. This new "aging with memory" phase presents aging on a marginal manifold below the threshold in a confined space (memory of the initial condition). From the theoretical study of the energy landscape at $T = 0$, we have shown that the confinement justifies the under-threshold behavior. We have seen that there is some almost temperature independent (T') behavior in the aging dynamics, also in the new "aging with memory" region. This behavior has allowed to define theoretically an onset temperature T_{on}. This same analysis should be carried out at different T. In any case, the question of how to solve analytically this enigma remains open. One possible path that should be followed is the study of isolated eigenvalues of the Hessian spectrum, both of the energy landscape and of the TAP free energy landscape. Some isolated direction could allow this under-threshold dynamics. We look forward to new developments.

Chapter 3 References

[ASZ18] Gérard Ben Arous, Eliran Subag, and Ofer Zeitouni. "Geometry and temperature chaos in mixed spherical spin glasses at low temperature - the perturbative regime". In: *arXiv:1804.10573 [math]* (2018).

[Bov05] Anton Bovier. *Extreme values of random processes*. 2005.

[CGG99] Andrea Cavagna, Juan P. Garrahan, and Irene Giardina. "Quenched complexity of the mean-field p -spin spherical model with external magnetic field". en. In: *Journal of Physics A: Mathematical and General* 32.5 (1999).

[CK93] L. F. Cugliandolo and J. Kurchan. "Analytical Solution of the Off-Equilibrium Dynamics of a Long Range Spin-Glass Model". In: *Physical Review Letters* 71.1 (1993).

[FFR19] Giampaolo Folena, Silvio Franz, and Federico Ricci-Tersenghi. "Memories from the ergodic phase: the awkward dynamics of spherical mixed p-spin models". In: *arXiv:1903.01421 [cond-mat]* (2019).

[KL95] Jorge Kurchan and Laurent Laloux. "Phase space geometry and slow dynamics". en. In: (1995).

[LNV18] Giacomo Livan, Marcel Novaes, and Pierpaolo Vivo. "Introduction to Random Matrices - Theory and Practice". In: *arXiv:1712.07903 [cond-mat, physics:math-ph]* 26 (2018).

[Ros+19] Valentina Ros et al. "Complex Energy Landscapes in Spiked-Tensor and Simple Glassy Models: Ruggedness, Arrangements of Local Minima, and Phase Transitions". In: *Physical Review X* 9.1 (2019).

[SDS98] Srikanth Sastry, Pablo G. Debenedetti, and Frank H. Stillinger. "Signatures of distinct dynamical regimes in the energy landscape of a glass-forming liquid". en. In: *Nature* 393.6685 (1998).

Perspectives

I titled this section 'Perspectives' rather than 'conclusions', since I believe that my PhD research would be more effective in opening new 'doors' than closing opened ones. Let's start by giving an account of the principal elements discussed throughout this thesis.

The p-spin spherical model, as it is already suggested by its name, has been introduced as a model with p-body interactions. What I have tried to argue at different levels, is that, having only one kind of interaction brutally trivializes the structure of the model, in which each minimum of the energy landscape is completely independent to all others and can be followed up in temperature until it melts. This can be rephrased geometrically as, the TAP free energy minima are followed radially on the sphere. And as a consequence, using different analysis such as Franz-Parisi from equilibrium states, or selecting dominant states with Monasson method, give the same conclusions on the structure of states. From the point of view of the two temperature protocol out-of-equilibrium dynamics, if one starts inside a state (below T_{MCT}) state following holds. While, if one starts in the ergodic phase (above T_{MCT}), and quench below T_{MCT}, the aging dynamics to the threshold energy manifold holds. It goes to "the" threshold, since there exist only one threshold at which dominant stationary points of the energy landscape pass from saddle to minima. This whole behavior is very singular and connected to the simple geometry of the energy landscape in pure models.

The entire scenario completely changes when considering mixed models, in which different kinds of interactions compete. First of all, it is not possible anymore to follow energy minima in temperature, at least in average; the so-called "chaos in temperature". Then comparing different methods of selecting states they give different results. States followed from equilibrium to some temperature T (FP-potential) are distributed differently than states directly sampled at T (M-method). This static phenomenology reflects in the out of equilibrium dynamics. States can be followed

from equilibrium in the glassy phase (below T_{MCT}), but when cooled too much they can be lost. Concentrating in the gradient descent dynamics, the system shows different aging behaviors. From high temperature it shows aging to "the" threshold, while equilibrating the system near T_{MCT} a new out-of-equilibrium dynamical regime emerges. The system ages in a marginal manifold and keeps memory of the initial condition. This new phase is very difficult to characterize. From the numerical integration it seems to have the same effective temperature, predicted by the Cugliandolo-Kurchan solution ("the" threshold solution), but at the same time it relaxes to energies under the threshold.

We have seen that an approximate asymptotic description of this dynamics can be obtained by noting that there exist two master curves in the FDR analysis. This approximation supports the presence of an onset temperature T_{on}, below which the dynamics begins to deviate from the threshold manifold. Considering that the gradient descent dynamics corresponds to a search for the inherent structures, this same phenomenon is observed in simulations of finite dimensional systems and is connected to the onset of heterogeneous dynamics at equilibrium. The mixed p-spin spherical model has the same phenomenology despite the lack of any spatial structure, which is a very interesting fact, I believe. Another signature of the onset dynamics is given by the non-monotonous behavior of the lightest p-energy part of the Hamiltonian. We have also seen that the aging dynamics, both the threshold and under-threshold ones, show two temperature independent power laws (2/3 and 3/2) which, as we argued, are connected to the lower bound shape of the typical visited Hessian in the energy landscape.

From this panorama multiple paths of investigation naturally arises. First a new analytical ansatz for the asymptotic dynamics, which should take memory effects and aging into account is needed. Many elements could play an essential role in defining this asymptotic behavior. One hypothesis is that there are some isolated eigenvalues of the Hamiltonian Hessian which open paths to the underthreshold dynamics already at short times. Because the dynamics from temperatures near T_{MCT} already goes under-threshold at short times. Another hypothesis is that the same constrained analysis must take into consideration the volume of the starting basin of attraction, as in PEL mind-setting. Apart from many different theoretical paths, one very fruitful way, in order to better understand all the out-of-equilibrium scenarios, would be to succeed in writing a stable algorithm that can achieve 'very large' times. Many have tried, but no one has succeeded. It is full of directions to explore, which one to follow?

What I find most fascinating, is that how from a so simple Hamiltonian, a complex universe has emerged. Over 30 years, the analysis of the properties of this model

has been deepening and reinforcing. In all these pages, I tried to summarize what in my belief are the main results, plus what has been my contribution. One should notice that the main purpose of such a model is to guide the comprehension of more complex models, not to give exact predictions. And in this sense, I think that the model is mature enough to consider its employment as a pedagogical tool. It gives a coherent apparatus of relations, conceptually organized in a very small core. All these relations have some counterparts in real systems, and therefore can guide the exploration. One could object that this apparatus can be misleading regarding the real world, however, I think that this is always the case. The more the model is essential, the more it misses the peculiar aspects of each reality but it is capable of unifying a lot of coherent rules. And I very much enjoy the internal coherence of abstract models.

What is sure, is that a new phase emerges, and this new phase is still far to be understood theoretically. Many ropes have been thrown. We hope that some will guide new comprehensions.

A

Appendices

A.1 Gaussian Correlation of Disorder

From the definition of p-spin model the disorder is Gaussian s.t.:

$$\begin{aligned}\overline{H[\sigma]} &= 0\\ \overline{H[\sigma]H[\tau]} &= Nf(\tfrac{\sigma\cdot\tau}{N})\end{aligned}$$

thus, the associated moment-generating function is:

$$\overline{e^{\int d\sigma H[s]\beta[s]}} = e^{\frac{1}{2}\int dsdt\beta[s]\overline{H[s]H[t]}\beta[t]} = e^{\frac{N}{2}\int dsdt f(\frac{s\cdot t}{N})\beta[s]\beta[t]}$$

where $\beta[\sigma]$ is the conjugated variable to $H[\sigma]$. Inserting $\beta[s] = \delta(s-\sigma)+\delta(s-\tau)$, an important identity follows:

$$\overline{e^{H[\sigma]+H[\tau]}} = e^{\frac{1}{2}\overline{(H[\sigma]+H[\sigma])^2}} = e^{\frac{N}{2}\left(2f(1)+2f(\frac{\sigma\cdot\tau}{N})\right)}$$

this is for two replicas τ and σ, but can be easily extended to n-replicas. Moreover, it can be extended to any linear operator D_σ acting on $H[\sigma]$:

$$\overline{e^{D_\sigma H[\sigma]}} = e^{\frac{1}{2}\lim_{\tau\to\sigma} D_\sigma D_\tau \overline{H[\sigma]H[\tau]}} = e^{\frac{1}{2}ND_\sigma D_\tau f(\frac{\sigma\cdot\tau}{N})|_{\tau=\sigma}}$$

Given any observable which is writable as $O[\sigma] = D_\sigma H[\sigma]$, its gaussian fluctuations can be directly characterized by acting with D_σ on the correlation function f:

$$\overline{O[\sigma]O[\tau]} = D_\sigma D_\tau f(\tfrac{\sigma\cdot\tau}{N}) \tag{A.1}$$

For example, given the gradient linear operator $D_\sigma = \partial_{\sigma_i}$ and $D'_\sigma = \partial_{\sigma_j}$:

$$\begin{aligned}\overline{\partial_i H[\sigma]\partial_j H[\tau]} &= \partial_{\sigma_i}\partial_{\tau_j} N f(\tfrac{\sigma\cdot\tau}{N}) \\ &= \partial_{\sigma_i}(\sigma_j f'(\tfrac{\sigma\cdot\tau}{N})) \\ &= \delta_{ij} f'(\tfrac{\sigma\cdot\tau}{N}) + N^{-1}\sigma_i\sigma_j f''(\tfrac{\sigma\cdot\tau}{N})\end{aligned}$$

For further derivatives the general algebra is:

$$\begin{aligned}\partial f &= \sigma f' \\ \partial\partial f &= \delta f' + N^{-1}\sigma\sigma f'' \\ \partial\partial\partial f &= N^{-1}\delta\sigma f'' + 2 \text{ perm.} + N^{-2}\sigma\sigma\sigma f''' \\ \partial\partial\partial\partial f &= N^{-2}\delta\delta f'' + 2 \text{ perm.} + N^{-3}\delta\sigma f''' + 2 \text{ perm.} + N^{-4}\sigma\sigma\sigma\sigma f'''' \\ &\dots\end{aligned}$$

each derivative of f brings out a term N^{-1}. And in the thermodynamic limit only the biggest power in N contributes. In particular in the main text we will refer to these correlations:

$$\begin{aligned}\lim_{N\to\infty} \overline{H[\sigma]H[\tau]} &= N f(\tfrac{\sigma\cdot\tau}{N}) \\ \lim_{N\to\infty} \overline{H'_i[\sigma]H'_j[\tau]} &= \delta_{ij} f'(\tfrac{\sigma\cdot\tau}{N}) \\ \lim_{N\to\infty} \overline{H''_{ij}[\sigma]H''_{kl}[\tau]} &= N^{-1}\delta_{(ij)(kl)} f''(\tfrac{\sigma\cdot\tau}{N})\end{aligned} \tag{A.2}$$

the first one comes directly from the definition of the disorder in the model and corresponds to fluctuation of the Hamiltonian, the second gives the typical correlations of the gradient, the third one the typical correlations of the element of the Hessian, which in the particular case $\sigma = \tau$ gives the variance of the GOE Hessian on the sphere, which we will explore in detail in the next section.

A.1.1 The typical Hessian belongs to the GOE

We want to show that the typical Hessian of the Hamiltonian of p-spin spherical models belong to the Gaussian Orthogonal Ensemble (GOE). Given the Hessian element of matrix:

$$G_{ij} \equiv \partial_i\partial_j H[s] + \mu\delta_{ij} \propto N^{-1}$$

The matrix G belongs to the GOE if:

$$\overline{G_{ij}G_{kl}} = \frac{1}{N}\Delta_G^2(\delta_{(ij)(kl)} + \delta_{(ij)(lk)}) + \frac{1}{N^2}B_{(ij)(kl)} \tag{A.3}$$

and

$$\overline{G_{ij}^4} = \frac{1}{N^2} 3\Delta_G^4 \tag{A.4}$$

the symmetric $\delta_{ik}\delta_{jl}+\delta_{il}\delta_{jk}$ comes from the fact that the Hessian is symmetric and so $\overline{G_{ij}G_{kl}} = \overline{G_{ij}G_{lk}}$. We will put apart the $\mu\delta_{ij}$ part of G_{ij} that will give only a constant drift of the spectrum, and consider only the part $\partial_i\partial_j H[s]$, and we will restrict the space with the spherical constrain $s\cdot s = N$. Let's check the first condition:

$$\begin{aligned}
\overline{\partial_i\partial_j H[s]\partial_k\partial_l H[s]}\big|_{s\cdot s=N} &= \lim_{s'\to s} N\partial_i\partial_j\partial'_k\partial'_l f(\frac{s\cdot s'}{N})\big|_{s\cdot s=N} \\
&= \lim_{s'\to s} N\partial_i\partial_j s_k s_l \frac{1}{N^2} f''(\frac{s\cdot s'}{N})\big|_{s\cdot s=N} \\
&= N(\delta_{ik}\delta_{jl}+\delta_{il}\delta_{jk})\frac{1}{N^2}f''(1) \\
&\quad + N(\delta_{ik}s_j s_l + \delta_{il}s_j s_k + \delta_{jk}s_i s_l + \delta_{jl}s_i s_k)\big|_{s\cdot s=N}\frac{1}{N^3}f'''(1) \\
&\quad + N(s_i s_j s_k s_l)\big|_{s\cdot s=N}\frac{1}{N^4}f''''(1)
\end{aligned}$$

The strength of last two terms depends on the components of a typical vector s on the sphere of radius N. But the product $s_i s_j$ will typically behave as $O(1)$ and thus, the two last terms give a sub-leading contribution. Therefore, we obtain the variance of the GOE:

$$\Delta_G^2 = f''(1)$$

To check the second condition on fourth moment we must evaluate:

$$\overline{(\partial_i\partial_j H[s])^4}\big|_{s\cdot s=N} = \lim_{s'''\to s''\to s'\to s} N^2\partial_i\partial_j\partial'_i\partial'_j\partial''_i\partial''_j\partial'''_i\partial'''_j[f(\frac{s\cdot s'}{N})f(\frac{s''\cdot s'''}{N})+2perm.]\big|_{s\cdot s=N}$$

now as in the previous calculation each derivative of f will give a weaker contribution since it carries out an N^{-1} which cannot be compensated by the typical component of a vector on the sphere of radius N. Thus, we will directly consider the terms with less derivatives of f. But these are:

$$\overline{(\partial_i\partial_j H[s])^4}\big|_{s\cdot s=N} = N^2\frac{1}{N^4}(3f''(1)^2) = \frac{1}{N^2}3\Delta_G^4$$

which is the expected result.

A.2 k-RSB q-extremization

Let's look at the extremization of $F_\beta[\hat{\lambda}(q)]$, given a k-RSB ansatz for $\hat{\lambda}(q)$ (see 2.41):

$$\begin{aligned}\delta F_\beta &= \int \frac{\delta F_\beta}{\delta \lambda}\delta\hat{\lambda} \\ \delta\hat{\lambda} &\equiv \sum_{i=0}^{k+1} dq_i\Big(\delta(q_i-q)(q_i-q)(x_i-x_{i+1}) + \theta(q_i-q)(x_i-x_{i+1})\Big) \\ &\quad + (dx_i - dx_{i+1})\theta(q_i-q)(q_i-q)\end{aligned} \tag{A.5}$$

Therefore, the condition of stationarity with regard to the r-overlap q_r reads:

$$0 = \partial_{q_r} F_\beta = \int \frac{\delta F_\beta}{\delta\lambda}\partial_{q_r}\delta\hat{\lambda} \quad \Rightarrow \quad \int_0^{q_r} dq\,\Big(f''(q) - \beta^{-2}\hat{\lambda}(q)^{-2}\Big) = 0 \tag{A.6}$$

It is not required that $\frac{\delta F_\beta}{\delta\lambda}$ is identically zero, as it would be if $\lambda(q)$ did not have to be concave, but that for each r-step its integral is zero:

$$\begin{aligned} f'(q_0) &= \beta^{-2} q_0 \lambda_0^{-2} \\ f'(q_r) - f'(q_{r-1}) &= \beta^{-2}\Big(\int_{q_{r-1}}^{q_r} dq\ \hat{\lambda}(q)^{-2}\Big) \qquad \forall r \geq 0 \end{aligned} \tag{A.7}$$

If we consider the first equation together with the stability condition $\lambda(q_0)^{-2} \geq \beta^2 f''(q_0)$(eq. 2.46), we obtain the general inequality:

$$f'(q_0) \geq q_0 f''(q_0)$$

which is satisfied only by $q_0 = 0$. This same condition was obtained in the 1-RSB case. Therefore, the lowest value of Q^{kRSB}, i.e. the minimum possible overlap between replicas, is always zero in absence of an external field.

A.3 Algebra of Overlap Matrices

A.3.1 Derivatives

$$\partial_{q_{ab}} \log\det Q = \partial_{q_{ab}} \log(q_{ab}M_{ab} + ...) = \frac{M_{ab}}{\det Q} = [q^{-1}]_{ba}$$

$$\partial_{q_{de}}\big(q_{ab}[q^{-1}]_{bc} = \delta_{ab}\big) \Rightarrow \delta_{(ad)(be)}[q^{-1}]_{bc} + q_{ab}\partial_{q_{de}}[q^{-1}]_{bc} = 0 \Rightarrow \partial_{q_{de}}[q^{-1}]_{bc} = -[q^{-1}]_{db}[q^{-1}]_{ec}$$

A.3.2 Algebra of RS Matrices

Given $A, B \in Q^{RS}$ the product $C = A * B \in Q^{RS}$ and is equal to:

$$C = A * B = \lim_{n\to 0}(\alpha I + a)(\beta I + b) = \lim_{n\to 0}\Big(\alpha\beta I + (\alpha b + a\beta) + nab\Big) = \alpha\beta I + (\alpha b + a\beta) \tag{A.8}$$

Therefore, B is the inverse of A if:

$$\beta = 1/\alpha \qquad b = -a/\alpha^2 \tag{A.9}$$

Let's evaluate the product of matrices $[q^{-1}]_{ac}[q^{-1}]_{bd}$ in the RS case. We have that the inverse of $q_{ab} = \delta_{ab}(1-q) + q$ is the matrix $[q^{-1}]_{ab} = \delta_{ab}(1-q)^{-1} - q(1-q)^{-2}$. Therefore:

$$\begin{aligned}[q^{-1}]_{ac}[q^{-1}]_{bd} &= (\delta_{ac}(1-q)^{-1} - q(1-q)^{-2})(\delta_{bd}(1-q)^{-1} - q(1-q)^{-2}) \\ &= \delta_{ac}\delta_{bd}(1-q)^{-2} - (\delta_{ac} + \delta_{bd})q(1-q)^{-3} + q^2(1-q)^{-4}\end{aligned}$$

A.4 TAP Free Energy

In mean-field models which present a first-order transition, in order to study metastable states, one needs to consider free energies written in terms of extensive variables $(M, E, V, ...)$. Unfortunately the majority of calculations are doable only in the dual space, the one of intensive variables $(h, T, P, ...)$, and here all metastabilities are lost. To overcome this issue, three main techniques have been developed. The Plefka's expansion (PE), which is based on a perturbative expansion around a known point of the theory (e.g. infinite temperature) [Ple82; YG90]. Another way is the cavity method (CM), which considers the linear response field of all neighbors on a particle and the auto-induced field of the particle through neighbors [MPV87; Bar97]. And finally the Bethe-Peierls approximation (also called Belief Propagation BP), which approximates the local topology of the neighbors as tree-like and then writes auto-consistent equations for local fields. All three methods agree on results (so far) for mean-field models i.e. completely connected models. In what follows, I present the PE up to second order in inverse-temperature β which gives an exact result for mean-field disorder models in the thermodynamic limit.

Let's write the PE for a generic model and then focus on the mixed p-spin case. The goal of the game is to write a free energy $G[m]$, which is a function of the average magnetization $m_i = \langle s_i \rangle$. The minima of this function locates (meta)stable states of the system. As it is usual habits in perturbative expansions, we decompose the cost function of our model in two parts, a zero-model $H_0[\sigma]$ for which the free energy $G_0[m]^*$ is known and a $\beta H[\sigma]$ which we process perturbatively. Let's now introduce the functional:

$$G_\beta[h; m] \equiv -\log(\mathrm{Tr}_\sigma e^{-\beta H[\sigma] - h\cdot\delta\sigma} e^{-H_0[\sigma]}) = F_\beta[h] - h \cdot m \tag{A.10}$$

where $\delta\sigma_i \equiv \sigma_i - m_i$ and $F_\beta[h] \equiv \log(\mathrm{Tr}_\sigma e^{-\beta H[\sigma] - h\cdot\sigma} e^{-H_0[\sigma]})$ is the usual free energy†. G_β can also be seen as the cumulant generator around the zero-model and around the magnetization m_i. Taking derivatives with respect to β and h_i we have first order moments:

$$\left.\frac{\partial G_\beta[h;m]}{\partial \beta}\right|_{\substack{\beta=0\\h_i=0}} = \langle H \rangle_0 \qquad \left.\frac{\partial G_\beta[h;m]}{\partial h_i}\right|_{\substack{\beta=0\\h_i=0}} = \langle \delta\sigma_i \rangle_0$$

where $\langle\rangle_0$ stands for expectation value over the zero-model ($\beta = 0$). And similarly for high orders. Extremizing the functional (A.10) with respect to h_i is equivalent of

*which is the entropy at infinite temperature

†a part from a β rescaling

calculating the Legendre transform of $F[h]$:

$$G_\beta[m] \equiv \inf_h G_\beta[h;m] = \inf_h (F_\beta[h] - h \cdot m) = F_\beta[h_\beta[m]] - h_\beta[m] \cdot m \tag{A.11}$$

This extremization defines the non-injective map $h_\beta[m]$, which at every inverse-temperature β returns the *right* field h that would allow an average magnetization m. One could naively evaluate $F_\beta[h]$ for arbitrary β and then do a Legendre transformation, however, in this way all non-convexities are lost ($m_\beta[h]$ is a non-surjective map). So the idea is to fix a certain magnetization m_i in the zero-model and to follow the evolution of its correspondent free energy by changing the parameter β. At this point, it is possible to write the total derivative of an averaged observable changing β as:

$$\frac{d\langle O\rangle_\beta}{d\beta} = \langle \frac{dO}{d\beta}\rangle_\beta - \langle OH\rangle^c_\beta - \langle O\delta\sigma_j\rangle^c_\beta \cdot \frac{dh_j}{d\beta} \tag{A.12}$$

where $\langle O\rangle_\beta = \mathrm{Tr}_\sigma O[s] e^{-\beta H[\sigma] - h_\beta[m]\cdot\delta\sigma} e^{-H_0[\sigma]}/Z$ i.e. the expectation over the β-model, the superscript c stands for connected correlations and h_j stands for the component j of $h_\beta[m]$. At this point we notice that, since we defined $h_\beta[m]$ such that $\langle\delta\sigma_i\rangle_\beta = 0$, evaluating derivatives we have a full set of equalities, the first of which reads (see A.12):

$$\frac{d\langle\delta\sigma_i\rangle_\beta}{d\beta} = 0 \quad \Longrightarrow \quad 0 = -\langle\delta\sigma_i H\rangle^c_\beta - \langle\delta\sigma_i\delta\sigma_j\rangle^c_\beta \frac{dh_j}{d\beta} \tag{A.13}$$

We are now ready to write the Taylor expansion of the free energy $G_\beta[m] \equiv G_\beta[h_\beta[m], m]$, obtained by fixing m in the zero-model and following it with the field $h_\beta[m]$:

$$G_\beta[m] = G_0[m] + \beta \frac{dG_\beta[m]}{d\beta}\Big|_{\beta=0} + \frac{\beta^2}{2}\frac{d^2G_\beta[m]}{d\beta^2}\Big|_{\beta=0} + O(\frac{1}{N}) \tag{A.14}$$

At a coherent perturbative order we must expand the field:

$$h_\beta[m] = h_0[m] + \beta \frac{dh_\beta[m]}{d\beta}\Big|_{\beta=0} + \frac{\beta^2}{2}\frac{d^2h_\beta[m]}{d\beta^2}\Big|_{\beta=0} + O(\frac{1}{N})$$

The first order derivative reads (see A.12):

$$\frac{dG_\beta[m]}{d\beta}\Big|_{\beta=0} = -\langle H\rangle_0 - \langle\delta\sigma_i\rangle_0 \frac{dh_i}{d\beta}\Big|_{\beta=0} = -\langle H\rangle_0$$

since $\langle\delta\sigma_i\rangle_0 = 0$. And from the Legendre duality $h_i = -\partial_{m_i} G_\beta$ we deduce the relative field derivative:

$$\frac{dh_i}{d\beta}\Big|_{\beta=0} = \partial_{m_i}\langle H\rangle_0$$

And for the second order derivative (using again A.12 and A.13):

$$\begin{aligned}\frac{d^2G_\beta[m]}{d\beta}\Big|_{\beta=0} &= \frac{d}{d\beta}(-\langle H\rangle_\beta - \langle\delta\sigma_i\rangle_\beta\frac{dh_i}{d\beta})\Big|_{\beta=0}\\ &= (\langle H^2\rangle^c_\beta + \langle H\delta\sigma_i\rangle^c_\beta\frac{dh_i}{d\beta})\Big|_{\beta=0}\\ &= \langle H^2\rangle^c_0 - \langle\delta\sigma_j\delta\sigma_i\rangle^c_0\frac{dh_j}{d\beta}\frac{dh_i}{d\beta}\Big|_{\beta=0}\\ &= \langle H^2\rangle^c_0 - \langle\delta\sigma_i^2\rangle_0(\partial_{m_i}\langle H\rangle_0)^2\end{aligned}$$

where in the last line, we have used the first order expansion of the field and taken the *further assumption* that the zero-model is factorized in the sites i.e. $\langle\delta\sigma_j\delta\sigma_i\rangle_0 = \langle\delta\sigma_j\rangle_0\langle\delta\sigma_j\rangle_0$. Putting first and second order together, we get the so-called TAP free energy:

$$G_\beta[m] = G_0[m] - \beta\langle H\rangle_0 + \beta^2(\langle H^2\rangle^c_0 - \langle\delta\sigma_i^2\rangle_0(\partial_{m_i}\langle H\rangle_0)^2)/2 \tag{A.15}$$

It can be shown that in completely connected models any further order derivatives will give non-extensive contributions i.e. $O(1/N)$.

Some interesting developments of the Plefka expansion can be found in the recent literature [BSO16; KH18]

Now we can focus on the mixed p-spin spherical model and evaluate its TAP free energy [Bir99; Zam10]. Our zero-model is the infinite temperature model i.e. a random point σ_i on a N-dimensional sphere and $G_0[m]$ is the entropy of the points on the sphere with given average magnetization m i.e. the volume of an N-dimensional sphere of squared radius $r^2 = 1 - q = 1 - \sum_i m_i^{2*}$:

$$G_0[m] = \log(V_N r^N) = \log(V_N) + \frac{N}{2}\log(1-q)$$

where V_N is the volume factor. Knowing the zero-model, we can perturb it with the quenched disorder Hamiltonian $H[\sigma] = \sum_k \alpha_k J_k\sigma^{\otimes k}$ with correspondent disorder covariances $\overline{H[\sigma]H[\tau]} = N\sum_k \alpha_k^2 q^k \equiv Nf(q)$ where $\overline{()}$ is the average over the quenched

*Thus $H_0[\sigma] = -\frac{1}{2}\mu(\sigma\cdot\sigma - N)$ with μ Lagrange multiplier. The related free energy is $F_0[h] = \frac{N}{2}\log(\frac{2\pi}{\mu}) + \frac{1}{2\mu}h\cdot h + \frac{1}{2}\mu N$ and $m_i = \partial_{h_i}F_0[h] = h_i^*/\mu$, and we have:

$$G_0[m] = F_0[h^*] - m\cdot h^* = \frac{N}{2}\log(\frac{2\pi}{\mu}) + \frac{N}{2}\mu(1-q) = \frac{N}{2}\log(1-q) + const$$

where the Lagrange multiplier has the value $\mu = (1-q)^{-1}$ and $q = \sum_i m_i^2/N$.

disorder. To evaluate the TAP free energy we just use (A.15), obtaining:

$$G_\beta[m] = \frac{N}{2}\log(1-q) - \beta\sum_k \alpha_k J_k m^{\otimes k} + \beta^2\frac{N}{2}(f(1) - f(q) - (1-q)f'(q)) \quad \text{(A.16)}$$

where we have used the equalities $\langle H^2\rangle_0 \approx \overline{\langle H^2\rangle}_0 = \overline{\sum_k \alpha_k^2 J_k^2 (\sigma^2)^{\otimes k}} = f(1)$, $\langle H\rangle_0^2 \approx \overline{\langle H\rangle}_0^2 = \overline{\sum_k \alpha_k^2 J_k^2 (m^2)^{\otimes k}} = f(q)$ and $(\partial_{m_i}\langle H\rangle_0)^2 \approx \overline{(\partial_{m_i}\langle H\rangle_0)^2} = f'(q)$.

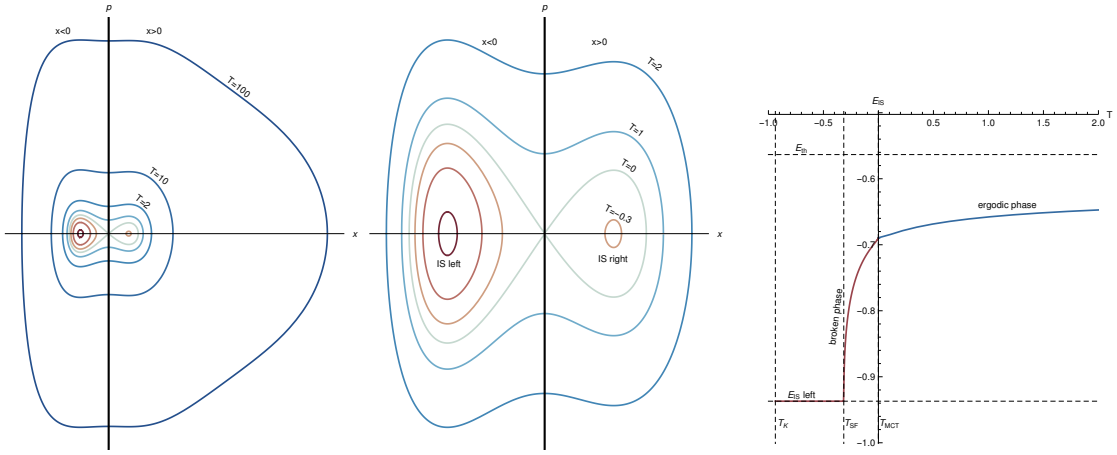

Figure A.1: (**left,center**): orbits of the bi-stable pendulum for high and small energies. The energy of the orbit is parameterized by the relative temperature T. (**right**): dependence of the final average energy E_{IS} after a quench from orbits at different temperature T. We define T_{MCT}, T_{SF}, T_K in analogy with the mixed p-spin model.

A.5 A Toy Model with Memory from the Ergodic Phase

In this small section, I present a uni-dimensional model that despite its simplicity illustrates the effect of memory from the ergodic phase. It's a bi-stable pendulum with Hamiltonian:

$$H(x,p) = \frac{1}{2}p^2 + V(x/L) \qquad \text{with} \qquad \begin{cases} \lim_{L\to\infty} V(x/L) = -x^2 + \frac{x^3}{3} + \frac{x^4}{4} \\ \lim_{L\to 0} V(x/L) = \frac{1}{2b^2}\theta(x)x^2 \end{cases} \tag{A.17}$$

If L is taken very large, we see that $V(x)$ is a standard asymmetric double-well potential with two minima divided by a saddle at $x = 0$. We look at this model from a microcanonical point of view. To each energy corresponds an orbit in the phase space (x, p). The $L \to 0$ limit is build in such a way that iso-energetic curves describe a half ellipse with an x-axis long b-times the p-axis. The relative entropic weight of finding a configuration in a certain portion of the orbit is proportional to the length of it, since the differential entropy is $dS = dxdp$. At high energies - which in our analogy with the p-spin dynamics corresponds to high temperatures - orbits are *ergodic*, in the sense that the dynamics explore both wells. Doing a quench, i.e. a gradient descent dynamics ($p \to 0$) from a point on a given orbit, the positive minimum is reached

with a probability equal to (positive orbit length)/(total length). Going down with the energy (temperature in our analogy), the probability of being in the basin of attraction of the right basin decreases, until at the certain temperature the orbit partitions into two disconnected parts at T_{MCT}, and at an even lower temperature the right minimum completely disappears (T_{SF}), leaving space only to the deeper state which continues its existence till T_K. This is a very simple model that already presents memory from the ergodic phase, i.e. in which there is a dependency of the average inherent structure energy onto the initial temperature for $T > T_{MCT}$.

A.6 Equilibrium Integration

The non-linear step

Let's suppose that we know $C_i \equiv C(t_i)$ exactly on a finite set of N points $\{t_i\}_{i\leq N}$ until a time $t_N \equiv \tau$ and we want to evaluate it at $t_{N+1} \equiv \tau + \Delta\tau$. The time $\Delta\tau$ can be very large, but the change $\Delta C_N \equiv C(\tau+\Delta\tau) - C(\tau)$ should be small. In this sense, we can capture very different time scales.
Therefore, we want to solve (see section 2.6):

$$\dot{C}(\tau+\Delta\tau) = -TC(\tau+\Delta\tau) - \beta \int_0^{\tau+\Delta\tau} ds f'(C(\tau+\Delta\tau-s))\dot{C}(s)$$

The question is: fixing $\Delta\tau$ (a posteriori checked), which value of $\underline{C_{N+1}}$ is the 'bets' $(A.6)$ knowing exactly all the past $\{C_i\}_{i\leq N}$?

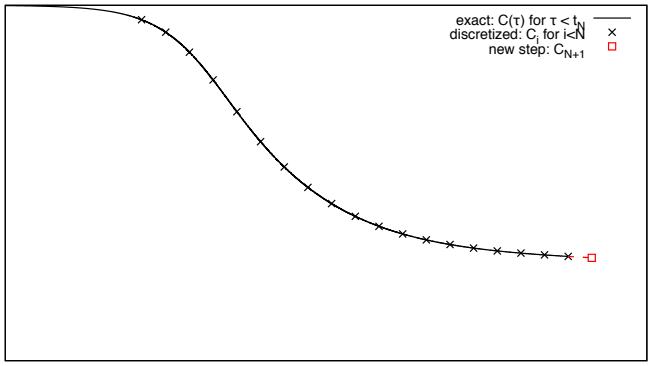

LHS - finite difference method

The LHS, i.e. $\dot{C}(\tau+\Delta\tau)$, can be approximated to the order $O(\Delta\tau^k)$ by a linear combination of $\{C_i\}_{N-k<i\leq N}$ and $\underline{C_{N+1}}$. This is the so-called finite difference (FD) method. Up to the second order the LHS becomes:

$$\begin{aligned}\dot{C}(\tau+\Delta\tau) &\equiv D(\{C_i\}_{N-k<i\leq N}, \underline{C_{N+1}}; \Delta\tau) \\ &= \frac{1}{\Delta\tau}(a_{N-1}C_{N-1} + a_N C_N + a_{N+1}\underline{C_{N+1}}) + O(\Delta\tau^2)\end{aligned} \tag{A.18}$$

where, in general, the coefficients $\{a_i\}_{N-k<i\leq N}$ depend on the time-discretization $\{t_i\}_{N-k<i\leq N}$.

RHS - integral evaluation

To evaluate the RHS of $(A.6)$, we need to split the convolution integral into an interior part, which only depends on the previous steps and a border part which depends explicitly on $\underline{C_{N+1}}$:

$$\int_0^{\tau+\Delta\tau} ds f'(C(\tau+\Delta\tau-s))\dot{C}(s) = I_{inter}(\{C_i\}_{i\leq N};\Delta\tau) + I_{bord}(\underline{C_{N+1}};\Delta\tau);$$

where:

$$\begin{aligned} I_{inter}(\{C_i\}_{i\leq N};\Delta\tau) &\equiv \int_{\Delta\tau}^{\tau} ds f'(C(\tau+\Delta\tau-s))\dot{C}(s) \\ I_{bord}(\underline{C_{N+1}};\Delta\tau) &\equiv \int_0^{\Delta\tau} ds f'(C(\tau+\Delta\tau-s))\dot{C}(s) \\ &\quad + \int_{\tau}^{\tau+\Delta\tau} ds f'(C(\tau+\Delta\tau-s))\dot{C}(s) \end{aligned} \tag{A.19}$$

The first term has a precision that depends on the discretization choice $\{t_i\}_{i\leq N}$. If at every interval in which the integral is decomposed we make an error $O(\Delta\tau^2)$ the total error will be of order $N\Delta\tau^2$.
To evaluate $I_{bord}(\underline{C_{N+1}};\Delta\tau)$ we integrate the first term by parts:

$$\begin{aligned} I_{bord}(\underline{C_{N+1}};\Delta\tau) =& f'(C(\tau+\Delta\tau-s))C(s)\big|_0^{\Delta\tau} \\ &- \int_0^{\Delta\tau} ds C(s)\dot{f}'(C(\tau+\Delta\tau-s)) - \int_0^{\Delta\tau} ds f'(C(s))\dot{C}(\tau+\Delta\tau-s) \end{aligned}$$

this cancels the dependence on the integral of $f'(C)$ on the border zone.
Going on, $I_{bord}(\underline{C_{N+1}};\Delta\tau)$ can be approximated as:

$$\begin{aligned} I_{bord}(\underline{C_{N+1}};\Delta\tau) =& (f'(C_N)C(\Delta\tau) - f'(\underline{C_{N+1}})C_0) \\ &+ \overline{C}_0(\Delta\tau)(f'(\underline{C_{N+1}}) - f'(C_N)) \\ &+ \overline{f'}_0(\Delta\tau)(\underline{C_{N+1}} - C_N) + O(\Delta\tau^2) \end{aligned} \tag{A.20}$$

where $\overline{g}_i(t) \equiv \frac{\int_{t_i}^t g(s)ds}{t-t_i}$. Which means that $I_{bord}(\underline{C_{N+1}};\Delta\tau)$ is a non-linear function of $\underline{C_{N+1}}$.

Non-linear equation for $\underline{C_{N+1}}$

Putting all the approximations together, equation $(A.6)$ becomes:

$$D(\{C_i\}_{N-k<i\leq N}, \underline{C_{N+1}};\Delta\tau) = -T\underline{C_{N+1}} - \beta(I_{inter}(\{C_i\}_{i\leq N};\Delta\tau) + I_{bord}(\underline{C_{N+1}};\Delta\tau)) \tag{A.21}$$

This is a non-linear equation for $\underline{C_{N+1}}$. Putting all the C_{N+1}-linear parts in the LHS and the non-linear in the RHS, we finally obtain:

$$\underline{C_{N+1}} = (a + bf'(\underline{C_{N+1}}))/d \tag{A.22}$$

where

$$\begin{aligned} a \equiv & -\frac{a_{N-1}}{\Delta\tau}C_{N-1} - \frac{a_N}{\Delta\tau}C_N - \beta(I_{inter}(\{C_i\}_{i\leq N}; \Delta\tau) \\ & + f'(C_N)C(\Delta\tau) - \overline{C}_0(\Delta\tau)f'(C_N) - \overline{f'}_0(\Delta\tau)C_N) \\ b \equiv & \beta(C_0 - \overline{C}_0(\Delta\tau)) \\ d \equiv & \frac{a_{N+1}}{\Delta\tau} + T + \beta\overline{f'}_0(\Delta\tau) \end{aligned}$$

To solve fix point equation $(A.22)$, we just run self-consistence dynamics:

$$\underline{C_{N+1}^{(l+1)}} = \frac{a + bf'(\underline{C_{N+1}}^{(l)})}{d} \qquad \text{with} \qquad \underline{C_{N+1}^{(0)}} = C_N$$

This algorithm was developed from the ideas firstly developed in [Fuc+91].

A.7 Out of Equilibrium Integration

In this appendix, we would like to introduce the two numerical methods, currently used to integrate mean-field dynamical equations of the p-spin spherical model (pure and mixed). In particular we will concentrate on the equations that describe the dynamics, following a sudden quench from T' to T. Thus, the correlation and the response of the system evolves according to the two-dimensional non-linear integro-differential equations:

$$\begin{aligned}
\partial_t C_{tt'} =& -\mu_t C_{tt'} + \int_{t'}^{t} f''(C_{ts}) R_{ts} C_{st'} ds \\
&+ \int_0^{t'} \big(f''(C_{ts}) R_{ts} C_{t's} ds + f'(C_{ts}) R_{t's} \big) ds + \beta' f'(C_{t0}) C_{t'0} \\
\partial_t R_{tt'} =& \delta_{tt'} - \mu_t R_{tt'} + \int_{t'}^{t} f''(C_{ts}) R_{ts} R_{st'} ds \\
\mu_t =& T + \int_0^t \big(f''(C_{ts}) R_{ts} C_{ts} ds + f'(C_{ts}) R_{ts} \big) ds + \beta' f'(C_{t0}) C_{t0}
\end{aligned} \tag{A.23}$$

where the Lagrange multiplier μ_t is such that $\lim_{t \to t'_+} \partial_t C_{tt'} = -T$. T is the bath temperature and β' is the initial inverse-temperature. $f'(\cdot)$ is a polynomial function that depends on the specific p-spin model considered (simple or arbitrary mixed).

The first method is based on a simple discretization of the two time indexes. The second, in the attempt to reach larger times, it uses a rescaling of times, in the same fashion of the 1d integration presented in A.6.

A.7.1 Fixed-step Algorithm

In order to integrate the p-spin MFDE, we homogeneously discretize the equations (A.23) with fixed time step Δt and integrate them according to a simple Euler algorithm. This fixed-step algorithm was firstly introduced in [FM94] to study a model of Random Media. It was then specialized to the p-spin case in [FP95] and [BBM96]. Here we won't describe the details, but just comment on the error analysis. The integration error in the Euler algorithm is linear in the integration step Δt. In order to check that we are considering the regime of linear error, three Δt are considered. Both a linear and quadratic fit are performed and the discrepancy between the two is evaluated. If the two fits 'agree', we can extrapolate $\Delta t \to 0$ since we are in the linear regime.

A.7.2 Rescaling Algorithm

An ad-hoc numerical method has been developed following the hint of [Fuc+91]. This method is capable of taking care of relaxations that have very different time scales (of many orders of magnitude). The algorithm as been specialized to p-spin models in [KL01] and its structure has been reported with some details in the appendices of [Ber+07].

The equations (A.23) are composed by five types of contributions (let's consider the correlation C):

1. **Local part:** $\partial_t C_{tt'}$
2. **Rescaling (R):** $\mu_t C_{tt'}$
3. **Crossed Integral (CI):** $\int_{t'}^{t} ds f''(C_{ts}) R_{ts} C_{st'}$
4. **Parallel Integral (PI):** $\int_0^{t'} ds (f'(C_{ts}) R_{t's} + f''(C_{ts}) R_{ts} C_{t's})$
5. **Initial Configuration (ic):** $\beta' f'(C_{t0}) C_{t'0}$

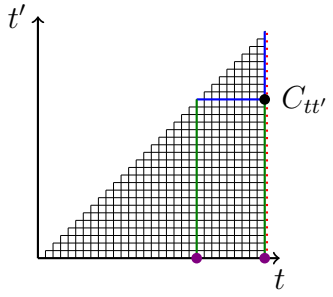

with any linear change of observables, the structure of the equations remain the same. In the following, we will consider an algorithm to integrate these equations.

$$\begin{aligned} \partial_t C_{tt'} &= -\mu(t) C_{tt'} + CI_C[C,R]_{tt'} + PI_C[C,R]_{tt'} + \beta' f'(C_{t0}) C_{t'0} \\ \partial_t R_{tt'} &= -\mu(t) R_{tt'} + CI_R[C,R]_{tt'} \\ \mu(t) &\equiv T + PI_\mu[C,R](t) + \beta' f'(C_{t0}) C_{t0} \end{aligned} \tag{A.24}$$

A.7.3 Structure and Approximations

In this section, we introduce the structure of the algorithm to integrate A.23. We will use the same ingredients at the basis of the one-time algorithm:

1. **Discretization → Grid**
2. **Non-linear Propagation → Self-Consistence equations**
3. **Time rescaling → Contraction**

Grid: storing data

To store $C_{tt'}$ until the time t (and all other two-time functions needed in the integration), we will make use of a half-grid of fixed side N.

Each **node** of the grid corresponds to one correlation value:

$$C_{i,j} \equiv C_{i\Delta t j\Delta t}$$

and each **segment** between two nodes corresponds to an average:

$$\bar{C}^h_{i,j} \equiv \frac{1}{\Delta t}\int_{t-\Delta t}^{t} dsC_{st'}$$

for horizontal segments. And

$$\bar{C}^v_{i,j} \equiv \frac{1}{\Delta t}\int_{t'}^{t'+\Delta t} dsC_{ts}$$

for vertical segments.
The same grid is build for $R_{tt'}$, $f'(C_{tt'})$ and $f''(C_{tt'})$.

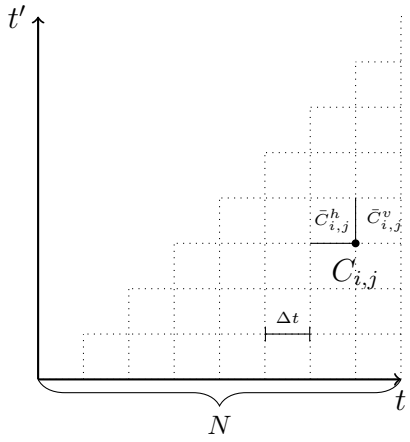

Self-Consistence Equations: non-linear step

Here, we briefly explain the core of the algorithm: the non-linear step. In analogy of what we have seen for the 1d integration (appendix A.6), let's admit that we know exactly $C(s,s')$ and $R(s,s')$ for any s,s' s.t. $s' \leq s \leq t-\Delta t$ in a discrete set of values (stored in the **grid**). What is the value of $C_{tt'}$ and $R_{tt'}$ for all t' s.t. $t' < t$?
To this end, we must expand lhs and rhs of A.24:

$$\begin{aligned} D[C,\underline{C}]_{i,j} &= -\mu[\underline{C},\underline{R}]_i \underline{C_{i,j}} \\ &\quad + CI_C[f'',C,R,\underline{C},\underline{R}]_{i,j} \\ &\quad + PI_C[f',f'',C,R,\underline{C},\underline{R}]_{i,j} \\ &\quad + \beta' f'(\underline{C_{i,0}})C_{j,0} \end{aligned} \qquad \text{(A.25)}$$

$$\begin{aligned} D[R,\underline{R}]_{i,j} &= -\mu[\underline{C},\underline{R}]_i \underline{R_{i,j}} \\ &\quad + CI_R[f'',C,R,\underline{C},\underline{R}]_{i,j} \end{aligned}$$

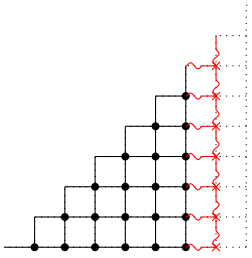

where the indexes i and j correspond respectively to the times t and t'.
$D[]$ is a linear operator that gives an approximation of the t-derivative of the function at time i,j given the value of the function at that time and previous nearby times ($\{C_{k,j}\}_{k\lesssim i}$). The operators $CI[]$ and $PI[]$ (see appendix give an approximation of the integrals in A.24 given all the past points of $C, R, f'(C), f''(C)$.

To evaluate $C_{i,j}$ and $R_{i,j}$ we put the equation $A.25$ in the form:

$$\begin{aligned} C_{i,j} &= \frac{a^C_{i,j} + f^C_{i,j}(\{C_{i,k}\}_{0\leq k\leq i}; \{R_{i,k}\}_{0\leq k\leq i})}{b^C_{i,j}} \\ R_{i,j} &= \frac{a^R_{i,j} + f^R_{i,j}(\{C_{i,k}\}_{0\leq k\leq i}; \{R_{i,k}\}_{0\leq k\leq i})}{b^R_{i,j}} \end{aligned} \tag{A.26}$$

These equations define the self-consistence loop. A starting set of $\{C_{i,k}\}_{0\leq k\leq i}$ and $\{R_{i,k}\}_{0\leq k\leq i}$ is given to the rhs (the same values of the previous time $t - \Delta t$) and a new set is obtained in the lhs. These are then reinserted in the rhs and the procedure is repeated until convergence. This fixed point method is very fast and stable.

Contraction: here comes the trouble

After having integrate until the end of the grid, the time step is rescaled $\Delta t \to 2\Delta t$ and the grid is contracted, in the sense that all the information is compressed in the first half of the grid.
We take one **node** each four:

$$C_{i,j} = C_{2i,2j}$$

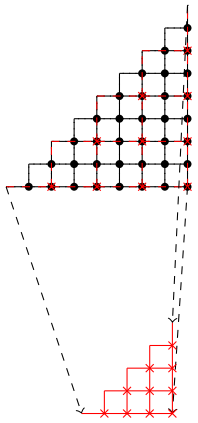

and one **segment** each four :

$$\bar{C}^h_{i,j} = \frac{1}{2}(\bar{C}^h_{2i-1,2j} + \bar{C}^h_{2i,2j})$$

for horizontal segments. And

$$\bar{C}^v_{i,j} = \frac{1}{2}(\bar{C}^v_{2i,2j} + \bar{C}^v_{2i,2j+1})$$

for vertical segments.

These contractions of the grid in half, is the major point of the algorithm and also its weakness. Thanks to this procedure many orders of magnitude can be explored, but this scaling of the past information is sometimes too brutal and the algorithm crashes. Some examples of this problem will be shown in the next section.

A.7.4 Simple Aging

Let's first present one very interesting result, obtainable with this algorithm. The numerical confirmation of the 1-RSB ansatz for the Fluctuation Dissipation Relation used in the CK aging solution:

$$\begin{aligned} \chi_{tt'} &= \beta C_{tt'} \qquad \text{for} \quad q < C_{tt'} < 1 \\ \chi_{tt'} &= \beta x C_{tt'} \qquad \text{for} \quad 0 < C_{tt'} < q \end{aligned} \tag{A.27}$$

The results are presented in section 2.7.4. The value of q and x that come from the asymptotic CK solution is perfectly retrieved in the numerical integration (see fig. 2.16). The algorithm is capable of reaching times of the order of 10^6 in standard units. The integration is performed with a grid of side 2^{12}. The same integration was firstly presented by B. Kim e A. Latz [KL01]. Here we wish to remark that the chosen dynamics in that work was particularly favorable for this rescaling algorithm. In many other cases the same algorithm is not capable of comparable performances, in particular when the bath temperature T is low or when the parental temperature T' is close to T_{MCT}. In the next session, we will discuss what is believed to be the main cause of the algorithm limits.

A.7.5 Limits and Errors

Now we will briefly explore one of the major limits of the Rescaling Algorithm and how it can be corrected. Each time the algorithm performs a contraction of the gird, there is a part of the information contained in the grid that gets lost. One way to quantify it is to look at an observable, before and after the contraction. In particular, we focus on the Lagrange multiplier $\mu(t)$. In fig. A.2 the integrated correlation $C(t,0)$ is shown (full lines), and the relative error made in the contraction of μ (symbols). The same computation for different sizes of the grid and for aging regime is shown, on the left a quench from random condition to $T \approx 0$ and on the right a quench from random condition to $T = 0.5$, which corresponds to the conditions chosen by Kim e Latz and shown in fig. 2.16). We see that there is a direct correspondence between the time dependence of the relative error over μ, following each contraction, and the stability of the correlation. Whenever the relative error reaches the threshold of 10^{-1}, the correlation starts to consistently deviate from the solution given by the biggest grid $N = 2048$. In the case of $T \approx 0$ this happens very soon and even the biggest grid cannot reach integration times bigger than 10^2.

It follows that one of the most important limits of the algorithm comes in the process of storing the information of the passed integration. The fixed size grid is

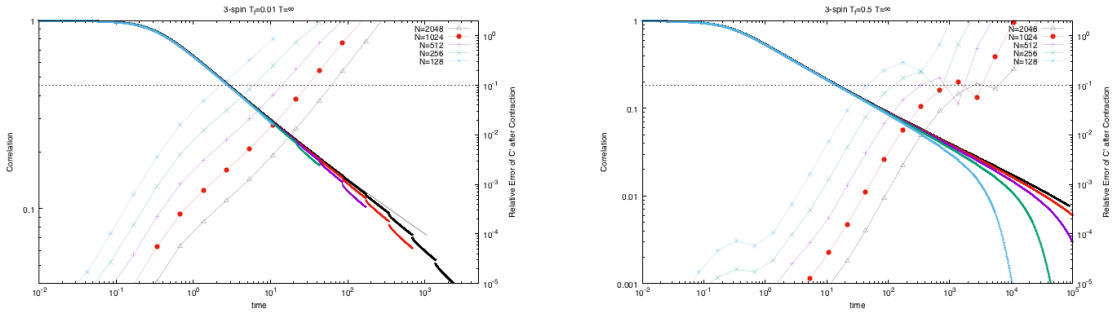

Figure A.2: Correlation with the initial configuration $C(t,0)$ (full lines) and relative error in the contraction of the grid. There is a net dependence of the performances of the algorithm and the error in the contraction. (**left**): aging from random condition to $T = 0.01$. Here the error diverge at small times. (**right**): aging from random condition to $T = 0.5$, which is the dynamics studied by Kim e Latz [KL01]. Here the error diverge for later times and an integration till 10^6 is feasible.

a good structure in this regard. A possible alternative could come from a more flexible grid that concentrates on the time regions which intrinsically detain more information: a flexible grid. The question remains open. What is sure, is that a 'good' algorithm, capable to reach times of the order of 10^6, would be an important tool in the investigation of aging dynamics in mixed p-spin and other models.

A.8 Formulario p-spin

Condition for 1-RSB Transition

$$\partial_q^2[f''(q)^{-1/2}] \geq 0$$

Mode Coupling Transition

$$q_{MCT} \quad \text{s.t.} \quad 1 - q_{MCT} = \frac{f'(q_{MCT})}{q_{MCT} f''(q_{MCT})}$$
$$T_{MCT} = \sqrt{\frac{1 - q_{MCT}}{q_{MCT}} f'(q_{MCT})}$$

Kauzmann Transition

$$q_K \quad \text{s.t.} \quad -\frac{(1 - q_K)}{q_K^2}\big(q_K - \log(1 - q_K)\big) = \frac{f(q_K)}{q_K f'(q_K)}$$
$$T_K = \sqrt{\frac{1 - q_K}{q_K} f'(q_K)}$$

RS Stability

$$\lambda_L = -\left(\beta^2 f''(q) - \frac{1}{(1-q)^2}\right) + \frac{2q}{(1-q)^3}$$
$$\lambda_R = -\left(\beta^2 f''(q) - \frac{1}{(1-q)^2}\right)$$

Marginality

$$T_{mg} = (1 - q_{mg})^{-1} f''(q_{mg})^{-1/2}$$
$$K_{mg} = \frac{f'(q_{mg})}{q_{mg} f''(q_{mg})}$$

Equilibrium

$$T_{eq} = \sqrt{\frac{(1 - q_{eq}) f'(q_{eq})}{q_{eq}}}$$
$$K_{eq} = 1 - q_{eq}$$

Equilibrium Plateau

$$\lambda_{pl} = \frac{1}{2\beta_{MCT}} \frac{f'''(q_{MCT})}{f''(q_{MCT})^{3/2}}$$
$$a_{pl} \quad \text{s.t.} \quad \frac{\Gamma(1-a_{pl})^2}{\Gamma(1-2a_{pl})} = \lambda_{pl}$$
$$b_{pl} \quad \text{s.t.} \quad \frac{\Gamma(1+b_{pl})^2}{\Gamma(1+2b_{pl})} = \lambda_{pl}$$

Threshold at T=0

$$\mu_{mg} = 2f''(1)^{1/2}$$
$$\chi_{mg} = f''(1)^{-1/2}$$
$$y_{th} = \frac{1}{\chi_{mg} f'(1)} - \chi_{mg}$$
$$E_{th} = -\chi_{mg} f'(1) - y_{th} f(1)$$

1RSB solution

$$K(q,\beta) = \frac{\beta^2 f'(q)(1-q)^2}{q}$$
$$\text{s.t.} \qquad \frac{K(K-1-2S-\log K)}{(1-K)^2} = \frac{f(q)}{qf'(q)}$$

which directly comes out from $\Sigma_{M}(q,\beta) = S$. This allows to draw isocomplexity lines.

Monasson Method

All the quantities are expressed as a function of the inverse-temperature β and the in-state overlap q.

$$x_{M}(q,\beta) = \frac{1}{\beta^2 f'(q)(1-q)} - \frac{(1-q)}{q} = (K^{-1}-1)\frac{(1-q)}{q}$$
$$F_{M}(q,\beta) = -\frac{\beta}{2}\Big(f(1) - f(q) + 2x_{M} f(q) + f'(q)(1-q)\Big) - \frac{\beta^{-1}}{2}\log(1-q)$$
$$E_{M}(q,\beta) = -\beta\big(f(1) - f(q)\big) - \beta x_{M} f(q)$$
$$\Sigma_{M}(q,\beta) = \frac{1}{2}\Big(- \beta^2 x_{M}^2 f(q) - \frac{q x_{M}}{1-(1-x_{M})q} + \log\frac{1-(1-x_{M})q}{1-q}\Big)$$

in all expressions is intended $x_{M} \equiv x_{M}(q, \beta)$.

Cugliandolo-Kurchan solution

$$\begin{aligned} q_{CK} = q_{mg} x_{CK}(\beta) &= x_{M}(q_{mg}, \beta) \\ F_{CK}(\beta) &= F_{M}(q_{mg}, \beta) \\ E_{CK}(\beta) &= E_{M}(q_{mg}, \beta) \\ &\dots \end{aligned}$$

Franz-Parisi Method

All the quantities are expressed as a function of the inverse-temperature β and the in-state overlap q.

$$\begin{aligned} \breve{q}_{FP}(q,\beta) &= \sqrt{q - \beta^2(1-q)^2 f'(q)} = q\sqrt{1-K} \\ \beta'_{FP}(q,\beta) &= \frac{\breve{q}_{FP}}{\beta(1-q)f'(\breve{q}_{FP})} \\ F_{FP}(q,\beta) &= -\frac{\beta}{2}\Big(f(1) - f(q) + 2\beta^{-1}\beta'_{FP} f(\breve{q}_{FP}) + f'(q)(1-q)\Big) - \frac{\beta^{-1}}{2}\log(1-q) \\ E_{FP}(q,\beta) &= -\beta\big(f(1) - f(q)\big) - \beta'_{FP} f(\breve{q}_{FP}) \\ \Sigma_{FP}(q,\beta) &= \frac{1}{2}\big(- \beta'^{2}_{FP} f(q_{eq}(\beta'_{FP})) - q_{eq}(\beta'_{FP}) - \log(1 - q_{eq}(\beta'_{FP}))\big) \\ \Sigma^{eq}_{FP}(q) &= \frac{1}{2}\left(-\frac{q}{(1-q)}\frac{f(q)}{qf'(q)} - q - \log(1-q)\right) \end{aligned}$$

in all expressions is intended $\breve{q}_{FP} \equiv \breve{q}_{FP}(q,\beta)$ and $\beta'_{FP} \equiv \beta'_{FP}(q,\beta)$. $q_{eq}(\beta)$ is the overlap that dominates the partition function at inverse temperature β i.e. s.t. $q_{eq}/(1-q_{eq}) = \beta^2 f'(q_{eq})$

Stability condition:

$$-\frac{W}{4\beta(1-q)^2\breve{q}^2_{FP}}\left(W(1-q)\left(\frac{\breve{q}_{FP} f''(\breve{q}_{FP})}{f'(\breve{q}_{FP})} - 1\right) - 2\breve{q}^2_{FP}\right) > 0$$

$$W = 1 + 2\beta^2 f'(q)(1-q) + \beta^2 f''(q)(1-q)^2 \quad \text{(A.28)}$$

TAP Method

All the quantities are expressed as a function of the Energies E_p and the in-state overlap q. Actung E_p are not the energies of the minima in mixed models, are just

decomposition weights.

$$
\begin{aligned}
H_{TAP}(q,\{E_p\}) &= \sum_p E_p q^{p/2} \\
H'_{TAP}(q,\{E_p\}) &= \sum_p p E_p q^{p/2-1} \\
\beta_{TAP}(q,\{E_p\}) &= \frac{1}{(1-q)\big(\sqrt{H'^2_{TAP}-f''(q)}-H'_{TAP}\big)} \\
F_{TAP}(q,\{E_p\}) &= H_{TAP}-\frac{\beta}{2}\Big(f(1)-f(q)-f'(q)(1-q)\Big)-\frac{\beta^{-1}}{2}\log(1-q) \\
E_{TAP}(q,\{E_p\}) &= H_{TAP}-\beta\left(f(1)-f(q)-f'(q)(1-q)\right) \\
\Sigma_{TAP}(E_{IS}) &= -E_{IS}^2+\log\Big(\frac{\sqrt{H'^2_{TAP}-f''(q)}-H'_{TAP}}{f'(q)}\Big)+\frac{H'_{TAP}}{\sqrt{H'^2_{TAP}-f''(q)}-H'_{TAP}}\Bigg|_{q=1}
\end{aligned}
$$

in all expressions is intended $H_{TAP} \equiv H_{TAP}(q,\{E_p\})$. $\Sigma_{TAP}(E_{IS})$ is valid only for pure models.

Universal Complexity

$$
\Sigma_{UN}(K,q) = \frac{1}{2}\Big(K-1-\frac{(1-K)^2}{K}\frac{f(q)}{qf'(q)}-\log(K)\Big)
$$

$$
\begin{aligned}
\text{for general } \beta \qquad & K_M = \frac{\beta^2 f'(q)(1-q)^2}{q} \Rightarrow \Sigma_{UN}(K_M,q) \equiv \Sigma_M(q,\beta) \\
\text{at } T=0 \qquad & K_0 = \chi^2 f'(1) \Rightarrow \Sigma_{UN}(K_0,1) \equiv \Sigma_0^{dm}(\chi) \\
\text{at equilibrium} \qquad & K_{eq} = 1-q_{eq} \Rightarrow \Sigma_{UN}(K_{eq},q_{eq}) \equiv \Sigma_{FP}^{eq}(q_{eq})
\end{aligned}
$$

A.9 Nomenclature

FP Franz-Parisi potential
M Monasson method
q_{MCT} value of the typical overlap at the Mode-Coupling transition
E_{eq} equilibrium energy
E_{IS} inherent structure energy
$\tau = t - t'$ stationary time
t' waiting time
RFOT random first order transition
MFDE mean-field dynamical equations
IS inherent structure
TTI time translation invariance
FDT fluctuation dissipation theorem
GD gradient descent
TS time sector
FDR fluctuation dissipation ratio
SCL supercooled liquid
VFT Vogel-Fulcher-Tamman
CA calorimetric analysis

Bibliography

[AAC10] A. Auffinger, G. Ben Arous, and J. Cerny. "Random Matrices and complexity of Spin Glasses". In: *arXiv:1003.1129 [math-ph]* (2010).

[ABM04] T. Aspelmeier, A. J. Bray, and M. A. Moore. "Complexity of Ising Spin Glasses". In: *Physical Review Letters* 92.8 (2004).

[ADG01] G. Ben Arous, A. Dembo, and A. Guionnet. "Aging of spherical spin glasses". en. In: *Probability Theory and Related Fields* 120.1 (2001).

[Aff+05] F. Affouard et al. "Onset of slow dynamics in difluorotetrachloroethane glassy crystal". In: *The Journal of Chemical Physics* 123.8 (2005).

[AG65] Gerold Adam and Julian H. Gibbs. "On the Temperature Dependence of Cooperative Relaxation Properties in Glass-Forming Liquids". In: *The Journal of Chemical Physics* 43.1 (1965).

[Ago+17] Elisabeth Agoritsas et al. "Out-of-equilibrium dynamical mean-field equations for the perceptron model". In: *arXiv:1710.04894 [cond-mat]* (2017).

[Ang+00a] L. Angelani et al. "Potential Energy Landscape and Long Time Dynamics in a Simple Model Glass". In: *Physical Review E* 61.2 (2000).

[Ang+00b] L. Angelani et al. "Saddles in the Energy Landscape Probed by Supercooled Liquids". In: *Physical Review Letters* 85.25 (2000).

[Ang+00c] C. A. Angell et al. "Relaxation in glassforming liquids and amorphous solids". In: *Journal of Applied Physics* 88.6 (2000).

[Ang88] C. A. Angell. "Perspective on the glass transition". en. In: *Journal of Physics and Chemistry of Solids* 49.8 (1988).

[Ang95] C. A. Angell. "The old problems of glass and the glass transition, and the many new twists". en. In: *Proceedings of the National Academy of Sciences* 92.15 (1995).

[AS82] C. A. Angell and D. L. Smith. "Test of the entropy basis of the Vogel-Tammann-Fulcher equation. Dielectric relaxation of polyalcohols near Tg". In: *The Journal of Physical Chemistry* 86.19 (1982).

[ASZ18] Gérard Ben Arous, Eliran Subag, and Ofer Zeitouni. "Geometry and temperature chaos in mixed spherical spin glasses at low temperature - the perturbative regime". In: *arXiv:1804.10573 [math]* (2018).

[Ban+17] Atreyee Banerjee et al. "Determination of onset temperature from the entropy for fragile to strong liquids". In: *The Journal of Chemical Physics* 147.2 (2017).

[Bar97] A. Barrat. "The p-spin spherical spin glass model". In: *arXiv:cond-mat/9701031* (1997).

[BB04] Jean-Philippe Bouchaud and Giulio Biroli. "On the Adam-Gibbs-Kirkpatrick-Thirumalai-Wolynes scenario for the viscosity increase in glasses". In: *The Journal of Chemical Physics* 121.15 (2004).

[BB09] G. Biroli and J. P. Bouchaud. "The Random First-Order Transition Theory of Glasses: a critical assessment". In: *arXiv:0912.2542 [cond-mat]* (2009).

[BB11] Ludovic Berthier and Giulio Biroli. "Theoretical perspective on the glass transition and amorphous materials". In: *Reviews of Modern Physics* 83.2 (2011).

[BBM96] A. Barrat, R. Burioni, and M. Mézard. "Dynamics within metastable states in a mean-field spin glass". In: *Journal of Physics A: Mathematical and General* 29.5 (1996).

[Ber+07] Ludovic Berthier et al. "Spontaneous and induced dynamic correlations in glass-formers II: Model calculations and comparison to numerical simulations". In: *The Journal of Chemical Physics* 126.18 (2007).

[Ber+17] Ludovic Berthier et al. "Configurational entropy measurements in extremely supercooled liquids that break the glass ceiling". en. In: *Proceedings of the National Academy of Sciences* 114.43 (2017).

[Ber11] Ludovic Berthier. "Dynamic heterogeneity in amorphous materials". In: *Physics* 4 (2011).

[BFP97] A. Barrat, S. Franz, and G. Parisi. "Temperature evolution and bifurcations of metastable states in mean-field spin glasses, with connections with structural glasses". In: *Journal of Physics A: Mathematical and General* 30.16 (1997).

[BG13] Giulio Biroli and Juan P. Garrahan. “Perspective: The glass transition”. In: *The Journal of Chemical Physics* 138.12 (2013).

[BGS84] U. Bengtzelius, W. Gotze, and A. Sjolander. “Dynamics of supercooled liquids and the glass transition”. en. In: *Journal of Physics C: Solid State Physics* 17.33 (1984).

[Bir99] Giulio Biroli. “Dynamical TAP approach to mean field glassy systems”. In: *Journal of Physics A: Mathematical and General* 32.48 (1999).

[BM80] A. J. Bray and M. A. Moore. “Metastable states in spin glasses”. en. In: *Journal of Physics C: Solid State Physics* 13.19 (1980).

[Bou+97] Jean-Philippe Bouchaud et al. “Out of equilibrium dynamics in spin-glasses and other glassy systems”. In: *arXiv:cond-mat/9702070* (1997).

[Bov05] Anton Bovier. *Extreme values of random processes*. 2005.

[Bro+00] Kurt Broderix et al. “Energy Landscape of a Lennard-Jones Liquid: Statistics of Stationary Points”. In: *Physical Review Letters* 85.25 (2000).

[BSO16] Barbara Bravi, Peter Sollich, and Manfred Opper. “Extended Plefka Expansion for Stochastic Dynamics”. In: *Journal of Physics A: Mathematical and Theoretical* 49.19 (2016).

[BV15] R. Baviera and M. A. Virasoro. “A method that reveals the multi-level ultrametric tree hidden in p-spin glass like systems”. In: *Journal of Statistical Mechanics: Theory and Experiment* 2015.12 (2015).

[Cal+12] F. Caltagirone et al. “Critical Slowing Down Exponents of Mode Coupling Theory”. In: *Physical Review Letters* 108.8 (2012).

[Cap+06] Barbara Capone et al. “Off-equilibrium confined dynamics in a glassy system with level-crossing states”. In: *Physical Review B* 74.14 (2006).

[Cas06] Tommaso Castellani. “The multi p-spin model: comparing tap states and out-of-equilibrium dynamics”. PhD thesis. 2006.

[Cav09] Andrea Cavagna. “Supercooled Liquids for Pedestrians”. In: *Physics Reports* 476.4-6 (2009).

[CC05] Tommaso Castellani and Andrea Cavagna. “Spin-Glass Theory for Pedestrians”. In: *Journal of Statistical Mechanics: Theory and Experiment* 2005.05 (2005).

[CE96] Marcus T. Cicerone and M. D. Ediger. “Enhanced translation of probe molecules in supercooled o-terphenyl: Signature of spatially heterogeneous dynamics?” In: *The Journal of Chemical Physics* 104.18 (1996).

[CG10] David Chandler and Juan P. Garrahan. "Dynamics on the Way to Forming Glass: Bubbles in Space-Time". In: *Annual Review of Physical Chemistry* 61.1 (2010).

[CGG99] Andrea Cavagna, Juan P. Garrahan, and Irene Giardina. "Quenched complexity of the mean-field p -spin spherical model with external magnetic field". en. In: *Journal of Physics A: Mathematical and General* 32.5 (1999).

[CGP01] Andrea Cavagna, Irene Giardina, and Giorgio Parisi. "Role of saddles in mean-field dynamics above the glass transition". In: *Journal of Physics A: Mathematical and General* 34.26 (2001).

[CGP97a] Andrea Cavagna, Irene Giardina, and Giorgio Parisi. "An investigation of the hidden structure of states in a mean field spin glass model". In: *Journal of Physics A: Mathematical and General* 30.20 (1997).

[CGP97b] Andrea Cavagna, Irene Giardina, and Giorgio Parisi. "Barriers between metastable states in the p-spin spherical model". In: *arXiv:cond-mat/9702069* (1997).

[CGP98] Andrea Cavagna, Irene Giardina, and Giorgio Parisi. "On the stationary points of the TAP free energy". In: *Physical Review B* 57.18 (1998).

[Cha+14a] Patrick Charbonneau et al. "Fractal free energy landscapes in structural glasses". en. In: *Nature Communications* 5 (2014).

[Cha+14b] Patrick Charbonneau et al. "Hopping and the Stokes-Einstein relation breakdown in simple glass formers". In: *Proceedings of the National Academy of Sciences* 111.42 (2014).

[CHS93] A. Crisanti, H. Horner, and H.-J. Sommers. "The spherical p-spin interaction spin-glass model". en. In: *Zeitschrift für Physik B Condensed Matter* 92.2 (1993).

[CK93] L. F. Cugliandolo and J. Kurchan. "Analytical Solution of the Off-Equilibrium Dynamics of a Long Range Spin-Glass Model". In: *Physical Review Letters* 71.1 (1993).

[CK94] L. F. Cugliandolo and J. Kurchan. "On the Out of Equilibrium Relaxation of the Sherrington - Kirkpatrick model". In: *Journal of Physics A: Mathematical and General* 27.17 (1994).

[CK95] L. F. Cugliandolo and J. Kurchan. "Weak-ergodicity breaking in mean-field spin-glass models". In: *Philosophical Magazine B* 71.4 (1995).

[CL04] A. Crisanti and L. Leuzzi. “Spherical $2+p$ Spin-Glass Model: An Exactly Solvable Model for Glass to Spin-Glass Transition”. In: *Physical Review Letters* 93.21 (2004).

[CL06] Andrea Crisanti and Luca Leuzzi. “The spherical 2+p spin glass model: an analytically solvable model with a glass-to-glass transition”. In: *Physical Review B* 73.1 (2006).

[CL07] Andrea Crisanti and Luca Leuzzi. “Amorphous-amorphous transition and the two-step replica symmetry breaking phase”. In: *Physical Review B* 76.18 (2007).

[CLP11] Andrea Crisanti, Luca Leuzzi, and Matteo Paoluzzi. “Statistical mechanical approach to secondary processes and structural relaxation in glasses and glass formers”. In: *The European Physical Journal E* 34.9 (2011).

[CNB19] Daniele Coslovich, Andrea Ninarello, and Ludovic Berthier. “A localization transition underlies the mode-coupling crossover of glasses”. en. In: *SciPost Physics* 7.6 (2019).

[Com+08] Pierre Comon et al. “Symmetric tensors and symmetric tensor rank”. In: *SIAM Journal on Matrix Analysis and Applications* 30.3 (2008).

[CP17] Wei-Kuo Chen and Dmitry Panchenko. “Temperature Chaos in Some Spherical Mixed p-Spin Models”. en. In: *Journal of Statistical Physics* 166.5 (2017).

[CS92] A. Crisanti and H.-J. Sommers. “The spherical p-spin interaction spin glass model: the statics”. en. In: *Zeitschrift für Physik B Condensed Matter* 87.3 (1992).

[CS95] A. Crisanti and H.-J. Sommers. “Thouless-Anderson-Palmer Approach to the Spherical p-Spin Spin Glass Model”. In: *Journal de Physique I* 5.7 (1995).

[Cug02] Leticia F. Cugliandolo. “Dynamics of glassy systems”. In: *arXiv:cond-mat/0210312* (2002).

[Der80] B. Derrida. “Random-Energy Model: Limit of a Family of Disordered Models”. In: *Physical Review Letters* 45.2 (1980).

[DP01] Catherine. Dreyfus and Robert M. Pick. “Relaxations and vibrations in supercooled liquids”. en. In: *Comptes Rendus de l’Académie des Sciences - Series IV - Physics-Astrophysics* 2.2 (2001).

[DS01] Pablo G. Debenedetti and Frank H. Stillinger. "Supercooled liquids and the glass transition". en. In: *Nature* 410.6825 (2001).

[Dyr06] Jeppe C. Dyre. "Colloquium: The glass transition and elastic models of glass-forming liquids". In: *Reviews of Modern Physics* 78.3 (2006).

[EA75] S. F. Edwards and P. W. Anderson. "Theory of spin glasses". en. In: *Journal of Physics F: Metal Physics* 5.5 (1975).

[ECG09] Yael S. Elmatad, David Chandler, and Juan P. Garrahan. "Corresponding States of Structural Glass Formers". In: *The Journal of Physical Chemistry B* 113.16 (2009).

[Edi00] M. D. Ediger. "Spatially Heterogeneous Dynamics in Supercooled Liquids". In: *Annual Review of Physical Chemistry* 51.1 (2000).

[EH12] M. D. Ediger and Peter Harrowell. "Perspective: Supercooled liquids and glasses". In: *The Journal of Chemical Physics* 137.8 (2012).

[Fer+12] U. Ferrari et al. "Two-step relaxation next to dynamic arrest in mean-field glasses: Spherical and Ising p-spin model". In: *Physical Review B* 86.1 (2012).

[FFR19] Giampaolo Folena, Silvio Franz, and Federico Ricci-Tersenghi. "Memories from the ergodic phase: the awkward dynamics of spherical mixed p-spin models". In: *arXiv:1903.01421 [cond-mat]* (2019).

[FM94] Silvio Franz and Marc Mézard. "On mean field glassy dynamics out of equilibrium". en. In: *Physica A: Statistical Mechanics and its Applications* 210.1 (1994).

[Fol+20] G. Folena et al. "manuscript in preparation". In: (2020).

[FP95] S. Franz and G. Parisi. "Recipes for metastable states in Spin Glasses". In: *Journal de Physique I* 5.11 (1995).

[FPV92] S. Franz, G. Parisi, and M. Virasoro. "The replica method on and off equilibrium". In: *Journal de Physique I* 2.10 (1992).

[Fuc+91] M. Fuchs et al. "Comments on the alpha -peak shapes for relaxation in supercooled liquids". en. In: *Journal of Physics: Condensed Matter* 3.26 (1991).

[Gol69] Martin Goldstein. "Viscous Liquids and the Glass Transition: A Potential Energy Barrier Picture". In: *The Journal of Chemical Physics* 51.9 (1969).

[Göt09] W. Götze. *Complex Dynamics of Glass-Forming Liquids: A Mode-Coupling Theory*. OUP Oxford, 2009.

[Göt99] Wolfgang Götze. "Recent tests of the mode-coupling theory for glassy dynamics". en. In: *Journal of Physics: Condensed Matter* 11.10A (1999).

[GS92] W. Gotze and L. Sjogren. "Relaxation processes in supercooled liquids". en. In: *Reports on Progress in Physics* 55.3 (1992).

[Gue03] Francesco Guerra. "Broken Replica Symmetry Bounds in the Mean Field Spin Glass Model". en. In: *Communications in Mathematical Physics* 233.1 (2003).

[Hal89] Timothy Halpin-Healy. "Diverse Manifolds in Random Media". In: *Physical Review Letters* 62.4 (1989).

[Hec+08] Tina Hecksher et al. "Little evidence for dynamic divergences in ultraviscous molecular liquids". en. In: *Nature Physics* 4.9 (2008).

[Heu08] Andreas Heuer. "Exploring the potential energy landscape of glass-forming systems: from inherent structures via metabasins to macroscopic transport". en. In: *Journal of Physics: Condensed Matter* 20.37 (2008).

[HS08] Andreas Heuer and Aimorn Saksaengwijit. "Properties of ideal Gaussian glass-forming systems". In: *Physical Review E* 77.6 (2008).

[HS18] Philip H. Handle and Francesco Sciortino. "Potential energy landscape of TIP4P/2005 water". In: *The Journal of Chemical Physics* 148.13 (2018).

[Jai+16] Abhishek Jaiswal et al. "Onset of Cooperative Dynamics in an Equilibrium Glass-Forming Metallic Liquid". In: *The Journal of Physical Chemistry B* 120.6 (2016).

[KA94] Walter Kob and Hans C. Andersen. "Scaling Behavior in the $\ensuremath{\beta}$-Relaxation Regime of a Supercooled Lennard-Jones Mixture". In: *Physical Review Letters* 73.10 (1994).

[KA95a] Walter Kob and Hans C. Andersen. "Testing mode-coupling theory for a supercooled binary Lennard-Jones mixture I: The van Hove correlation function". In: *Physical Review E* 51.5 (1995).

[KA95b] Walter Kob and Hans C. Andersen. "Testing mode-coupling theory for a supercooled binary Lennard-Jones mixture. II. Intermediate scattering function and dynamic susceptibility". In: *Physical Review E* 52.4 (1995).

[Kau48] Walter. Kauzmann. “The Nature of the Glassy State and the Behavior of Liquids at Low Temperatures.” In: *Chemical Reviews* 43.2 (1948).

[KH18] Tobias Kühn and Moritz Helias. “Expansion of the effective action around non-Gaussian theories”. In: *Journal of Physics A: Mathematical and Theoretical* 51.37 (2018).

[KL01] B. Kim and A. Latz. “The dynamics of the spherical p-spin model: from microscopic to asymptotics”. In: *Europhysics Letters (EPL)* 53.5 (2001).

[KL95] Jorge Kurchan and Laurent Laloux. “Phase space geometry and slow dynamics”. en. In: (1995).

[Kob+97] Walter Kob et al. “Dynamical Heterogeneities in a Supercooled Lennard-Jones Liquid”. In: *Physical Review Letters* 79.15 (1997).

[KPV93] J. Kurchan, G. Parisi, and M. Virasoro. “Barriers and metastable states as saddle points in the replica approach”. In: *Journal de Physique I* 3.8 (1993).

[KT87a] T. R. Kirkpatrick and D. Thirumalai. “Dynamics of the Structural Glass Transition and the p-Spin—Interaction Spin-Glass Model”. In: *Physical Review Letters* 58.20 (1987).

[KT87b] T. R. Kirkpatrick and D. Thirumalai. “p-spin-interaction spin-glass models: Connections with the structural glass problem”. In: *Physical Review B* 36.10 (1987).

[KTW89] T. R. Kirkpatrick, D. Thirumalai, and P. G. Wolynes. “Scaling concepts for the dynamics of viscous liquids near an ideal glassy state”. In: *Physical Review A* 40.2 (1989).

[KZ09] Florent Krzakala and Lenka Zdeborová. “Hiding Quiet Solutions in Random Constraint Satisfaction Problems”. In: *Physical Review Letters* 102.23 (2009).

[KZ87] Mehran Kardar and Yi-Cheng Zhang. “Scaling of Directed Polymers in Random Media”. In: *Physical Review Letters* 58.20 (1987).

[Leu84] E. Leutheusser. “Dynamical model of the liquid-glass transition”. In: *Physical Review A* 29.5 (1984).

[LNV18] Giacomo Livan, Marcel Novaes, and Pierpaolo Vivo. “Introduction to Random Matrices - Theory and Practice”. In: *arXiv:1712.07903 [cond-mat, physics:math-ph]* 26 (2018).

[LSS06] Emilia La Nave, Srikanth Sastry, and Francesco Sciortino. "Relation between local diffusivity and local inherent structures in the Kob-Andersen Lennard-Jones model". In: *Physical Review E* 74.5 (2006).

[LW07] Vassiliy Lubchenko and Peter G. Wolynes. "Theory of Structural Glasses and Supercooled Liquids". In: *Annual Review of Physical Chemistry* 58.1 (2007).

[Mal+10] Francesco Mallamace et al. "Transport properties of glass-forming liquids suggest that dynamic crossover temperature is as important as the glass transition temperature". en. In: *Proceedings of the National Academy of Sciences* 107.52 (2010).

[Man+19] Stefano Sarao Mannelli et al. "Passed & Spurious: Descent Algorithms and Local Minima in Spiked Matrix-Tensor Models". en. In: *International Conference on Machine Learning*. 2019.

[Méz99] Marc Mézard. "How to compute the thermodynamics of a glass using a cloned liquid". In: *Physica A: Statistical Mechanics and its Applications* 265.3 (1999).

[Mon95] R. Monasson. "The structural glass transition and the entropy of the metastable states". In: *Physical Review Letters* 75.15 (1995).

[Mor16] Sebastian Morel-Balbi. "Multi-replica effective potential for state following in disordered systems". PhD thesis. 2016.

[MP90] M. Mezard and G. Parisi. "Interfaces in a random medium and replica symmetry breaking". en. In: *Journal of Physics A: Mathematical and General* 23.23 (1990).

[MPV87] M. Mezard, G. Parisi, and M. Virasoro. *Spin Glass Theory and Beyond: An Introduction to the Replica Method and Its Applications*. en. World Scientific Publishing Company, 1987.

[Nan+15] Manoj Kumar Nandi et al. "Unraveling the success and failure of mode coupling theory from consideration of entropy". In: *The Journal of Chemical Physics* 143.17 (2015).

[Par02] Giorgio Parisi. "The physical Meaning of Replica Symmetry Breaking". In: *arXiv:cond-mat/0205387* (2002).

[Par79a] G. Parisi. "Infinite Number of Order Parameters for Spin-Glasses". In: *Physical Review Letters* 43.23 (1979).

[Par79b] G. Parisi. "Toward a mean field theory for spin glasses". en. In: *Physics Letters A* 73.3 (1979).

[Pet+13] N. Petzold et al. "Evolution of the dynamic susceptibility in molecular glass formers: Results from light scattering, dielectric spectroscopy, and NMR". In: *The Journal of Chemical Physics* 138.12 (2013).

[Ple82] T. Plefka. "Convergence condition of the TAP equation for the infinite-ranged Ising spin glass model". en. In: *Journal of Physics A: Mathematical and General* 15.6 (1982).

[PSD18] Ulf R. Pedersen, Thomas B. Schrøder, and Jeppe C. Dyre. "Phase diagram of Kob-Andersen type binary Lennard-Jones mixtures". In: *Physical Review Letters* 120.16 (2018).

[RA98] R. Richert and C. A. Angell. "Dynamics of glass-forming liquids. V. On the link between molecular dynamics and configurational entropy". In: *The Journal of Chemical Physics* 108.21 (1998).

[RC03] T. Rizzo and A. Crisanti. "Chaos in Temperature in the Sherrington-Kirkpatrick Model". In: *Physical Review Letters* 90.13 (2003).

[RC05] David R. Reichman and Patrick Charbonneau. "Mode-coupling theory". en. In: *Journal of Statistical Mechanics: Theory and Experiment* 2005.05 (2005).

[Ric84] Pascal Richet. "Viscosity and configurational entropy of silicate melts". en. In: *Geochimica et Cosmochimica Acta* 48.3 (1984).

[Ros+19] Valentina Ros et al. "Complex Energy Landscapes in Spiked-Tensor and Simple Glassy Models: Ruggedness, Arrangements of Local Minima, and Phase Transitions". In: *Physical Review X* 9.1 (2019).

[RTV86] R. Rammal, G. Toulouse, and M. A. Virasoro. "Ultrametricity for physicists". In: *Reviews of Modern Physics* 58.3 (1986).

[Sas00] Srikanth Sastry. "Onset temperature of slow dynamics in glass forming liquids". en. In: *PhysChemComm* 3.14 (2000).

[Sas01] Srikanth Sastry. "The relationship between fragility, configurational entropy and the potential energy landscape of glass-forming liquids". en. In: *Nature* 409.6817 (2001).

[Sas02] Srikanth Sastry. "Onset of slow dynamics in supercooled liquid silicon". en. In: *Physica A: Statistical Mechanics and its Applications* 315.1 (2002).

[Sch+00] Thomas B. Schrøder et al. "Crossover to potential energy landscape dominated dynamics in a model glass-forming liquid". In: *The Journal of Chemical Physics* 112.22 (2000).

[Sci05] Francesco Sciortino. "Potential energy landscape description of supercooled liquids and glasses". en. In: *Journal of Statistical Mechanics: Theory and Experiment* 2005.05 (2005).

[SDS98] Srikanth Sastry, Pablo G. Debenedetti, and Frank H. Stillinger. "Signatures of distinct dynamical regimes in the energy landscape of a glass-forming liquid". en. In: *Nature* 393.6685 (1998).

[Sin+12] Murari Singh et al. "Structural correlations and cooperative dynamics in supercooled liquids". In: *The Journal of Chemical Physics* 137.2 (2012).

[Sun+12] YiFan Sun et al. "Following states in temperature in the spherical s+p-spin glass model". In: *Journal of Statistical Mechanics: Theory and Experiment* 2012.07 (2012).

[SW82] Frank H. Stillinger and Thomas A. Weber. "Hidden structure in liquids". In: *Physical Review A* 25.2 (1982).

[SW83] Frank H. Stillinger and Thomas A. Weber. "Dynamics of structural transitions in liquids". In: *Physical Review A* 28.4 (1983).

[SW84] Frank H. Stillinger and Thomas A. Weber. "Packing Structures and Transitions in Liquids and Solids". en. In: *Science* 225.4666 (1984).

[SW85] Frank H. Stillinger and Thomas A. Weber. "Computer simulation of local order in condensed phases of silicon". In: *Physical Review B* 31.8 (1985).

[SZ82] H. Sompolinsky and Annette Zippelius. "Relaxational dynamics of the Edwards-Anderson model and the mean-field theory of spin-glasses". In: *Physical Review B* 25.11 (1982).

[TAP77] D. J. Thouless, P. W. Anderson, and R. G. Palmer. "Solution of 'Solvable model of a spin glass'". In: *The Philosophical Magazine: A Journal of Theoretical Experimental and Applied Physics* 35.3 (1977).

[Wal12] David J. Wales. "Decoding the energy landscape: extracting structure, dynamics and thermodynamics". en. In: *Philosophical Transactions of the Royal Society A: Mathematical, Physical and Engineering Sciences* (2012).

[Wee+00] Eric R. Weeks et al. "Three-Dimensional Direct Imaging of Structural Relaxation Near the Colloidal Glass Transition". en. In: *Science* 287.5453 (2000).

[Wei+16] Nicholas B. Weingartner et al. “A Phase Space Approach to Supercooled Liquids and a Universal Collapse of Their Viscosity”. English. In: *Frontiers in Materials* 3 (2016).

[Win99] Eric Winsberg. “Sanctioning Models: The Epistemology of Simulation”. en. In: *Science in Context* 12.2 (1999).

[YG90] J. S. Yedidia and A. Georges. “The fully frustrated Ising model in infinite dimensions”. en. In: *Journal of Physics A: Mathematical and General* 23.11 (1990).

[Zam10] Francesco Zamponi. “Mean field theory of spin glasses”. In: *arXiv:1008.4844 [cond-mat]* (2010).

[Zin02] Jean Zinn-Justin. *Quantum Field Theory and Critical Phenomena*. en. Clarendon Press, 2002.

[ZK16] Lenka Zdeborová and Florent Krzakala. “Statistical physics of inference: thresholds and algorithms”. In: *Advances in Physics* 65.5 (2016).

[Zwa01] Robert Zwanzig. *Nonequilibrium Statistical Mechanics*. en. Oxford University Press, 2001.